MODULATION OF HIV_{GP120} ANTIGEN-SPECIFIC IMMUNE RESPONSES, IN VITRO AND IN VIVO, BY Δ^9-TETRAHYDROCANNABINOL AND CANNABINOID RECEPTORS 1 AND 2

By

Weimin Chen

A DISSERTATION

Submitted to
Michigan State University
in partial fulfillment of the requirements
for the degree of

Microbiology – Environmental Toxicology – Doctor of Philosophy

2014

ABSTRACT

MODULATION OF HIV_{GP120} ANTIGEN-SPECIFIC IMMUNE RESPONSES, IN VITRO AND IN VIVO, BY Δ^9-TETRAHYDROCANNABINOL AND CANNABINOID RECEPTORS 1 AND 2

By

Weimin Chen

Approximately 25% of HIV patients use marijuana for its putative therapeutic benefit; however, it is unknown how cannabinoids affect the immune function of immunocompromised HIV patients at the early stage. The goal of these studies was to investigate the immunomodulatory effects of cannabinoids on the early stage of the anti-HIV immune responses. A surrogate *in vitro* mouse model was first established to determine the effects of cannabinoids on HIV antigen-specific T cell effector function. Specifically, $CD8^+$ T cell proliferation and gp120-specific IFNγ production were induced, which were suppressed or enhanced by Δ^9-tetrahydrocannabinol (THC), the predominant psychoactive component in marijuana, depending on the magnitude of the control response. To further elucidate the molecular and cellular mechanisms by which cannabinoids differentially modulate T cell responses, phorbol ester, phorbol 12-myristate 13-acetate (PMA), in combination with the ionophore, ionomycin (Io) or anti-CD3/CD28 antibodies were used as activation stimuli, and another marijuana-derived cannabinoid, cannabidiol (CBD), was also investigated. THC or CBD suppressed or enhanced IFNγ and IL-2 production by mouse splenocytes under optimal or suboptimal stimulation, respectively. Similar differential effects of cannabinoids on cytokine production were also observed on nuclear translocation of nuclear factor of activated T cells (NFAT) and with human peripheral blood mononuclear cells (PBMCs) in response to PMA/Io stimulation. However, THC and CBD elevated intracellular calcium, regardless of

the stimulation level with PMA/Io, suggesting that the cannabinoid-induced calcium increase provides an appropriate signal for activation in suboptimally stimulated T cells but an anergic-like signal as a result of excessive calcium in optimally stimulated T cells. Together, these data demonstrate differential modulation by cannabinoids of a HIV antigen-specific response and identify a possible mechanism responsible for this effect.

To investigate whether THC produced similar effects *in vivo*, a mouse model to induce HIV_{gp120}-specific immune responses was then developed. The gp120-expressing plasmid, pVRCgp120, or the vector plasmid, pVRC2000, was injected intramuscularly into mice. Both the gp120-specific IFNγ and IL-2 responses were detected, when splenocytes were restimulated with gp120-derived peptide IIGDIRQAHCNISRA (#81), which was identified as being immunodominant among 211 tested peptides. In addition, T cell and non-T cell populations were all activated in response to pVRCgp120 stimulation followed by peptide restimulation, as evidenced by increased expression levels of surface markers (e.g., CD69, CD80, major histocompatibility complex II [MHC II]). The gp120-specific IFNγ response and the magnitude of cellular activation were enhanced by THC in C57Bl/6 wild-type (WT) mice but suppressed or not affected by THC in cannabinoid receptors 1 (CB_1) and 2 (CB_2) knockout ($CB_1^{-/-}CB_2^{-/-}$) mice. Furthermore, $CB_1^{-/-}CB_2^{-/-}$ mice exhibited an augmented immune response phenotype compared with WT mice on IFNγ production. Collectively, these *in vivo* findings suggest that THC modulates HIV antigen-specific immune responses *in vivo* in both a CB_1/CB_2-dependent and -independent manner. The significance of this dissertation work is that it provides novel insights into the understanding of cannabinoid-mediated effects on antigen-specific immune responses and the associated mechanisms.

ACKNOWLEDGEMENTS

First of all, I would like to acknowledge my thesis advisor, Dr. Norbert Kaminski, for his excellent mentorship during my years in his laboratory. He inspired me with great projects and ideas, trained me to become a motivated and meticulous researcher, and provided tremendous support for my research and other activities at the Society of Toxicology, which made my Ph.D. experience in his laboratory productive as well as beneficial for my future career.

I would also like to thank my guidance committee for providing helpful suggestions and insights during discussions of my dissertation research. Specifically, I thank Dr. Andrea Amalfitano for valuable discussions on HIV biology and vaccine research; Dr. Barbara Kaplan for being my go-to person in the lab and all her great inputs in many experiments and manuscript writings; Dr. James Pestka for sharing critical thinking on experimental designs; Dr. Kefei Yu for sharing his expertise in cell and molecular immunology; former committee member Dr. Ian York for nurturing my interest in the immunology field and providing valued suggestions on the model systems.

Additionally, I would like to thank current and former Kaminski lab members: Dr. Schuyler Pike, Dr. Peer Karmaus, Dr. Thitirat Ngaotepprutaram, Dr. Ale Manzan, Dr. Haitian Lu, Dr. Ashwini Phadnis-Moghe, Dr. Priya Raman, Dr. Collin North, Natasha Kovalova, Jose Suarez Martinez, Jinpeng Li, Bob Crawford, Kimberly Hambleton, Tony Bach, Shawna D'Ingillo, Sara Fox, and Sonia Dantas, for providing me a wonderful working environment, helping me with many aspects of my projects, and being great friends. I also want to express my appreciation to the Department of Microbiology & Molecular Genetics and Center for

Integrative Toxicology for giving me the opportunity to be part of the programs. They have been a great source of help and support all these years I have spent here.

Last but not least, I would like to thank my parents for bringing me up and giving their encouragement in my oversea study and life. Their love is always a major source of strength to me. I would also like to thank my husband Dr. Kezhen Huang for his encouragement, enduring love and support all these years, which have made me through my Ph.D. and will leave an everlasting impression in my life, and my baby girl Leah (Zixuan) for being such an angel and bringing so much love, happiness & joy to my life.

TABLE OF CONTENTS

LIST OF TABLES ix

LIST OF FIGURES x

KEY TO ABBREVIATIONS xiii

INTRODUCTION 1
I. Human Immunodeficiency Virus (HIV) 1
A. HIV Classification and Genome 1
B. HIV-1 Prevalence 2
C. HIV-1 Infection 3
II. Innate Immune Responses to HIV-1 4
A. Cytokines/Chemokines 4
B. DCs 5
C. NK Cells 5
III. Antigen Processing and Presentation 6
A. MHC I and MHC II Pathways 6
B. DC Maturation 8
IV. Adaptive Immune Responses to HIV-1 8
A. $CD8^+$ T Cell Responses 8
B. $CD4^+$ T Cell Responses 10
C. B Cell Mediated Immune Responses 11
D. Implications for Vaccine Development 12
V. T Cell Signaling Cascades 12
A. T Cell Activation Signaling Pathways 12
B. T Cell Stimulation *In Vitro* 14
VI. Cannabinoids and Cannabinoid Receptors 14
A. Cannabis Use 14
B. Cannabinoids 15
C. Pharmacokinetics of THC 18
D. Physiological Effects of THC 19
E. Toxicity of THC 19
F. Cannabinoid Receptors 20
1) CB_1 and CB_2 20
2) Signaling Events Associated with CB_1/ CB_2 21
3) Other Targets for Cannabinoid Ligands 25
VII. Cannabinoid and CB_1/ CB_2-Mediated Immune Modulation 26
A. T Cells 27
B. B Cells 29
C. NK Cells 30
D. APCs 31
E. *In Vivo* Host Resistance Models 32

F. Involvement of CB_1/ CB_2 in Cannabinoid-Mediated Immune Modulation 33
VIII. Rationale and Objectives 36

MATERIALS AND METHODS 39
I. Chemicals and Reagents 39
II. Mice 39
III. Cell Culture Conditions 40
IV. Lentiviral Plasmid Construction 40
V. $DC2.4_{gp120}$ and $EL4_{gp120}$ Cell Line Construction 43
VI. *In Vivo* Immunizations Using Plasmids 43
VII. Real Time PCR 44
VIII. Western Blotting Analysis 45
IX. Elicitation of Splenocytes with $DC2.4_{gp120}$ Cells 46
X. THC Treatment *In Vivo* 46
XI. Necropsy and Tissue Preparation 47
XII. Enumeration of Cytokine Secreting Cells by ELISPOT Assays 50
XIII. Cell Staining for Flow Cytometry 51
XIV. T Cell Purification 53
XV. ELISA 53
XVI. Calcium Determinations 54
XVII. Low Density Array Mouse Immune Panel 55
XVIII. Verification of Genotype 55
XIX. Statistical Analysis 56

EXPERIMENTAL RESULTS 58
I. *In Vitro* Cannabinoid-Mediated Effects on T Cell Response to HIV_{gp120} 58
A. Expression of gp120 mRNA and protein in transduced DC2.4 and EL4 clones . 58
B. Elicitation of gp120-specific $CD8^+$ T cell response 59
C. Differential effects of cannabinoids on $CD8^+$ T cell IFNγ production and proliferation 67
D. Differential effects of cannabinoids on IL-2 response 80
E. Differential effects of cannabinoids on cytokine production were correlated with effects on NFAT nuclear translocation 86
F. Cannabinoid enhanced intracellular calcium regardless of the magnitude of cellular activation 90
II. *In Vivo* Cannabinoid-Mediated Effects on Immune Responses to HIV_{gp120} 93
A. pVRCgp120 induced gp120-specific cytokine production by ELISPOT assay .. 93
B. pVRCgp120-induced T cell activation 97
C. pVRCgp120-induced activation on non-T cells 97
D. pVRCgp120-induced B cell responses 98
E. THC treatment enhanced pVRCgp120-induced IFNγ production by lymphocyte populations in the spleens of WT but not $CB_1^{-/-}CB_2^{-/-}$ mice 103
F. THC treatment enhanced pVRCgp120-induced activation of T cells in WT but not $CB_1^{-/-}CB_2^{-/-}$ mice 104
G. THC treatment enhanced pVRCgp120-induced B cell activation in WT but not $CB_1^{-/-}CB_2^{-/-}$ mice 109

H. THC treatment enhanced pVRCgp120-induced activation of non-T/non-B cells in WT but not $CB_1^{-/-}CB_2^{-/-}$ mice 109
I. THC modulated mRNA expression of genes induced by pVRCgp120 110

DISCUSSION 114
I. *In vitro* cannabinoid-mediated effects on T cell responses to HIV_{gp120} 114
II. *In vivo* cannabinoid-mediated effects on immune responses to HIV_{gp120} 119
III. Significance and concluding remarks 126

APPENDIX 131

BIBLIOGRAPHY 175

LIST OF TABLES

Table 1. Sequences of PCR primer/probe sets 42

Table 2. Differential gene expression in response to pVRCgp120 injection and THC treatment in WT and $CB_1^{-/-}CB_2^{-/-}$ mice 113

Table 3. Grafting amount and size of SNPs 150

Table 4. Grafting data from different size SNPs terminated with carboxylic acids 151

LIST OF FIGURES

Figure 1. Chemical structures of selected cannabinoids 17

Figure 2. Simplified signaling pathways associated with CB_1/CB_2 24

Figure 3. Experimental model of *in vitro* elicitation of gp120-specific T cells 48

Figure 4. Protocol for the administration of THC or CO into the mice immunized with pVRCgp120/pVRC2000 49

Figure 5. Plasmid cassette constructs for expression of gp120 and $puro^r$ in DC2.4 (top) or gp120 and neo^r in EL4 cells (bottom) 60

Figure 6. Expression of gp120 transcript and protein in transduced $DC2.4_{gp120}$ or $EL4_{gp120}$ clones 61

Figure 7. Proliferation of gp120-specific $CD8^+$ T cells was elicited in the *in vitro* model 63

Figure 8. gp120-specific IFNγ production by $CD8^+$ T cells was elicited in the *in vitro* model 64

Figure 9. Differentiation of gp120-specific $CD8^+$ T cells was elicited in the *in vitro* model 66

Figure 10. Differential effects of THC on IFNγ production 68

Figure 11. Differential effects of THC on $CD8^+$ T cell proliferation 71

Figure 12. THC-mediated effects on IFNγ response in a CB_1/CB_2-dependent manner 75

Figure 13. Effects of cannabinoids on IFNγ production in response to different stimuli 78

Figure 14. Effects of cannabinoids on IL-2 production in response to different stimuli 81

Figure 15. Enhancement of the IL-2 response by CBD in purified T cells 83

Figure 16. Enhancement of cytokine response by CBD in different cellular populations 84

Figure 17. Differential effects of CBD on IL-2 response in human PBMC 85

Figure 18. Cannabinoids differentially regulated IFNγ steady state mRNA expression 87

Figure 19. Cannabinoids differentially regulated IL-2 steady state mRNA expression 88

Figure 20. Cannabinoids differentially modulated nuclear translocation of NFAT2... 89

Figure 21. Cannabinoids increased intracellular calcium regardless of activation level 91

Figure 22. gp120-specific cytokine production by splenocytes 94

Figure 23. Identification of immunodominant gp120 peptide for restimulation 96

Figure 24. Activation of T cells in response to pVRCgp120 stimulation 99

Figure 25. Activation of non-T cells in response to gp120 antigen stimulation..... 100

Figure 26. B cell responses to pVRCgp120 stimulation..... 102

Figure 27. THC-mediated enhancement on gp120-specific IFNγ response in WT but not $CB_1^{-/-}CB_2^{-/-}$ mice..... 105

Figure 28. THC-mediated enhancement on gp120-specific T cell activation in WT but not $CB_1^{-/-}CB_2^{-/-}$ mice 107

Figure 29. THC-mediated enhancement on gp120-specific B cell activation in WT but not $CB_1^{-/-}CB_2^{-/-}$ mice 111

Figure 30. THC-mediated enhancement on gp120-specific non-T/non-B cell activation in WT but not $CB_1^{-/-}CB_2^{-/-}$ mice..... 112

Figure 31. Synthesis of different SNPs 142

Figure 32. Surface chemistry of modified SNPs with different functional groups and at different sizes 149

Figure 33. Aqueous dispersion stability of LTM40PTrg4PEG SNPs in *in vitro* culture media 153

Figure 34. Aqueous dispersion stability of SNPs with -OH functional group in *in vitro* culture media 154

Figure 35. Aqueous dispersion stability of SNPs with –NH2 functional group in *in vitro* culture media 155

Figure 36. Aqueous dispersion stability of SNPs with -COOH functional group in *in vitro* culture media 156

Figure 37. SIINFEKL concentration-dependent activation of $CD8^+$ T cell responses . 158

Figure 38. Enhancement by modified LTM40PTrg4PEG on $CD8^+$ T cell responses induced by a suboptimal concentration of SIINFEKL 163

Figure 39. Absence of enhancement by SNPs with different functional groups on $CD4^+$ T cell responses under suboptimal $OVA_{323-339}$ stimulation 165

Figure 40. Effect of -COOH SNPs at different sizes on $CD8^+$ T cell responses under suboptimal induction 167

KEY TO ABBREVIATIONS

2-AG	2-arachidonoyl glycerol
AC	adenylate cyclase
AEA	anandamide
AFC	antibody forming cell
Akt	activation of protein kinase B
AHR	airway hyperesponsiveness
AP-1	activator protein-1
APC	antigen presenting cell
ART	antiretroviral drug therapy
BALF	bronchoalveolar lavage fluid
BCS	bovine calf serum
bmDCs	bone marrow-derived DCs
BSA	bovine serum albumin
cAMP	cyclic adenosine 3’,5’-monophosphate
CB_1	cannabinoid receptor 1
CB_2	cannabinoid receptor 2
$CB_1^{-/-}CB_2^{-/-}$	CB_1 and CB_2 null
CBD	cannabidiol
CBN	cannabinol
CCR	chemokine co-receptor
CD40L	CD40 ligand
CNS	central nervous system

CO	corn oil
conA	concanavalin A
CRAC	calcium release-activated channels
CREB/ATF	cAMP-response element binding protein/activation transcription factor
CTL	cytotoxic T lymphocytes
DAG	diacylglycerol
DC	dendritic cell
$DC2.4_{gp120}$	gp120-expressing DC2.4 cells
DLS	dynamic light scattering
DYRK1A	dual-specificity tyrosine-phosphorylation regulated kinase 1A
$EL4_{gp120}$	gp120-expressing EL4 cells
ERK	extracellular signal-regulated kinases
FTIR	fourier transform infrared spectroscopy
$G\alpha_i$	inhibitory heterotrimeric G proteins
$G\alpha_s$	stimulatory heterotrimeric G proteins
GPCR	G protein-coupled receptor
GSK-3	glycogen synthase kinase-3
HIV	Human Immunodeficiency Virus
HLA	human leukocyte antigen
iCD3/CD28	immobilized anti-CD3 plus soluble anti-CD28 antibodies
IFN	interferon
i.m.	intramuscular
Io	ionomycin

IP_3	inositol trisphosphate
ITAMs	the immunoreceptor tyrosine-based activation motifs
JNK	c-Jun N-terminal kinases
KIR	killer cell immunoglobulin-like receptor
KO	knockout
K_V	the voltage-gated potassium channels
LN	lymph node
LPS	lipopolysaccaride
MAPK	mitogen-activated protein kinases
MCP-1	monocyte chemotactic protein-1
NEAA	non-essential amino acids
neo^r	neomycin resistance
NFAT	nuclear factor of activated T cells
NF-κB	nuclear factor kappa-light-chain-enhancer of activated B cells
NK	natural killer
NT	no treatment
OVA	ovalbumin
PBMC	peripheral blood mononuclear cells
PBS	phosphate buffered saline
pDC	plasmacytoid DCs
PEG	polyethylene glycol
P/I	PMA/Io
PIP_2	phosphatidylinositol 4,5-bisphosphate
PKA	protein kinase A

PMA	phorbol 12-myristate 13-acetate
PPAR	peroxisome proliferators-activated receptors
PTK	protein tyrosine kinase
$puro^r$	puromycin resistance
S	SIINFEKL
sCD3/CD28	soluble anti-CD3 plus soluble anti-CD28 antibodies
SEM	scanning electron microscopy
SIV	simian immunodeficiency virus
SNP	silica nanoparticle
sRBC	sheep red blood cell
STIM	stromal interaction molecule
TAP	transporters associated with antigen processing
TCR	T cell receptor
TEM	transmission electron microscopy
TGA	thermogravimetric analyses
THC	Δ^9-Tetrahydrocannabinol
TLR	toll-like receptors
TNF	tumor necrosis factor
TRPA1	transient receptor potential ankyrin 1
TRPC1	transient receptor potential canonical 1
TRPV1	transient receptor potential vanilloid 1
VH	vehicle
WT	wild-type

INTRODUCTION

I. Human Immunodeficiency Virus (HIV)

A. HIV Classification and Genome

HIV is a single-stranded (ss) RNA (positive-sense) virus, belonging to the retroviridae family. There are two known types of HIV, HIV-1 and HIV-2. HIV-1 is more infective and virulent, causing the majority of infections in the world, whereas HIV-2 is less infective upon exposure and mainly found in West Africa [1]. Therefore, only HIV-1 is discussed in this dissertation. HIV-1 viruses are divided into different groups, including the major group M, which is responsible for 90% of the infections worldwide. Group M viruses are further subdivided into various subtypes through A to K, also referred to as clades, based on their genome sequences [2]. Subtype B viruses are predominant in Western countries [2, 3].

HIV-1 genome contains nine identified genes, including *gag*, *pol*, *env*, *tat*, *rev*, *nef*, *vif*, *vpr*, and *vpu*, encoding a total of 19 proteins [4]. The structural proteins of the virus consist of Gag, protease, integrase, RNase H, reverse transcriptase, and envelope protein (Env), which have their particular functions. For example, the Gag protein, also called p55, consists of four smaller parts: the matrix (p17) responsible for particle stabilization [5] or nuclear transportation [6], the capsid (p24) to form the core of viral particles, the nucleocapsid (p9) involved in recognition of packaging signal [7], and p6 needed for interaction with Vpr protein [8]. In particular, the Env protein is cleaved to the transmembrane domain p41 and the surface protein gp120, which mediates the

entry of virus into target cells by interacting with the surface CD4 molecule as well as a chemokine co-receptor (CCR), CXCR4 or CCR5, depending on the viral tropism [9].

There are two regulatory proteins, including the transcriptional activator Tat involved in viral replication [10], and the RNA binding protein Rev associated with transportation of RNA from the nucleus to the cytoplasm [11].

In addition to the structural and regulatory proteins, HIV-1 genome also encodes the following accessory proteins. Nef protein is involved in decreasing surface CD4, major histocompatibility complex (MHC) I, and MHC II expression, therefore down-regulating T cell activation and increasing HIV-1 infectivity [12-14]. Vif protein is required for HIV-1 replication in some cells [15]. Vpr protein causes cell accumulation at the G2/M division [16]. Vpu protein is known to increase viral release from infected cells [17].

B. HIV-1 Prevalence

HIV-1 is associated with high mortality in the US. At the end of 2009, approximately 1.1 million people were infected with HIV-1 in the United States, and an estimation of half a million people have died due to acquired immune deficiency syndrome (AIDS) [18]. According to estimates by the Center for Disease Control, each year there are about 50,000 new HIV-1 infections in the United States, and an estimated 47,500 people were newly infected in 2010 (the most recent year that data are available) [19].

C. HIV-1 Infection

HIV-1 exposure mainly occurs through the mucosal route of transmission, including reproductive and gastrointestinal routes. Upon exposure in the mucosal tissues, the virus infects immune cells locally by interacting with CD4 receptor and a chemokine coreceptor, CCR5 or CXCR4 [20]. CCR5-tropic HIV-1 viruses are the predominant ones in chronically infected patients [21]. Since it is impossible to study the physiological events in the early stage of HIV-1 infection in humans *in vivo*, simian immunodeficiency virus (SIV) infection in rhesus macaque monkeys has been used as a model system to provide a fundamental understanding of HIV infection. $CD4^+$ T cells have been demonstrated as the major initial targets for SIV replication in the lymphoid tissue in the mucosa [22].

Free virus and/or virus-infected cells then travel to the other lymphoid tissues where they further infect more immune cells, including $CD4^+$ T cells, dendritic cells (DC), and macrophages. In the acute phase of HIV-1 infection, the viral load increases exponentially to reach a peak by 2-3 weeks, which accompanies a dramatic decrease of $CD4^+$ T cell counts, establishing a pool of latently infected $CD4^+$ T cells [23]. Meanwhile, HIV-1 specific immune responses are developed (see below), followed by a decrease of viremia and a partial recovery of peripheral blood $CD4^+$ T cell counts [24]. The viral load falls over the next 3-5 months to reach a stable level, known as the viral set point [25], which determines the intensity, the magnitude, and the kinetics of disease progression in the chronic infection stage in the absence of antiretroviral drug therapy (ART). Over the next 10 years, the $CD4^+$ T cell numbers

slowly decrease and the viremia slowly increases, along with any potentially opportunistic tumors and viral infections in the AIDS patients [26, 27].

Upon entry into host cells, HIV-1 viral RNA is reverse transcribed by the reverse transcriptase into double-stranded cDNA, which is then transported into the cell nucleus and integrated into the DNA genome of host cells by the viral integrase [28]. Upon integration, the virus may become latent to protect itself and the host cells from being detected by the immune system [28]. The integrated DNA provirus can also be transcribed in activated T cells, making new RNA and viral proteins that are packaged into new viruses [29, 30]. During the replication process, HIV-1 virus mutates rapidly, which makes the virus highly genetically-variable and thus increases the difficulty of developing HIV-1 vaccines [31].

II. Innate Immune Responses to HIV-1

A. Cytokines/Chemokines

When there is HIV-1 infection, the innate immune response is the first line of defense. As the plasma viremia increases, toll-like receptors (TLRs), which recognize viral RNAs and proteins [32], are activated, leading to the production of acute-phase cytokines and chemokines. Type I interferons (IFNs), such as IFNα, interleukin-15 (IL-15), and CXC-chemokine ligand 10 (CXCL10) are produced rapidly upon infection, followed by production of tumor necrosis factor (TNF) α, IFNγ, and IL-18, and IL-10 [33]. Type I IFNs are known to have antiviral activities by inhibiting HIV replication [34]. Type I IFNs, IL-15, and IL-18 can also enhance innate and adaptive

immune responses. During the acute phase of HIV-1 infection, cytokines and chemokines can be produced by infected $CD4^+$ T cells, DCs, monocytes, macrophages, natural killer (NK) cells, and NKT cells [35].

B. DCs

DCs and macrophages were demonstrated to be infected either through the $CD4^+CCR5^+$ route or through the DC-specific intracellular adhesion molecule-3-grabbing non-integrin (also known as CD209) receptor on the cell surface [36]. In particular, plasmacytoid DCs (pDCs) were shown to be activated in response to HIV-1 infection, which led to activation of TLR7 by viral ssRNA [37] as well as production of IFNα to inhibit HIV-1 replication and promote $CD4^+$ T cell expansion [38, 39]. Infected conventional DCs were found to further activate $CD4^+$ and $CD8^+$ T cells in the adaptive immune responses [40].

C. NK Cells

NK cells also play an important role in controlling HIV viremia during acute infection. NK cells are activated by pro-inflammatory cytokines secreted by DCs and monocytes, including IL-15 and IFNα [41]. Depending on the functionality of killer cell immunoglobulin-like receptors (KIRs), NK cells might have activating or inhibitory functions on HIV-1 replication. For example, NK cells that expressed the activating receptor KIR3DS1 binding to its human leukocyte antigen (HLA) class I ligands, HLA class I molecules of the HLA-Bw4-80I family, were found to inhibit

HIV-1 replication in $CD4^+$ T cells [42] and therefore slowed down HIV-1 disease progression [43]. In contrast, expression of inhibitory receptor KIR3DL1 in combination with the same HLA family as mentioned above by NK cells might have an opposite effect [44]. In addition, NK cells can also secrete antiviral cytokines and chemokines as well as cytotoxic granules that mediate the antiviral activities to further induce apoptosis of infected cells. Furthermore, NK cells were demonstrated to eliminate immature DCs, therefore leaving the mature DCs to induce antiviral T cell responses [45].

III. Antigen Processing and Presentation

A. MHC I and MHC II Pathways

Antigen presentation links the innate and adaptive immune responses. As reviewed by Cresswell et al. [46], endogenous antigens are usually presented by MHC I molecules, whereas exogenous antigens are presented by MHC II molecules. However, exceptions exist under certain conditions (see below). Endogenous antigens, including viral proteins, intracellular bacteria, tumor antigens, and misfolded proteins, are escorted to the proteasome after ubiquitin tagging and are processed into peptide fragments in the cytosol. These antigenic fragments are then transported to the endoplasmic reticulum (ER) by transporters associated with antigen processing (TAP) to be further trimmed by ER aminopeptidases (ERAPs) to peptides of 8-10 amino acids in length and loaded onto MHC I molecules. This process is coordinated by the peptide-loading complex that contains several proteins. Finally, peptide-loaded

MHC I complexes are exported to the cell surface to allow for immune surveillance by $CD8^+$ T cells. On the other hand, exogenous antigens, such as extracellular bacteria, parasitic worms, and free viruses, are endocytosed by antigen presenting cells (APCs). The endosome compartments fuse with lysosomes where the antigens are processed to fragments that are further degraded to peptides (~13-18 amino acids) by proteases in the lysosome MHC class II compartment (MIIC). Meanwhile, MHC II molecules assembled in ER traffic to MIIC where the invariant chain (li) is cleaved to class II-associated li peptide (CLIP) in the peptide-binding groove prior to binding with high affinity-peptides. Then antigenic peptides bind to MHC II molecules, which are transported to the cell surface to allow for immune surveillance by $CD4^+$ T cells (as reviewed in [47]). All nucleated cells express MHC I molecules, whereas only professional APCs, such as DC, macrophages, and B cells, express MHC II molecules. There are exceptions that extracellular antigens taken up via endosomes may be retrotranslocated into the cytosol and presented on MHC I molecules by some DC and macrophages, referred to as cross-presentation [46]. In addition, endogenously expressed proteins may traffic to the MIIC through autophagy for presenting on the MHC II molecules [48]. In the case of HIV-1 infection, viral proteins are processed to antigenic peptides in the APCs, which will then be presented in the context of MHC I and II molecules to be recognized by $CD8^+$ and $CD4^+$ T cells, respectively.

B. DC Maturation

DCs have been demonstrated to be more effective to present antigens to naïve T cells than other APCs [49]. Upon capturing antigens, DCs mature and migrate to lymphoid tissues to activate T cells. DC maturation involves up-regulation of MHC I and II molecules, co-stimulatory molecules, CD80 and CD86, and changes in cell morphology [49]. Proinflammatory cytokines TNF-α, IL-1, IL-6, type I and type II interferons, and pathogen-associated molecules, such as ssRNA, dsRNA, and lipopolysaccaride (LPS) are known to induce DC maturation [49].

IV. Adaptive Immune Responses to HIV-1

A. $CD8^+$ T Cell Responses

As the viremia increases to the peak level, HIV-specific $CD8^+$ T cells develope. T cells are activated upon the engagement of interactions between T cell receptor (TCR) and antigen-MHC complexes on APCs. The co-stimulatory signal from the binding of CD28 on T cells by CD80 and CD86 on APCs is also required for T cell activation (see below). Once T cells are activated, they clonally expand and differentiate to effector T cells. Virus-specific cytotoxic T lymphocytes (CTLs) can recognize HIV-infected cells presenting MHC I-restricted peptides on cell surface, and eliminate infected cells. Therefore, clearance of virus in the acute infection stage correlates with the appearance of HIV-specific CTLs [50]. CTLs produce and release granules containing cytolytic proteins, such as perforin and granzymes. Upon degranulation, they directly act on target cells presenting the same antigens and induce apoptosis of

target cells [51, 52]. An alternative route of triggering target cell apoptosis is mediated through the interaction between FasL on CTLs and Fas on infected target cells [53]. In addition, cytokines, such as IFNγ, TNF-α, and IL-2, secreted by CTLs following recognition of target epitopes, can promote the cytolytic activity of CTLs and help maintain the growth, differentiation and survival of CTL [51, 52]. Moreover, CTLs can secret chemokines, such as MIP-1α, MIP-1β, and RANTES, which can bind to the CCR5 coreceptor on infected cells, therefore destroying the entry of viruses, and also facilitate the cytolytic activity of CTLs among other functions [54]. Recently, presence of multifunctional $CD8^+$ T cells, which possess more than two functions simultaneously, including cytokine/chemokine production and degranulation, was detected in HIV elite controllers coincident with low viremia in the plasma [55]. Collectively, CTLs play a critical role in controlling HIV, resulting in a decrease of viral load in the plasma until reaching the set point in the acute phase of HIV infection. A more robust immune response after acute infection will lead to a lower viral set point, which might slow the disease progression to AIDS. Thus, the viral set point is an important indicator of the initial immune responses as well as the longer-term prognosis of the patient.

Although CTL induction helps to set a low viral set point, the virus sequence still mutates rapidly at multiple epitopes in order to escape from the recognition by $CD8^+$ T cells [56, 57]. Changes in amino acid sequence were often found to occur upstream of the sequence that could be recognized by T cells, and were suggested to be involved in antigen processing [58, 59]. T cell responses elicited against Env and Nef proteins in particular were indicated to control early viremia, while T cell responses against

other viral proteins, such as Gag and Pol, were more involved in maintaining the viral set point [56, 60]. Once the escape mutants were selected, the magnitude of the initial T cell responses decreased [56]. A lower viral set point was observed when T cell responses were induced against immunodominant viral epitopes [61]. In addition, it has been suggested that $CD8^+$ T cell responses to conserved epitopes played a more important role in long-term control of HIV-1 infection [56, 62].

B. $CD4^+$ T Cell Responses

Naïve $CD4^+$ T cells upon activation can proliferate and differentiate to T helper cells. Typically, $CD4^+$ T helper cells can produce various soluble mediators, including cytokines and chemokines. Th1 cytokines, such as IL-2 and IFNγ, are secreted to maintain effective CTL functions (Th1 response). Th2 cytokines, such as IL-4, IL-5, IL-6, and IL-10, are secreted to assist in the humoral response (Th2 response). Particularly among patients with HIV infection, stronger CD4 responses were correlated with lower viral loads, whereas weaker CD4 responses were correlated with higher viral loads [63]. CD4 responses in HIV antiviral immunity were determined by measuring $CD4^+$ T cell proliferation as well as production of IFNγ [63]. In addition to IFNγ, production of other cytokines, such as TNF-α and IL-2, or chemokines, such as RANTES, MIP-1α, and MIP-1β, by $CD4^+$ T cells derived from peripheral blood mononuclear cells (PBMCs) of HIV patients in response to HIV antigens *in vitro*, was also detected [63-65]. Moreover, stronger CD4 helper responses

were demonstrated to correlate with stronger CTL responses [66]. Since $CD4^+$ T cells are targets of HIV infection, loss of $CD4^+$ T cells is rapid due to a combination of direct viral killing, increased rate of apoptosis, and CTL killing of infected cells. However, the $CD4^+$ T cell arm is still partially functional according to above investigations. Due to activation and proliferation of $CD4^+$ T cells, more cellular targets for HIV will be produced, which will further induce more HIV specific T cell responses [23, 67].

C. B Cell Mediated Immune Responses

B cells also provide protection against HIV-1 by producing neutralizing antibodies, which have been demonstrated to block the interaction between the virus and the cellular receptors to prevent virus from entry into the cells [68]. B cell activation requires $CD4^+$ T helper cells for providing the necessary signals, including one signal from cross-linking the antigens and the other signal from co-stimulation between CD40 ligand on T cells and CD40 on B cells, therefore the B cell response is usually delayed compared to other leukocytes [69]. Once B cells differentiate into plasma cells, they first produce IgM, and after affinity maturation through somatic hypermutation they undergo class switching to IgG and IgA [70]. Neutralizing antibodies against autologous virus have been shown to develop slowly, approximately 12 weeks or longer after HIV-1 transmission, and antibodies against heterologous virus were only effective in about 20% of the patients years after infection [71, 72]. In addition, neutralizing antibodies induced in clade B or clade C

HIV-1 infections were found to be specific only for the initial transmitted virus isolates [71, 73, 74]. Thus broadly reactive neutralizing antibodies are rarely generated.

D. Implications for Vaccine Development

In vaccine research, the focus of vaccine development against HIV-1 (the most common and pathogenic strain) is to induce both antigen-specific T cell responses and neutralizing antibodies [75-77]. $CD8^+$ T cells play an important role on controlling the virus in the early stage of HIV-1 infection, when the immune system is still functionally normal. An effective vaccine would be expected to induce $CD8^+$ T cell responses to multiple epitopes, especially to those that are conserved among different virus variants [78, 79]. In addition, broadly reactive antibodies need to be generated, which can target multiple neutralizing epitopes and induce a rapid secondary response.

V. T Cell Signaling Cascades

A. T Cell Activation Signaling Pathways

T cells are activated via two signals, including the first signal mediated through TCR and the second signal mediated through the costimulatory molecule CD28, which then activate the cytosolic protein tyrosine kinases (PTKs), such as Lck and Fyn, to further phosphorylate the immunoreceptor tyrosine-based activation motifs (ITAMs) on the cytosolic side of the CD3 domain in the TCR complex (reviewed in [80]). Subsequently, zeta-chain associated protein kinase (Zap-70) is recruited to the

TCR/CD3 complex by ITAMs, and phosphorylated Zap-70 will further phosphorylate the downstream adaptor or scaffold proteins. Phospholipase C γ1 (PLCγ1) is phosphorylated, leading to hydrolysis of phosphatidylinositol 4,5-bisphosphate (PIP_2) to produce the second messengers, diacylglycerol (DAG) and inositol trisphosphate (IP_3). DAG activates PKCθ and the mitogen-activated protein kinase (MAPK) pathways, which activate the transcription factor nuclear factor kappa-light-chain-enhancer of activated B cells (NF-κB) (reviewed in [81]), while IP3 induces intracellular Ca^{2+} release from the ER, which causes extracellular Ca^{2+} to be transported into cells via the calcium release-activated channels (CRAC). Ca^{2+}-bound calmodulin activates the phosphatase calcineurin, which results in activation of transcription factors, including nuclear factor of activated T cells (NFAT), NF-κB, and activator protein-1 (AP-1), with NFAT being the main target of the Ca^{2+} signaling (reviewed in [82]). On the other hand, ligation of CD28 leads to activation of phosphoinositide 3-kinase (PI3K), which converts PIP_2 to phosphatidylinositol 3,4,5-trisphosphate (PIP_3) resulting in activation of protein kinase B (Akt) (reviewed in [83]). Phosphorylated Akt inhibits glycogen synthase kinase-3 (GSK-3) from phosphorylating NFAT, and thereby promotes its nuclear translocation [84]. In addition, CD28 activates JNK pathway to phosphorylate transcription factors such as JUN and AP-1 [85]. Activation of the above transcription factors leads to increased expression of regulated genes, including cytokines and chemokines, such as IL-2, IFNγ and TNFα [86, 87].

B. T Cell Stimulation *In Vitro*

Traditionally, T cells can be activated *in vitro* using pharmacological stimuli such as the phorbol ester, phorbol 12-myristate 13-acetate (PMA), in combination with the ionophore, ionomycin (Io). PMA can directly activate PKC bypassing the ligation of TCR [88, 89], while Io can directly increase the level of intracellular Ca^{2+} [90]. In addition, a more physiologically relevant approach is used by stimulating T cells with anti-CD3 and anti-CD28 antibodies, which activates T cells through the TCR/CD28 signaling pathways.

VI. Cannabinoids and Cannabinoid Receptors

A. Cannabis Use

Despite legal restriction, cannabis, also known as marijuana, is used for recreational purposes. More than 100 million Americans have tried cannabis at least once, and use of cannabis has increased particularly among young adults aged 18 to 25, about 21% of whom report using of marijuana every month [91]. Cannabis intoxication leads to relaxation, sleepiness, and mild euphoria (getting high), but might also increase the incidence of possible health issues, such as schizophrenia or depression [92]. As of 2013 in the US, 20 states and the District of Columbia, including Michigan in 2008, have legalized marijuana use for medical purposes. Medical marijuana is used in cancer patients to reduce nausea, vomiting, and pain that are associated with chemotherapy [93]. In addition, marijuana is also used by

approximately 25% of AIDS patients to stimulate appetite and ameliorate HIV-associated nausea, pain and wasting syndrome [94, 95]. However, effects of marijuana-derived compounds on immune function of these immunocompromised patients are still not well understood, which has led to our research interests.

B. Cannabinoids

Cannabinoids are a group of compounds originally extracted from the cannabis plant. Δ^9-Tetrahydrocannabinol (THC) is the main psychoactive constituent among over 60 structurally-related congeners in the cannabis plant [96]. It is lipophilic and has a tricyclic ring structure, which contains a phenol ring with a 5-carbon alkyl chain, a central dihydrobenzopyran ring, and a mono-unsaturated cyclohexyl ring (Fig. 1) (see [97] for review). These terpenophenolic compounds are primarily produced by the female plants from their glandular trichomes [98]. In addition to THC, cannabidiol (CBD) and cannabinol (CBN) are also well studied compared with the other constituents. CBD is highly abundant in the fresh plant, making up about 40% of the whole extract, and CBN is the primary product during THC oxidation [99]. These phytocannabinoids exhibit varying binding affinities to the two identified cannabinoid receptors, cannabinoid receptor 1 (CB_1) and 2 (CB_2). For instance, THC exhibits similar affinity to CB_1 and CB_2 and is psychotropic, whereas CBD exhibits weak affinity to both receptors and is therefore, not psychotropic. CBN has weak affinity to CB_1, but high affinity to CB_2, which is still lower compared with THC, and therefore has little psychotropic activity [100-102].

In addition to the plant-derived cannabinoids, there are endogenously produced cannabinoids by humans and animals, also known as endocannabinoids, which are ligands for CB_1 and/or CB_2 [103]. Two well-characterized endocannabinoids are N-arachidonoylethanolamine or anandamide (AEA) and 2-arachidonoyl glycerol (2-AG) (Fig. 1). AEA is different in chemical structure from THC and is converted to the arachidonic acid, which is one of the most abundant fatty acid in the brain, by fatty acid amide hydrolase (FAAH). AEA exhibits affinity to CB_1 and, to a lesser extent, CB_2, whereas 2-AG binds to CB_1 and CB_2 with similar affinity [104]. Endocannabinoids are synthesized upon demand and function by maintaining homeostasis in the body related to neuronal system, immune system, metabolism, and energy [105].

The third category of cannabinoids is synthetic cannabinoids. These are the compounds produced in laboratories and structurally-related to the phytocannabinoids or having binding affinities to CB_1 and/or CB_2. For example, Dronabinol (Marinol®) is synthetic THC, a drug approved by FDA to be used in cancer and AIDS patients for treating appetite loss, nausea, vomiting and pain [106]. Cyclohexylphenol (CP) 55,940, developed by Pfizer in the 1970s, and HU-210, developed by Raphael Mechoulam at the Hebrew University in the 1960s, are two other representative synthetic cannabinoids, which have structural similarity to THC, but possess more potency than THC [107] (Fig. 1). WIN 55,212-2 is another example of synthetic cannabinoid (Fig. 1), the non-classical prototypic aminoalkylindole cannabinoid, which is functionally similar but structurally different to THC [108].

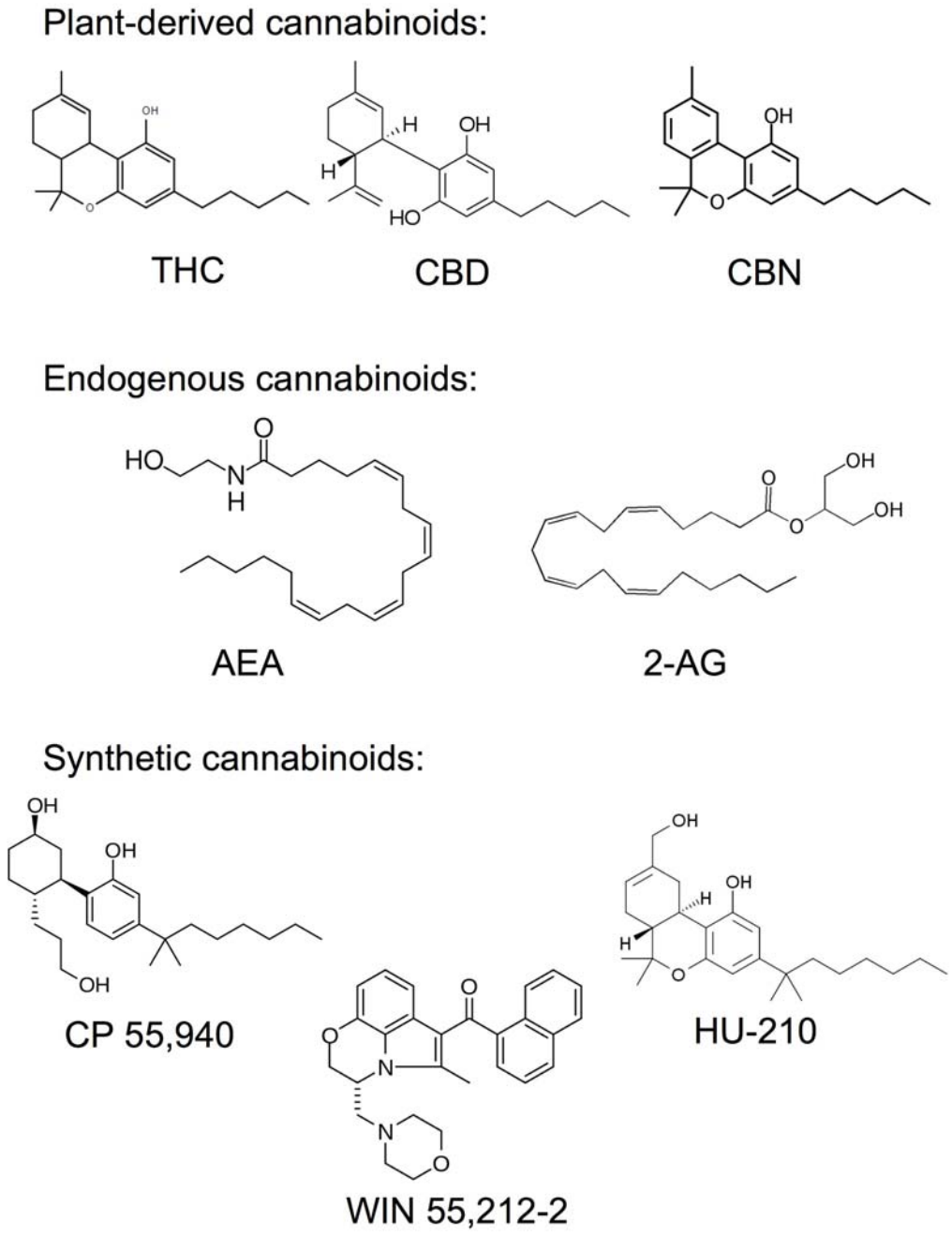

Figure 1. Chemical structures of selected cannabinoids.

C. Pharmacokinetics of THC

Cannabis products are usually administered by two main routes, inhalation or oral consumption, and therefore the pharmacokinetic profile of THC is different. With inhalation by smoking cannabis cigarettes, THC is absorbed through the lungs and rapidly reaches the bloodstream and the brain within minutes [109]. The bioavailability of THC in the plasma ranged between 10 to 35%, depending on the number of puffs and the extent of breath holding during smoking [109, 110]. On the other hand, the absorption of THC after oral use is very slow, and peak plasma concentration reached up to 6 hours post administration, so the bioavailability of THC is less than when using the same amount for inhalation [111]. Within the low pH environment of the stomach and the gut, THC was found to degrade to CBD [112].

The plasma concentration of THC decreases as THC rapidly distributes to various tissues including liver, heart, lung, kidney, spleen, thyroid, fat, and pituitary glands, but only about 1% distributes to the brain [113]. Since THC is highly lipophilic, the tissue clearance half-life of THC was found to take about 7 days, and complete clearance after a single dose might take up to 30 days [114]. Further metabolism of THC mainly happens in the liver where it is hydroxylated and oxidized by the enzymes of the cytochrome P450 (CYP) complex, [115, 116]. The major metabolite after THC hydroxylation in humans is 11-OH-THC, and subsequent oxidation produces THC-COOH, which may be glucuronidated to 11-nor-9-carboxy-THC glucuronide [117]. In addition, 11-OH-THC may also be conjugated with fatty acids to be stored in tissues [118].

D. Physiological Effects of THC

THC has modulatory effects on various physiological systems, as reviewed in [119, 120]. For example, THC can lead to euphoria, anxiety, dysphoria, and increased sensory perception. The effect of THC on the cognition and motor functions may include fragmented thinking, disturbed memory, ataxia, and slurred speech. THC may also cause muscle relaxation, appetite stimulation, analgesia, and neuroprotection in hypoxia in the nervous system. In addition, THC may trigger hypertension, vasodilation, and enhanced heart rate in the cardiovascular system. Moreover, impaired cell-mediated and humoral immune responses have been demonstrated to be mediated by THC (see below for details). Furthermore, growth retardation, and impairment of fetal development might be associated with THC use as well.

E. Toxicity of THC

Studies have been conducted to compare acute oral toxicity of THC in different species. In rats, oral THC resulted in a median lethal dose (LD_{50}) of 800-1900 mg/kg. In dogs and monkeys, oral THC at doses up to 3000 mg/kg and 9000 mg/kg, respectively, did not induce any fatality, but animals showed symptoms of drowsiness and ataxia [121]. In humans, no fatal cases have been demonstrated due to toxicity following acute THC treatment; however, death might be induced due to THC-triggered myocardial infarction [122, 123]. The harmful effects of medical marijuana use are suggested to include impaired cognition, decreased motor function, and cardiovascular diseases, such as hypertension and vasodilation, but these adverse effects are considered minimal or comparable to the adverse effects caused by other

medications [124, 125]. Whether long-term use of cannabis could cause any physical or cognitive dysfunction is still controversial, which might depend on the existing health condition of the individuals.

F. Cannabinoid Receptors

1) CB_1 and CB_2

Both CB_1 and CB_2 are $G_{i/o}$ protein-coupled receptors (GPCR) [97]. CB_1 was originally cloned from rat cerebral cortex [102], and its human homolog was identified soon after [126]. The amino acid sequence of CB_1 is very conserved among different mammalian species, with 81% homology between human and rat, and 93% homology between rat and mouse [101, 127-129]. CB_1 is expressed throughout the body, but mainly expressed in the central nervous system (CNS), including cerebellum, hippocampus, and basal ganglia, to suppress the release of various neurotransmitters that are associated with multiple functions, such as cognition, memory, motor and metabolism [97, 130]. The psychotropic effect of THC is mediated through CB_1 [102]. CB_2 was originally cloned from HL60 after CB_1 was identified [101]. The amino acid sequence of human CB_2 shares 44% homology with CB_1 [101]. CB_2 is predominantly expressed in the periphery, including the immune system [101], and was recently found in neurons and glial cells of the CNS [131, 132]. In the immune system, CB_2 expression is higher than CB_1, with human B cells having the highest mRNA levels of CB_2 than the other immune cells, including NK cells, monocytes,

neutrophils, $CD4^+$ T cells, and $CD8^+$ T cells [133, 134]. In addition, the expression levels of CB_1 and CB_2 can be altered under certain conditions. For example, CB_1 mRNA expression was up-regulated in activated human T cell line [135], whereas CB_1 mRNA and protein levels were down-regulated during B cell differentiation [136].

2) Signaling Events Associated with CB_1/CB_2

As members of the GPCR family, cannabinoid receptors have the transmembrane structure with seven α-helices, an extracellular glycosylated N-terminus, and an intracellular C-terminus [101, 102]. Both CB_1 and CB_2 are known to couple to $G_{i/o}$ proteins, but they might have differential binding affinities. For example, human CB_1 expressed in *Spodoptera frugiperda* cells showed similar binding affinity to G_i and G_o proteins (the pertussis toxin sensitive G proteins), whereas CB_2 was only found to bind to G_i protein [137]. G_i is known as an inhibitory G protein to activate downstream signaling events (see below), and G_o is a similar protein in the G_i class, but its function is yet to be determined. In addition, the nature of the ligands for CB_1 and CB_2 determine the magnitude of $G_{i/o}$ protein activation. For example, THC partially activated G_i protein through CB_1; however WIN 55,212-2, HU-210, and AEA induced CB_1-mediated activation of G_i to a much higher extent [137]. On the

other hand, HU-210 was the only agonist that could elicit CB_2-mediated G_i activation to the maximal level.

It has been demonstrated that stimulation of $G_{i/o}$ protein by cannabinoids inhibited the activity of adenylate cyclase (AC), which decreased the levels of intracellular cyclic adenosine 3',5'-monophosphate (cAMP) [134, 138]. The schematic description of signaling events mediated by CB_1 and CB_2 is illustrated in Fig. 2. The level of cAMP is critical for activation of protein kinase A (PKA) to further phosphorylate the cAMP-response element binding protein/activation transcription factor (CREB/ATF) family of transcription regulators, including CREB, ATF, and cAMP response element modulator (CREM) [138]. CREB is the best studied among the three transcription factors, and it could associate with other transcription factors for binding to cAMP regulatory element (CRE) DNA sequences in the promoter region of various genes [139, 140]. In fact, cannabinoids were demonstrated to inhibit PKA activity and the binding of CREB/ATF to CRE [140]. In addition, CREB might form heterodimers with transcription factors in the Fos and Jun family to bind to the promoter region of inducible regulatory factors, such as AP-1 [141, 142].

CBN was shown to suppress PMA/Io-induced CREB binding at the AP-1 proximal site in the IL-2 promoter region, which inhibited IL-2 expression [140]. Furthermore, cannabinoids, including THC, were found to increase intracellular Ca^{2+} levels in resting splenic T cells, which was further enhanced in activated splenocytes potentially mediated through the calcium channel TRPC1 [143, 144]. CBN was shown to inhibit the activation of ERK MAPK, which functions downstream of the

calcium signaling pathways [145]. Moreover, it has also been reported that PKA can phosphorylate IκB, resulting in dissociation of IκB from NFκB, to facilitate NFκB activation and its bind to the NFκB site in the promoter region of various genes, such as IL-2 [146]. By extension, suppression of PKA activity by cannabinoids might represent a mechanism that could explain impairment of NFκB.

In addition to binding to $G_{i/o}$ proteins, studies have shown that under certain conditions cannabinoid receptors could also interact with the stimulatory G protein, G_S, which in turn increased AC activity upon CB agonist binding. It was shown that pertussis toxin treatment of CB_1 attenuated HU-210-mediated inhibition of AC activity to increase cAMP accumulation and unmasked an agonist-mediated stimulation of the enzyme in the presence of a costimulant such as forskolin [147, 148]. WIN 55,212-2 at high concentrations was found to increase cAMP accumulation in the absence of pertussis toxin or costimulant, which was blocked by CB_1 antagonist SR141716A [149]. It is still unclear whether CB_1 simultaneously binds to G_S and G_i proteins or different populations of CBs are involved. In addition, different AC isoforms have also been suggested to contribute to the differential effects mediated by cannabinoids. Activation of the cannabinoid receptors CB_1 or CB_2 by the agonists, HU-210 and WIN 55,212-2, inhibited the activity of AC isoforms I, III, V, VI, and VIII, whereas activation of CB_1 and CB_2 by cannabinoids stimulated the activity of AC isoforms II, IV, and VII [150].

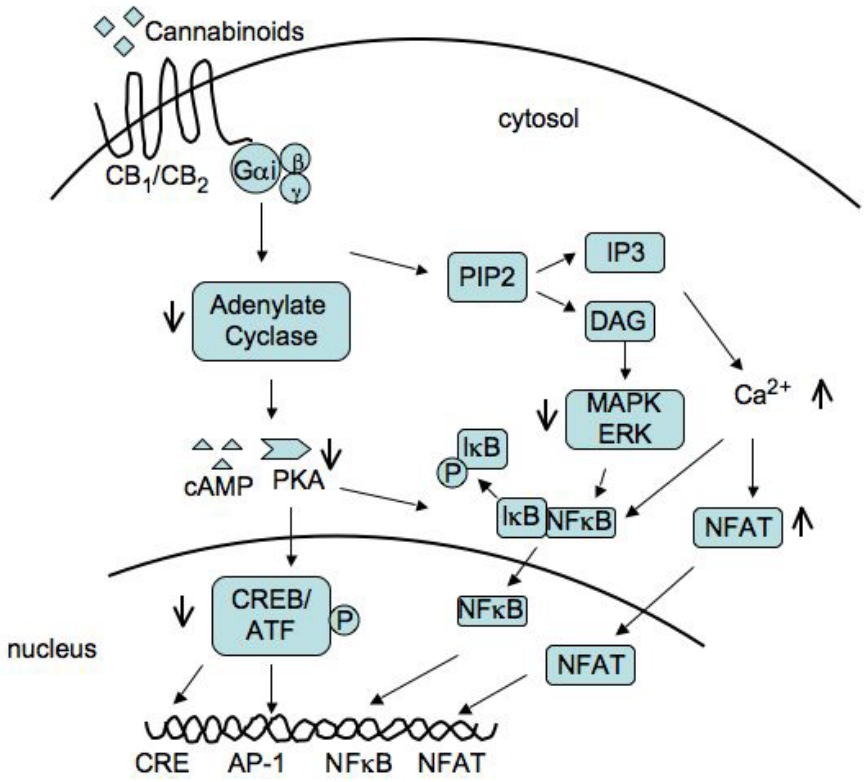

Figure 2. Simplified signaling pathways associated with CB_1/CB_2.

3) Other Targets for Cannabinoid Ligands

It has been demonstrated that some effects of cannabinoids are not mediated through CB_1 or CB_2, suggesting the existence of other targets for cannabinoid ligands, which are classified as nonclassical cannabinoid receptors.

The established targets include GPCRs, ion channels and nuclear receptors. For example, orphan GPCRs, such as GPR18, GPR55, and, GPR119, have recently been found to interact with phytocannabinoids, endocannabinoids, or synthetic cannabinoids, although the functions of these GPCRs remain unclear [107]. GPR55 shares low amino acid sequence similarity to CB_1 (13.5%) and CB_2 (14.4%), and it is most closely related to lysophosphatidic acid (LPA) receptors (30% similarity) [151, 152]. GPR55 has been shown to couple with $G_{\alpha 13}$, G_q, G_{12}, or G_{13}, which activate GTPase RhoA and PLC for signal transduction, and therefore affect intracellular Ca^{2+}, actin cytoskeleton, and growth of neural pathways (reviewed in [97]). THC and N-arachidonoyl glycine have been shown as ligands of GPR18 to affect intracellular Ca^{2+} mobilization [153]. Oleylethanolamide (OEA) has high affinity for GPR119, which is involved in controlling glucose-dependent insulin release in the pancreatic tissues [154].

In addition, the transient receptor potential vanilloid 1 (TRPV1) has been reported to interact with AEA, N-arachidonoyl dopamine, and a lower affinity with CBD, but not 2-AG. These agonists affect intracellular Ca^{2+} levels, cation currents in the neurons, and release of vasodilatory peptides from sensory neurons [155, 156]. Apart

from TRPV1, other TRPV channels and other TRP channels, such as TRPV2, -3, -4, -5, -6, TRP ankyrin 1 (TRPA1), TRP canonical 1 (TRPC1) have also showed evidence of being activated by cannabinoids (reviewed in [97]). Moreover, endogenous cannabinoids, such as AEA, can activate calcium, potassium, and sodium channels (reviewed in [97]).

Other than the putative receptors described above, peroxisome proliferators-activated receptors (PPARs) have been found to interact with endocannabinoids, phytocannabinoids, and synthetic cannabinoids, such as AEA, 2-AG, THC, and WIN55212 (review in [97]). For examples, 2-AG was found to suppress IL-2 production through impairment of NFAT activity, due to binding of a putative cyclooxygenase (COX)-2 metabolite of 2-AG, 15-deoxy-Δ12,14-prostaglandin J2-glcyerol ester, to PPARγ receptor [157, 158]. So far, there is not enough evidence indicating these other receptors or channels as identified cannabinoid receptors, so they are considered as putative targets for cannabinoid ligands, and therefore, further investigations are needed.

VII. Cannabinoid and CB_1/CB_2-Mediated Immune Modulation

Over forty years of studies have demonstrated that THC possesses broad modulatory effects on the immune system in a CB_1/CB_2-dependent and -independent manner. In this section, the effects of THC and the role of CB_1/CB_2 on multiple immune cell populations will be discussed.

A. T Cells

T cells have been demonstrated as one of the most sensitive targets of cannabinoids. THC has been demonstrated to modulate various T cell functions, including T cell activation, proliferation, and production of cytokines. For example, THC and other cannabinoids were found to suppress mitogen-induced T cell activation, proliferation, and production of IL-2, IFNγ, and other cytokines [140, 159-162]. In addition, inhibition of DNA binding activity of transcription factors regulating IL-2, e.g. NFAT and AP-1, as well as temporal dysregulation of intracellular Ca^{2+} signaling in resting T cells by THC or CBN have been suggested, at least in part, as mechanisms for cytokine suppression [143, 144, 159, 161, 163].

Effects of THC on CTL functions as well as the associated mechanisms have also been extensively studied. For example, cytolytic function of CTLs was reduced by THC and 11-OH-THC in response to allogeneic or 2,4,6-trinitrophenyl (TNP)-modified stimulators *in vivo* and *in vitro*, which was due to suppression of differentiation and maturation of precursor $CD8^{+}$ T cells or cytolytic activity of CTL after binding to the target cells [164]. Moreover, CTL activity to herpes simplex virus type 1 (HSV1)-infected cells as well as CTL cytoplasmic polarization toward the infected target cells were suppressed by THC [165]. Furthermore, kinetic and time of addition studies indicated that the effect of THC on T cell functions occurred in the early stage during activation [166]. This was consistent with a recent finding using an *in vitro* P815 allogeneic model to elicit CTL responses based on MHC mismatch, which revealed that THC suppressed CTL activation, cytolytic activity, and IFNγ production, when present during the elicitation phase but not the effector phase [167].

Likewise, $CD4^+$ T cell-derived cytokine production was modulated by THC and other cannabinoids. *In vivo*, both acute and chronic THC treatment in mice was found to cause a decrease in serum IL-2 and IFNγ levels as well as the number of T cells [168]. In addition, with allogeneic DC stimulation *in vitro*, T cell proliferation and Th1 cytokine (IFNγ, IL-2) production were suppressed by THC, but Th2 cytokine (IL-4, IL-5) expression was increased by THC, which were attenuated by CB_2 antagonist, SR144528, suggesting a modulation of the balance between Th1/Th2 cytokines in the T cells by THC in a CB_2-dependent manner [169].

Interestingly, depending on experimental conditions, such as cannabinoid concentration, cell types, and specific immune stimuli, enhancement of T cell responses by cannabinoids has also been reported in a number of studies. For example, it was first demonstrated that THC treatment of anti-CD3 stimulated spleen cells resulted in an enhancement in cellular proliferation, whereas using cells from lymph nodes or concanavalin A (conA) or phytohemagglutinin for stimulation led to THC-mediated suppression [170]. In addition to differences between various stimuli and organ sources, the age of animals was also suggested to play a role in cannabinoid-mediated differential effects [171]. Moreover, CP55,940 at nanomolar concentrations was found to increase the expression of IL-8 and beta-chemokine monocyte chemotactic protein-1 (MCP-1) in CB_2-transfected HL60 cells, which was sensitive to pertussis toxin [172]. Although HL60 cells are not T cells, these studies are mentioned here to support the differential effects of cannabinoids in T cells. Low concentrations of cannabinoids were also observed to produce enhancement in B cells

[173]. Furthermore, positive regulation of IL-2 expression by cannabinol has been observed when EL4 T cells were suboptimally activated with low concentrations of PMA, due to binding of NFAT to a distal site in the IL-2 promoter region [174, 175]. In addition, CBN-mediated enhancement was also observed with THC, CP55,940 and CBD, which was not abrogated by CB_2 antagonist SR144528, suggesting a CB-independent mechanism.

B. B Cells

Since B cells express higher levels of CB_2 compared with other immune cells as discussed earlier, THC and other cannabinoids have shown modulatory effects on B cell functions, such as proliferation and antibody production responses, mediated through this receptor. For example, many studies have found that cannabinoids suppress plasma cell formation in response to the T cell-dependent antigen, sheep red blood cells (sRBCs), both *in vivo* and *in vitro* [162, 176-178]. To identify the cellular targets for THC, further studies have shown that the antibody forming cell (AFC) response to T cell-independent antigen, DNP-Ficoll, or polyclonal B cell activator, LPS, was not suppressed by THC, and T cell proliferation in response to sRBCs was indeed suppressed by THC, collectively suggesting that THC might target T cells rather than directly affecting B cells [179]. However, THC and other cannabinoids, such as 2-AG, were also found to suppress proliferation of B cells in response to LPS [180, 181]. In addition, recent studies have shown that the CD40 ligand (CD40L)-induced IgM AFC response was suppressed by THC [162]. Moreover, studies from this laboratory have demonstrated that THC decreased IgM production by human

peripheral blood B cells activated by CD40L plus recombinant cytokines (IL-2, -6, and -10). THC also suppressed expression of activation marker CD80 on B cells as well as STAT3 phosphorylation [182], which is involved in B cell survival, proliferation, and differentiation [183]. Furthermore, in human studies, serum immunoglobulin levels in chronic marijuana smokers were altered; however, which immunoglobulin isotype, including IgG, IgM, IgA, IgD, and IgE, was changed in particular is still controversial among different studies [184-186]. Interestingly, enhancement of B cell responses by cannabinoids has also been observed. For example, ligation of CD40-induced proliferation of B cells isolated from human tonsillar tissue, which was in fact enhanced rather than suppressed by THC at nanomolar concentrations [173].

C. NK Cells

NK cell function is also susceptible to modulation by THC. The lytic activity by splenic NK cells on target cells was found to be suppressed by THC and its primary metabolite 11-OH-THC in a dose-dependent manner [187]. Similarly, the cytolytic activity of IL-2 stimulated cloned NK cells against YAC-1 and EL4 target cells and proliferation of NK cells were suppressed by THC and 11-OH-THC, but the binding of cloned NK cells to target cells was not inhibited by THC [188]. Suppression of IL-2 receptor expression by THC was suggested as a mechanism by which THC mediated inhibition on the killing activity of NK cells [189]. In addition, migration of NK cells induced by 2-AG was abolished by CB_2 antagonist, SR144528, which suggested that the 2-AG-mediated effect occurred in a CB_2-dependent manner [190]. Also, THC at

micromolar concentrations attenuated the protein and mRNA production of TNFα from human NK cells in response to *C. albicans* [191]. ConA-induced IFNγ production by NK cells was reduced by THC, and both CB_1 and CB_2 antagonists reversed the effect [192].

D. APCs

APCs are critical cellular populations to link the innate and adaptive immune responses. Antigen processing and presentation as well as cytokine production by APCs were reported to be modulated by THC and other cannabinoids [193]. For instance, DCs and macrophages are known to express CB_1 and the voltage-gated potassium (K_V) channels [194, 195]. The CB_1 agonist arachidonylcyclopropylamide as well as AEA attenuated K_V channel-mediated outward currents in DCs, which resulted in a decrease of surface MHC II expression on DCs and therefore a reduced T cell response, suggesting the modulation of DC function by cannabinoids via CB_1 signaling [196]. Most recently, THC was found to suppress LPS-induced maturation of bone marrow-derived DCs (bmDCs), as evidenced by reduced MHC II, CD80, and CD86 expression, which in turn decreased IFNγ production by $CD8^+$ T cells after the co-culture of bmDCs and splenocytes [197]. In addition, THC was shown to suppress gene expression as well secretion of cytokines, such as IL-1α, IL-1β, TNFα, and IL-6, by activated macrophages [198-200]. Moreover, THC was demonstrated to inhibit NO production in macrophages in the CNS, by affecting NOS gene expression or synthesis via acting on the transcription factor NF-κB/RelA [146, 201]. Furthermore, the level of CB_2 expression in the macrophages was suggested to be altered depending

on the activating stage of the cells. THC and other CB_2 agonists were reported to inhibit chemotaxis as well as antigen processing and presentation in macrophages that were at the responsive or primed stage [202, 203].

E. *In Vivo* Host Resistance Models

Since THC and other cannabinoids have been shown to modulate immune function in humans and animals, the possible adverse effects on human health and disease have been a concern. Animal models have been used to study the effects of cannabinoids on host resistance to infection with viral and microbial pathogens. Due to the immunosuppressive properties of THC, increased host susceptibility to infections has been reported in a number of studies.

For example, in a mouse model with *Legionella pneumophila* infection, serum levels of Th1-promoting cytokines, IL-12 and IFNγ, were increased in Balb/c mice, which were suppressed by THC treatment administered prior to bacterial challenge. In contrast, *Legionella*-induced production of Th2-promoting cytokine, IL-4, was further increased by THC treatment, which was also observed in IL-4 knockout mice, suggesting that THC-mediated suppression of Th1 immunity to *Legionella* infection was due to a decrease in IL-12 and IFNγ production but not an increase in IL-4 production [204]. Moreover, it was indicated that both CB_1 and CB_2 played a role in THC-mediated effects on cytokine production by using CB antagonists [205].

Recently, this laboratory has established a mouse model of influenza virus challenge to study the effects of THC and the role of CB_1 and CB_2 on host resistance

to influenza. THC increased viral load in the lungs, which was, in part, through decreasing the infiltration of $CD4^+$, $CD8^+$, and macrophages to the lung [206]. In addition, CB_1 and CB_2 double knockout mice ($CB_1^{-/-}CB_2^{-/-}$) showed a lower viral burden in the lung than wild-type mice. THC increased the viral load in both genotypes when compared to the respective vehicle controls. Also, inflammatory cell infiltration, T cell activation and cytokine production were increased in $CB_1^{-/-}CB_2^{-/-}$ mice, when compared to wild-type mice [207, 208]. These findings suggest that THC-mediated effects on airway immune responses to influenza may be through CB_1/CB_2-dependent and -independent mechanisms. Further studies have implied that the exacerbated immune response phenotype in $CB_1^{-/-}CB_2^{-/-}$ mice might be due to a more mature function of APCs [208], and THC treatment suppressed APC-stimulated cytokine production by $CD8^+$ T cells in a CB_1/CB_2-dependent manner [197].

F. Involvement of CB_1/CB_2 in Cannabinoid-Mediated Immune Modulation

To study mechanisms for immune modulation by cannabinoids, one crucial factor that needs to be considered is the role of cannabinoid receptors involved in the biological activities of cannabinoids. Receptor antagonists, receptor agonists, or receptor knockout mice are the important and widely used approaches in identifying receptor-specific effects of cannabinoids. Both CB_1/CB_2-dependent and -independent mechanisms have been reported to be involved in cannabinoid-mediated immunomodulatory effects. For example, suppression of PMA/Io-induced IL-2

production in mouse splenocytes by cannabinoids, including CBN, CBD, and WIN55,212, was not attenuated by a CB_1 antagonist SR141716A and a CB_2 antagonist SR144528, suggesting a CB_1/CB_2-independent mechanism [144]. In addition, elevated intracellular calcium concentration in the presence of cannabinoids in resting splenocytes was attenuated by both CB_1 and CB_2 antagonists, suggesting a CB-dependent mechanism [144]. However, the role of CB_1 and CB_2 in cannabinoid-mediated actions based on receptor agonists and antagonists studies has been controversial. For example, SR141716A and SR144528 have been found to have inverse agonist activity by inhibiting GPCR signaling [209-211]. Other studies have shown that SR141716A and SR144528 exhibited partial agonist properties mimicking the actions of CB_1/CB_2 agonist, HU-210, by decreasing left ventricular developed pressure and maximum rates of contraction and relaxation [212]. Additional studies have also suggested off-target effects of CB antagonists. CB_1 or CB_2 antagonists attenuated THC-, CBN-, and HU-210-mediated elevation of intracellular Ca^{2+} levels in T cells, which was in fact independent of CB_1 and CB_2 as demonstrated using $CB_1^{-/-}CB_2^{-/-}$ mice, suggesting the existence of putative receptors that are also sensitive to CB antagonists [163].

$CB_1^{-/-}CB_2^{-/-}$ mice (on a C57Bl/6 background) have been used as an experimental tool to study the role of both CBs in cannabinoid-mediated immune modulation, which would avoid the issues with antagonists as described above. Although the

specific CB played a role in mediating the effects in these studies can not be discerned by using $CB_1^{-/-}CB_2^{-/-}$ mice, the involvement of one or both of these receptors can be determined. As described by Springs et al. [162], $CB_1^{-/-}CB_2^{-/-}$ mice do not show any phenotypic defects, except for a higher tendency to develop conjunctivitis in aged animals. The proportions of various splenic cellular populations, including T cells, B cells, and macrophages, were similar between wild-type and $CB_1^{-/-}CB_2^{-/-}$ mice. Also, mitogen-induced lymphocyte proliferation and cytokine production (IL-2 and IFNγ) were comparable between the two genotypes. In response to sRBC *in vivo*, the IgM AFC response was suppressed by THC in wild-type mice but not in $CB_1^{-/-}CB_2^{-/-}$ mice. *In vitro*, the LPS-induced IgM response was not modulated by THC in both genotypes, but the IgM response induced by CD40L was suppressed by THC in wild-type but not in $CB_1^{-/-}CB_2^{-/-}$ mice. Together, these findings suggest that the THC-mediated effects on immune responses may involve both a CB_1/CB_2-dependent and -independent mechanism.

In addition, the lack of CB_1 and CB_2 potentially leads to an enhanced immune response. For example, in a model for cutaneous contact hypersensitivity, $CB_1^{-/-}CB_2^{-/-}$ mice developed chronic ear ulceration with contact to nickel-containing ear clips, and exhibited exacerbated ear swelling compared with wild-type mice in response to the contact sensitizer, 2,4-dinitrofluorobenzene [213]. Additionally, CB antagonists SR141716A and SR144528 further enhanced allergic inflammation, whereas CB

agonist, THC, attenuated the responses, suggesting the involvement of endocannabinoids in the protection against allergic responses [213]. Similarly, in a mouse model challenged with influenza, there was a more robust immune response in $CB_1^{-/-}CB_2^{-/-}$ mice in the absence of THC, as evidenced by a lower viral load in the lung when compared with wild-type mice. THC also increased pulmonary inflammation and lung injury in $CB_1^{-/-}CB_2^{-/-}$ mice when compared with wild-type mice [206, 207].

VIII. Rationale and Objectives

As described above, approximately 25% of HIV/AIDS patients use marijuana to ameliorate nausea, pain, and wasting syndrome that accompany with HIV infection [94]. However, the effects of cannabinoids on immune function of these immunocompromised patients are still not well understood. To date, only a few studies have demonstrated that short-term or chronic THC treatment neither increased HIV viral load nor decreased $CD4^+$ and $CD8^+$ lymphocyte counts using patients or nonhuman primate models, therefore suggesting that cannabinoid treatment does not have adverse effects on disease progression in the early stage of infection [214-216]. In-depth studies are needed to investigate the involvement of cannabinoids and cannabinoid receptors on immune responses to HIV antigens, especially on antigen-specific responses. The objective for the studies presented in this dissertation was to test the hypothesis that *THC impairs the anti-HIV immune responses in a CB_1/CB_2-dependent mechanism*.

The specific aim for the first part of this dissertation research was to characterize the effect of THC and the role of CB_1/CB_2 on the elicitation and effector functions of antigen-specific $CD8^+$ T cells, and to investigate the associated molecular mechanisms. A novel mouse model of HIV_{gp120} antigen presentation was established, which was designed to elicit a broad antiviral immune response against multiple gp120-derived antigenic epitopes, to closely resemble aspects of host antiviral immunity in the initial phase of HIV infection. Since both cell-mediated and humoral immune responses against gp120 have been reported previously, gp120 was used as a representative HIV protein against which to induce an immune response in our models [217-219]. A C57Bl/6 mouse-derived DC line, DC2.4, and the T lymphoma cell line, EL4, were transduced with gp120 ($DC2.4_{gp120}$ and $EL4_{gp120}$, respectively), and used as APCs and target cells to restimulate CTL, respectively. $DC2.4_{gp120}$ cells were co-cultured with mouse spleen cells to activate T cells. The effect of THC on CTL elicitation and IFNγ production was investigated. The cellular and molecular mechanisms responsible for THC-mediated effects were then determined using more titratable T cell activators: specifically, PMA/Io or anti-CD3/CD28. These studies provide a possible mechanism to explain the widely reported discrepancy regarding cannabinoid effects on immune responses in the literature.

The specific aim for the second part of this dissertation research was to determine the effect of THC and the role of CB_1/CB_2 on antigen-specific immune responses *in*

vivo. In vaccine research, the focus of vaccine development against HIV-1 is to induce both antigen-specific T cell responses and neutralizing antibodies [75-77]. Plasmid DNA encoding viral proteins is often used as a more potent vaccine than using viral proteins directly in animal models to induce CTL, Th cell, and antibody responses [220]. Here, plasmid $pVRC_{gp120}$, encoding HIV envelope protein gp120, is used as the immunogen, which is injected intramuscularly into mice in this model system. To assess gp120-specific responses, splenocytes from treated mice were restimulated with immunodominant gp120-derived peptides. The effect of THC was studied in C57Bl/6 wild-type mice as well as $CB_1^{-/-}CB_2^{-/-}$ mice. Our findings provide an in-depth understanding of cannabinoid effects on HIV antigen-specific immune responses *in vivo*.

MATERIALS AND METHODS

I. Chemicals and Reagents

THC and CBD were obtained from the National Institute on Drug Abuse (Bethesda, MD). RPMI 1640 media, penicillin/streptomycin, MEM non-essential amino acids (NEAA), sodium pyruvate, and L-glutamine were obtained from Gibco Invitrogen (Carlsbad, CA). Restriction endonucleases and ligase were purchased from New England Biolabs (Ipswich, MA). Unless otherwise specified, all other reagents were purchased from Sigma (St. Louis, MO).

II. Mice

Female C57Bl/6 or B6C3F1 mice were purchased from Charles River (Portage, MI). Female $CB_1^{-/-}CB_2^{-/-}$ mice on C57Bl/6 background were bred at the University Laboratory Animal Resources (Michigan State University). $CB_1^{-/-}CB_2^{-/-}$ mice were a kind gift from Dr. Andreas Zimmer at the University of Bonn, Germany. Mice were used between the ages of 8-12 weeks and randomly assigned to experimental groups. They were provided with food (Purina Certified Laboratory Chow) and spring water *ad libitum*. Rooms were kept on a 12-hr light/dark cycle at 21-24°C and 40-60% humidity. All experiments followed the guidelines set forth by Michigan State University Institutional Animal Care and Use Committee.

III. Cell Culture Conditions

DC2.4 (a kind gift from Dr. Kenneth Rock at University of Massachusetts), EL4, $DC2.4_{gp120}$, and $EL4_{gp120}$ cells were maintained in complete RPMI media (10% bovine calf serum [BCS; HyClone, Logan, UT]; 100 units/ml penicillin and 100 μg/ml streptomycin [Pen/Strep]). HEK293T cells were cultured in Dulbecco's Modified Eagle's Medium (DMEM) with 10% BCS and Pen/Strep. Splenocytes were isolated aseptically from female C57Bl/6 mouse spleens unless otherwise specified and made into single-cell suspensions. In the elicitation phase of the gp120 response (see below), "CTL media" (RPMI plus 5% BCS, Pen/Strep, 2 mM MEM NEAA, 2 mM sodium pyruvate, 2 mM L-glutamine, and 50 μM 2-mercaptoethanol) supplemented with 5 ng/ml recombinant mouse IL-12 was utilized (R&D Systems, Inc., Minneapolis, MN). In the effector phase, 2% BCS and 1 ng/ml IL-12 were substituted in the CTL media. In the other experiments, splenocytes were cultured in complete RPMI media with 2% BCS, Pen/Strep and 50 μM 2-mercaptoethanol. Human leukocyte packs were obtained commercially from anonymous donors (Gulf Coast Regional Blood Center, Houston, TX). PBMC were enriched from each pack by density gradient centrifugation using Ficoll-Paque Plus (GE Healthcare, Piscataway, NJ). Human PBMC were cultured in complete RPMI media with 2% BCS and Pen/Strep.

IV. Lentiviral Plasmid Construction

HIV gp120 cDNA, derived from the HIV-1 IIIB (HXBc2) strain, was amplified from plasmid, pVRC2000-gp120 [221] (a kind gift from Dr. Norman Letvin, Beth Israel Deaconess Medical Center, Boston, MA) using primers gp-FP and gp-RP (Table 1). To

generate pLexPuro-gp120, the gp120 amplicon was digested with SpeI and NotI (underlined in gp-FP and gp-RP, respectively) and ligated into the pLexMCS plasmid containing the IRES-puromycin resistance ($puro^r$) gene cassette (Trans-Lentiviral™ pLex Packaging System, Open Biosystems, Huntsville, AL). A similar plasmid, pLexNeo-gp120, was made by replacing the IRES-$puro^r$ cassette of pLexMCS with an IRES-neomycin resistance (neo^r) cassette and inserting gp120 as above. The IRES-neo^r cassette was amplified from plasmid pIRESneo3 (Clontech Laboratories, Inc. Mountain View, CA) using primers IRES5' and Neo3' (Table 1) with respective XhoI and HpaI sites. Each ligate was transformed into competent *E. coli* cells, Stbl3™ (Invitrogen) or 10-beta (C3019, New England Biolabs). Transformants were selected on LB plus ampicillin plates. Individual colonies were expanded in LB broth plus ampicillin and 0.5% glycerol. Plasmids were isolated using a HiSpeed Plasmid Maxi kit (Qiagen, Valencia, CA).

Table 1. Sequences of PCR primer/probe sets.

Primer/probe sets	Sequence (5' – 3')
gp-FP	TACGTACTAGTTGGCAAGAGAAGGCCAGAAAC
gp-RP	TGACTGCGGCCGCTCCTCAGCTCTTCTCGCTCT
IRES5'	AAAAAACTCGAGTATGCATCTAGGGCGGCCAATTC
neo3'	AAAAAAGTTAACTTCAGAAGAACTCGTCAAGAAGGCGA
gp120 (3' end)	CCTTGCCCACCTTCTG
gp120 (5' end)	CACCAGCACCACCTCC
$puro^r$	CCGGGAACCGCTCAAC
neo^r	TCCGGTGCCCTGAATG

V. $DC2.4_{gp120}$ and $EL4_{gp120}$ Cell Line Construction

Packaging plasmids (Trans-Lentiviral™ pLex Packaging System, OpenBiosystems) were co-transfected with either pLexPuro-gp120 or pLexNeo-gp120 into HEK293T cells according to the manufacturer's protocol. Lentiviral particles were collected and incubated with 6 mg/ml polybrene at RT for 5 min. The polybrene/particle (gp120-$puro^r$ or gp120-neo^r) mixtures were added to DC2.4 or EL4 cells, respectively, in 24-well plates (750 μl/well), and centrifuged at 800 x g for 2h. Media was replaced with complete RPMI media and incubated for 48h. Transduced cells were cultured in 1.5 μg/ml puromycin for $DC2.4_{gp120}$ cells and 400 μg/ml of G418 for $EL4_{gp120}$ cells. Cloning by limiting dilution was performed by seeding heterogeneous mixtures of transduced cells at approximately one cell per three wells in 96-well U-Bottom plates (200 μl/well) to select individual clones, which were cultured for screening by Real Time PCR (primer/probe sets in Table 1) and Western blotting.

VI. *In Vivo* Immunizations Using Plasmids

The control vector plasmid pVRC2000 was constructed by digestion of the pVRCgp120 plasmid with the restriction enzyme, ScaI (New England Biolabs, Ipswich, MA), to remove the gp120 cassette and ligated with T4 DNA ligase (New England Biolabs). Each plasmid was transformed into competent *E. coli* 10-beta cells. Transformants were selected on LB plus kanamycin plates. Individual clones were expanded in LB broth plus kanamycin. Plasmid DNA was isolated using Endofree plasmid Mega Kit (Qiagen, Valencia, CA), according to the manufacturer's instructions.

Both C57Bl/6 and $CB_1^{-/-}CB_2^{-/-}$ mice (n=5/group) were randomly placed into different treatment groups one week prior to the start of the experiment. The prime-boost immunization scheme, the route of administration and the amount of DNA per injection were based on studies in the literature and then optimized for the present investigation in order to stimulate robust antigen-specific immune responses [222-225]. Mice were injected intramuscularly (i.m.) in each quadricep muscle with 50 μg pVRCgp120 or pVRC2000 plasmid DNA in 50 μl final volume of Endofree water. Injections were performed twice per mouse over a one-week interval (day 1 and day 8).

VII. Real Time PCR

For gp120-transduced cells, total RNA was extracted using the SV Total RNA Isolation System (Promega, Madison, WI) following manufacturer's protocols. For cytokine production, splenocytes (5×10^6 cells) were treated with vehicle (VH, 0.1% ethanol) or CBD for 30 min at 37°C, and activated with 10x P/I (4 nM/0.05 μM) or 1x P/I (40 nM/0.5 μM) for 2, 6 or 24 hr at 37°C. Total RNA was isolated using the TRI Reagent method as previously reported [159]. In brief, cells were harvested, placed in TRI Reagent and frozen at -80°C. Upon thaw, bromochloropropane was added (0.1 ml per 1 ml TRI reagent) and phases were separated by centrifugation at 12,000 x g for 15 min. After isolation of the aqueous phase, RNA was precipitated with isopropranol, washed twice with 75% ethanol, dried at room temperature and suspended in nuclease-free water. In all experiments, equal amounts of RNA were reverse transcribed with random primers using the High Capacity cDNA Reverse Transcription Kit (Applied Biosystems, Foster City, CA). Real time PCR amplification and detection was performed with Taqman

primer/probe sets for mouse IL-2 (Mm00434256_m1, Applied Biosystems), or IFNγ (Mm00801778_m1, Applied Biosystems) on a 7900 HT Fast Real Time PCR System (Applied Biosystems). Assessment of genomic DNA contamination was performed using controls without reverse transcriptase (RT) during the cDNA reaction and demonstrated more than 10 Ct value difference between samples with and without RT for 18S and no detectable signal or above 35 Ct value for target genes in samples without RT. Fold-change values were calculated using the ΔΔCt method [226].

VIII. Western Blotting Analysis

Cytosolic protein was isolated from $DC2.4_{gp120}$ and $EL4_{gp120}$ clones. Briefly, cells were washed with phosphate buffered saline, lysed with lysis buffer (1% Igepal CA-630, 0.5% sodium deoxycholate, 50 mM Tris, 150 mM NaCl, pH 8.0, supplemented with EDTA containing protease inhibitors [Complete, Mini Protease Inhibitor Cocktail Tablets, Roche Applied Science, Indianapolis, IN]) at $\leq 4 \times 10^7$ cells/ml on ice for 5 min, and centrifuged at 25,000 x g at 4°C for 5 min. Supernatants were collected, and 20 μg protein for each sample was loaded per lane into a 7% denaturing polyacrylamide gel. Proteins from parental DC2.4 or EL4 were negative controls and 500 ng purified gp120 protein ($HIV\text{-}1_{96ZM651}$ gp120, NIH AIDS Research & Reference Reagent Program) was the positive control. Nuclear protein was isolated from splenocytes (5×10^7 cells) that were treated with VH or CBD for 30 min at 37°C, then activated with 10x or 1x P/I for 30 min at 37°C as previously described [227]. Protein extract was then loaded into an 8% denaturing polyacrylamide gel to ensure resolution of several bands that correspond to

NFAT2 [228]. All protein samples were transferred to nitrocellulose membranes using a semi-dry electroblotter in transfer buffer (0.025 M Tris, 0.2 M glycine, 10% methanol for NFAT or 20% methanol for gp120). Membranes were blocked in 5% milk or 1% bovine serum albumin (BSA) in tris-buffered saline in Tween (0.01 M tris, 0.15 M NaCl, 0.1% Tween-20) overnight at 4°C. Gp120 was detected using a polyclonal HIV-1 gp120 antibody (Prosci, Inc., Poway, CA), and NFATc1 (NFAT2) was detected using an anti-mouse NFAT2 antibody (Affinity Bioreagents/Thermo Scientific, Rockford, IL), followed by horseradish peroxidase-conjugated sheep anti-mouse IgG (GE Healthcare, Buckinghamshire, United Kingdom) and west pico chemiluminescent substrate development (Thermo Scientific).

IX. Elicitation of Splenocytes with DC2.4$_{gp120}$ Cells

The experimental model for *in vitro* elicitation of gp120-specific T cells is illustrated in Fig. 3. DC2.4$_{gp120}$ cells were irradiated with 35 gray of X-ray to prevent proliferation, washed 3 times, and adjusted to 1 x 10^6 cells/ml. Splenocytes (1 x 10^7 cells/ml) were treated with THC (1, 5, 10, and 15 μM) or VH (0.1% ethanol) for 30 min, and then co-cultured with DC2.4$_{gp120}$ cells (100 μl of each cell type in 96 U-bottom plates) for 5 days of elicitation in 5% CTL media.

X. THC Treatment *In Vivo*

THC was obtained from the National Institute on Drug Abuse (NIDA, Bethesda, MD). Two days post the injection of pVRCgp120 or pVRC2000 plasmid (day 1 and day 8),

mice received corn oil (CO) vehicle or THC (75 mg/kg/day per mouse) by oral gavage for three consecutive days (day 3-5 and day 10-12) (Fig. 4). The dose and dosing regimen were chosen based on historical data [206, 207, 229, 230], and the resulted THC concentrations in mouse serum are expected to be comparable with the finding from a previous study, in which 75 mg/kg of THC for 5 consecutive days resulted in 66.2 ng/ml of THC in mouse serum [206]. This is physiologically relevant to human plasma levels of THC, which typically ranged from 57 to 268 ng/ml in marijuana smokers [229]. There were total of four experimental groups for each genotype: CO-pVRC2000, CO-pVRCgp120, THC-pVRCgp120 using n=5/group and naïve (NA) using n=3/group.

XI. Necropsy and Tissue Preparation

Three days following the last THC dose, mice were sacrificed by decapitation for immunological assays. Trunk blood was collected into plasma separator tubes on ice (BD Medical, Franklin Lakes, NJ), and centrifuged at 3500 rpm (2536 x g) for 15 min at 4°C. Splenocytes were isolated from the spleen and made into single-cell suspensions in ice-cold RPMI 1640 medium (Gibco Invitrogen, Carlsbad, CA). Splenocytes were centrifuged at 300 x g for 4 min and resuspended in RPMI supplemented with 2% bovine calf serum (BCS), 100 U/ml penicillin, 100 μg/ml streptomycin, 2 mM non-essential amino acids, 2 mM sodium pyruvate, 2 mM L-glutamine, and 50 μM 2-ME (Gibco Invitrogen).

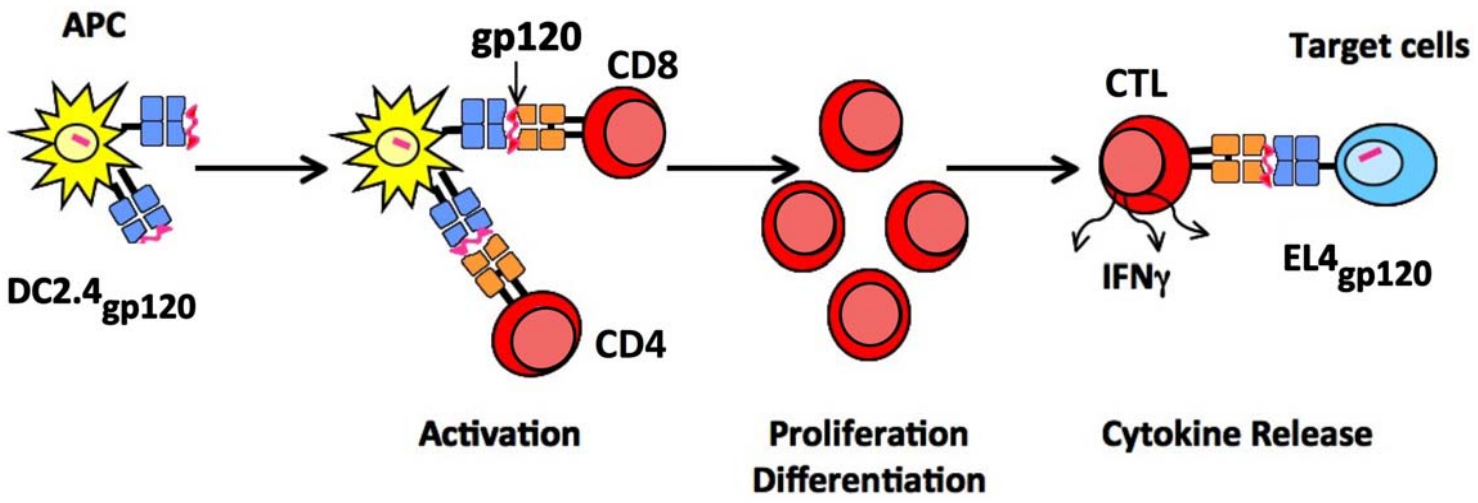

Figure 3. Experimental model of *in vitro* elicitation of gp120-specific T cells.

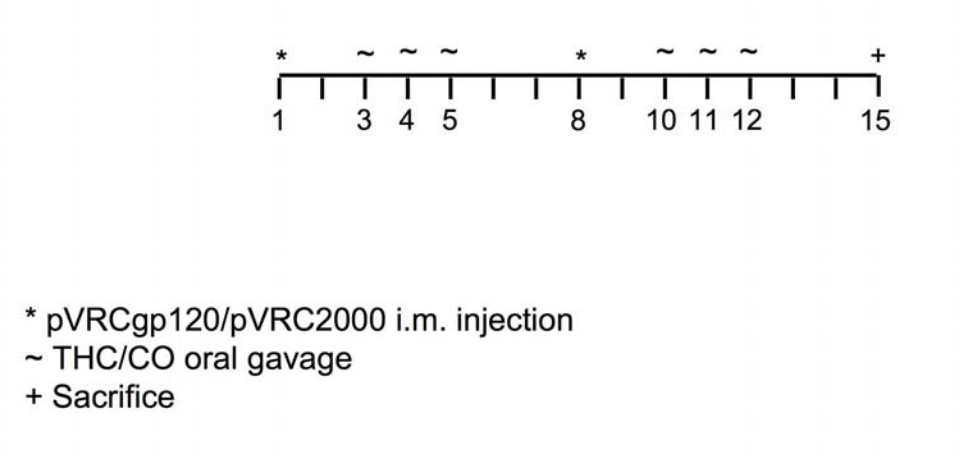

Figure 4. Protocol for the administration of THC or CO into the mice immunized with pVRCgp120/pVRC2000.

XII. Enumeration of Cytokine Secreting Cells by ELISPOT Assays

For *in vitro* studies, after five days of co-culture, elicited effector splenocytes (2×10^7 cells/ml) were restimulated with $EL4_{gp120}$ or parental EL4 target cells (1×10^6 cells/ml) in 2% CTL media. 50 μl of each for effectors and targets were plated in ELISPOT wells overnight. A CTL only group (no target restimulation) was included as a control to assess background nonspecific CTL activity.

For *in vivo* studies, 1×10^6/well splenocytes in 100 μl of 2% BCS RPMI medium were restimulated with gp120-derived peptides *ex vivo*. A 211-peptide library, comprising the HIV-1 IIIB envelope protein region, was obtained from the NIH AIDS Reagent Program (https://www.aidsreagent.org/). These peptides are 15 amino acids in length, with 11-amino acid overlaps between sequential peptides. Splenocytes were restimulated *ex vivo* overnight with 100 μl media containing one of the following treatments: 1). 53 pools of 4 peptides (except for 3 peptides in pool 53) from the library (0.2 μg/well of each peptide) individually; 2). 0.2 μg/well of the most immunogenic peptide from the library; 3). VH control for the peptides (0.1% dimethyl sulfoxide [DMSO]); 4). no treatment (NT).

ELISPOT assays were performed as described previously [231]. Ninety six-well Multiscreen-HA filter plates (Millipore, Billerica, MA) were pre-coated with purified mouse anti-IFNγ or anti-IL-2 antibody (10 μg/ml, BD PharMingen, San Diego, CA) overnight, washed and blocked with phosphate buffered saline (PBS) containing 5% bovine serum albumin (BSA), prior to the addition of cells (described above). ELISPOT plates were then washed and incubated with biotin-conjugated mouse anti-IFNγ or IL-2 antibody (1 μg/ml, BD PharMingen), followed by the incubation with a 1/1000 dilution of

streptavidin peroxidase (Sigma, St. Louis, MO). Spots were developed with AEC Chromogen Kit (Sigma) and enumerated with the Cellular Technology ImmunoSpot system (Cellular Technology, Shaker Heights, OH).

XIII. Cell Staining for Flow Cytometry

For *in vitro* studies, splenocytes (5 x 10^6/ml) were labeled with 5 μM CellTrace Violet dye (Cell Proliferation Kit, Invitrogen) following the manufacturer's protocol. Proliferation was assessed on days 1-5 post co-culture of labeled splenocytes with $DC2.4_{gp120}$ cells, and IFNγ production was assessed after restimulation as described above. In some studies, splenocytes were treated with VH (0.1% ethanol) or CBD at various concentrations for 30 min, then activated with 1x P/I (4 nM/0.05 μM) for 18-24 hr at 37°C. Cells were incubated with LIVE/DEAD Fixable Near-IR or Aqua Dead Cell Stain (Invitrogen) to assess cell viability according to the manufacturer's instructions. Fc receptors were blocked with purified rat anti-mouse CD16/CD32 (BD Pharmingen) in FACS buffer (1 x HBSS containing 1% BSA and 0.1% sodium azide), and stained for extracellular and intracellular proteins using the following antibodies from Biolegend (San Diego, CA): PE/Cy7- or PE/Cy5-CD8α (clone 53-6.7), FITC-CD62L (clone MEL-14), APC/Cy7-CD3 (clone 145-2c11), PE/Cy7-CD4 (clone GK1.5), FITC-CD49b (clone DX5), APC-IL-2 (clone JES6-5H4), and PE-IFNγ (clone XMG1.2) following previously described protocols [208]. Brefeldin A (Biolegend) was added during the last 6 h of restimulation incubation to block cytokine secretion allowing the identification of cytokine producing T cells. Violet staining from each day was compared to the day 1 control, and a decrease of fluorescence intensity is indicative of cell proliferation. Single

stain controls were included in all experiments to compensate for fluorescence interference between detectors. Cells were assessed on a FACS Canto II flow cytometer (BD Biosciences, San Jose, CA), and analyzed with FlowJo v8.8.6 (Tree Star, Ashland, OR) or Kaluza 1.1 (Beckman Coulter, Miami, FL) software. Linear regression was performed using GraphPad Prism version 4.0a (Graphpad Software, San Diego, CA).

For *in vivo* studies, splenocytes (1×10^6/well) isolated from different treatment groups were restimulated *ex vivo* with the most immunogenic peptide from the gp120 library (0.2 μg/well) overnight in 2% BCS RPMI medium in a 96-well U-bottom plate. VH for the peptide (0.1% DMSO) or NT were included as controls. A mouse IFNγ secretion assay (Miltenyi Biotec Inc., Auburn, CA) was used to quantify IFNγ secretion by splenocytes after peptide restimulation, according to the manufacturer's instructions. Briefly, 1×10^6 splenocytes were centrifuged at 300 x g for 10 min at 4°C and incubated with mouse IFNγ catch reagent in cold MACS buffer (PBS containing 0.5% BSA and 2 mM EDTA, pH 7.2) for 5 min on ice. Splenocytes were then diluted with warm (37°C) medium and incubated for 45 min at 37°C under slow continuous rotation. Subsequently, cells were washed with cold buffer and incubated with mouse antibodies (Biolegend, San Diego, CA) specific for IFNγ (PE), CD8 (PE/Cy7), CD4 (PE/Cy5), and NK1.1 (APC) for 10 min on ice. Next, cells were stained with LIVE/DEAD Fixable Near-IR cell stain to assess cell viability, fixed with Cytofix, and resuspended in FACS buffer. For cell activation studies, peptide restimulated splenocytes were first stained with LIVE/DEAD Fixable Aqua cell stain, followed by FcR blocking and cell staining for extracellular proteins using the following

antibodies from Biolegend: PE-CD69, PE/Cy5-CD80, FITC-MHC II, PE/Cy7-CD8α, APC-CD4, and Pacific Blue-CD19. Cells were assessed and analyzed as described above.

XIV. T Cell Purification

T cells were purified from splenocytes by negative selection using the Pan T Cell Isolation Kit according to the manufacturer's instructions (Miltenyi Biotec, Auburn, CA). Purity of T cells was determined using immunofluorescence analysis with anti-CD3 antibody (clone 145-2c11, BD Pharmingen), and generally exceeded 98%. Purified T cells were subsequently used for ELISA analysis.

XV. ELISA

For cytokine ELISA, in 48-well plates, splenocytes (8×10^5 cells/well) or human PBMC (2×10^6 cells/well) were treated with VH, THC or CBD for 30 min at 37°C, then activated with 10x or 1x P/I for 18-24 hr at 37°C. In some studies, cells were activated with anti-CD3 plus anti-CD28 antibodies (BD Pharmingen). For optimal stimulation, plates were coated with 0.1 μg/well purified NA/LE hamster anti-mouse CD3e antibody (clone 145-2C11) overnight at 4°C, washed twice with RPMI, and overlaid with splenocytes in the presence of 0.8 μg/well purified NA/LE hamster anti-mouse CD28 antibody (clone 37.51) for 2 days at 37°C. For suboptimal stimulation, splenocytes were activated with 0.8 μg/well of each of anti-CD3 and anti-CD28. Quantification of IL-2 and IFNγ was determined by ELISA as previously described [159]. Briefly, recombinant purified mouse IL-2 or IFNγ (BD Pharmingen) or human IL-2 (BD Pharmingen) served as

standards from which the amount of each cytokine in the samples could be determined. Ninety-six well ELISA plates (Immulon 4 HBX strips, Thermo Scientific, Milford, MA) were coated with capture antibodies, purified anti-mouse IL-2 or IFNγ or anti-human IL-2 antibody. Detection antibodies were biotinylated anti-mouse IL-2 or IFNγ or anti-human IL-2 (BD Pharmingen). Color development was performed using streptavidin peroxidase followed by tetramethylbenzidine. Reactions were stopped with 6N H_2SO_4, after which samples were read at 450 nm using the BioTek Synergy HT (BioTek, Winooski, VT).

For antibody ELISA, serum anti-gp120 antibody response from immunized mice was quantified by ELISA. ELISA plates were coated with 50 μl/well of 2 μg/ml purified recombinant IIIB gp120 (NIH AIDS Reagent Program) in 0.1 M $NaHCO_3$ buffer (pH 9.6) at 4°C overnight. Plates were washed with PBS containing 0.05% tween-20 and blocked with 3% BSA-PBS for 1.5-2 h at 37°C. Serum samples were added into the wells and incubated for 1-1.5 h at 37°C. Plates were washed again and incubated with a 1/1000 dilution of a peroxidase-conjugated goat anti-mouse IgG secondary antibody (Sigma) for 1-1.5 h. Plates were washed and developed with 1 mg/ml ABTS substrate (Roche Applied Science, Branford, CT). Samples were read at 450 nm every minute for 1 hr on kinetic mode using the BioTek Synergy HT plate reader.

XVI. Calcium Determinations

Splenocytes (2×10^7 cells) were incubated with 2 μM Fluo-3 (Invitrogen) and 5 μM Fura Red (Invitrogen) for 30-60 min at RT in the dark. Cells were analyzed on a FACSCalibur (BD Biosciences) using the kinetic acquisition setting over 5-min intervals.

Baseline analysis was conducted for 1 min, after which cells received various treatments (VH or THC or CBD at 1 min, cellular activation at 2 min). Kinetic analyses were performed with FlowJo software.

XVII. Low Density Array Mouse Immune Panel

RNA was isolated from splenocyte samples using the TRI Reagent method as described above. cDNA was synthesized using the High Capacity cDNA Reverse Transcription Kit with 500 ng of RNA in a total volume of 40 μl following the manufacturer's instructions. TaqMan low density array mouse immune panel (Applied Biosystems) was utilized according to manufacturer's instructions. In brief, 50 ng of cDNA in a total volume of 100 μl was loaded into each row on the plate, followed by centrifugation at 1100 rpm at 1 min twice using a Sorvall Legend T centrifuge (Thermo Fisher, Waltham, MA). Analysis was performed using the Applied Biosystems 7900HT Real-Time PCR system. Thresholds for Ct values were determined by setting baseline fluorescence at 2-5 cycles for the internal control, 18S rRNA gene, and 2-13 cycles for target genes. Fold changes were calculated using the ΔΔCt method [226] when comparing CO-pVRCgp120 group to the control CO-pVRC2000, and comparing THC-pVRCgp120 group to the control CO-pVRCgp120. Genes that were differentially regulated by at least 1.5-fold were selected.

XVIII. Verification of Genotype

Real-time PCR was performed using genomic DNA samples extracted from WT and $CB_1^{-/-}CB_2^{-/-}$ mouse-tails to verify the genotype. Genomic DNA from WT and KO

mouse-tails was extracted using the DirectPCR Lysis Reagent according to the manufacturer's instructions (Viagen Biotech, Los Angeles, CA). One μl of isolated genomic DNA was assayed in a total volume of 20 μl, containing Taqman Universal Master mix (Applied Biosystems, Foster City, CA) and primers, in a real-time PCR reaction using standard amplification procedures (50°C for 2 min, 95°C for 10 min, 40 cycles of 95°C for 15 sec, and 60°C for 1 min) with a 7900 HT Thermocycler (Applied Biosystems). The presence of CB1 and CB2 was determined using commercial primers for *cnr1* (Mm00432621-s1) and custom primers for *cnr2* (forward 5′-CCTGATAGGCTGGAAGAAGTATCTAC-3′, reverse 5′-ACATCAGCCTCTGTTTCTGTAACC-3′) [232] from Applied Biosystems. The average of Ct value for CB_1 and CB_2 in the WT mice was 24.70 ± 1.22 and 26.84 ± 2.14, respectively. All Ct values for both genes in the $CB_1^{-/-}CB_2^{-/-}$ mice were below the level of detectable product and were reported as undetermined.

XIX. Statistical Analysis

Statistical analyses were performed using GraphPad Prism version 4.0a (GraphPad Software, La Jolla, CA). The mean ± SE is displayed in all bar graphs. Differences between means of each treatment group were determined using parametric ANOVA. When significant differences were detected, treatment groups were compared to the appropriate control using Dunnett's post-tests. Following a two-way ANOVA, all groups were compared using Bonferroni's post-tests. For cytokine PCR or low density array data, Grubb's outlier test was performed for each treatment group using ΔCt ($Ct_{target\ gene}$

- Ct_{18S}). Fold-change values were transformed using natural log (fold-change + 1) for statistical analysis using ANOVA or unpaired t test. P value of < 0.05 was deemed statistically significant.

EXPERIMENTAL RESULTS

I. *In Vitro* Cannabinoid-Mediated Effects on T Cell Response to HIV_{gp120}

A. Expression of gp120 mRNA and protein in transduced DC2.4 and EL4 clones

DC2.4 and EL4 were transduced with pLexPuro-gp120 and pLexNeo-gp120, respectively (Fig. 5). Importantly, because all $DC2.4_{gp120}$ cells endogenously expressed cellular proteins are sampled and expressed within the context of MHC, including gp120, any peptide recognized as "nonself" has the potential of eliciting an immune response. To ensure that the immune response being measured during the effector phase of the CTL response was against gp120 but not an antibiotic resistance gene, each cell line (i.e., $DC2.4_{gp120}$ and $EL4_{gp120}$) was engineered to express a different antibiotic resistance gene. All transduced $DC2.4_{gp120}$ clones (C1, C2, C3, and C4) expressed $puro^r$ transcript compared with parental DC2.4, as shown by lower Ct values (Fig. 6A). However, only C1 and C4 expressed gp120 transcript but not C2 and C3 (Fig. 6A). The presence of gp120 protein was detected in C1, but not in parental DC2.4 or C4 (Fig. 6B). Two tested $EL4_{gp120}$ clones, C135 and C149, showed expression of both gp120 and neo^r transcripts, compared with parental EL4 (Fig. 6C), and both clones expressed high levels of gp120 protein (Fig. 6D). Subsequent experiments were conducted with $DC2.4_{gp120}$ C1 for elicitation and $EL4_{gp120}$ C135 as target cells in the effector phase. Furthermore, the presence of gp120 transcript and protein in $DC2.4_{gp120}$ C1

and $EL4_{gp120}$ C135 was verified after cells had been passaged several times in culture, confirming stable insertion of the cassette into the genome of clones. The clones will be referred to as $DC2.4_{gp120}$ and $EL4_{gp120}$, respectively, in the following sections.

B. Elicitation of gp120-specific $CD8^+$ T cell response

Following co-culture stimulation with $DC2.4_{gp120}$, proliferation of $CD8^+$ T cells in splenocytes was observed, and approximately 80% of total viable $CD8^+$ T cells had divided at least once by day 5 (Fig. 7). IFNγ ELISPOT was performed as a proof-of-principle experiment to demonstrate a gp120-specific CTL response. $DC2.4_{gp120}$ elicited a greater IFNγ response against $EL4_{gp120}$ than against parental EL4 target cells (Fig. 8A) used to assess the contribution to the IFNγ response from putative antigens derived from BCS, EL4 tumor antigens, or antibiotic resistance peptides. The IFNγ response was low when there was no antigenic restimulation (CTL only group in Fig. 8A), demonstrating the requirement of target cell restimulation for measuring effector activity. The same trend of gp120-specific CTL response was confirmed by intracellular IFNγ staining (Fig. 8B). Furthermore, almost all viable $IFN\gamma^+CD8^+$ T cells had proliferated (Fig. 8C). Finally, the percent of $CD62L^{low}CD8^+$ T cell (differentiated $CD8^+$ T cell) population increased after elicitation with $DC2.4_{gp120}$ for 5 days, compared with naïve $CD8^+$ T cells from the splenocytes (Fig. 9A), and most $IFN\gamma^+CD8^+$ cells were also the $CD62L^{low}$ population (Fig. 9B).

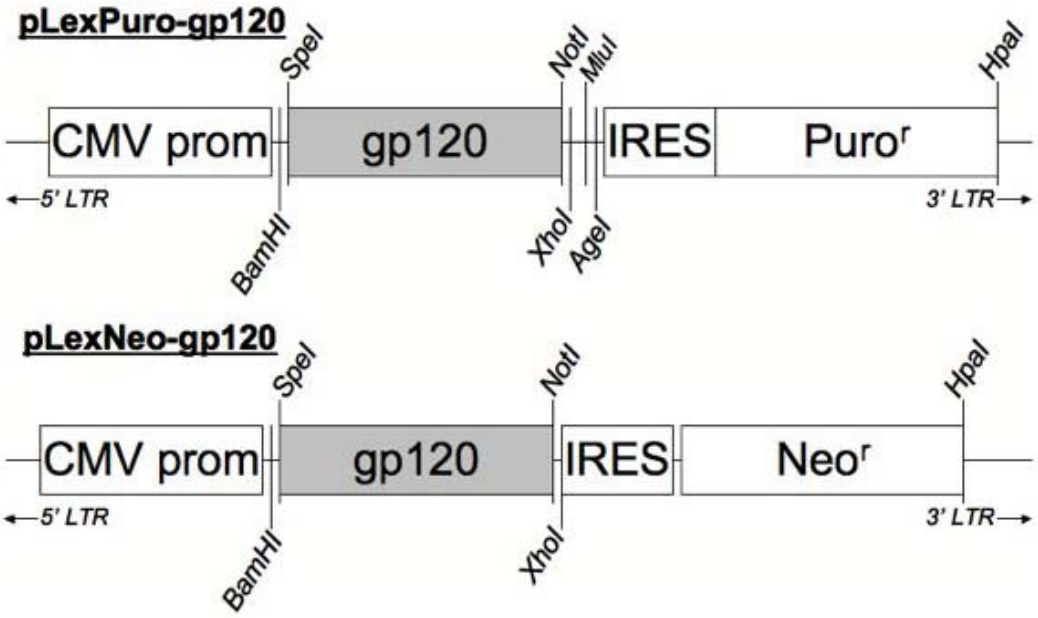

Figure 5. Plasmid cassette constructs for expression of gp120 and puro^r in DC2.4 (top) or gp120 and neo^r in EL4 cells (bottom).

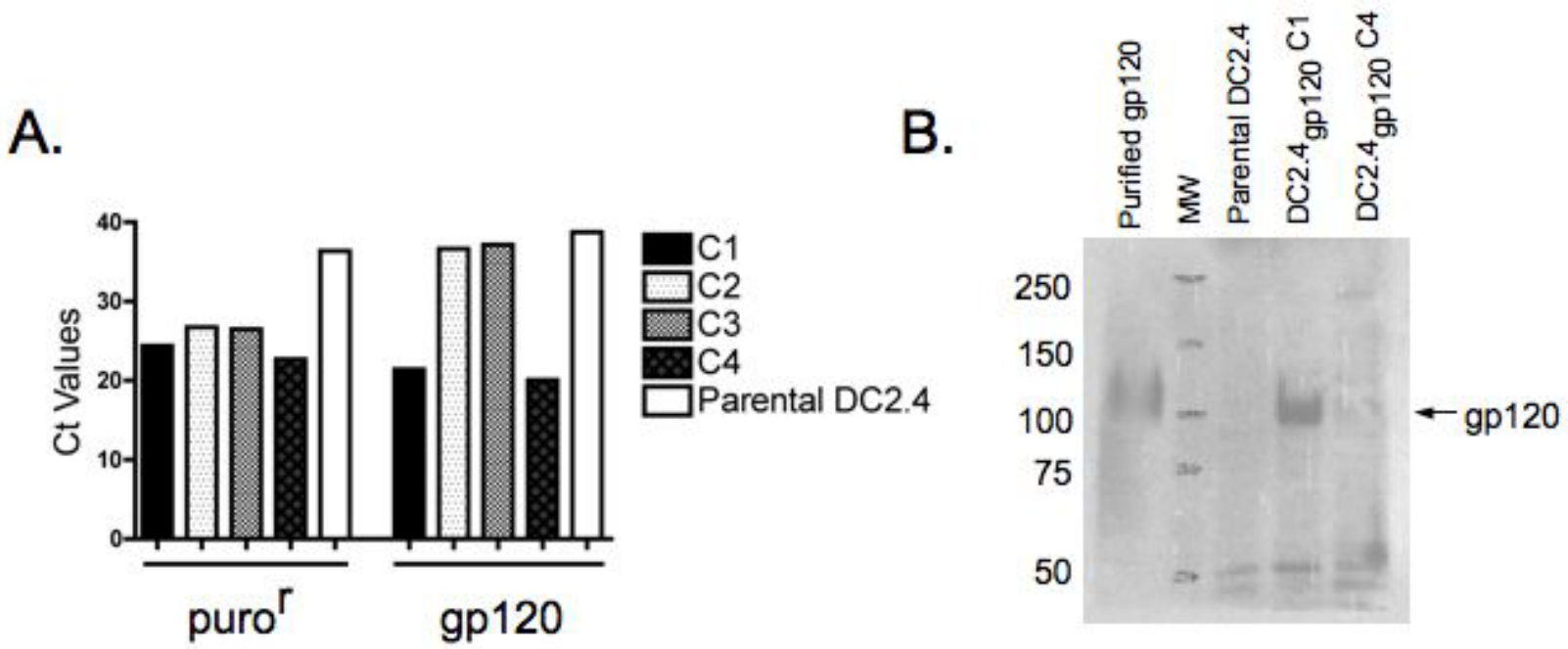

Figure 6. Expression of gp120 transcript and protein in transduced DC2.4$_{gp120}$ or EL4$_{gp120}$ clones. (A, C) Total RNA was extracted from DC2.4$_{gp120}$ clones (C1, C2, C3, C4), parental DC2.4 cells, EL4$_{gp120}$ clones (C135, C149), or parental EL4 cells. Puro^r, Neo^r and gp120 transcript levels were analyzed by Real Time PCR. Data are presented as Ct values. Results shown are from gp120 3' end Taqman primers, and 5' end primers gave similar values. (B, D) Cytosolic proteins were isolated from DC2.4$_{gp120}$ C1 and C4, EL4$_{gp120}$ C135 and C149. 20 μg of each sample was assessed by Western blotting for gp120 expression. Protein extract from parental DC2.4 or EL4 was included as a negative control, and purified gp120 protein (500 ng) was included as a positive control. (A-D) Data are representative of at least three separate experiments.

Figure 6 (cont'd)

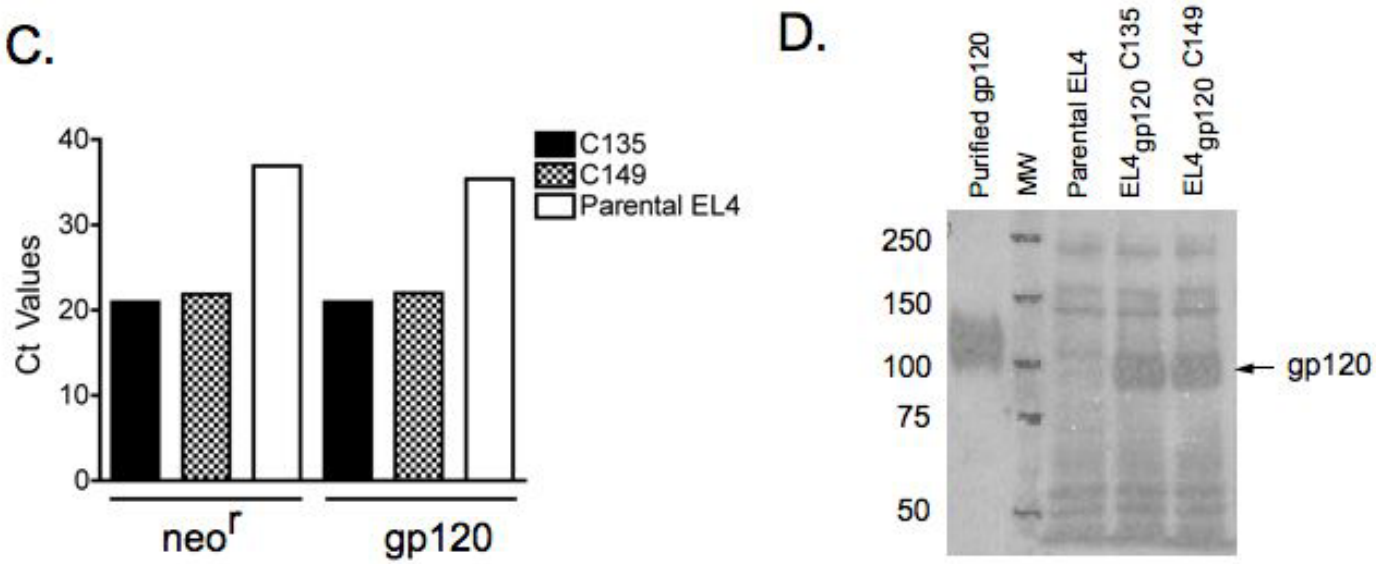

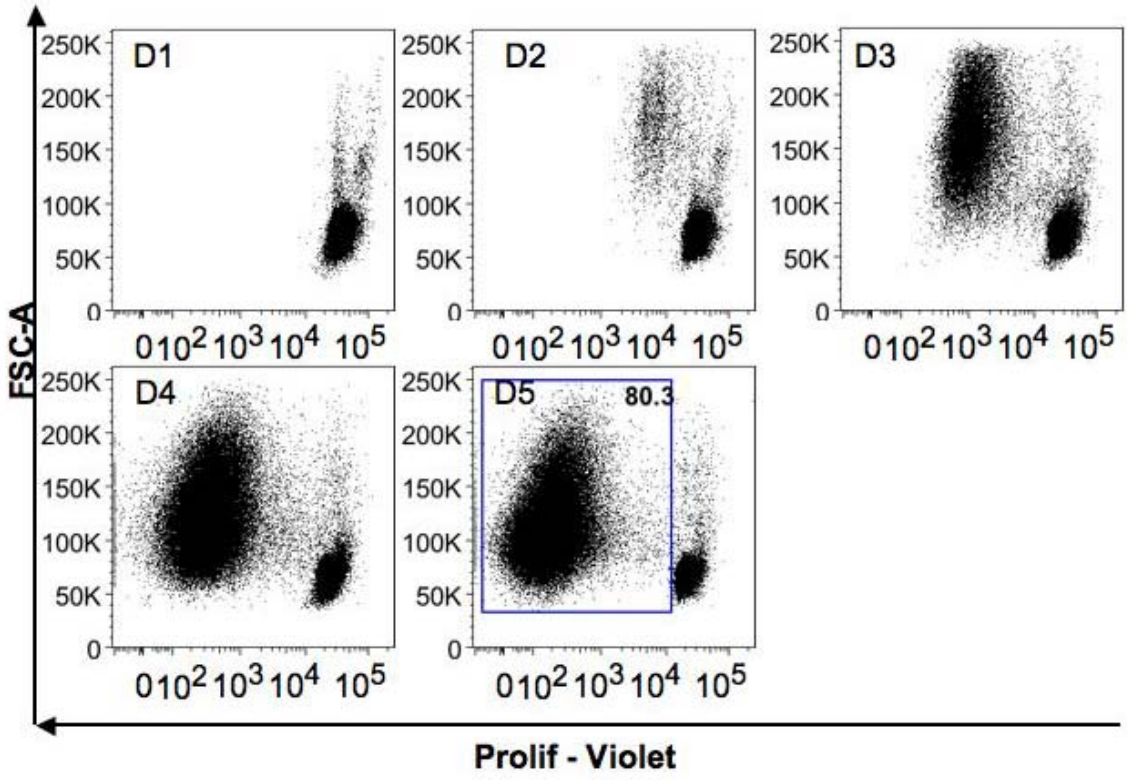

Figure 7. Proliferation of gp120-specific CD8$^+$ T cells was elicited in the *in vitro* model. CellTrace Violet-labeled splenocytes (1 x 10^6 cells/well) from C57Bl/6 mice were incubated with irradiated DC2.4$_{gp120}$ cells (1 x 10^5 cells/well). On days 1-5 (D1 – D5) post initiation of the co-culture, cells were stained for viability and CD8 and assessed by flow cytometry for proliferation of CD8$^+$ T cells. Cells were gated on singlet, viable, lymphocyte, and CD8$^+$ populations. The percent of proliferated CD8$^+$ T cell population on D5 is indicated in the plot.

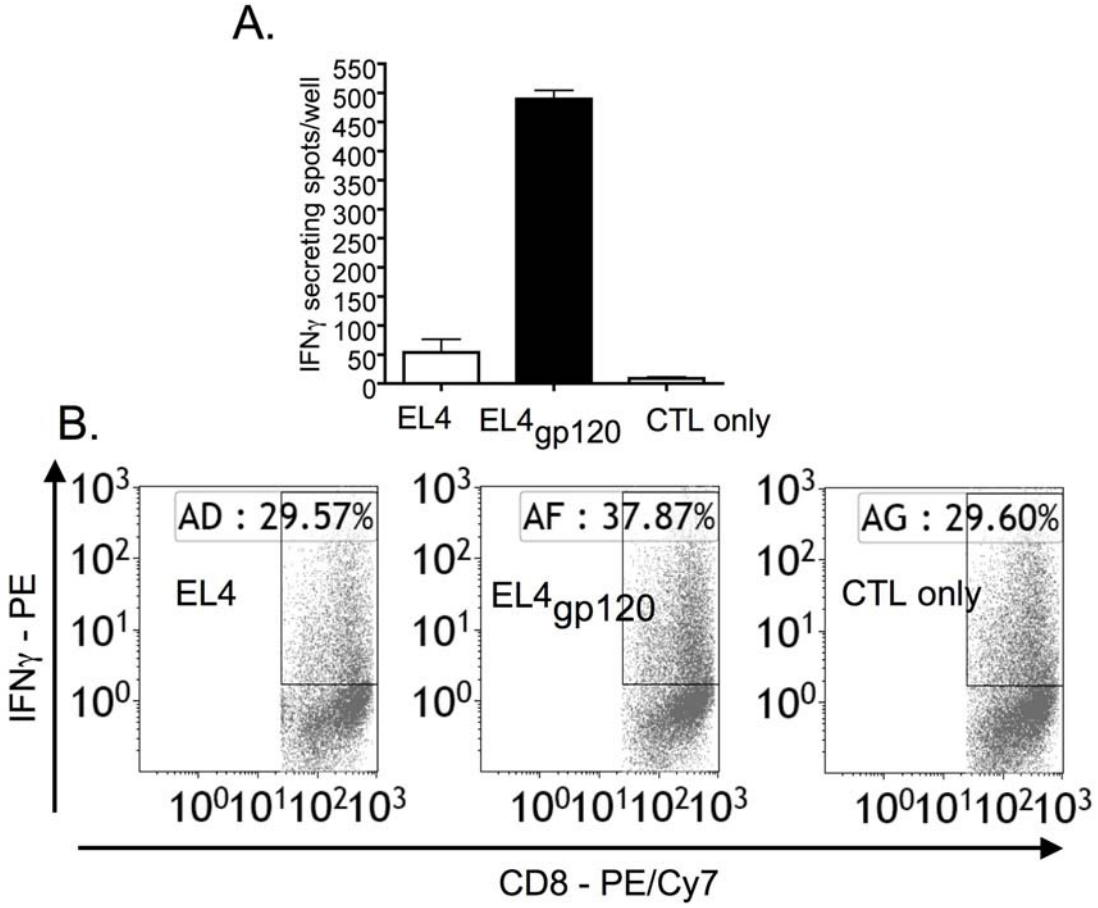

Figure 8. gp120-specific IFNγ production by CD8$^+$ T cells was elicited in the *in vitro* model. (A) Splenocytes (1 x 10^6 cells/well) were co-cultured with irradiated DC2.4$_{gp120}$ cells (1 x 10^5 cells/well) for 5 days. Elicited cells were assayed for CTL activity against EL4$_{gp120}$ or parental EL4 target cells. IFNγ secretion was measured by ELISPOT. Each well received 1 x 10^6 effectors and 5 x 10^4 target cells. No target cells were added to the CTL only group. (B-C) Labeled splenocytes were co-cultured with irradiated DC2.4$_{gp120}$ cells and restimulated with EL4$_{gp120}$ or parental EL4 target cells at a ratio of 20:1 as in A. Brefeldin A was added during the last 6 h of incubation. Cells were stained for viability, surface CD8, and intracellular IFNγ. Cells were gated on singlet, viable, lymphocyte, and CD8$^+$ populations. Cells were analyzed for IFNγ production and CD8$^+$ T cell proliferation in the plots.

Figure 8 (cont'd)

C.

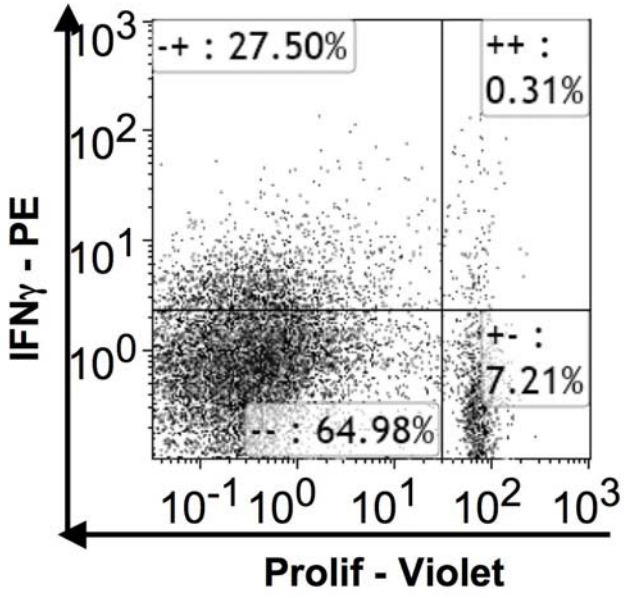

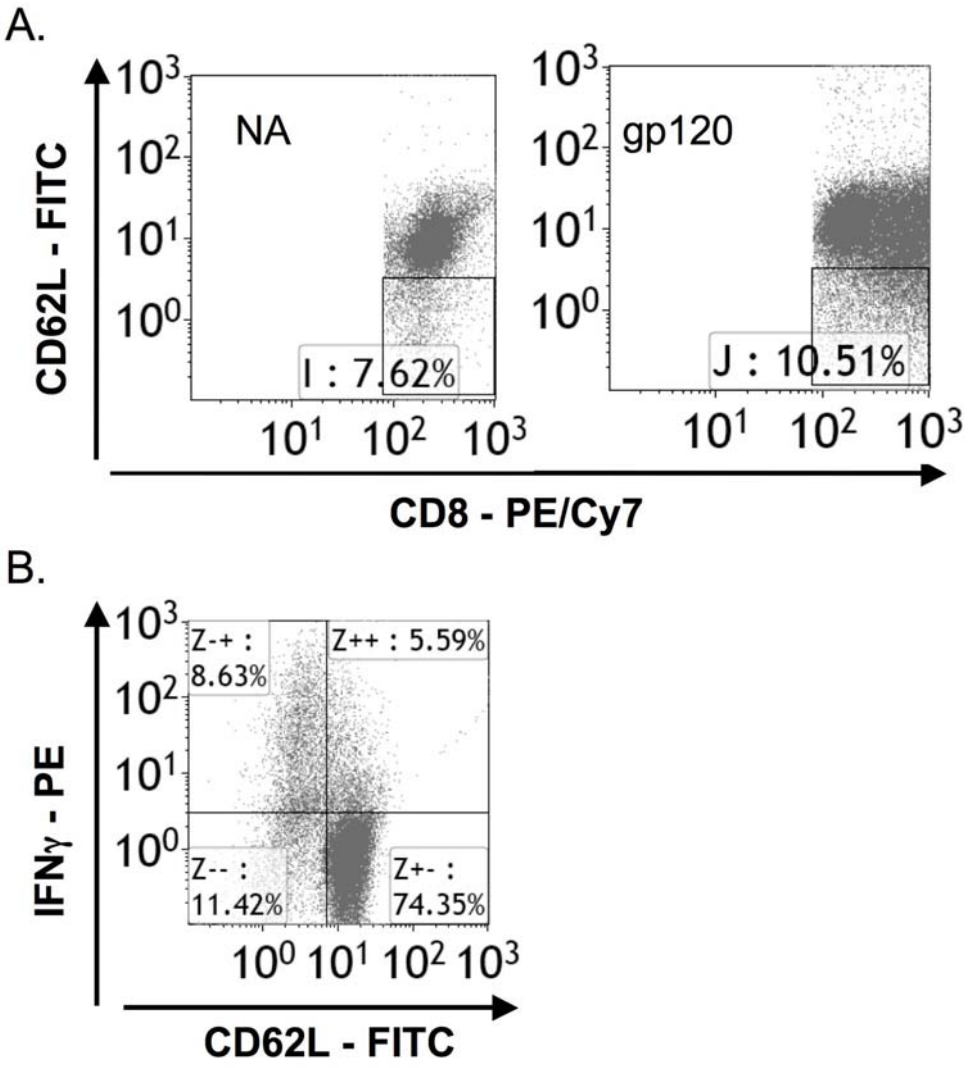

Figure 9. Differentiation of gp120-specific CD8$^+$ T cells was elicited in the *in vitro* model. (A) Splenocytes (1 x 10^6 cells/well) from C57Bl/6 mice were incubated with irradiated DC2.4$_{gp120}$ cells (1 x 10^5 cells/well). DC2.4$_{gp120}$-elicited (gp120, day 5) and naive (NA) splenocytes were stained for viability, CD8, and CD62L. The percent of CD62L^{low} cells within CD8$^+$ T cells is presented in each plot. (B) Elicited cells were restimulated with EL4$_{gp120}$ target cells and analyzed for IFNγ and CD62L expression by CD8$^+$ T cells in one plot. (A-B) Three replicates were concatenated for each treatment in the flow cytometric analysis.

C. Differential effects of cannabinoids on $CD8^+$ T cell IFNγ production and proliferation

When THC was added at the initiation of the co-culture, IFNγ release by CTL was suppressed with increasing concentrations of THC (Fig. 10A), suggesting modulation by THC during the elicitation of CTL effectors. Interestingly, enhancement of the CTL IFNγ response by THC was also observed in some experiments (Fig. 10B). The overall THC effect was modest, but the trend towards suppression or enhancement was clear. An inverse correlation between THC effect and the level of IFNγ response, represented by percent of $IFN\gamma^+CD8^+$ T cells in the VH group, was drawn based on the data from eight separate experiments (Fig. 10C; $p = 0.0272$, $R^2 = 0.5841$).

In light of the differential modulation on the CTL IFNγ response by THC (Fig. 10C) and the correlation between the IFNγ response and $CD8^+$ T cell proliferation by day 5 (Fig. 8C), we sought to investigate the effect of THC on $CD8^+$ T cell proliferation during the elicitation phase. These experiments were performed on day 5 because the majority of $CD8^+$ T cells exhibited a fully proliferative phenotype by day 5 following elicitation (Fig. 7). Again, an inverse correlation was observed between the effect of THC and the magnitude of stimulation: THC decreased the percent of proliferating $CD8^+$ T cells under conditions in which the IFNγ response was suppressed (Fig. 11A), but increased the percent of proliferating $CD8^+$ T cells under conditions in which the IFNγ response was enhanced (Fig. 11B). The inverse relationship can be seen in Fig. 11C ($p = 0.0099$, $R^2 = 0.6968$).

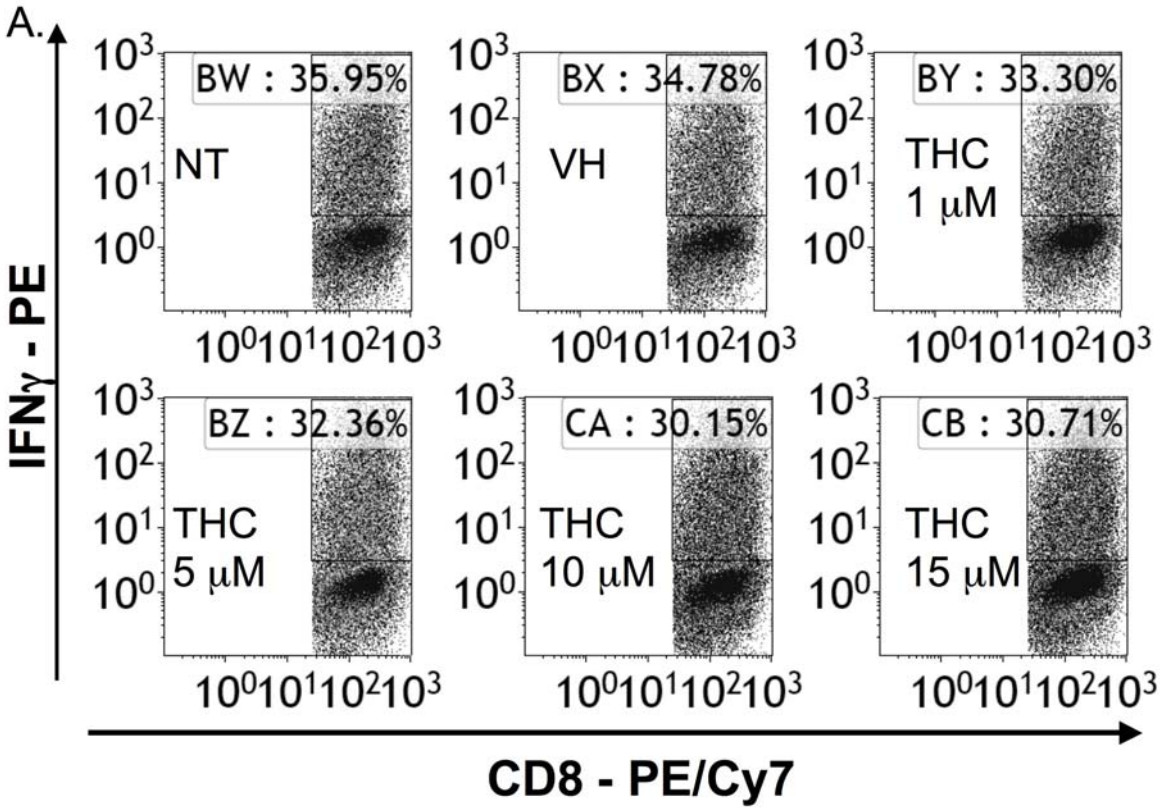

Figure 10. Differential effects of THC on IFNγ production. (A-B) Splenocytes (1 x 10^6 cells/well) were co-cultured with irradiated DC2.4$_{gp120}$ cells (1 x 10^5 cells/well) in the presence of THC (1, 5, 10, 15 μM) or VH (0.1% ethanol) or no treatment (NT). On day 5, elicited cells (1 x 10^6 cells/well) were restimulated with EL4$_{gp120}$ or parental EL4 target cells (5 x 10^4 cells/well). Brefeldin A was added during the last 6 h of incubation. Cells were stained for viability, surface CD8, and intracellular IFNγ. Cells were gated on singlet, viable, lymphocyte, and CD8$^+$ populations. The percent of IFNγ$^+$ cells within the CD8$^+$ T cell population were analyzed, and data from the EL4$_{gp120}$ target group are presented here. One example of THC-mediated suppression is presented in panel A, and one example of THC-mediated enhancement is presented in panel B. (C) The inverse correlation between the magnitude of IFNγ response in VH and the THC effect on the response was evaluated using data collected from eight independent experiments.

Figure 10 (cont'd)

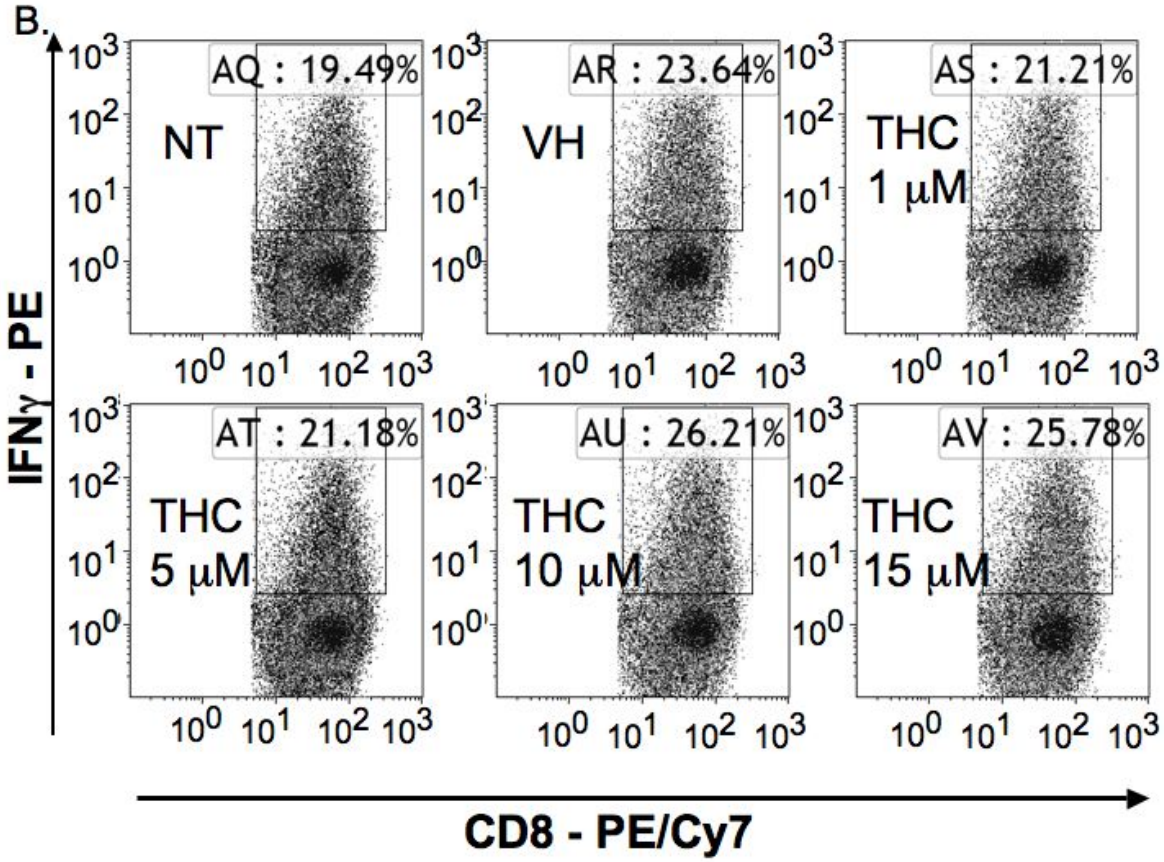

Figure 10 (cont'd)

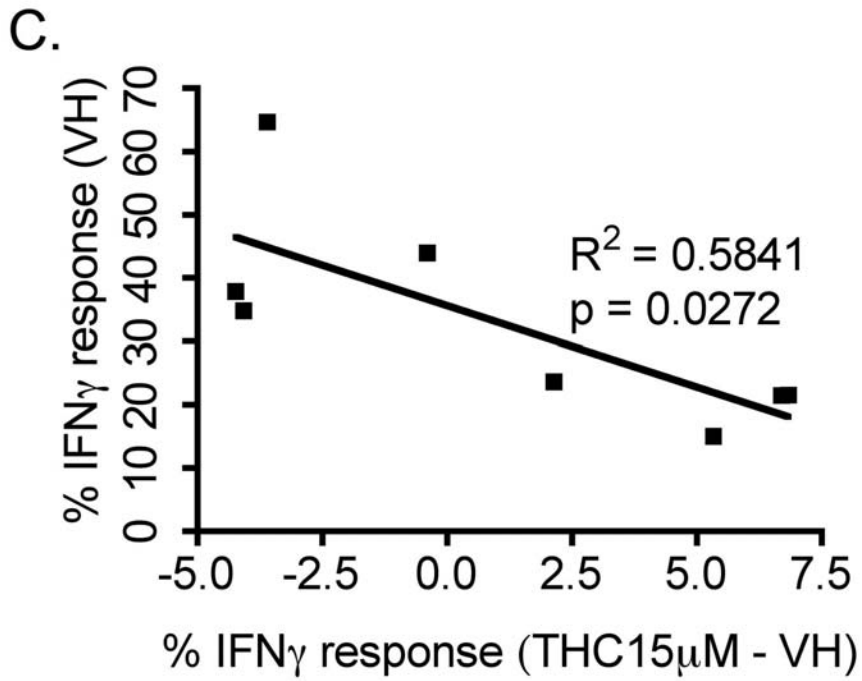

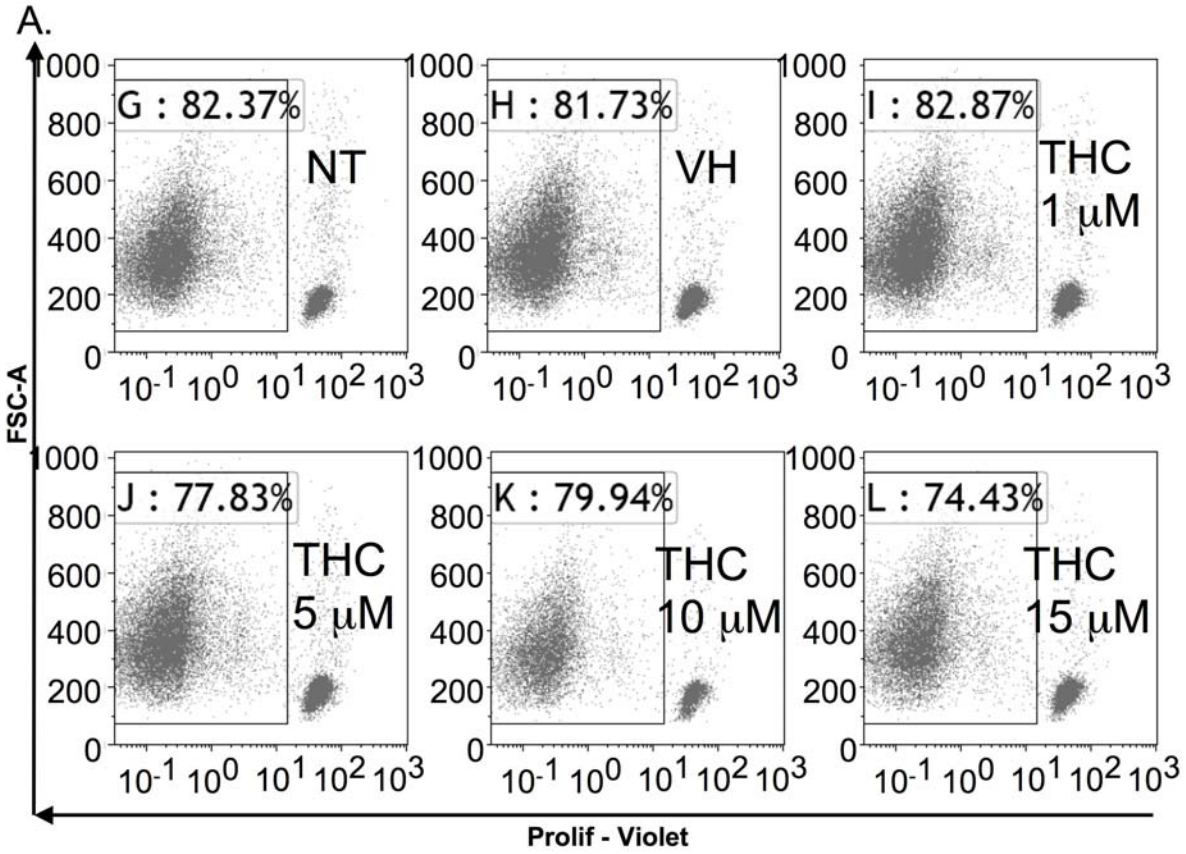

Figure 11. Differential effects of THC on CD8$^+$ T cell proliferation. (A-B) CellTrace Violet-labeled splenocytes (1 x 10^6 cells/well) were co-cultured with irradiated DC2.4$_{gp120}$ cells (1 x 10^5 cells/well) in the presence of THC (1, 5, 10, 15 μM) or VH (0.1% ethanol) or no treatment (NT). Cells were stained for viability and surface CD8. Cells were gated on singlet, viable, lymphocyte, and CD8$^+$ populations. The percent of the proliferated CD8$^+$ T cell population is presented. One example of THC-mediated suppression is presented in panel A, and one example of THC-mediated enhancement is presented in panel B. (C) The inverse correlation between the magnitude of proliferation in VH and the THC effect was evaluated using data collected from eight independent experiments.

Figure 11 (cont'd)

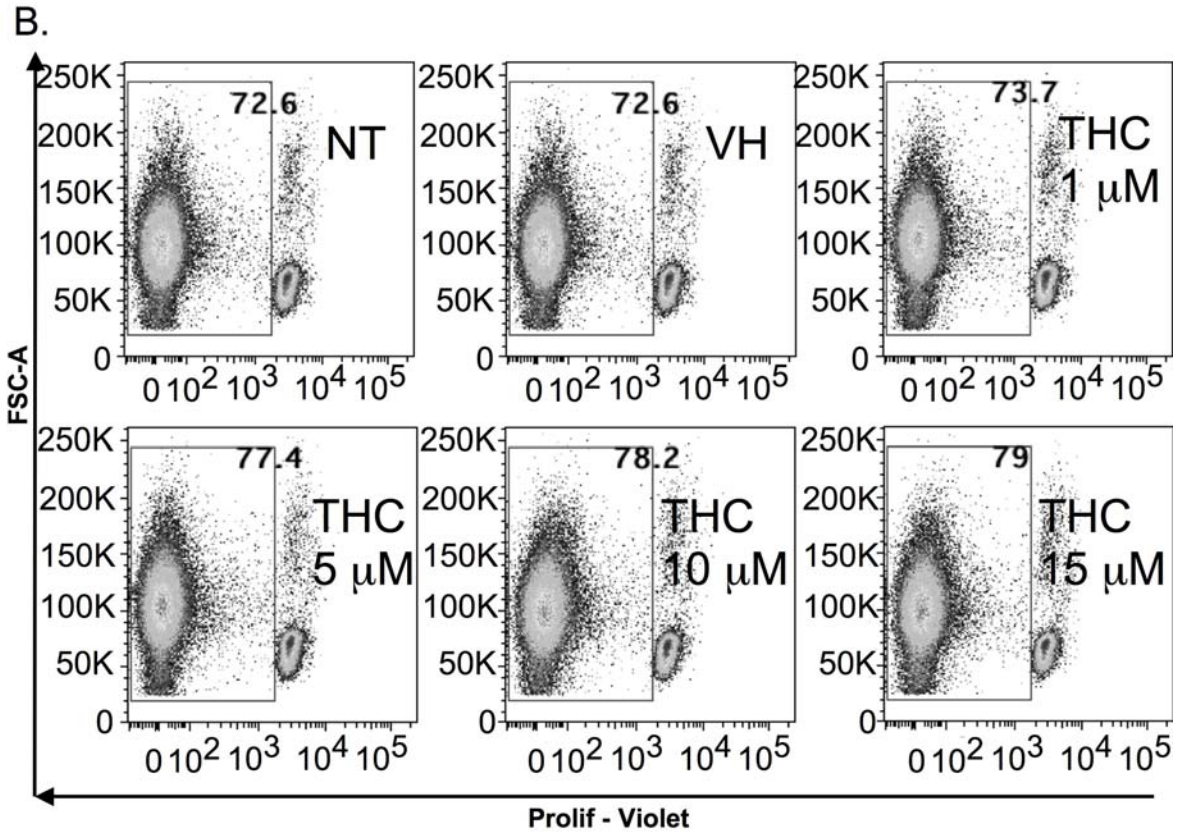

Figure 11 (cont'd)

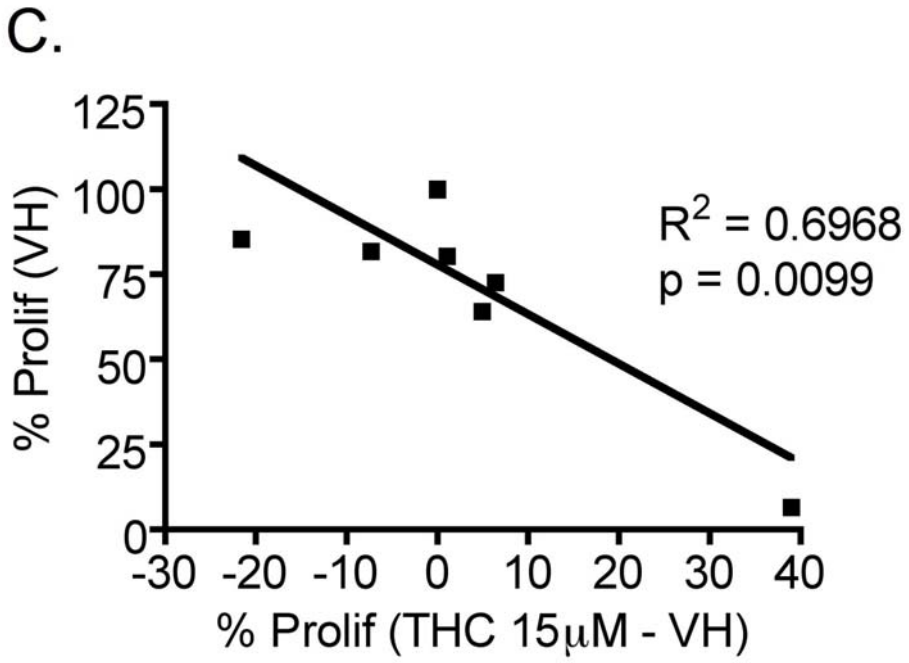

The role of CB_1/CB_2 in the THC-modulated differential effects was also investigated using $CB_1^{-/-}CB_2^{-/-}$ (KO) mice. Both C57Bl/6 wild-type (WT) and KO $CD8^+$ T cells exhibited a gp120-specific IFNγ response, and KO $CD8^+$ T cells showed an enhanced response when compared with WT $CD8^+$ T cells (Fig. 12A). In addition, in three separate experiments, THC produced a concentration-dependent enhancement on gp120-specific IFNγ production in WT $CD8^+$ T cells, with the effect at 10 and 15 μM being significantly different from the VH control (Fig. 12B). On the other hand, THC produced a trend toward enhancement on gp120-specific IFNγ response in KO $CD8^+$ T cells, but to a much lesser extent when compared with the response in WT $CD8^+$ T cells and the effect was not significant (Fig. 12B), suggesting a CB_1/CB_2-dependent mechanism.

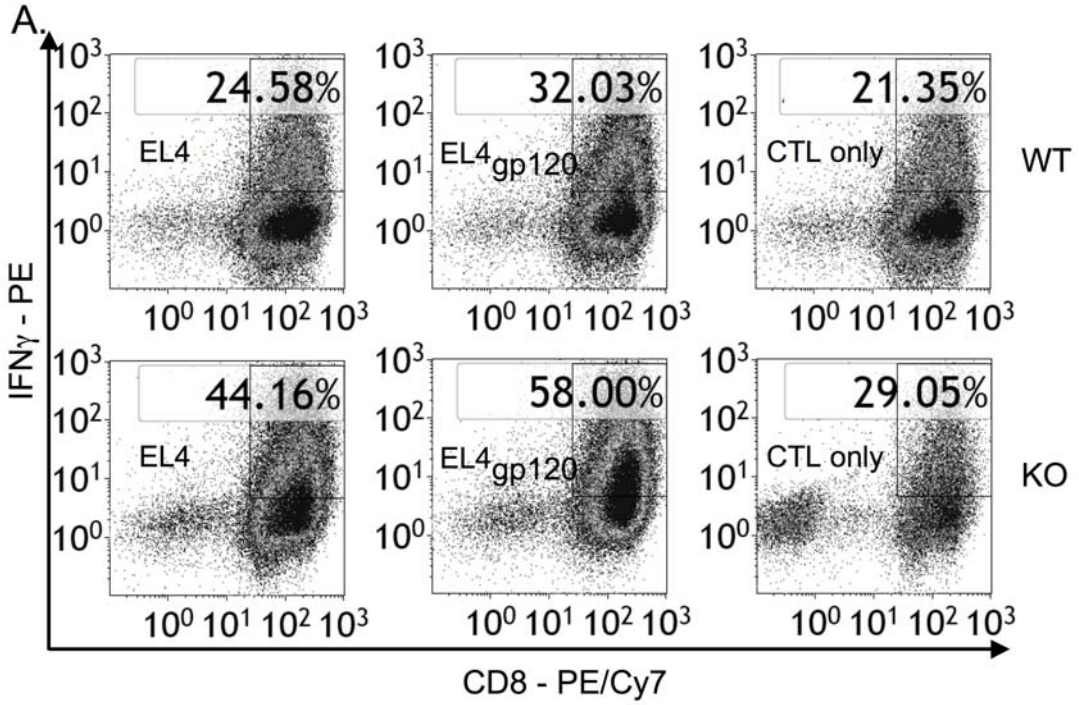

Figure 12. THC-mediated effects on IFNγ response in a CB_1/CB_2-dependent manner. (A) Splenocytes (1 x 10^6 cells/well) from C57Bl/6 wild-type (WT) and $CB_1^{-/-}CB_2^{-/-}$ (KO) mice were co-cultured with irradiated $DC2.4_{gp120}$ cells (1 x 10^5 cells/well), respectively. On day 5, elicited cells (1 x 10^6 cells/well) were restimulated with $EL4_{gp120}$ or parental EL4 target cells (5 x 10^4 cells/well). Brefeldin A was added during the last 6 h of incubation. Cells were stained for viability, surface CD8, and intracellular IFNγ. Cells were gated on singlet, viable, lymphocyte, and $CD8^+$ populations. The percent of $IFN\gamma^+$ cells within the $CD8^+$ T cell population are presented. (B) Splenocytes from WT and KO mice were co-cultured with $DC2.4_{gp120}$ cells as described in A, in the presence of THC (1, 5, 10, 15 μM) or VH (0.1% ethanol). The correlation between the magnitude of IFNγ response in VH and the effect of THC at various concentrations on the response was evaluated using data collected from three independent experiments. * $p < 0.05$, ** $p < 0.01$ as compared to respective VH.

Figure 12 (cont'd)

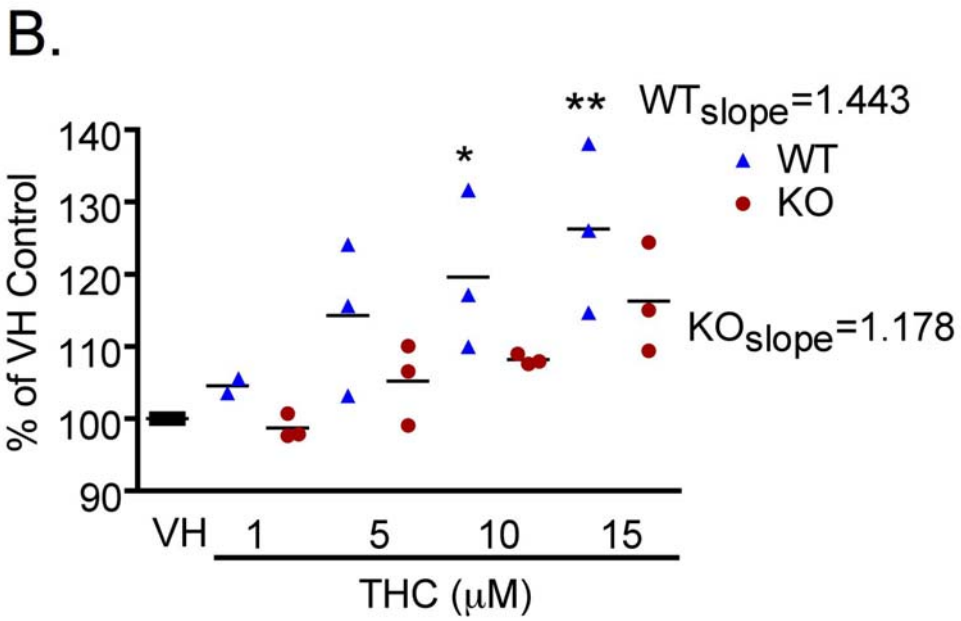

The differential effects of THC on the IFNγ response were reminiscent of previous reports in the literature in which both positive and negative modulatory effects of cannabinoids have been observed [144, 159-161, 170, 172, 174, 175, 233]. However, the mechanisms for such differential effects of cannabinoids have produced significant confusion in the literature and are poorly understood. Thus, we sought to determine if the correlation between the magnitude of stimulation and the cannabinoid-mediated effect was broadly observed using two plant-derived cannabinoids (THC and CBD) and readily titratable T cell activators. THC and CBD were compared since they possess different affinities for CB_1 and CB_2 [101, 102]. We anticipated that the effects of THC and CBD would be similar since we had previously demonstrated that cannabinoid-mediated modulation of T cell function occurred independent of cannabinoid receptors [159, 162, 208]. In response to "optimal" stimulation with either 10x P/I (40 nM/0.5 μM) or immobilized anti-CD3 plus soluble anti-CD28 antibodies (iCD3/CD28), IFNγ was robustly induced, which was suppressed by THC and CBD, similar to previous findings [144, 159, 162] (Fig. 13A, B and C). In contrast, IFNγ production following "suboptimal" stimulation using 1x P/I (4 nM/0.05 μM) was low, and was enhanced by CBD, but not THC (Fig. 13A, and B). Interestingly, in response to soluble anti-CD3 plus soluble anti-CD28 antibodies (sCD3/CD28), which was previously used as a suboptimal activation for IL-2 [174, 175], IFNγ production was robustly induced and then suppressed by both THC and CBD (Fig. 13D).

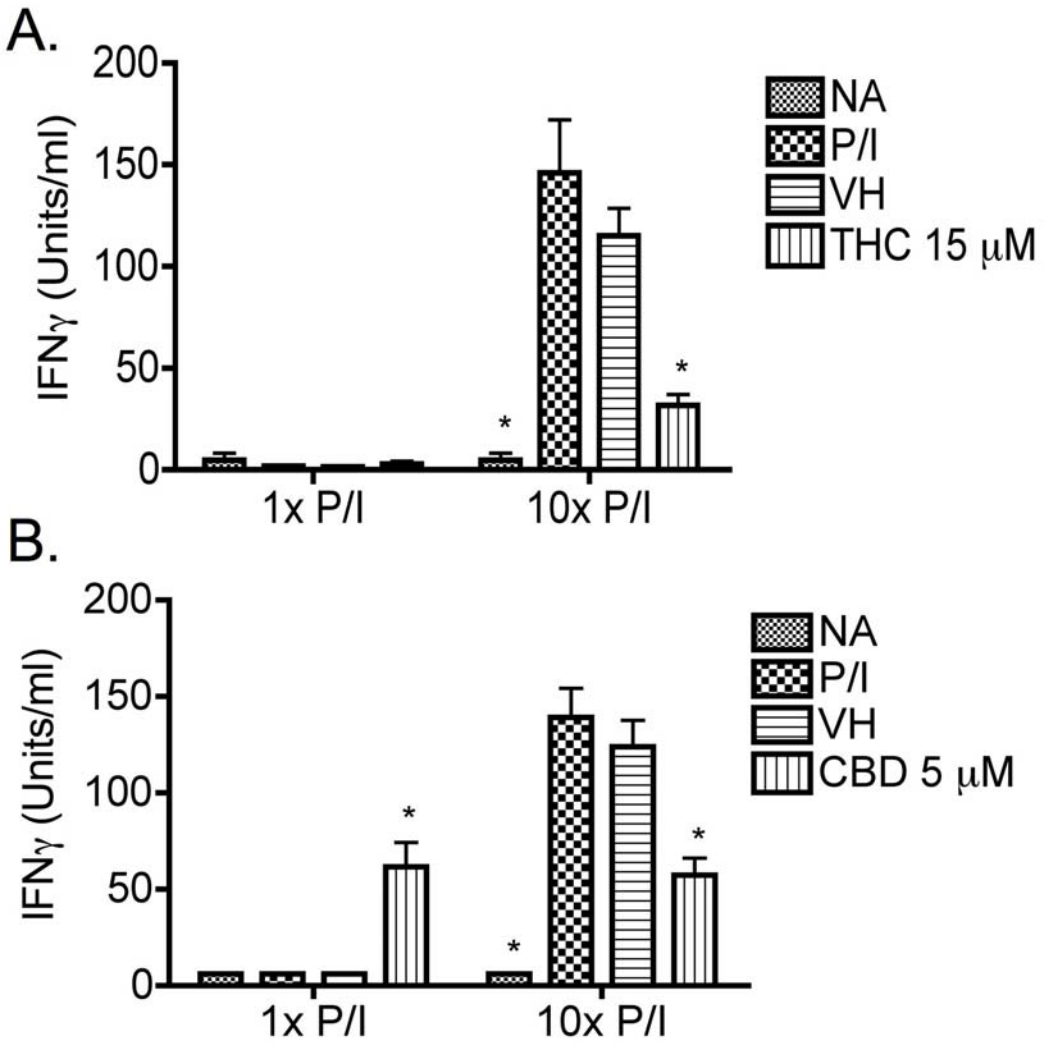

Figure 13. Effects of cannabinoids on IFNγ production in response to different stimuli. B6C3F1 splenocytes (8 x 10^5 cells/well) were treated with THC (15 μM; A) or CBD (5 μM; B) for 30 min, and then activated with P/I (40 nM/0.5 μM, 10x P/I or 4 nM/0.05 μM, 1x P/I) for 18-24 h. (C-D) B6C3F1 splenocytes (8 x 10^5 cells/well) were treated with THC or CBD at various concentrations for 30 min, and then activated with immobilized anti-CD3 plus soluble anti-CD28 (iCD3/CD28; C) or soluble anti-CD3 plus soluble anti-CD28 (sCD3/CD28; D) for 2 days. (A-D) IFNγ in the supernatant was quantified by ELISA. Data are presented as the mean units/ml ± S. E. of triplicate cultures. * $p < 0.05$ as compared to respective VH. Data are representative of at least two separate experiments.

Figure 13 (cont'd)

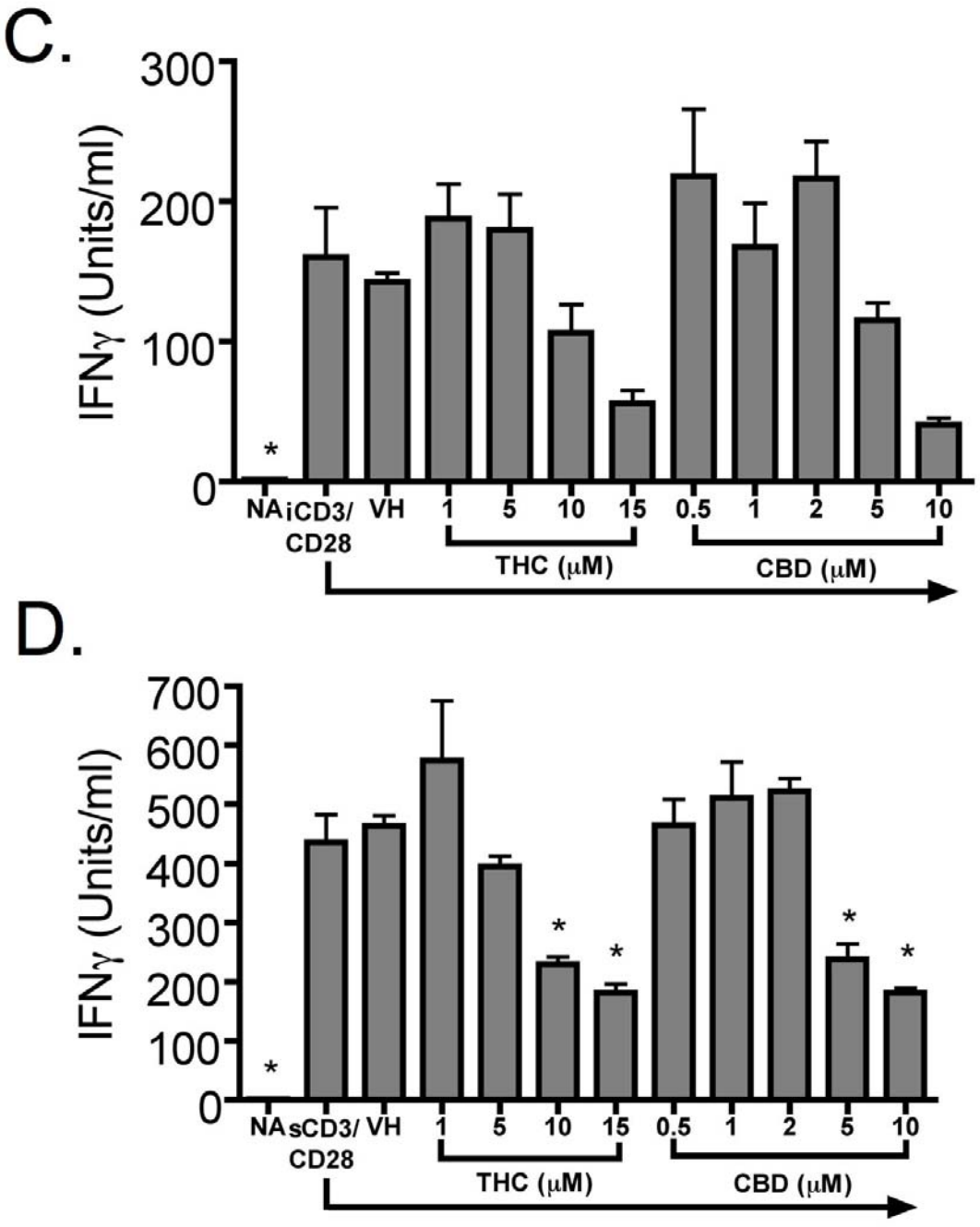

D. Differential effects of cannabinoids on IL-2 response

With the demonstration that THC differentially modulated $CD8^+$ T cell proliferation in response to $DC2.4_{gp120}$ stimulation, IL-2 production in the presence of P/I or anti-CD3/CD28 and the effect of cannabinoids were evaluated. Optimal stimulation, 10x P/I or iCD3/CD28, induced robust IL-2 production, which was significantly suppressed by THC and CBD, similar to previous reports [144, 159, 162, 175] (Fig. 14A and B). In response to 1x P/I, CBD, but not THC, enhanced IL-2 production (Fig. 14A), consistent with the differential cannabinoid effects on the IFNγ response. Again, using sCD3/CD28 as a suboptimal stimulation for IL-2, as previously performed [174, 175], IL-2 production was low, and was enhanced by both THC and CBD (Fig. 14C).

Additional experiments were conducted in order to decipher the mechanisms by which cannabinoids differentially affected cytokine production with a focus on 1x P/I and CBD. Since P/I likely activated all cells in the splenocyte population, a comparison between splenocytes and purified T cells in response to 1x P/I was performed and demonstrated that the CBD-induced enhancement of the IL-2 response also occurred in purified T cells (Fig. 15). Moreover, FACS analysis of the cytokine-producing cells in splenocytes in response to 1x P/I plus CBD demonstrated that $CD4^+$ T cells produced most of the IL-2, whereas $CD4^+$ and $CD8^+$ T cells and NK cells all contributed to IFNγ production (Fig. 16). Finally, in order to determine whether the differential effects of cannabinoids also occur in human PBMC, human IL-2 production was quantified. CBD suppressed IL-2 production when using 10x P/I, and enhanced IL-2 production when using 1x P/I (Fig. 17).

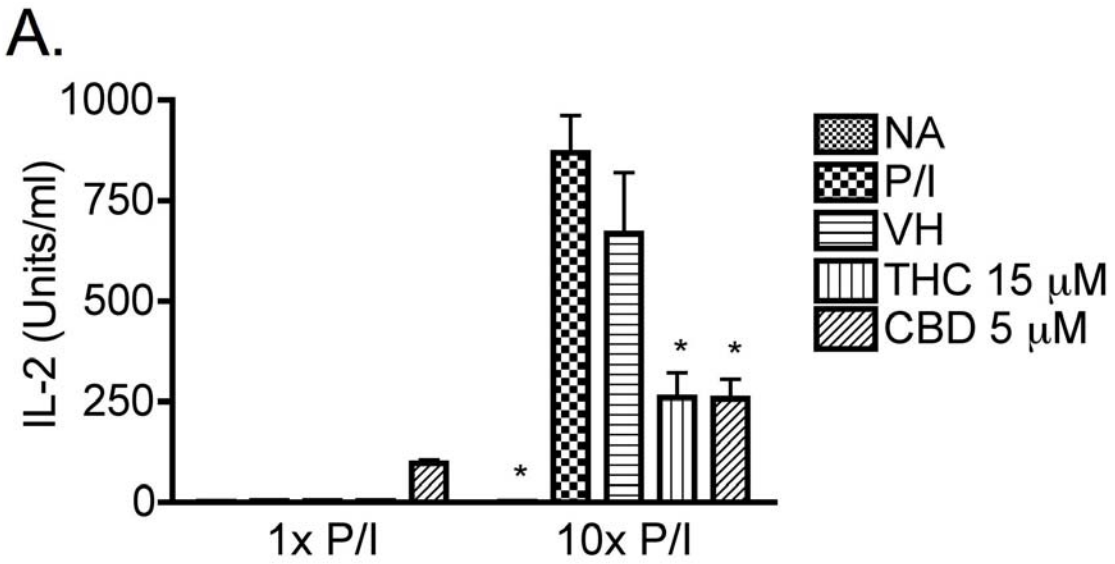

Figure 14. Effects of cannabinoids on IL-2 production in response to different stimuli. (A) B6C3F1 splenocytes (8 x 10^5 cells/well) were treated with THC (15 μM) or CBD (5 μM) for 30 min, and then activated with P/I (40 nM/0.5 μM, 10x P/I or 4 nM/0.05 μM, 1x P/I) for 18-24 h. (B-C) B6C3F1 splenocytes (8 x 10^5 cells/well) were treated with THC or CBD at various concentrations for 30 min, and then activated with immobilized anti-CD3 plus soluble anti-CD28 (iCD3/CD28; B) or soluble anti-CD3 plus soluble anti-CD28 (sCD3/CD28; C) for 2 days. (A-C) IL-2 in the supernatant was quantified by ELISA. Data are presented as the mean units/ml ± S. E. of triplicate cultures. * $p < 0.05$ as compared to respective VH. Data are representative of at least two separate experiments.

Figure 14 (cont'd)

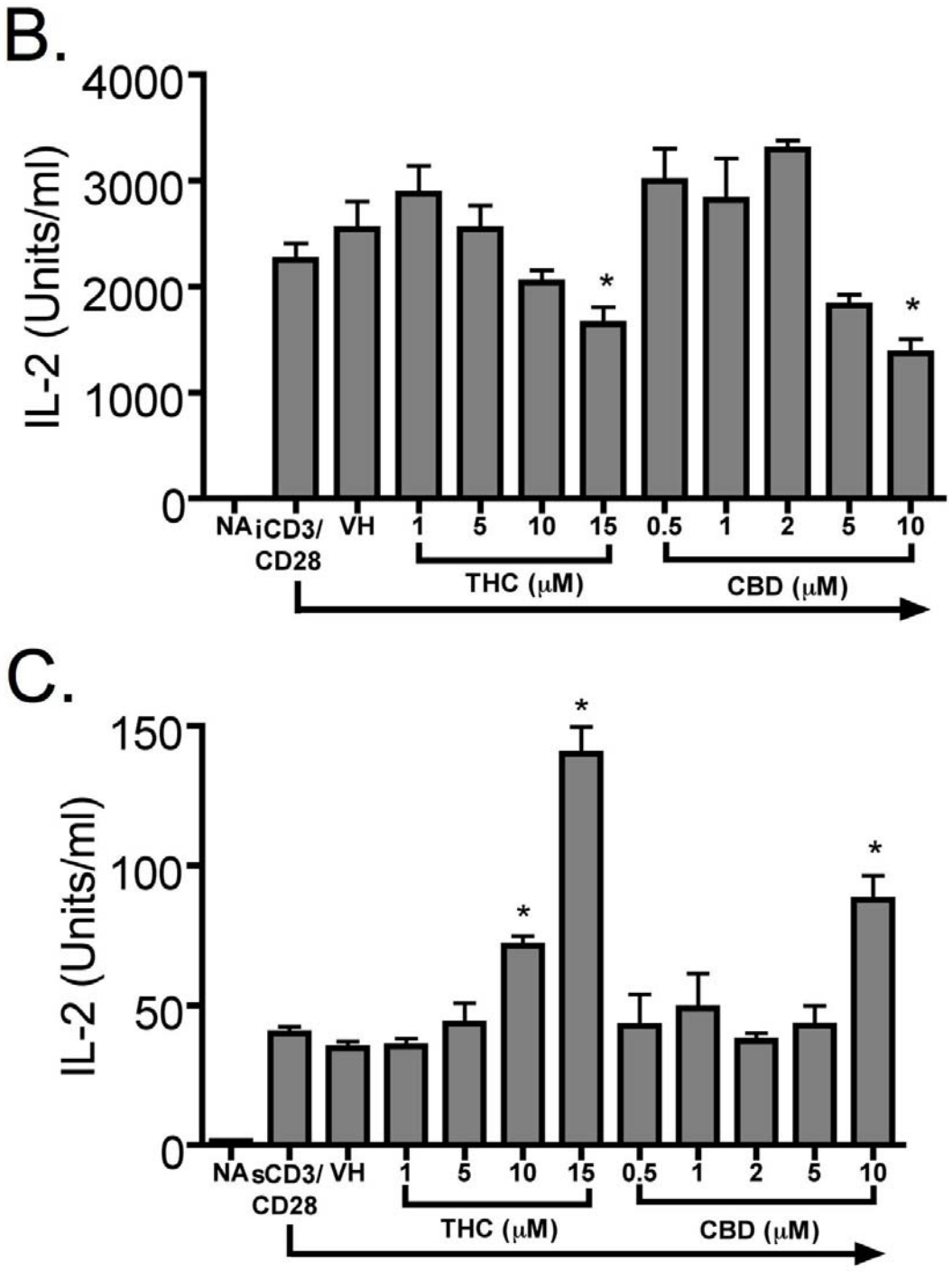

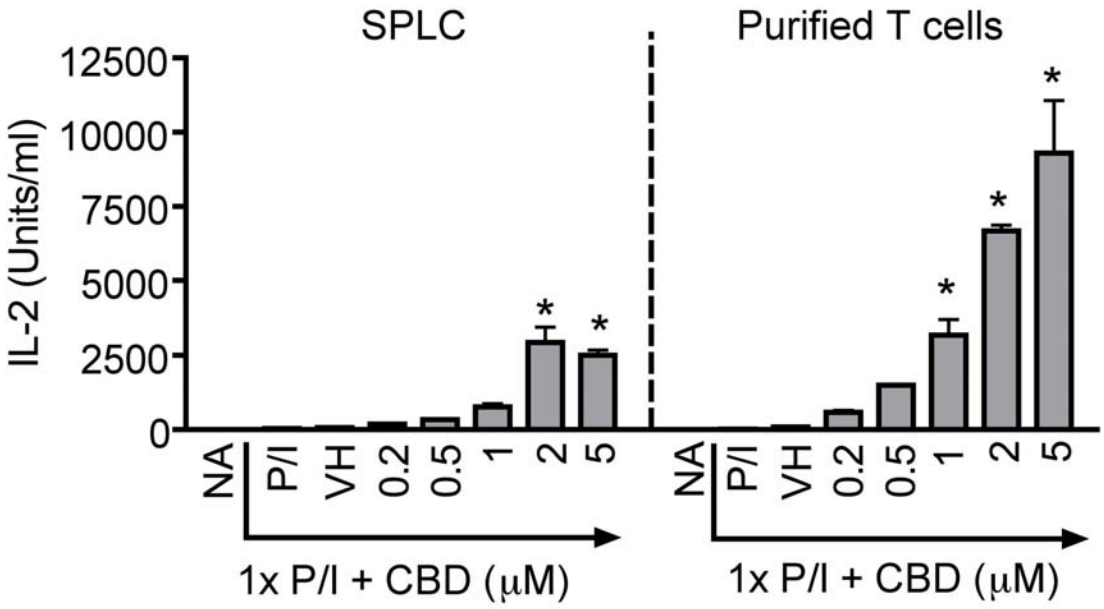

Figure 15. Enhancement of the IL-2 response by CBD in purified T cells. B6C3F1 splenocytes or T cells purified from the splenocytes (SPLC, 8 x 10^5 cells/well) were treated with 0.2 – 5 μM CBD for 30 min, then activated with 1x P/I for 48 h. IL-2 in the supernatant was quantified by ELISA. Data are presented as the mean units/ml ± S. E. of triplicate cultures. * $p < 0.05$ as compared to respective VH. Data are representative of at least two separate experiments.

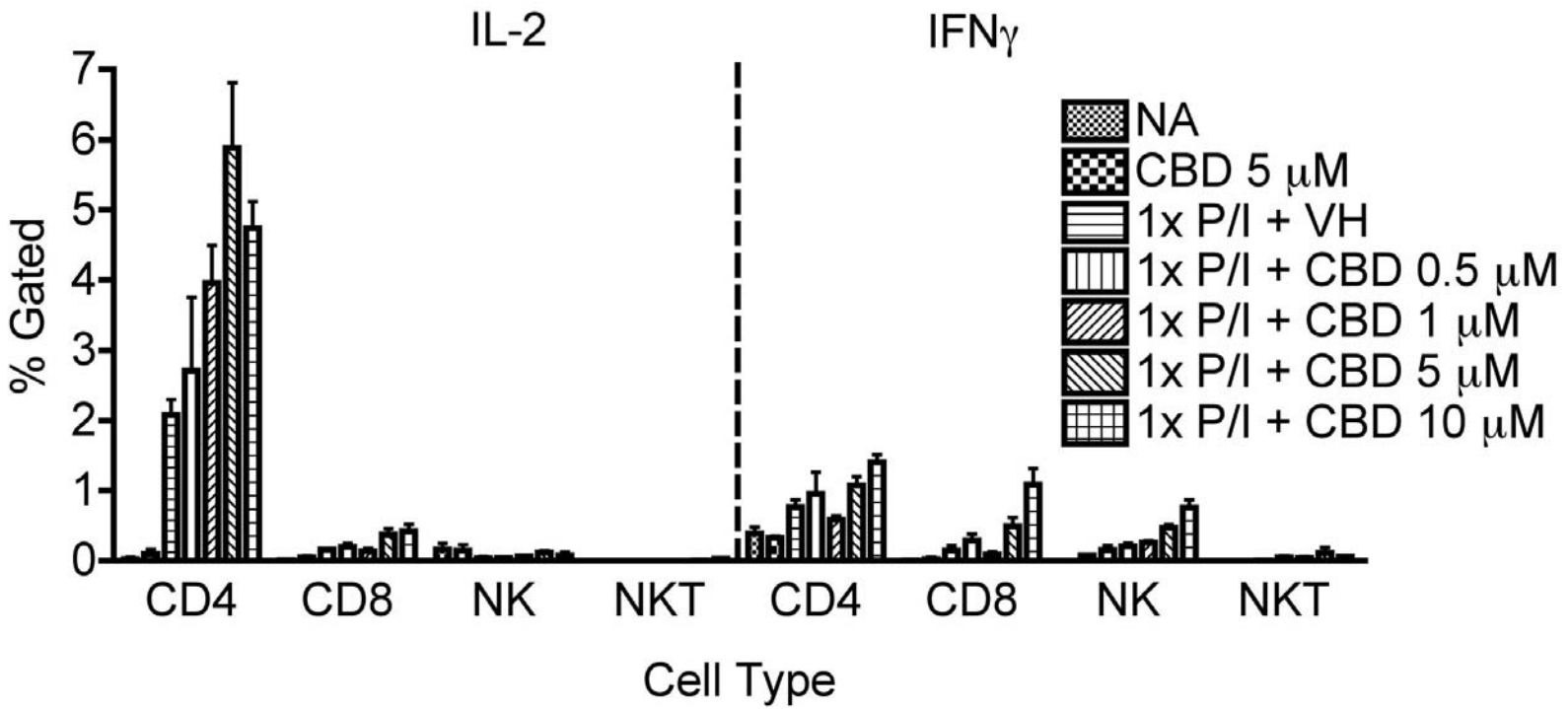

Figure 16. Enhancement of cytokine response by CBD in different cellular populations. B6C3F1 splenocytes (8 x 10^5 cells/well) were treated with 0.5 – 10 μM CBD for 30 min, followed by activation with 1x P/I for 18-24 h. Cells were also treated with Brefeldin A 4 h prior to harvest. Cells were stained for viability and extracellular markers, CD4, CD8, CD3 and CD49b, as well as intracellular IL-2 and IFNγ.

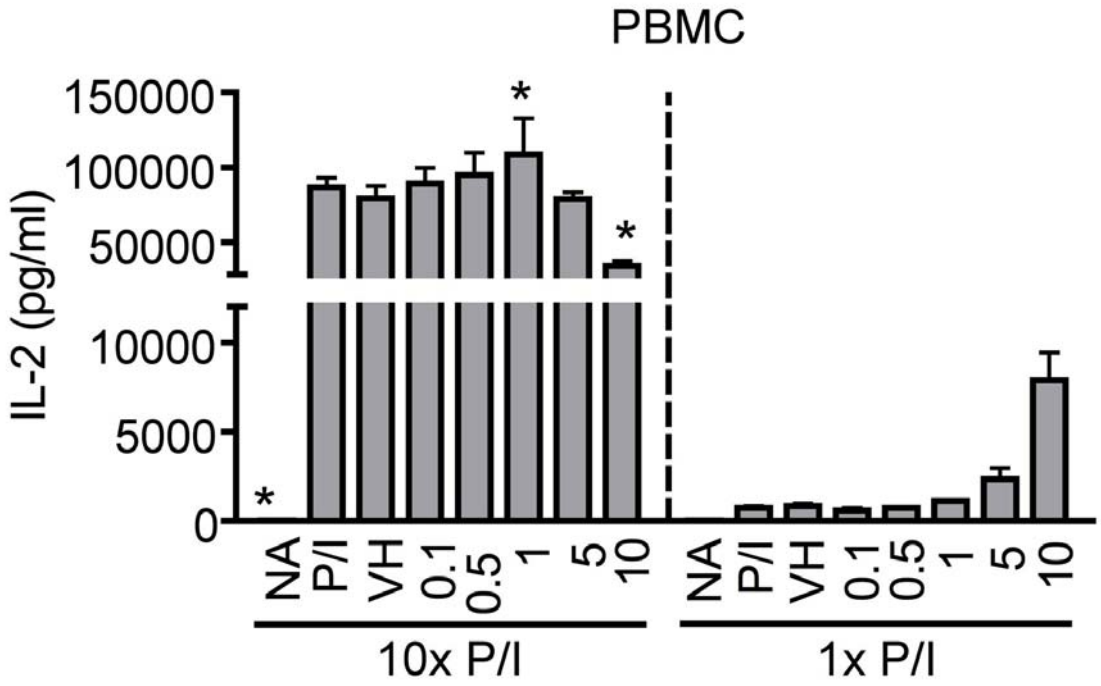

Figure 17. Differential effects of CBD on IL-2 response in human PBMC. PBMC were enriched from human leukocyte packs by density gradient centrifugation. PBMC (2 x 10^6 cells/well) were treated with 0.1 – 10 μM CBD for 30 min, then activated with 1x or 10x P/I for 18-24 h. IL-2 in the supernatant was quantified by ELISA. Data are presented as the mean units/ml ± S. E. of triplicate cultures. * $p < 0.05$ as compared to respective VH. Data are representative of at least three separate experiments.

E. Differential effects of cannabinoids on cytokine production were correlated with effects on NFAT nuclear translocation

The differential effects of cannabinoids on cytokine production was also observed at the steady state mRNA level as CBD suppressed or enhanced IFNγ and IL-2 mRNA expression in response to 10x or 1x P/I, respectively, at several time points following stimulation (Fig. 18A and 19A). In addition, CBD-induced IFNγ and IL-2 mRNA expression was increased in a concentration-dependent manner in response to 1x P/I (Fig. 18B and 19B). The concentration-dependent suppression of IFNγ and IL-2 mRNA expression by CBD on 10x P/I-stimulated splenocytes at 24 hr has been reported previously [159]. These results suggested that CBD-induced modulation of cytokine production might occur at the level of transcription. NFAT family members NFAT1 (NFATc2) and NFAT2 (NFATc1) are the two predominant NFAT proteins expressed by T cells [234], and of the two, NFAT2 is the primary form induced under lower calcium or anergic conditions [235]. Since CBD enhanced cytokine production in response to suboptimal cellular activation, and NFAT plays an important role in IFNγ and IL-2 transcription [236-239], the effect of CBD on NFAT2 nuclear translocation was examined. 10x P/I induced nuclear translocation of NFAT2, which was modestly suppressed by CBD, whereas 1x P/I-stimulated NFAT2 translocation was enhanced by CBD (Fig. 20).

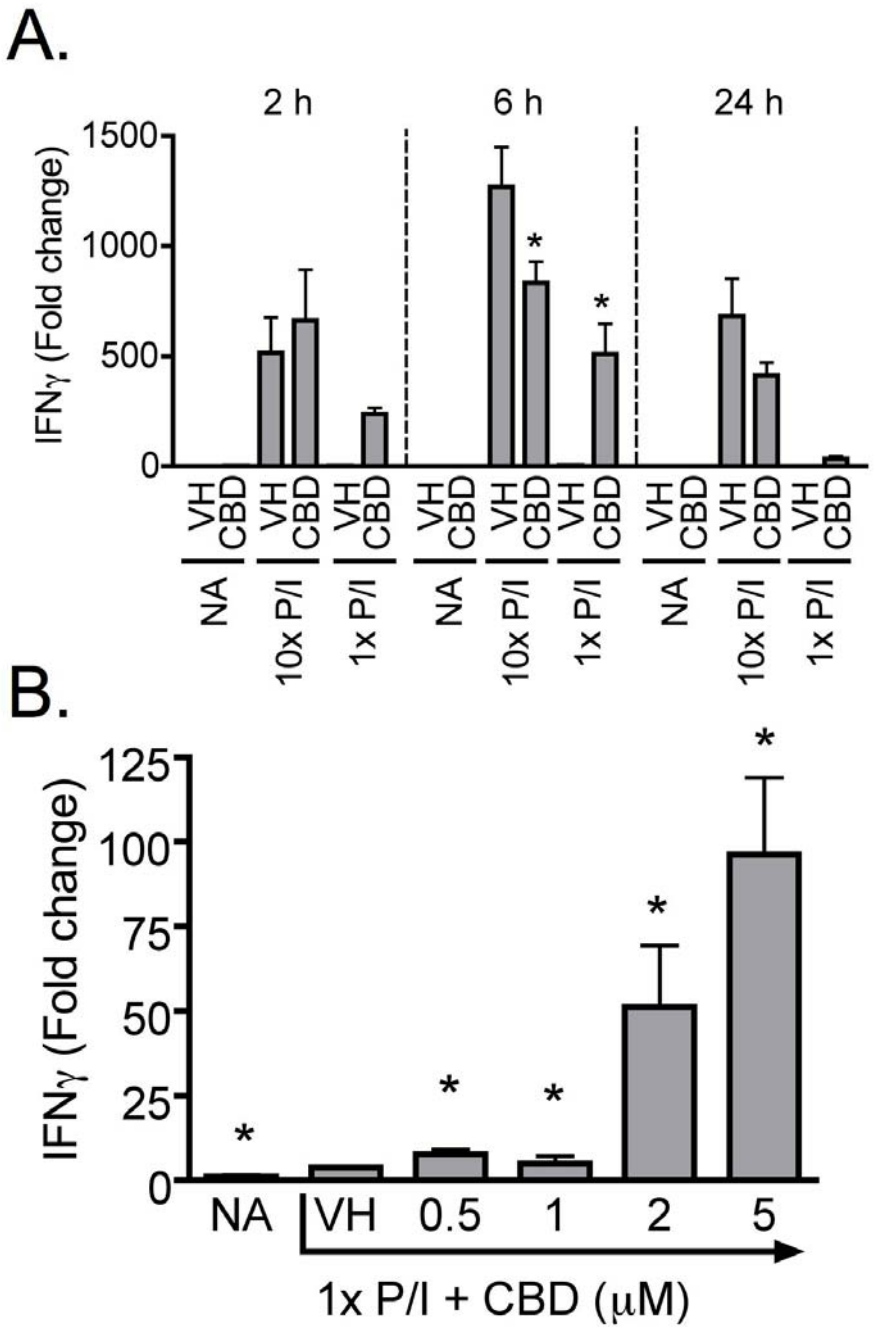

Figure 18. Cannabinoids differentially regulated IFNγ steady state mRNA expression. (A-B) B6C3F1 splenocytes (5 x 10^6 cells) were treated with CBD (0.5 – 5 μM) or VH (0.1% ethanol) for 30 min, then activated with P/I (40 nM/0.5 μM, 10x P/I or 4 nM/0.05 μM, 1x P/I) for various times. Total RNA was isolated and reverse transcribed, and Real Time PCR was performed for IFNγ. Data are expressed as the mean fold change ± S. E. of triplicate cultures. * $p < 0.05$ as compared to respective VH.

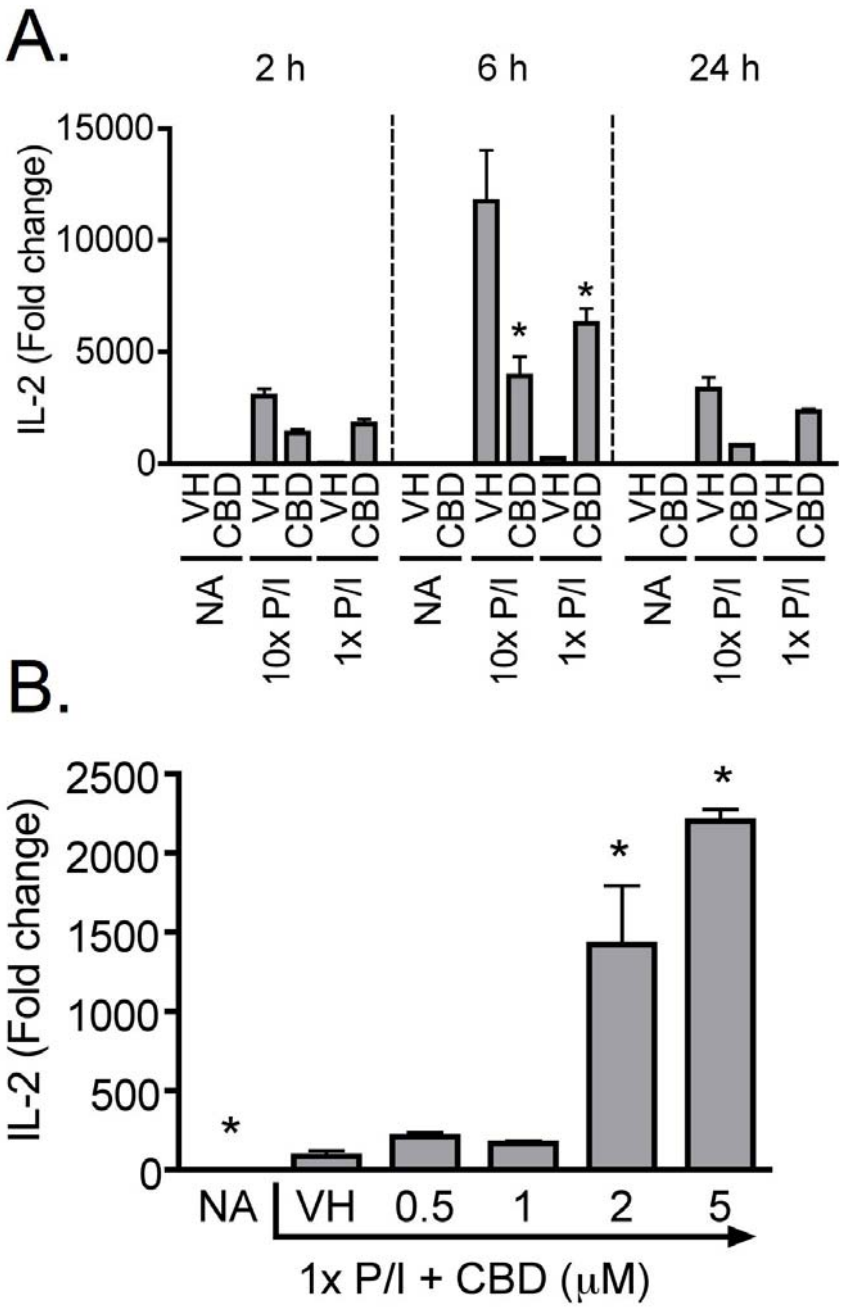

Figure 19. Cannabinoids differentially regulated IL-2 steady state mRNA expression. (A-B) B6C3F1 splenocytes (5 x 10^6 cells) were treated with CBD (0.5 – 5 μM) or VH (0.1% ethanol) for 30 min, then activated with P/I (40 nM/0.5 μM, 10x P/I or 4 nM/0.05 μM, 1x P/I) for various times. Total RNA was isolated and reverse transcribed, and Real Time PCR was performed for IL-2. Data are expressed as the mean fold change ± S. E. of triplicate cultures. * $p < 0.05$ as compared to respective VH.

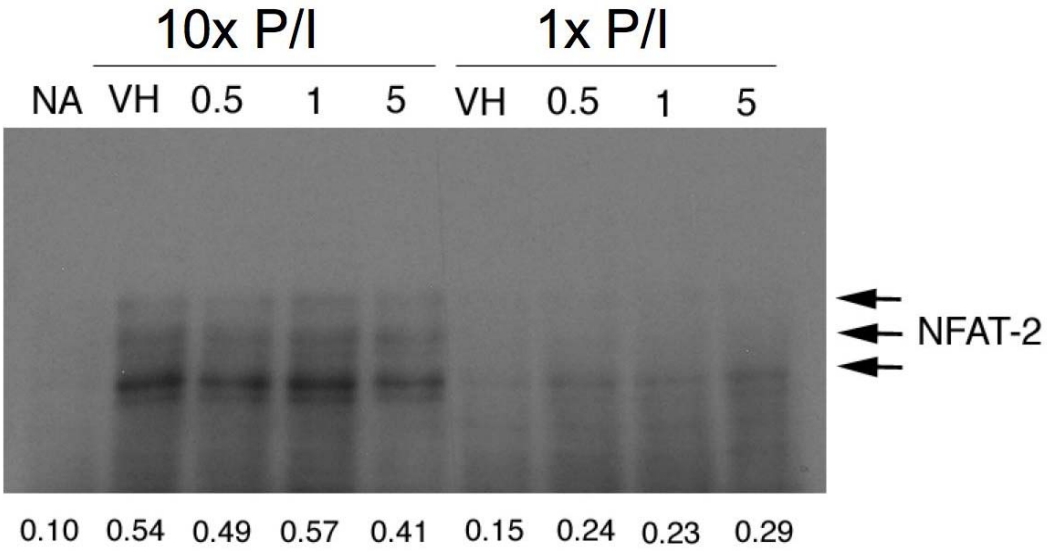

Figure 20. Cannabinoids differentially modulated nuclear translocation of NFAT2. B6C3F1 splenocytes (5 x 10^6 cells) were treated with 0.5 – 5 μM CBD or VH (0.1% ethanol) for 30 min, followed by activation with 1x or 10x P/I for 30 min. Nuclear protein was isolated and loaded into an 8% SDS-PAGE gel. NFAT2 is detected as multiple bands in the 100-130 kDa range.

F. Cannabinoids enhanced intracellular calcium regardless of the magnitude of cellular activation

Intracellular calcium is critical for activation of NFAT [236, 238], therefore we hypothesized that the effect of cannabinoids on intracellular calcium might correlate with the differential regulation of NFAT translocation and cytokine production. THC has been shown to induce intracellular calcium in resting lymphocytes [143, 163] and as seen in Fig. 21A, CBD also induced intracellular calcium in resting splenocytes in a concentration-dependent manner. 1x P/I modestly induced intracellular calcium, and both THC and CBD further elevated the level of intracellular calcium (Fig. 21B). 10x P/I robustly induced intracellular calcium, but unlike the effects of CBD or THC on NFAT nuclear translocation and cytokine production, THC and CBD further enhanced the intracellular calcium above the level induced by P/I alone (Fig. 21B).

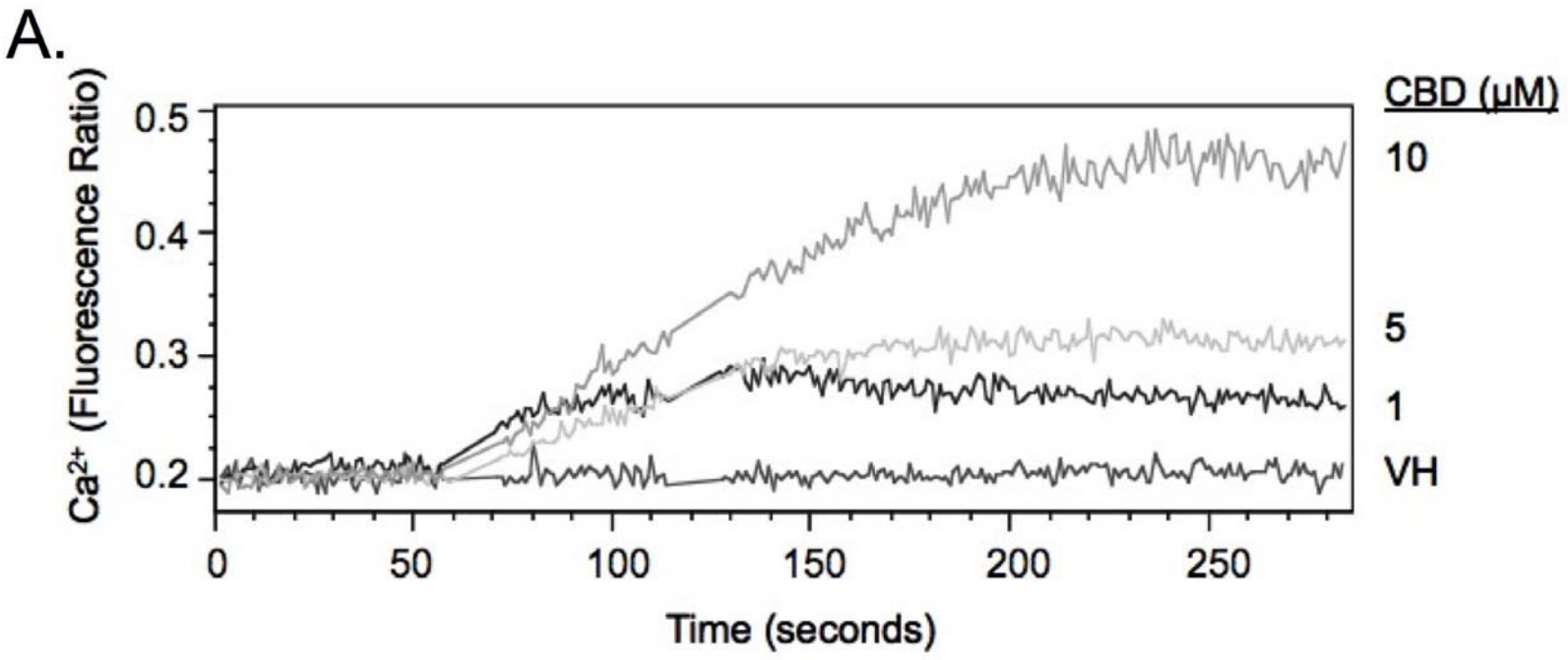

Figure 21. Cannabinoids increased intracellular calcium regardless of activation level. (A-B) B6C3F1 splenocytes (2 x 10^7 cells) were incubated with Fura Red and Fluo-3 for 30 – 60 min in the dark. Cells were then analyzed by flow cytometry, during which time they received CBD (1 – 10 μM) in panel A or THC (10 μM)/CBD (5 μM)/VH (0.1% ethanol) in panel B for 1 min followed by 1x or 10x P/I or VH (0.1% DMSO) for 3 additional min. Results are representative of at least two separate experiments.

Figure 21 (cont'd)

B.

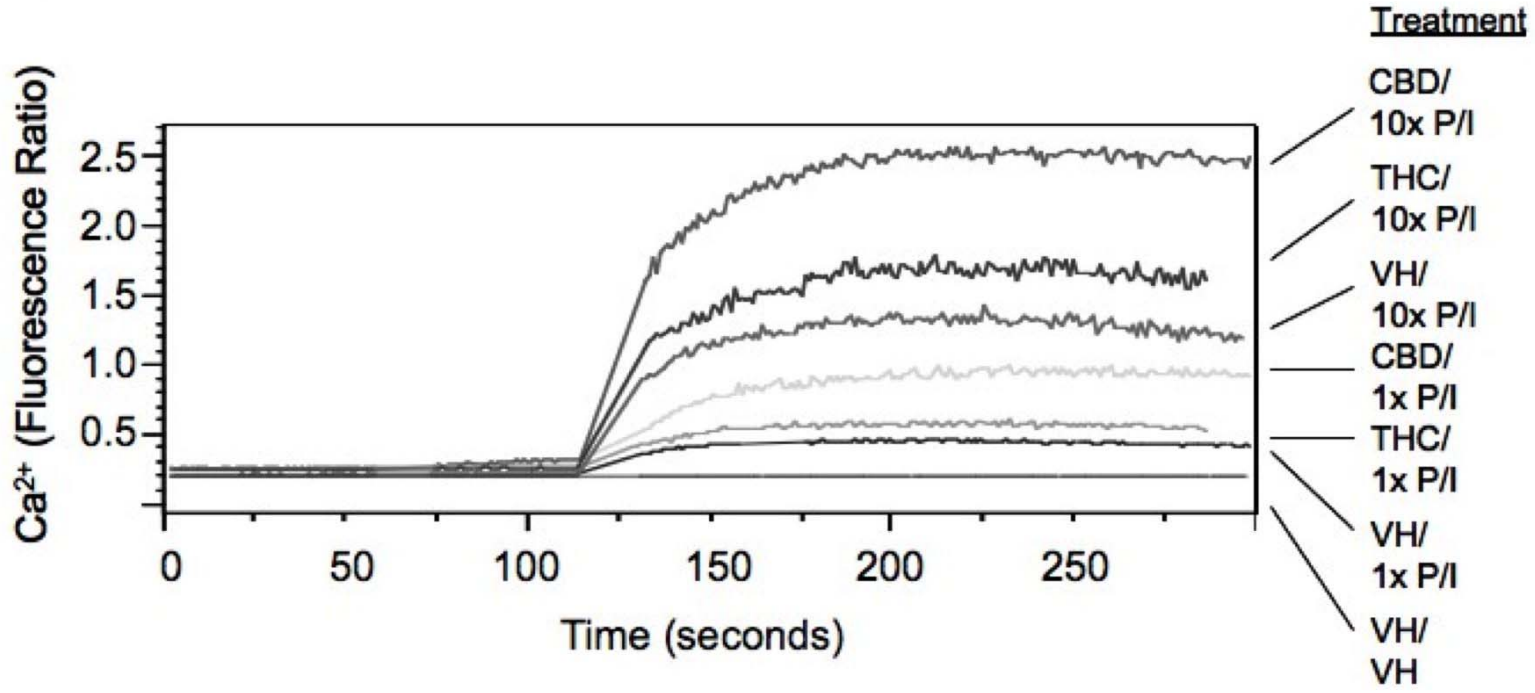

II. *In Vivo* Cannabinoid-Mediated Effects on Immune Responses to HIV_{gp120}

To investigate the effect of THC and the role of CB_1/CB_2 on gp120 antigen-specific immune responses *in vivo*, studies were designed such that the gp120-expressing plasmid was injected intramuscularly into WT and $CB_1^{-/-}CB_2^{-/-}$ mice to induce the immune responses and THC was orally given to the mice post each plasmid injection.

A. pVRCgp120 induced gp120-specific cytokine production by ELISPOT assay

To determine if pVRCgp120 plasmid DNA can elicit gp120-specifc T cell responses *in vivo*, peptides derived from HIV-1 IIIB envelope protein were split into 53 peptide pools and screened upon peptide restimulation. A robust IFNγ response by ELISPOT assay was detected when splenocytes from pVRCgp120-injected mice were restimulated with peptide pool 21 compared with the other 52 peptide pools (Fig. 22A). When peptide pool 21 was used to restimulate the splenocytes from pVRC2000-injected mice, the IFNγ response was minimal (Fig. 22B). This result suggests that pool 21 contains potentially-immunodominant peptide(s) to induce a gp120-specific T cell response. To further identify the immunogenic peptide(s) within pool 21, peptides 81-84 were tested individually. IFNγ production was significantly higher when peptide 81 (IIGDIRQAHCNISRA) was used for restimulation in the pVRCgp120 group as compared with the other three peptides within pool 21 ($p < 0.05$), suggesting that peptide 81 is the most immunogenic gp120 peptide (Fig. 23A). Also, an IFNγ response was not observed in the pVRC2000 control group. A similar profile was observed with IL-2 production in response to peptide 81 restimulation, although less IL-2 was produced compared to IFNγ (Fig. 23B).

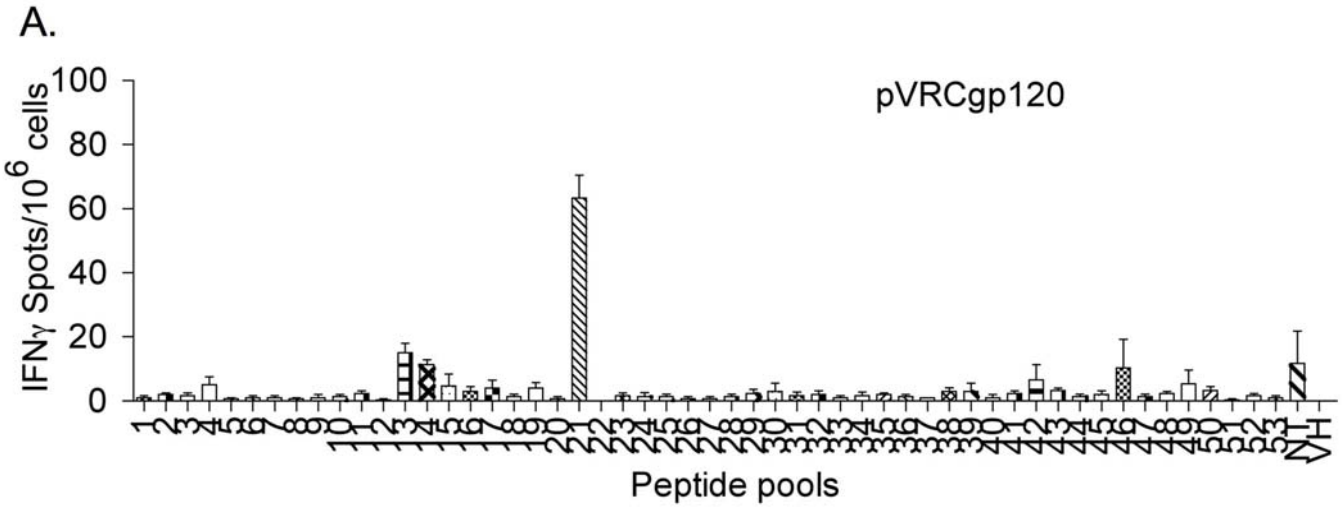

Figure 22. gp120-specific cytokine production by splenocytes. Splenocytes (1 x 10^6 cells/well) from pVRCgp120- (A) or pVRC2000- (B) injected C57Bl/6 mice were restimulated overnight with 53 peptide pools (0.2 μg/peptide/well) respectively, which are derived from the HIV envelope protein. IFNγ secretion was measured by ELISPOT. No treatment (NT) or VH (0.01% DMSO) were included as controls. Data are presented as the mean spots/10^6 cells of 5 samples in each treatment group.

Figure 22 (cont'd)

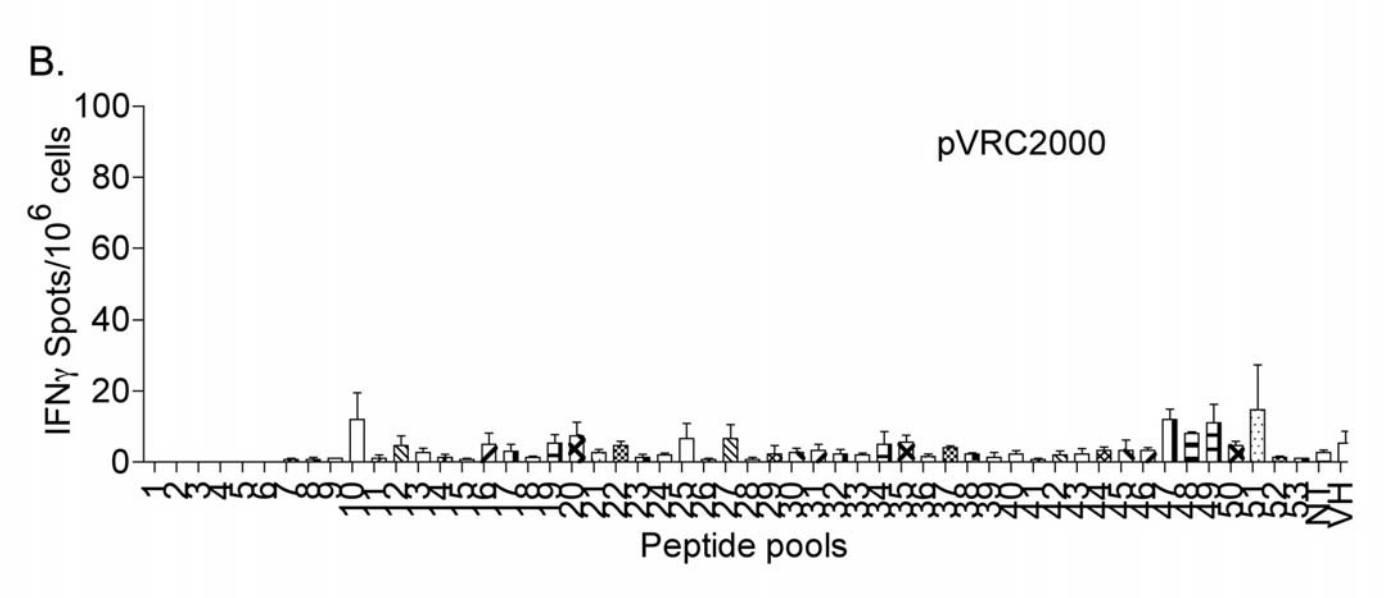

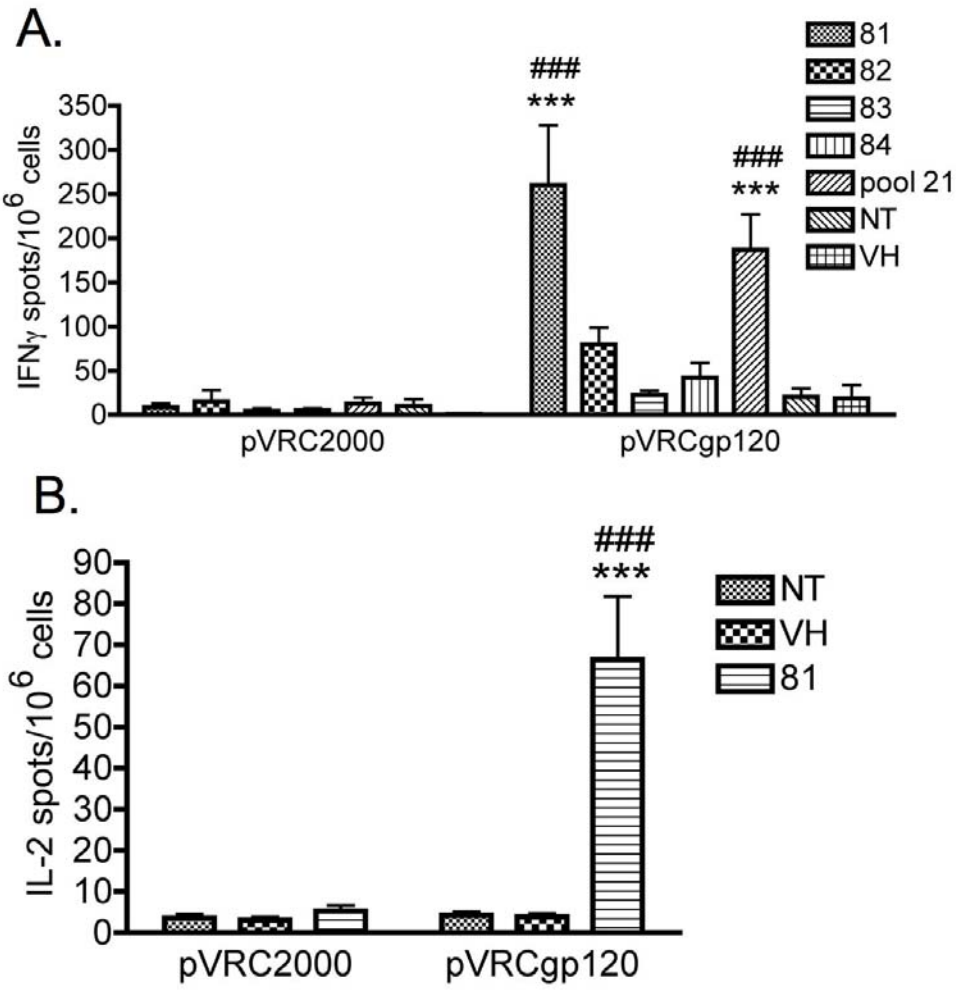

Figure 23. Identification of immunodominant gp120 peptide for restimulation. Splenocytes (1 x 10^6 cells/well) from pVRCgp120- or pVRC2000-injected C57Bl/6 mice were restimulated with the immunodominant peptide 81 (0.2 μg/well) overnight. IFNγ (A) or IL-2 (B) secretion was measured by ELISPOT. No treatment (NT) or VH (0.01% DMSO) were included as controls. Data are presented as the mean spots/10^6 cells of 5 samples in each treatment group. Data were analyzed using two-way ANOVA with Bonferroni post-tests: *** $p < 0.001$ as compared with respective VH in each treatment group; ### $p < 0.001$ as compared with pVRC2000 control for each peptide restimulation.

B. pVRCgp120-induced T cell activation

With the demonstration that gp120-specifc cytokine production was induced in response to pVRCgp120 antigens *in vivo*, activation of splenic T cell populations was assessed by measuring the expression level of the activation marker, CD69. MFI of CD69 on $CD8^+$ (Fig. 24A) and $CD4^+$ (Fig. 24B) T cells in the splenocyte populations was significantly increased when peptide 81 was used for restimulation in the pVRCgp120 group, when compared with the other three peptides within pool 21 ($p < 0.05$), once again confirming that peptide 81 is the immunodominant peptide. In addition, with peptide 81 restimulation, CD69 expression was higher in the pVRCgp120 group compared with the pVRC2000 control, which was statistically different for $CD4^+$ T cells (Fig. 24B, $p < 0.05$), hence demonstrating a gp120-specific T cell activation.

C. pVRCgp120-induced activation of non-T cells

In addition to T cells, activation of non-T cell populations using the same *in vivo* model system was also examined. The magnitude of activation marker expression, including CD69 (Fig. 25A), CD80 (Fig. 25B), and MHC II (Fig. 25C), on the non-T cell ($CD8^-CD4^-$) populations in the pVRCgp120 group was significantly increased in response to peptide 81 restimulation ($p < 0.05$), when compared with the other three peptides. Moreover, the expression levels of all three activation markers in the pVRCgp120 group were significantly higher than in the pVRC2000 control in the presence of peptide 81 restimulation, again demonstrating a gp120-specific response. Peptide 82 was also found to be immunogenic for some endpoints, but to a lesser extent than peptide 81, which is likely due to the sequence overlap between peptide 81 and 82.

D. pVRCgp120-induced B cell responses

In light of the fact that non-T cells demonstrated a gp120-specific response, B cells were assayed for antibody production in response to pVRCgp120 antigen stimulation *in vivo*. Expression levels of CD69 (Fig. 26A) and MHC II (Fig. 26B) on B cells ($CD19^{+}$) in the spleen were significantly increased in the pVRCgp120 group as compared with the pVRC2000 control ($p < 0.05$), in response to peptide 81 restimulation. Furthermore, a gp120-specific IgG response was detected using the serum samples from pVRCgp120-treated mice, which was significantly different from the pVRC2000 control and NA groups (Fig. 26C, $p < 0.05$), demonstrating the generation of a secondary antibody response.

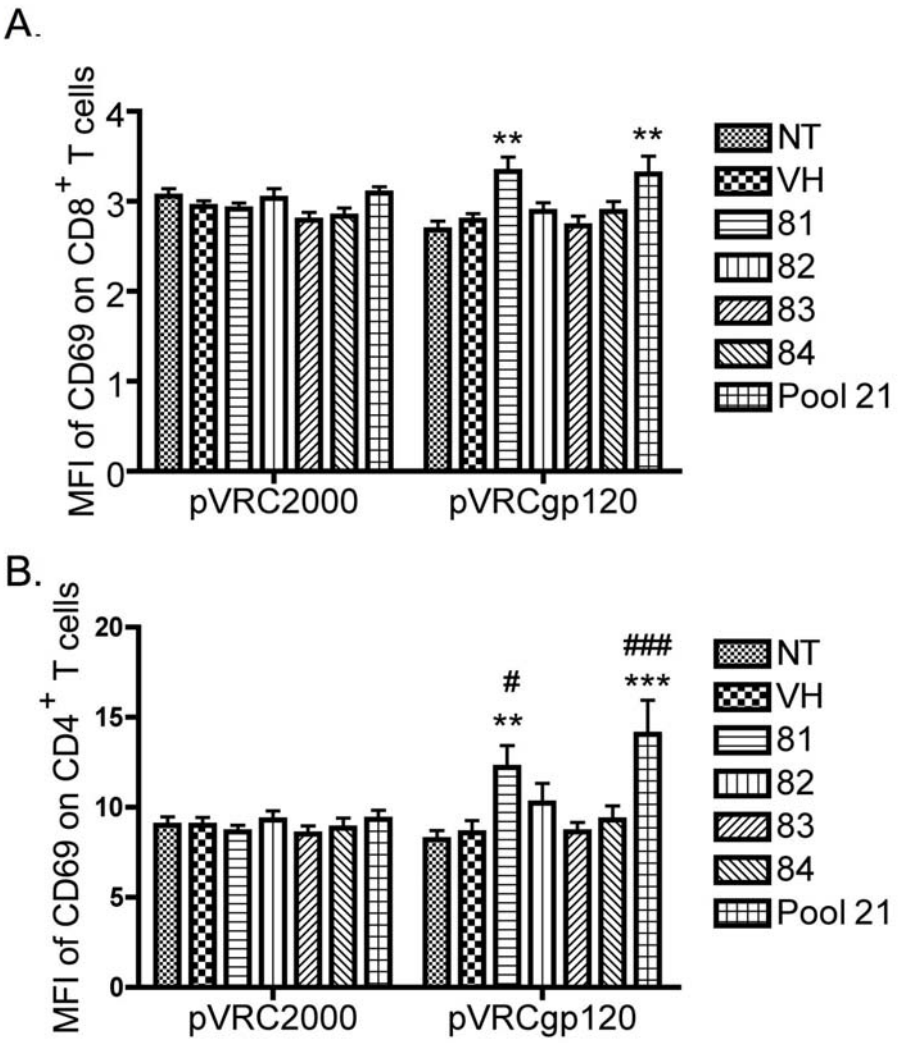

Figure 24. Activation of T cells in response to pVRCgp120 stimulation. (A-B) Splenocytes (1 x 10^6 cells/well) from pVRCgp120- or pVRC2000-injected C57Bl/6 mice were restimulated overnight with gp120-derived peptides 81, 82, 83, 84, or pool 21, containing all four peptides (0.2 μg/peptide/well). Cells were stained for viability, surface CD8, CD4, and CD69, and assessed by flow cytometry. Cells were gated on singlet, viable, lymphocyte, and $CD8^+/CD4^+$ populations. No treatment (NT) or VH (0.01% DMSO) were included as controls. Data are presented as MFI of CD69 from 5 samples in each treatment group. Data were analyzed using two-way ANOVA with Bonferroni post-tests: ** $p < 0.01$, *** $p < 0.001$ as compared with respective VH in each treatment group; # $p < 0.05$, ### $p < 0.001$ as compared with pVRC2000 control for each peptide restimulation.

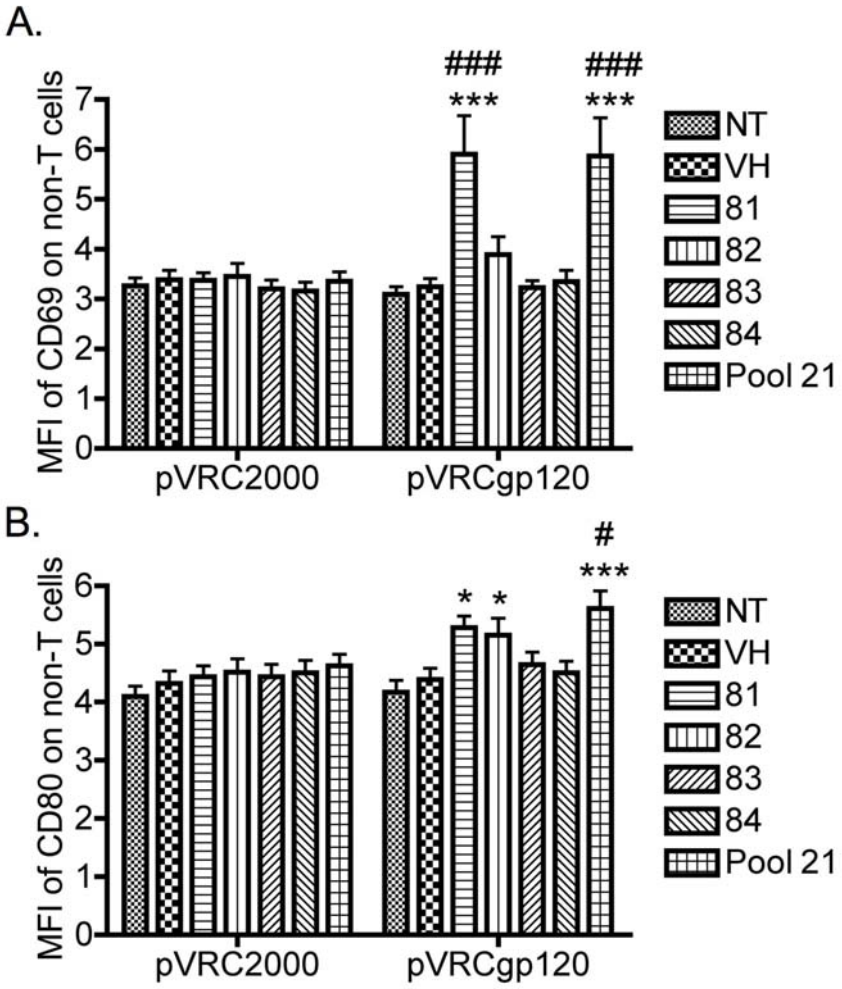

Figure 25. Activation of non-T cells in response to gp120 antigen stimulation. (A-C) Splenocytes (1 x 10^6 cells/well) from pVRCgp120- or pVRC2000-injected C57Bl/6 mice were restimulated overnight with gp120-derived peptides 81, 82, 83, 84, or pool 21, containing all four peptides (0.2 μg/peptide/well). Cells were stained for viability, surface CD8, CD4, CD69, CD80, and MHC II, and assessed by flow cytometry. Cells were gated on singlet, viable, lymphocyte, and $CD8^-CD4^-$ populations. No treatment (NT) or VH (0.01% DMSO) were included as controls. Data are presented as MFI of CD69 (A), CD80 (B), or MHC II (C) from 5 samples in each treatment group. Data were analyzed using two-way ANOVA with Bonferroni post-tests: ** $p < 0.01$, *** $p < 0.001$ as compared with respective VH in each treatment group; # $p < 0.05$, ### $p < 0.001$ as compared with pVRC2000 control for each peptide restimulation.

Figure 25 (cont'd)

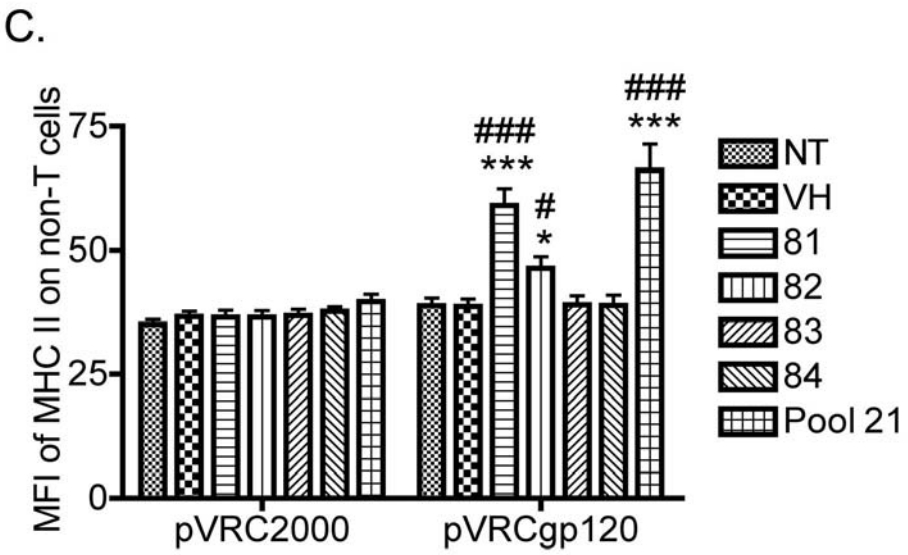

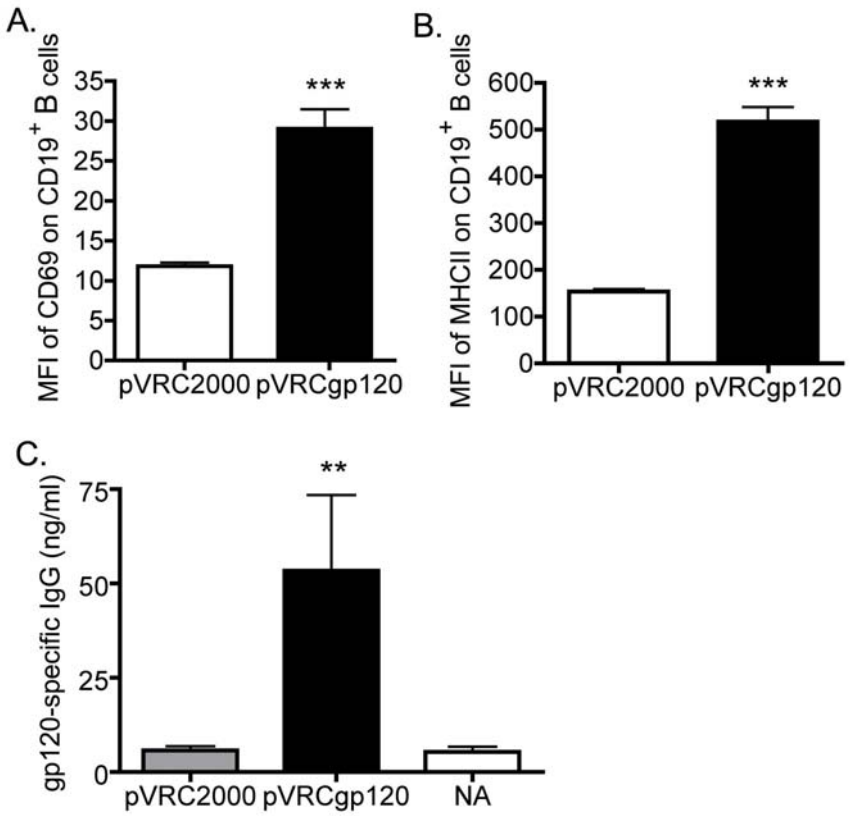

Figure 26. B cell responses to pVRCgp120 stimulation. (A-B) Splenocytes (1 x 10^6 cells/well) from pVRCgp120- or pVRC2000-injected C57Bl/6 mice were restimulated overnight with gp120-derived immunodominant peptide 81 (0.2 μg/well). Cells were stained for viability, surface CD19, CD69, and MHC II, and assessed by flow cytometry. Cells were gated on singlet, viable, lymphocyte, and $CD19^+$ populations. Data are presented as MFI of CD69 (A) or MHC II (B) from 5 samples in each treatment group. (C) Serum from trunk blood was collected from pVRCgp120- or pVRC2000-injected C57Bl/6 mice. IgG production in the serum was quantified by ELISA. Data are presented as the mean ng/ml of 5 samples in each treatment group. (A-C) Data were analyzed using two-tailed t test or one-way ANOVA with Dunnett's post-tests: ** $p < 0.01$, *** $p < 0.001$ as compared with the pVRC2000 control.

E. THC treatment enhanced pVRCgp120-induced IFNγ production by lymphocyte populations in the spleens of WT but not $CB_1^{-/-}CB_2^{-/-}$ mice

Using the *in vivo* model system, the effects of THC and the role of CB_1/CB_2 on gp120-specific immune responses in WT and $CB_1^{-/-}CB_2^{-/-}$ mice were investigated. In initial studies, we conducted THC treatment surrounding the DNA injection, similar to our studies examining effects of THC on influenza-induced immune responses [206]. However, given the likely differences in pharmacokinetics between intranasal injection of influenza virus and intramuscular injection of viral plasmid DNA, it was anticipated that initial gp120 immune response in the spleen following intramuscular injection would require some time. Thus, the studies were repeated using the regimen presented in Fig. 4. Overall, the experiment was repeated four times: twice in which THC dosing surrounded DNA injection and twice in which THC dosing was performed 2 days following DNA injection. Results presented are from the latter regimen (Fig. 4), but are representative of all four experiments.

In CO-treated mice, pVRCgp120 injection induced a higher percentage of $CD8^+$, $CD4^+$, and $NK1.1^+$ cells that produced IFNγ in response to peptide 81 restimulation when compared with pVRC2000 control in both WT and $CB_1^{-/-}CB_2^{-/-}$ mice (Fig. 27A and 27B). Interestingly, the percentage of $IFN\gamma^+$ cells in all three lymphocyte populations was further enhanced by THC treatment in WT mice (Fig. 27A). In contrast, there was a trend toward THC-mediated suppression on IFNγ production in $CB_1^{-/-}CB_2^{-/-}$ mice, demonstrating a CB_1/CB_2-independent

mechanism of THC modulation of the IFNγ response (Fig. 27B). On the other hand, the magnitude of the IFNγ response in the absence of THC was higher in $CB_1^{-/-}CB_2^{-/-}$ mice than in WT mice, suggesting endocannabinoid regulation of immune responses via CB_1 and/or CB_2 (Fig. 27B).

F. THC treatment enhanced pVRCgp120-induced activation of T cells in WT but not $CB_1^{-/-}$ $CB_2^{-/-}$ mice

Next, the effects of THC and the role of CB_1/CB_2 were studied on the magnitude of T cell activation. The same trend of THC effects was observed on T cell activation as on the IFNγ response in Fig. 27A and 27B. In the CO-treated mice, pVRCgp120 induced a higher percentage of $CD69^+CD8^+$ and $CD69^+CD4^+$ cells in response to peptide 81 restimulation in both WT and $CB_1^{-/-}CB_2^{-/-}$ mice, which was further increased by THC treatment in WT but not in $CB_1^{-/-}CB_2^{-/-}$ mice (Fig. 28A and 28B).

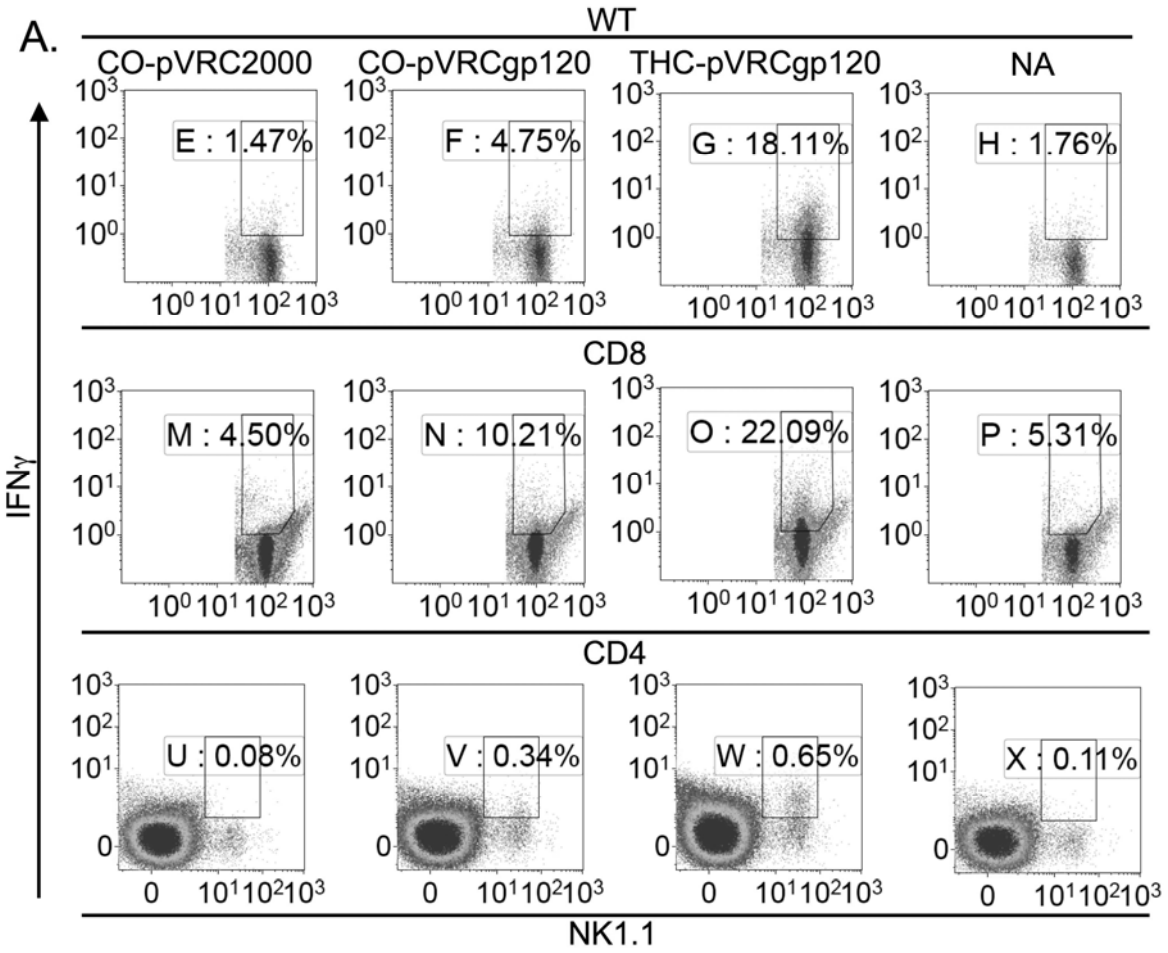

Figure 27. THC-mediated enhancement on gp120-specific IFNγ response in WT but not $CB_1^{-/-}CB_2^{-/-}$ mice. (A-B) Splenocytes (1 x 10^6 cells/well) from pVRCgp120- or pVRC2000-injected C57Bl/6 (WT, A) and $CB_1^{-/-}CB_2^{-/-}$ (KO, B) mice were restimulated overnight with gp120-derived immunodominant peptide 81 (0.2 μg/well). Cells were stained for viability, surface CD8, CD4, NK1.1, and intracellular IFNγ, and assessed by flow cytometry. Cells were gated on singlet, viable, lymphocyte, and $CD8^+/CD4^+/NK1.1^+$ populations. The percentage of IFNγ cells within each lymphocyte population is presented in the dot plots. Displayed are concatenated samples (n=5) of each treatment group.

Figure 27 (cont'd)

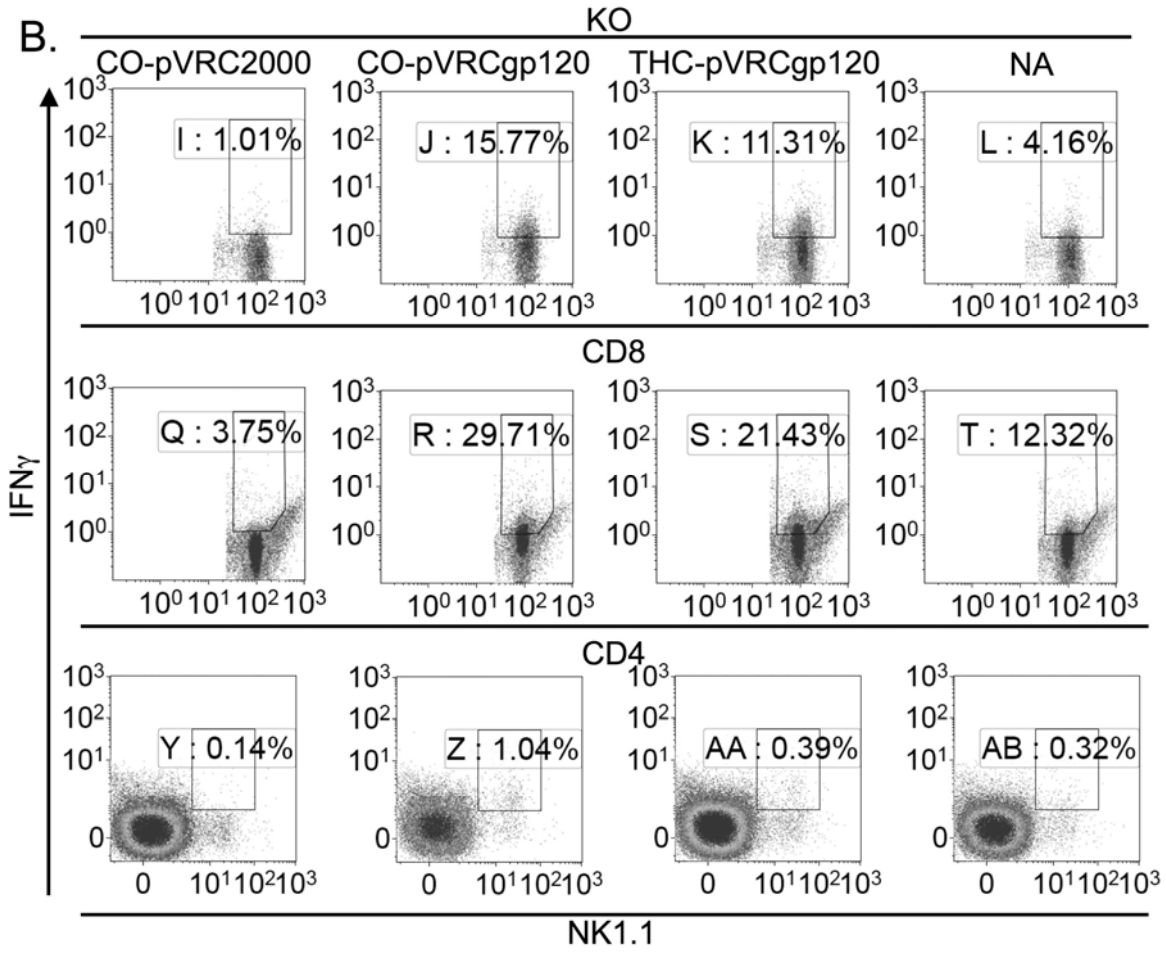

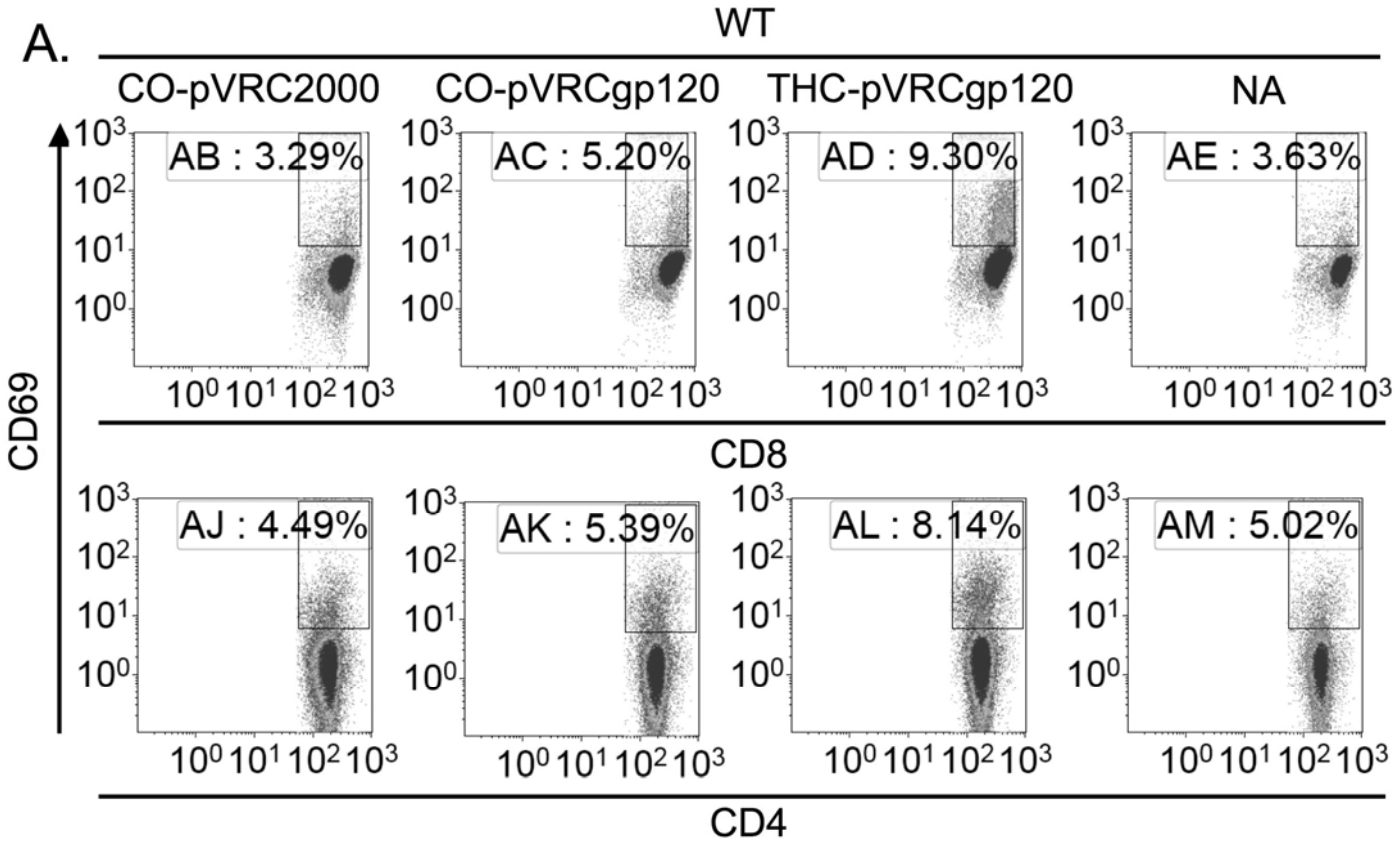

Figure 28. THC-mediated enhancement on gp120-specific T cell activation in WT but not $CB_1^{-/-}CB_2^{-/-}$ mice. (A-B) Splenocytes (1 x 10^6 cells/well) from pVRCgp120- or pVRC2000-injected C57Bl/6 (WT, A) and $CB_1^{-/-}CB_2^{-/-}$ (KO, B) mice were restimulated overnight with gp120-derived immunodominant peptide 81 (0.2 μg/well). Cells were stained for viability, surface CD8, CD4, and CD69, and assessed by flow cytometry. Cells were gated on singlet, viable, lymphocyte, and $CD8^+/CD4^+$ populations. The percentage of $CD69^+$ cells within $CD8^+$ or $CD4^+$ populations is presented in the dot plots. Displayed are concatenated samples (n=5) of each treatment group.

Figure 28 (cont'd)

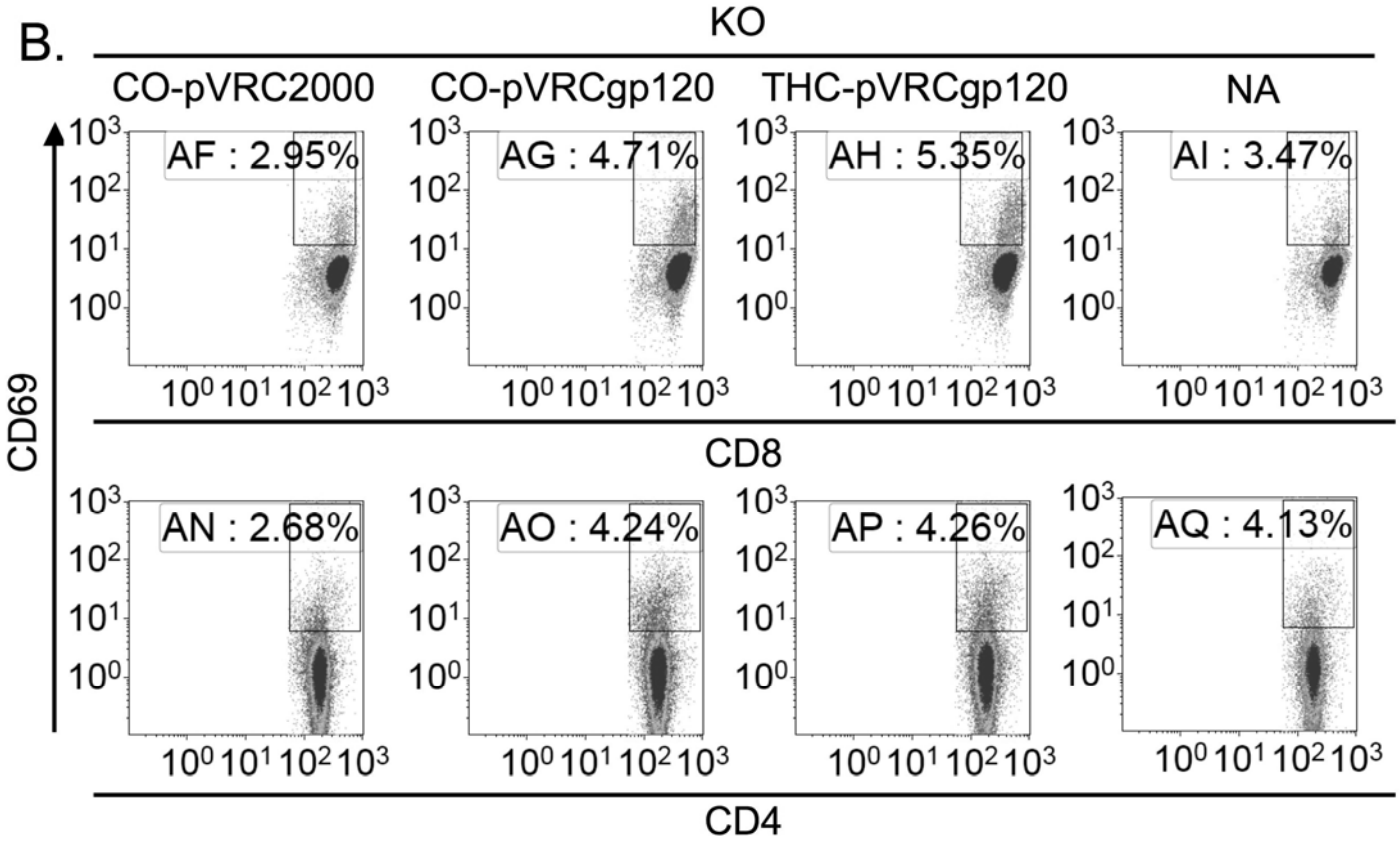

G. THC treatment enhanced pVRCgp120-induced B cell activation in WT but not $CB_1^{-/-}$ $CB_2^{-/-}$ mice

Expression levels of activation marker CD69 on B cells in the presence of THC treatment was also assessed. In response to peptide 81 restimulation, the MFI of CD69 expression on B cells ($CD19^{+}$) was higher in pVRCgp120-treated WT and $CB_1^{-/-}CB_2^{-/-}$ mice as compared with their corresponding control mice (Fig. 29A). Although the THC effect was modest, it clearly showed a trend toward enhancement on CD69 expression in WT but not $CB_1^{-/-}CB_2^{-/-}$ mice (Fig. 29A), which was consistent with its effects on other endpoints reported above. In addition, upon pVRCgp120 stimulation, MHC II expression on B cells was significantly increased in both WT and $CB_1^{-/-}CB_2^{-/-}$ mice as compared with the pVRC2000 control mice (Fig. 29B, $p < 0.05$). THC also significantly elevated the expression level of MHC II on B cells in pVRCgp120-treated WT mice but not in $CB_1^{-/-}CB_2^{-/-}$ mice (Fig. 29B, $p < 0.05$)

H. THC treatment enhanced pVRCgp120-induced activation of non-T/non-B cells in WT but not $CB_1^{-/-}CB_2^{-/-}$ mice

In addition to T cell and B cell populations, the splenic non-T/non-B cell population ($CD8^{-}CD4^{-}CD19^{-}$) was also studied is this model system. Both CD69 (Fig. 30A) and MHC II (Fig. 30B) expression levels on the non-T/non-B cells was higher in pVRCgp120-treated WT and $CB_1^{-/-}CB_2^{-/-}$ mice when compared with the pVRC2000 controls, with the increase being statistically significant for MHC II expression in $CB_1^{-/-}CB_2^{-/-}$ mice ($p < 0.05$). The

THC treatment group showed a trend toward enhancement in the MFI for CD69 and MHC II in WT mice but not in $CB_1^{-/-}CB_2^{-/-}$ mice. It is also noteworthy that $CB_1^{-/-}CB_2^{-/-}$ mice upon gp120 stimulation exhibited a higher MFI for CD69 and MHC II on non-T/non-B cells, when compared to the WT mice, which was significantly different for MHC II expression ($p < 0.05$).

I. THC modulated mRNA expression of genes induced by pVRCgp120

To further investigate the effects of THC on the anti-gp120 immune responses at gene transcript levels, a 96-gene immune array was employed with spleen RNA from WT and $CB_1^{-/-}CB_2^{-/-}$ mice on day 15 post pVRCgp120 injection. Differential gene expression was observed in treated WT and $CB_1^{-/-}CB_2^{-/-}$ mice. Specifically, in CO-treated mice, mRNA levels of several genes were increased in $CB_1^{-/-}CB_2^{-/-}$ mice in response to pVRCgp120 compared with the pVRC2000 control group, including cytokine *Il2*, chemokine receptor *Ccr4* and *Cxcr3*, and surface marker *Cd40lg* (Table 2). THC treatment upregulated expression of surface marker *Cd68* and downregulated expression of *Ctla4* compared with the CO control group in WT mice. In contrast, THC treatment downregulated expression of cytokines *Il17*, *Il12*, and *Il2*, negative regulators of cytokines *Socs1* and *Socs2*, and chemokine receptor *Ccr2* compared with the CO control group in $CB_1^{-/-}CB_2^{-/-}$ mice (Table 2).

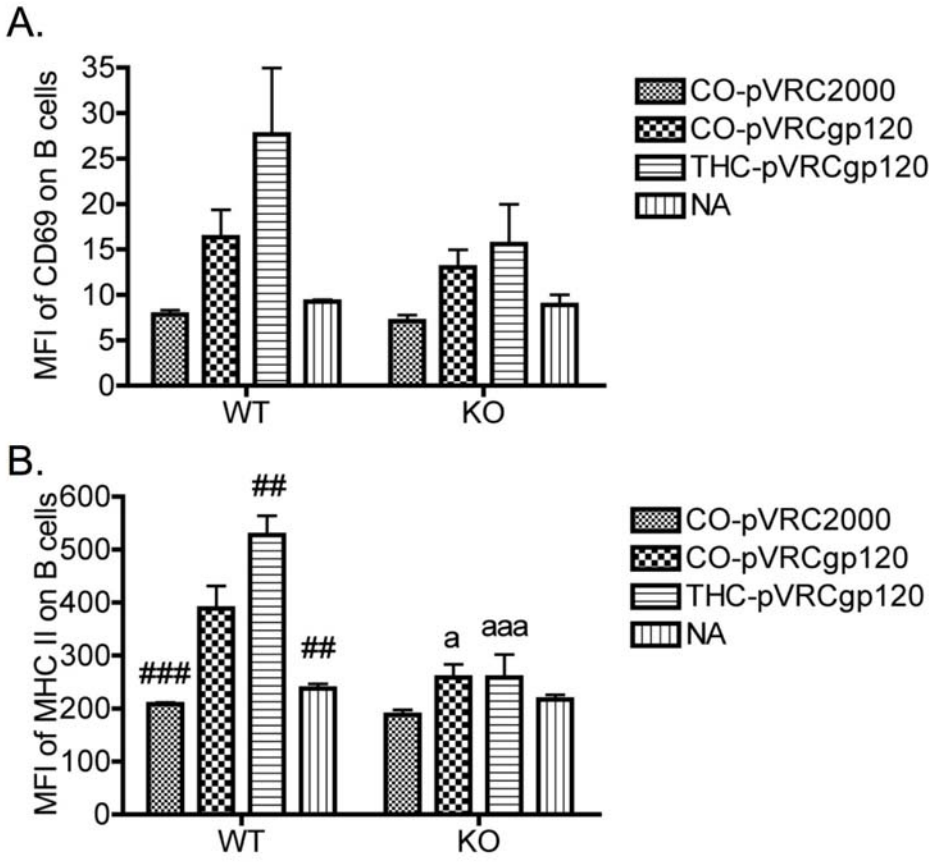

Figure 29. THC-mediated enhancement on gp120-specific B cell activation in WT but not $CB_1^{-/-}CB_2^{-/-}$ mice. (A-B) Splenocytes (1 x 10^6 cells/well) from pVRCgp120- or pVRC2000-injected C57Bl/6 (WT) and $CB_1^{-/-}CB_2^{-/-}$ (KO) mice were restimulated overnight with gp120-derived immunodominant peptide 81 (0.2 μg/well). Cells were stained for viability, surface CD19, CD69, and MHC II, and assessed by flow cytometry. Cells were gated on singlet, viable, lymphocyte, and $CD19^+$ populations. Data are presented as MFI of CD69 (A) and MHC II (B) from 5 samples in each treatment group. Data were analyzed using two-way ANOVA with Bonferroni post-tests: ## $p < 0.01$, ### $p < 0.001$ as compared with the respective CO-pVRCgp120 control for each genotype; a $p < 0.05$, aaa $p < 0.001$ as compared with the WT control.

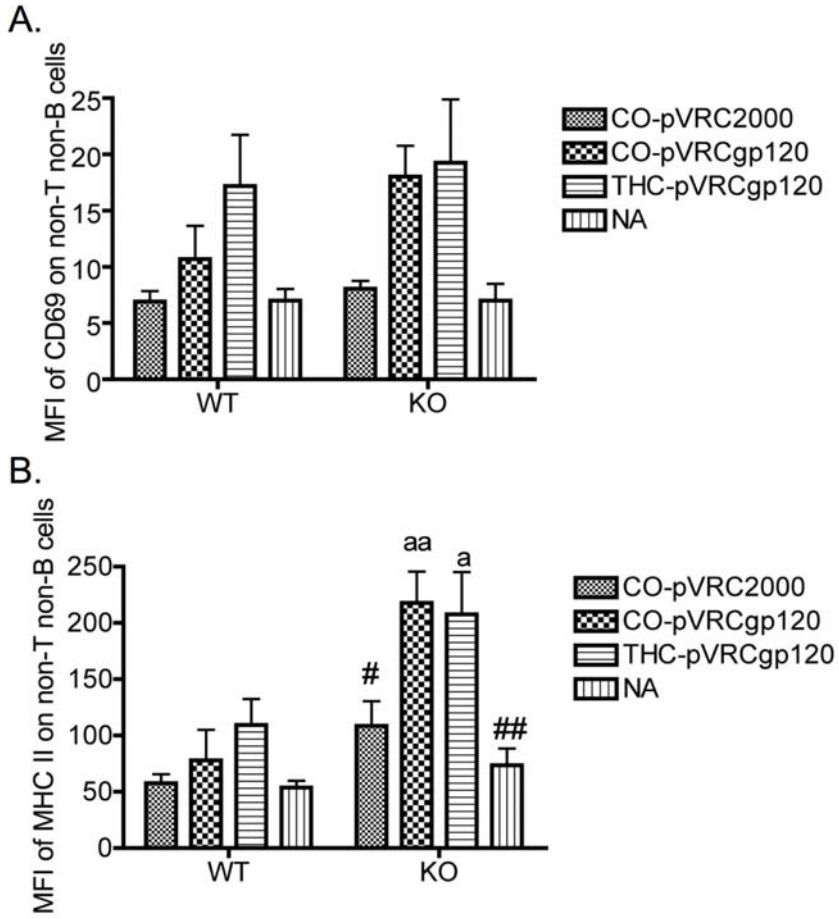

Figure 30. THC-mediated enhancement on gp120-specific non-T/non-B cell activation in WT but not $CB_1^{-/-}CB_2^{-/-}$ mice. (A-B) Splenocytes (1 x 10^6 cells/well) from pVRCgp120- or pVRC2000-injected C57Bl/6 (WT) and $CB_1^{-/-}CB_2^{-/-}$ (KO) mice were restimulated overnight with gp120-derived immunodominant peptide 81 (0.2 μg/well). Cells were stained for viability, surface CD8, CD4, CD19, CD69, and MHC II, and assessed by flow cytometry. Cells were gated on singlet, viable, and $CD8^-CD4^-CD19^-$ populations. Data are presented as MFI of CD69 (A) and MHC II (B) from 5 samples in each treatment group. Data were analyzed using two-way ANOVA with Bonferroni post-tests: # $p < 0.05$, ## $p < 0.01$ as compared with the respective CO-pVRCgp120 control for each genotype; a $p < 0.05$, aa $p < 0.01$ as compared with the WT control.

Table 2. Differential gene expression in response to pVRCgp120 injection and THC treatment in WT and $CB_1^{-/-}CB_2^{-/-}$ mice. Mice (n=3) were injected with pVRCgp120 or pVRC2000 prior to THC or CO treatment. Spleen RNA was isolated on day 15 and converted to cDNA, and gene expression levels were analyzed using a PCR-based low density immune array. Fold change values were calculated, and shown are genes differentially regulated by at least 1.5-fold when comparing CO-pVRCgp120 to the control CO-pVRC2000 group, and comparing THC-pVRCgp120 to the control CO-pVRCgp120 group in WT and $CB_1^{-/-}CB_2^{-/-}$ mice, respectively, with a p value of at lease 0.05. Red color indicates upregulation, and green color indicates downregulation.

CO-pVRCgp120 *vs* CO-pVRC2000		THC-pVRCgp120 *vs* CO-pVRCgp120	
WT	KO	WT	KO
	Ccr4	*Cd68*	*Ccr2*
	Cxcr3	*Ctla4*	*Il17*
	Il2		*Il12*
	Cd40lg		*Il2*
			Socs1
			Socs2

DISCUSSION

The effect of cannabinoids and the role of CB_1/CB_2 on HIV viral antigen-specific immune responses were determined throughout this dissertation work, which was divided into two parts. The first part focused on characterizing the effect of cannabinoid on HIV_{gp120}-specific T cell responses using an *in vitro* model. The second part focused on investigating the effects of cannabinoid and the role of CB_1/CB_2 on gp120-specific immune responses using an *in vivo* model.

I. *In vitro* cannabinoid-mediated effects on T cell responses to HIV_{gp120}

As described earlier, HIV patients use marijuana to mitigate AIDS-associated adverse effects [94], but there are no suitable mouse models that address the effect of cannabinoids, the active components of marijuana, on initial anti-HIV immune responses. The novel *in vitro* mouse model established here mimics the T cell response against HIV-associated antigens in the early stages of infection when T cells are critical in eliminating the virus, and was used to investigate the modulation of the T cell response by cannabinoids. Although only one HIV protein, gp120, was studied in our model, broad T cell responses against multiple viral epitopes of this protein are elicited. In this model, different engineered cell lines were employed, which provided the ability to study the response specific to gp120 antigens shared by both $DC2.4_{gp120}$ and $EL4_{gp120}$ cells, but not to antigens from BCS, parental cells, or antibiotic resistance markers. As demonstrated, $DC2.4_{gp120}$ was capable of eliciting $CD8^+$ T

cell proliferation, differentiation, and therefore, gp120-specific IFNγ production from CTL, indicating that APC $DC2.4_{gp120}$ cells, $CD8^+$ T cells, and target $EL4_{gp120}$ cells all play functional roles in this model system.

The present studies demonstrated that THC differentially modulated IFNγ production from gp120-specific CTL and proliferation of $CD8^+$ T cells in response to $DC2.4_{gp120}$ elicitation. This is the first report of the differential effect of cannabinoids on an antigen-specific T cell response. The experimental factors that control the magnitude of cellular activation in this *in vitro* system are unknown. Across eight independent experiments, a general trend was observed such that the magnitude of the immune response, as measured by IFNγ and $CD8^+$ T cell proliferation, appeared to be one important determinant of whether THC produced enhancement or suppression. Moreover, the suppression or enhancement produced by THC on the IFNγ response was consistent with its effect on $CD8^+$ T cell proliferation, indicating that THC modulated $CD8^+$ T cell effector function, in part, via regulating $CD8^+$ T cell proliferation first.

Due to the complexity of the factors involved in the gp120-induced response in this cognate model (i.e., magnitude of gp120 expression, gp120 processing and presentation associated with MHC, and initiation of T-cell receptor signaling), more direct activators of T cell effector function were employed to study the differential immune modulation by cannabinoids. The pharmacological activators, P/I and anti-CD3/CD28, facilitated a more readily controlled titration of the stimulus used to induce the immune response. In addition, CBD was also used in several studies in order to demonstrate that the differential effect of

cannabinoids was not specific to THC. THC exhibits affinity for CB_1 and CB_2, whereas CBD does not exhibit high affinity for either cannabinoid receptor [101, 102]. In fact, we anticipated that CBD and THC would produce similar effects since we have previously demonstrated that many effects of cannabinoids on T cells are mediated independently of either CB_1 or CB_2 [140, 159-162]. With one exception (cannabinoid effect in response to 1x P/I), the effects of THC and CBD were, in fact, similar. The effect of CBD on IFNγ and IL-2 production was, in part, dictated by the magnitude of stimulation delivered through either P/I or anti-CD3/CD28 treatment. Under conditions of relatively high stimulation (10x P/I, iCD3/CD28 or sCD3/CD28 only for IFNγ), CBD suppressed cytokine production, whereas under conditions of relatively low stimulation (1x P/I or sCD3/CD28 only for IL-2), CBD enhanced cytokine production. The effect of THC on IFNγ and IL-2 production followed the same pattern as CBD, with the exception that THC did not enhance cytokine production in response to 1x P/I. It was also unexpected that sCD3/CD28 induced robust IFNγ production since we previously showed that iCD3/CD28 was a stronger activation stimulus than sCD3/CD28 for IL-2 induction in splenocytes [174, 175], but THC and CBD still produced similar effects on sCD3/CD28-stimulated IFNγ. It is possible that suboptimal stimulation with sCD3/CD28 leads to T cell anergy or activation-induced cell death (AICD), which requires IFNγ for the production of caspases and also results in decreases in IL-2 production and proliferation to regulate T cell homeostasis [240-243].

These results are consistent with previous reports that cannabinoids either suppressed or enhanced immune function depending on the experimental conditions, such as cell type, immune stimuli, and cannabinoid concentrations [171-175, 233], which were described in the

Introduction chapter, but a clear mechanism has not been established. We hypothesize that the increase in intracellular calcium by cannabinoids prior to activation contributes to the downstream effects. That is, the combination of cannabinoids with suboptimal cellular activation provides an appropriate or optimal calcium signal to induce cytokine production, whereas the combination of cannabinoids with an optimal level of cellular activation might provide an anergic or cell death signal to suppress cytokine production, which has been suggested for immune suppression by CBD previously [144, 244]. Thus, it is unexpected that THC does not induce IL-2 or IFNγ in response to 1x P/I, especially since THC has been reported to increase intracellular calcium in lymphocytes [163, 245, 246]. In these studies, we demonstrated that CBD and THC increased calcium in splenocytes, regardless of the magnitude of activation. It is possible that since THC enhanced the calcium level to a lesser extent than CBD in the presence of 1x P/I, the induction on cytokine production was so modest that it is below the level of detection. It was notable that differential regulation of IL-2 production by CBD was also observed in human PBMC, implying that the differential effect of cannabinoids occurs in humans. Further investigations are needed to determine whether similar trends in the cannabinoid-mediated effects also occur in immunocompromised HIV patients.

As shown here and in previous studies, cannabinoids increased intracellular calcium in resting and activated splenocytes, suggesting that the differential regulation of NFAT nuclear translocation by cannabinoids must occur at a signal distal to increased intracellular calcium [163, 245, 246]. It is possible that cannabinoids in combination with optimal or suboptimal stimulation might differentially produce oscillatory calcium signals, and depending on the frequency of the signals NFAT activation as well as IL-2 expression were differentially

regulated, which have been demonstrated previously [247]. Alternatively, the "switch factor" for cannabinoid-induced modulation of NFAT2 nuclear translocation and subsequent cytokine production that must be distal to the increase in intracellular calcium could be cytoplasmic NFAT regulating factors, such as the calcium-sensing stromal interaction molecule (STIM) or calcium-release-activated calcium (CRAC) channel protein ORAI, or nuclear kinases that induce nuclear export of NFAT, such as dual-specificity tyrosine-phosphorylation regulated kinase 1A (DYRK1A) (reviewed in [248]). Another possibility is that the induction of different transcription factors distal to the increase in intracellular calcium dictates the effects on cytokine production. For example, whether the cells would undergo anergy or AICD may depend on the NFAT:AP-1 ratio, as a high AP-1 level is required for AICD [249, 250]. The putative differential effects of cannabinoids on AP-1 are presently unknown, but AP-1 activity has been shown to be suppressed by cannabinoid treatment under optimal stimulation conditions [140, 161, 227].

Overall, these *in vitro* studies demonstrated that cannabinoids suppressed or enhanced HIV_{gp120}-specific T cell responses. Such differential effects by cannabinoids also occur in response to other stimuli, such as P/I or anti-CD3/CD28, and demonstrated that cannabinoids differentially regulated NFAT nuclear translocation and cytokine production. Despite these opposing effects, cannabinoids elevated intracellular calcium regardless of the presence or absence, or even the magnitude, of cellular activation. These data indicated that the intracellular calcium level resulting from the combination of cannabinoid treatment and cellular activation, at least in part, determined the overall T cell response. In particular, cannabinoids in combination with suboptimal stimulation led to an optimal calcium level, increased nuclear translocation of NFAT, and therefore enhanced the T cell response. On the

other hand, cannabinoids plus optimal stimulation led to excessive intracellular calcium, which reduced NFAT nuclear translocation and resulted in suppression of the T cell response. Together, these data provide one potential mechanism to explain the many dichotomous reports in the literature in which cannabinoids either induce or suppress the same immune response [140, 144, 159-161, 170-172, 174, 175, 233]. Our observations also identify the need for more in-depth investigations on evaluating the effect of cannabinoid use on immune competence of HIV patients.

II. *In vivo* cannabinoid-mediated effects on immune responses to HIV_{gp120}

In light of the demonstration that cannabinoids produced differential effects on T cell responses against HIV_{gp120} antigen *in vitro*, the effect of cannabinoids on immune responses to HIV viral antigens *in vivo* was in turn characterized. In the second part of this dissertation work, a novel HIV mouse model was first developed in which viral DNA injections were used to stimulate gp120-specific responses in WT and $CB_1^{-/-}CB_2^{-/-}$ mice. This is a physiologically relevant model using intact animals to mimic the immune responses against multiple viral epitopes in the early stages of HIV infection. Using this model, a comprehensive immune response was induced, including both cell-mediated and humoral immunity, as evidenced by induction of gp120-specific cytokines, serum IgG production, and activation of various cellular populations. In fact, this is the first report in which the gp120-derived immunodominant peptide (IIGDIRQAHCNISRA) was identified in the C57Bl/6 mouse strain in response to the gp120 protein from the HIV-1 IIIB HXBc2 stain. Interestingly, C57Bl/6 T helper cells were found to respond predominantly to the peptide IIGDIRQAHCNISRE

derived from the envelope protein in HIV-1 isolate 1007 [251], which differs from ours by only one amino acid. It is also suggested that this immunodominant peptide is likely located in the variable (V) 3 region of gp120 [252], which is responsible for binding to the chemokine coreceptor CCR5 to allow virus entry into the target cells [253].

In the absence of THC treatment, $CB_1^{-/-}CB_2^{-/-}$ mice produced a greater level of IFNγ upon gp120 antigen stimulation compared with WT mice (Fig. 27A and 27B). Such hyper-reactivity in $CB_1^{-/-}CB_2^{-/-}$ mice has also been reported previously in other studies. For example, in a model of contact hypersensitivity, $CB_1^{-/-}CB_2^{-/-}$ mice showed a pronounced induction of type IV hypersensitivity with exacerbated ear swelling in response to contact sensitizer, 2,4-dinitrofluorobenzene [213]. In addition, in a host resistance model to influenza, $CB_1^{-/-}CB_2^{-/-}$ mice exhibited an exaggerated antiviral immune response to influenza challenge, as shown by less viral load in the lung and increased leukocyte infiltration in the bronchoalveolar lavage fluid [207]. Furthermore, more robust IFNγ production by $CD8^+$ T cells from $CB_1^{-/-}CB_2^{-/-}$ mice compared with WT mice was also observed in the *in vitro* model system (Fig. 12A). The mechanisms responsible for these findings are yet to be completely elucidated, but are consistent with the widely held premise that CB_1 and CB_2 are involved in dampening the immune response. CB_1 and CB_2 are primarily known as inhibitory heterotrimeric G protein coupled receptors ($G\alpha_{i/o}$) involved in down-regulating the activity of AC, which decreases the levels of intracellular cAMP [97, 134, 138]. The downstream signaling events are in turn influenced, such as decreased activity of transcription

factors, AP-1, NFAT, NF-κB, which are involved in regulation of cytokine production as described earlier [141, 142]. Therefore, the enhanced IFNγ response observed in $CB_1^{-/-}CB_2^{-/-}$ mice might be due to the lack of suppression on signaling events downstream of $G\alpha_{i/o}$ mediated by endogenous cannabinoids via CB_1 and CB_2. In addition, the CB_1 agonist AEA was found to attenuate the K_V channel-mediated outward currents in DCs, which resulted in a decrease of surface MHC II expression on DCs and therefore a reduced T cell response, suggesting the modulation of DC function by cannabinoids via CB_1 signaling [194-196]. Most recently, THC was found to suppress LPS-induced maturation of bone marrow-derived DCs, as evidenced by reduced MHC II, CD80, and CD86 expression, which in turn decreased IFNγ production by $CD8^+$ T cells after the co-culture [197]. Consistent with these observations, maturation of the non-T/non-B cell population, which is comprised of APCs, such as DCs, was more pronounced in $CB_1^{-/-}CB_2^{-/-}$ mice, as assessed by expression of surface markers CD69 and MHC II (Fig. 30). Hence, the enhanced immune response observed in $CB_1^{-/-}CB_2^{-/-}$ mice might also be due to the lack of suppression on APC function mediated by endogenous cannabinoids via CB_1/CB_2.

As extensively described in the Introduction chapter, THC is primarily known to suppress immune responses, such as host resistance to pathogens and tumor challenge [197, 204, 206, 254, 255]; however, depending on experimental conditions, including cell type, immune stimuli, and cannabinoid concentrations, enhancement by THC and other cannabinoids on immune function has also been reported in some studies. For example, cells from the spleen

or lymph nodes in combination with stimulation using anti-CD3, ConA or phytohemagglutinin could result in differential modulation on cellular proliferation by THC [170]. In addition, the age of animals was also found to be an important factor in determining whether cannabinoids produced immune enhancement or suppression [171]. Moreover, nanomolar concentrations of the synthetic cannabinoid, CP55,940, were demonstrated to increase IL-8 and beta-chemokine monocyte chemotactic protein-1 (MCP-1) production in CB_2-transfected HL60 cells [172], and low concentrations of cannabinoid-mediated enhancement were also observed in B cells [173]. Cannabinoid-mediated enhancement on IL-2 expression was also observed when EL4 T cells were suboptimally activated with low concentrations of PMA, due to binding of NFAT to a distal site in the IL-2 promoter region [174, 175]. Such enhancement was not abrogated by CB_2 antagonist SR144528, possibly suggesting a CB-independent mechanism [174, 175]. In particular, from the *in vitro* studies reported in the first half of this dissertation, we have also demonstrated that THC suppressed the CTL response specific to gp120 antigens when the magnitude of cellular activation was high, and THC enhanced the response when the magnitude of cellular activation was suboptimal. In the current *in vivo* studies, which were designed such that THC would be present at the time of immune activation, THC produced an enhanced effect in WT mice on the IFNγ response and activation of various cellular populations, as assessed by expression of CD69 and MHC II. The mechanisms by which THC produced immune enhancement in WT mice are not clear, but based on the above evidence it is possible that the current experimental conditions in this *in vivo* model system, including the amount of viral DNA employed and the THC dose, induced a modest antigen-specific responses, hence THC produced immune enhancement. In order to test this possibility, further investigations to boost the response, for

example, by increasing the number of epitopes or including an adjuvant, would help to resolve this possibility. In addition, it was clearly demonstrated here that the enhancement produced by THC in WT mice on the IFNγ response was consistent with its effect on the activation level of T cells, indicating that THC modulated T cell effector function, in part, via regulating T cell activation first. Moreover, although CB_1 and CB_2 are initially reported to interact with inhibitory $G\alpha_{i/o}$, they have also been shown to couple with stimulatory heterotrimeric G proteins ($G\alpha_s$) to activate AC and therefore the downstream signaling events [149, 256-258]. However, the binding affinity of CB_1 or CB_2 to G_s or G_i proteins or the expression levels of either G protein in certain tissues remain elusive. Furthermore, since it was shown that CB_1 or CB_2 agonists, HU-210 and WIN 55,212-2 inhibited the activity of AC isoforms I, III, V, VI, and VIII, but stimulated the activity of AC isoforms II, IV, and VII [150], involvement of different AC isoforms might be another contributing factor to the differential effects mediated by cannabinoids. Therefore, this *in vivo* model system, which includes numerous components such as THC, endogenous cannabinoids, CB_1, and CB_2 might lead to stimulation of different Gα subunits to cause differential effects on the downstream responses.

Although the overall THC effects were modest, the trend toward enhancement in WT mice was consistently observed. In contrast, a trend toward suppression by THC on IFNγ production was seen in $CB_1^{-/-}CB_2^{-/-}$ mice, but no THC-mediated effect was observed on the other endpoints. These results suggest that depending on the particular immune response, the observed THC-induced activity might be mediated through CB_1/CB_2-independent or -

dependent mechanisms. Interestingly, the observation that THC enhanced the relatively low magnitude of IFNγ response in WT mice, but suppressed the relatively strong IFNγ response in $CB_1^{-/-}CB_2^{-/-}$ mice was consistent with our findings from *in vitro* studies in which THC differentially modulated immune function depending on the magnitude of immune response. These results also suggest that the effects of THC could be mediated by receptors other than CB_1 and CB_2. So far, orphan GPCRs, such as GPR18, GPR55, and GPR119, and several TRP channels, such as TRPC1, TRPA1, and TRPV1-6, have all been implicated as targets for cannabinoid ligands [97, 107, 155, 156], but their functions in cannabinoid-mediated immune modulation remain uncertain. Whether any of these receptors plays a role in this *in vivo* model system is not known and will require further investigation.

At the gene transcript levels, increased cytokine (IL-2) production and expression of costimulatory molecule CD40L on T cells in $CB_1^{-/-}CB_2^{-/-}$ mice but not WT mice, is consistent with a more robust immune response in $CB_1^{-/-}CB_2^{-/-}$ mice compared with WT mice, as evidenced by augmented IFNγ production in $CB_1^{-/-}CB_2^{-/-}$ mice measured by flow cytometry. In response to THC treatment, the mRNA of inhibitory molecule CTLA-4 was downregulated when compared with the CO-pVRCgp120 control group in WT mice, suggesting an enhanced effect by THC on immune function. On the other hand in $CB_1^{-/-}CB_2^{-/-}$ mice, suppression of cytokine production by THC was observed when compared with the CO-pVRCgp120 control group, as evidenced by downregulation of lymphocyte-specific cytokines (IL-17 and IL-2) and APC-produced cytokine (IL-12) [259]. However, THC also attenuated the suppressive effect on cytokine production by downregulating the transcripts of

negative regulators *Socs1* and *Socs2*, suggesting opposing effects by THC in $CB_1^{-/-}CB_2^{-/-}$ mice. It is possible that the suppressive effect was more robust, therefore decreased IFNγ production by THC was evident in $CB_1^{-/-}CB_2^{-/-}$ mice as measured by flow cytometry.

Collectively, the *in vivo* studies identified an immunodominant peptide derived from HIV_{gp120}, which induced antigen-specific immune responses, including production of cytokines, IFNγ and IL-2, activation of different cellular populations, and the generation of a secondary antibody response. THC treatment enhanced HIV_{gp120}-induced expression levels of activation markers only in WT but not $CB_1^{-/-}CB_2^{-/-}$ mice, suggesting a CB_1/CB_2-dependent mechanism of THC-mediated activity, which might be due to the low magnitude of stimulation or activation of different Gα subunits upon ligation of CB_1 and/or CB_2. Furthermore, the absence of CB_1 and CB_2 in $CB_1^{-/-}CB_2^{-/-}$ mice led to a phenotype with enhanced immune responsiveness in some respects, such as cytokine production, suggesting the potential involvement of endogenous CB_1 and/or CB_2 ligands. Finally, THC enhanced IFNγ production in WT mice, but suppressed IFNγ production in $CB_1^{-/-}CB_2^{-/-}$ mice, suggesting a CB_1/CB_2-independent mechanism and the putative involvement of other receptors. Together, these studies provide an approach to investigate cannabinoid-mediated effects on viral antigen-specific immune responses *in vivo*, and suggest possible enhancement of immune function by cannabinoids in response to HIV antigens.

III. Significance and concluding remarks

The studies presented in this dissertation have made significant contributions to the understanding of the effect of cannabinoids in the immune system, in particular on HIV antigen-specific immune responses. By characterizing the immune responses induced by HIV_{gp120} viral antigens *in vitro* and *in vivo* using WT and $CB_1^{-/-}CB_2^{-/-}$ mice, the role of CB_1/CB_2 was also further elucidated.

AIDS is one of the leading causes of high death rates in the US [19]. It is known that HIV patients suffer severe pain, nausea, appetite loss and wasting syndrome associated with weight loss and cachexia. Approximately 25% of HIV/AIDS patients have been using cannabis as an appetite stimulant, anti-emetic and/or analgesic for alleviating some of the symptoms listed above. Use of cannabis has provided relief of anxiety, depression, and pain, improved appetite, and increased pleasure [94]. Since HIV patients are immunocompromised, they are more susceptible to further pathogen infections. At the same time, cannabinoids are primarily known to exert a negative impact on immune function as described in the Introduction chapter, therefore whether marijuana can further impair the immune competence of HIV patients has become a major concern. There is still a lack of research and knowledge on understanding the effect of cannabinoids on the immune function in HIV patients. So far, only a few studies have reported on the effects of short-term or chronic THC treatment on HIV viral load and T cell counts in human patients or nonhuman primate models [214-216]. However, it is important to emphasize that in these studies neither antigen-specific immune responses nor the associated molecular and cellular mechanisms were investigated. Therefore, the first unique contribution of this work is the establishment of two antigen-specific models.

Specifically, an *in vitro* model was first utilized to investigate basic parameters associated with T cell response against HIV_{gp120}, and a subsequent *in vivo* model using the same stimulation strategy was employed to test this model under physiological conditions of both antiviral immune responses and drug metabolism. This is a stepwise incremental approach to increase the complexity of the model system to make it gradually closer to the real life situation in HIV patients who use marijuana for treating HIV-associated adverse effects. These models are important experimental approaches and can be potentially applied to various cannabinoids or other xenobiotics and other HIV or non-HIV derived viral proteins. In addition, the immunodominant epitope(s) derived from interested viral proteins can be identified using a similar *in vivo* model system.

The second novel finding from these studies is that THC exhibits differential effects on HIV_{gp120} antigen-specific immune responses depending on the magnitude of the immune response. *In vitro*, THC was demonstrated to suppress gp120-specific IFNγ production and proliferation of $CD8^+$ T cells when the magnitude of response was high, but enhance the aforementioned responses when the magnitude of response was low. Although the experimental factors determining the magnitude of the response under the current conditions are not clear, such cannabinoid-mediated differential effects on cytokine (IFNγ and IL-2) production were also observed when pharmacological activators were used to stimulate the cells under optimal (10x P/I, iCD3/CD28, sCD3/CD28 only for IFNγ) or suboptimal (1x P/I, sCD3/CD28 only for IL-2) conditions. My findings suggested that the magnitude of cellular activation dictates the cannabinoid-mediated differential T cell response to HIV_{gp120}. Previous reports imply that experimental conditions, including cell type, cannabinoid

concentration, and stimuli, influence the effect of cannabinoids on immune responses [171-175, 233], and my results provide further insight into the decisive experimental factors.

The third important finding is that the modulatory effects of cannabinoids on immune function may be acting on various cellular components simultaneously. The *in vitro* and *in vivo* studies performed in this dissertation research are very comprehensive, which demonstrate that cannabinoids modulate the functions of $CD8^+$ T cells, $CD4^+$ T cells, NK cells, B cells, and non-T/non-B cells (consisting primarily of APCs). Due to the fact that DC2.4 cells express very limited amount of MHC II molecules, the $CD4^+$ T cell response was not detected, so the *in vitro* model mainly focused on the $CD8^+$ T cell response. However, the *in vivo* studies clearly show that multiple cellular populations are the targets of cannabinoid-mediated modulation.

In addition, we demonstrate that each stage in the development of cell-mediated and humoral immunity can be modulated by cannabinoids. *In vivo*, THC-mediated modulatory effects on T cell and B cell effector function, including cytokines specifically induced by gp120 and IgG production, which correlated with effects on the activation levels of T cells and B cells, as measured by expression levels of CD69, CD80, and MHC II. *In vitro*, the activity of THC on cytokine production by $CD8^+$ T cells was consistent with its effects on $CD8^+$ T cell proliferation. Therefore, the *in vitro* and *in vivo* studies complement each other, and together indicate that cannabinoids modulate activation, proliferation and the effector functions of the differentiated immune cells.

Furthermore, mRNA expression of IFNγ and IL-2 and nuclear translocation of transcription factor NFAT were also differentially regulated by cannabinoids under optimal

(10x P/I) or suboptimal (1x P/I) stimulation conditions, suggesting that cannabinoid-mediated modulation also occurs at the transcriptional levels. However, surprisingly, cannabinoids did not differentially regulate but increased intracellular calcium levels regardless of the stimulation condition. Therefore, we have speculated that optimal stimulation in combination with cannabinoids leads to excessive intracellular calcium, which decreases downstream cytokine production, whereas suboptimal stimulation in combination with cannabinoids results in an optimal level of intracellular calcium, which increases cytokine production. These results also imply that cannabinoids are likely to differentially modulate signaling events distal to increased intracellular calcium, which might be NFAT cytoplasmic regulators or nuclear kinases (e.g., STIM, ORAI, and DYRK1A). Although both suppressive and enhancing effects by cannabinoids on immune function have been reported previously by us and others, this is the first time a possible mechanism is suggested.

Lastly, the role of CB_1/CB_2 in cannabinoid-mediated immune modulation has been extensively elucidated mainly using the *in vivo* model. With the demonstration that THC produced enhancement on activation of various cellular populations in WT mice but no effect in $CB_1^{-/-}CB_2^{-/-}$ mice, a CB_1/CB_2-dependent mechanism is suggested. On the other hand, IFNγ production was enhanced by THC in WT mice but suppressed in $CB_1^{-/-}CB_2^{-/-}$ mice, hence suggesting a CB_1/CB_2-independent mechanism and the existence of additional receptors other than CB_1/CB_2. Therefore, depending on the response being measured, both CB_1/CB_2-dependent and -independent mechanisms may be involved in cannabinoid-mediated immune modulation. It is unknown what receptor(s) are responsible for the aforementioned

THC-mediated effects. Studies identifying the potential target(s) will provide further information on the mechanisms by which cannabinoids modulate immune responses. It is also noteworthy that consistent with findings from other studies [207, 213], $CB_1^{-/-}CB_2^{-/-}$ mice exhibited a phenotype of enhanced immune responsiveness when compared with WT mice, as shown by more robust IFNγ production, suggesting the involvement of CB_1/CB_2 in endocannabinoid-mediated immune suppression.

In summary, as described above, this dissertation research advances the knowledge of the effects of cannabinoids and the role of CB_1/CB_2 on immune regulation to viral antigens in several ways. In addition, our findings further elucidate the mechanisms by which cannabinoids and cannabinoid receptors influence immune modulation. Moreover, these studies provide a basis for developing future studies in which primary human PBMCs from healthy or HIV patients, who may also currently use marijuana for appetite stimulation, can be used to determine correlations between the data presented in this dissertation and human health. This work also begins to provide valuable information for HIV/AIDS patients who are currently using marijuana for therapeutic benefits.

APPENDIX

INDUCED T CELL CYTOKINE PRODUCTION IS ENHANCED BY ENGINEERED NANOPARTICLES

ABSTRACT

Engineered nanoparticles are widely used in commercial products and yet due to the paucity of safety information there are concerns surrounding potential adverse health effects, especially from inhaled nanoparticles and their putative contribution to allergic airway disease. The objective of this study was to investigate whether engineered nanoparticles possess adjuvant-like or immune enhancing properties on antigen-specific T cell responses using *in vitro* models. Ovalbumin (OVA)-derived peptides were presented to T cells by either spleen-derived endogenous APCs or a mouse DC line, DC2.4. In all models, IFNγ and IL-2 production by $CD8^+$ or $CD4^+$ T cells in response to peptide $OVA_{257-264}$ or $OVA_{323-339}$, respectively, was measured by flow cytometry. Silica nanoparticles (SNPs) were modified with alkyne-terminated surfaces and appended with polyethylene glycol (PEG) chains via "click" chemistry. Modified SNPs were not likely to agglomerate in *in vitro* culture media, suggesting that their effect on leukocyte function was the result of true nanoscale. Under suboptimal T cell stimulation conditions, modified SNPs (up to 10 μg/ml) enhanced the proportion of $CD8^+$, but not $CD4^+$, T cells producing IFNγ and IL-2. Various functional groups (-COOH, $-NH_2$, -OH) on modified SNPs enhanced IFNγ and IL-2 production to different levels, with -COOH SNPs being the most effective. Furthermore, 51 nm -COOH SNPs exhibited a greater enhancing effect on $CD8^+$ T cell response than other sized particles. Collectively, our results show that modified SNPs can enhance antigen-specific $CD8^+$ T cell responses, suggesting that certain modified SNPs exhibit potential adjuvant-like properties.

INTRODUCTION

Nanoparticles can occur naturally in the environment or can be artificially engineered for a wide range of applications in industry, such as electronics, medicine, food, clothing and cosmetics [260]. Nanoparticles have potentially beneficial effects; for example, their therapeutic use in vaccine development [261]. By contrast, the same mechanisms that account for their beneficial attributes in vaccine development can contribute to putative adverse effects on human health [262, 263]. Some of these concerns have arisen from animal studies, which have demonstrated that nanoparticles can exhibit adjuvant-like properties and can also contribute to allergic pulmonary disease through increased granulocyte infiltration, production of proinflammatory cytokines and allergen-specific antibodies [264, 265]. Little is presently known concerning the consequences resulting from interactions of engineered nanoparticles with the immune system, especially at the cellular level. The objective of this study was to investigate whether engineered nanoparticles can enhance antigen-driven T cell responses to provide a mechanism of nanoparticle-mediated adjuvant effects, and if so, whether these enhancing properties are influenced by the surface chemistry or specific size of the nanomaterials.

In the present investigation SNPs were synthesized, which were modified with alkyne-terminated surfaces and appended with PEG azides via "click" chemistry. Pegylated SNPs are dispersed in water and can readily interact with, as well as enter, cells [266, 267]. Preliminary *in vivo* studies using bronchoalveolar lavage fluid (BALF) and lymph node (LN) cells from OVA/SNP-treated mice have demonstrated the potential adjuvant-like effects of these SNPs on cell counts and activation of lymphocytes as well as other cell populations [268]. However, since *in vivo* study was limited by the amount of materials and the number

of T cells obtained in BALF and LN samples, *in vitro* models were chosen to delineate the effect of SNPs on T cell functions directly. In addition, these *in vitro* models could facilitate the study of mechanisms associated with SNP-mediated immune enhancing effect.

In this study, antigen-specific T cell responses *in vitro* were induced. T cells were obtained from spleens of OT-I ($CD8^+$ T cells) or OT-II ($CD4^+$ T cells) mice, which have been engineered to express transgenic T cell receptors specific for OVA-derived peptides $OVA_{257-264}$ (SIINFEKL) or $OVA_{323-339}$ (ISQAVHAAHAEINEAGR), respectively [269, 270]. In the OT-I model, $OVA_{257-264}$ peptides that bind to MHC I molecules were presented by either endogenous APCs from the splenic population or a mouse DC line, DC2.4, to activate OT-I $CD8^+$ T cells specifically. By using DC2.4 as APCs, OVA peptides were directly loaded onto DC2.4 cells, which were then co-cultured with splenic cells. In the OT-II model, $OVA_{323-339}$ peptides that bind to MHC II molecules were presented by endogenous APCs from the splenic population to OT-II $CD4^+$ T cells specifically. Production of cytokines, including IFNγ and IL-2, were used as a measure of T cell function.

The physical and chemical properties of the engineered nanoparticles determine their uptake by cells and therefore their activity in the cells [271-273]. Therefore, SNPs were synthesized in different sizes and with modifications to surface chemistry through the addition of functional groups, including -COOH, $-NH_2$, and -OH, which were not likely to agglomerate in *in vitro* culture media by performing dynamic light scattering (DLS) analysis. Using the above-mentioned antigen specific models, the objective of this study was to evaluate the effects of modified SNPs on T cell functions using suboptimally-activated $CD8^+$ and $CD4^+$ T cells.

METHODS

SNPs

LUDOX® TM-40 colloidal silica (LTM40, 40 wt% suspension in H_2O), 3-(triethoxysilyl)propyl isocyanate, propargyl alcohol, sodium ascorbate and sodium azide were purchased from Sigma-Aldrich (St. Louis, MO) and used as received. Colloidal silica SNOWTEX XS (SNTXS, 4-6 nm, 20 wt% suspension in H_2O), SNOWTEX 20L (SNT20L, 40-50 nm, 20 wt% suspension in H_2O), and SNOWTEX ZL (SNTZL, 71 nm, 40 wt% suspension in H_2O) were gifts from Nissan Chemical Industries, Ltd (Pasadena, TX). 1-azido-2-(2-(2-(2-methoxyethoxy)ethoxy)ethoxyethane (N34PEG) was synthesized according to a literature procedure [274]. Dialysis membranes (Spectra/Por® Biotech Cellulose ester, MWCO: 300K, 12-14K) were purchased from Spectrum Laboratories Inc. (Rancho Dominguez, CA). Ion exchange resin (Amberlite® IRC-748) was purchased from Alfa Aesar (Ward Hill, MA).

Instruments and SNP characterization

^{1}H Nuclear magnetic resonance (NMR) and ^{13}C NMR spectra were recorded in $CDCl_3$ on a Varian 300 MHz or VXR-500 MHz instrument (Agilent Technologies, Santa Clara, CA). The $CDCl_3$ resonance was used as the internal standard for ^{13}C NMR (δ = 77.0 ppm) and residual $CHCl_3$ for ^{1}H NMR (δ = 7.24 ppm). Fourier Transform Infrared spectroscopy (FTIR) spectra were recorded on a Mattson Galaxy series FTIR 3000 (Mattson Instruments, Inc., Madison, WI). Thermogravimetric analyses (TGA) were obtained in air from a Perkin-Elmer TGA 7 (Perkin Elmer Corporation, Norwalk, CT). Samples were held at 120 °C for 30 min to

remove adsorbed water from the particle surfaces, and then heated to 850 °C at a rate of 10 °C/min. All FTIR and TGA samples were dried under vacuum at room temperature for 24 h.

DLS data were obtained with a Malvern NanoZS ZetaSizer (Malvern Instruments Inc., Westborough, MA) with 178° backscattering detection. Intensity and average diameters were calculated from the autocorrelation function using Malvern's Zetasizer Software 6.12. Samples for DLS analyses were sonicated at 60 °C prior to measuring particle sizes at 25 °C (FS20H sonicator, Fisher Scientific, Pittsburgh, PA). For nanoparticle stability studies, particles were added to fresh *in vitro* culture media (see below), dispersed by vortex mixing, and characterized by DLS at 0, 4, 8, 21, 42, 68 h at 25 °C. Particles only and media only were included as experimental controls.

Synthesis of reagents for modifying nanoparticles and click chemistry

Synthesis of ((2-propynylcarbamate)propyl)triethoxysilane (PPTrEOS) (Fig. 31A). Propargyl alcohol (12 g, 0.21 mol) and triethylamine (19 g, 0.19 mol) were dissolved in 120 mL of dry CH_2Cl_2. The mixture was cooled in an ice bath, and under nitrogen, a solution of 3-(triethoxysilyl)propyl isocyanate (IPTEOS) (46 g, 0.18 mol) in 60 mL of dry CH_2Cl_2, was added dropwise to the flask. The reaction mixture was stirred for 24 h at room temperature and then filtered. CH_2Cl_2, excess propargyl alcohol, and NEt_3 were evaporated under reduced pressure to afford 50 g of PPTrEOS as pale-yellow oil. ^{1}H NMR (500 MHz, $CDCl_3$) 0.52 (t, 2H, J = 8Hz), 1.11 (t, 9H, J = 8 Hz), 1.52 (m, 2H), 2.37 (s, 1H), 3.08 (m, 2H), 3.71 (q, 6H, J = 7 Hz), 4.55 (s, 2H).

Synthesis of 2-[2-[2-[2-azidoethoxy]ethoxy]ethoxy]ethanol (N34PEGOH) (Fig.31B). A solution of TsCl (14 g, 0.071 mol) in 250 mL of tetrahydrofuran (THF) was added dropwise to a solution of tetraethylene glycol (34 g, 0.18 mol), triethylamine (14 mL) and THF (250 mL). After stirring the resulting solution for 36 h at room temperature, THF was removed by rotary evaporation and the crude product was dissolved in 200 mL of CH_2Cl_2. The organic layer was washed with water (3 × 150 mL), aqueous $NaHCO_3$ (200 mL), and brine (200 mL). After drying over Na_2SO_4, the solution was concentrated and dried under vacuum to give 18 g of a light yellow liquid comprised of a mixture of mono-tosylate (85%) and di-tosylate (15%), which corresponded to 14.3 g of mono-tosylate (58% yield). The product was used in the next step without further purification. ^{1}H NMR (500 MHz, $CDCl_3$) δ 7.77 (m, 2H), 7.32 (m, 2H), 4.29 (m, 2H), 3.69-3.50 (m, 14H), 2.5 (br, 1H), 2.42 (s, 3H). The tosylates were dissolved in dimethylformamide (DMF) (210 mL), treated with NaN_3 (10.4 g, 15 mmol), and then heated to 60 °C for 24 h. Then the mixture was concentrated, re-dissolved in ethyl acetate, filtered to remove the solid sodium tosylate, and concentrated under reduced pressure. The resulting oily product was dissolved in water and washed with hexane until α,ω-diazido tetraethylene glycol was not detected in the aqueous layer. Drying under vacuum gave the product as a light yellow liquid (8.0 g, 72%). ^{1}H NMR (500 MHz, $CDCl_3$) δ 3.69 (m, 2H), 3.64 (m, 10H), 3.58 (m, 2H), 3.36 (t, 2H, J = 5.5 Hz), 2.8 (br, 1H); ^{13}C NMR (125 MHz, $CDCl_3$) 72.41, 70.55, 70.51, 70.43, 70.18, 69.90, 61.56, 50.54.

Synthesis of 2-[2-[2-[2-azidoethoxy]ethoxy]ethoxy]ethyl amine (N34PEGNH2) (Fig. 31C). A solution of TsCl (39.9 g, 0.21 mol) in THF (150 mL) was added dropwise into an ice-cold mixture of tetraethylene glycol (13.5 g, 0.07 mol), aqueous KOH (100 g, 47%, w/w),

and THF (100 mL). After stirring the solution for 36 h at room temperature, THF was removed by rotary evaporation, and then CH_2Cl_2 (200 mL) was added to the residue. The organic layer was washed with water (3 × 150 mL), aqueous $NaHCO_3$ (200 mL), and brine (200 mL). After drying the organic layer over Na_2SO_4, the solution was concentrated and dried under vacuum to give 32 g of a light yellow liquid (91%), which was used in the next step without further purification. ^{1}H NMR (300 MHz, $CDCl_3$) δ 7.81(m, 4H), 7.36 (m, 4H), 4.20 (m, 4H), 3.70-3.65 (m, 12H), 2.47 (s, 6H). The di-tosylate of tetraethylene glycol was treated with NaN_3 (11.7 g, 18 mmol) in DMF (300 mL) at 90 °C for 24 h. The mixture was concentrated, dissolved in water, and extracted with CH_2Cl_2 (4 × 100 mL). The solution was dried over anhydrous Na_2SO_4 and concentrated under reduced pressure to give 12 g of a yellow liquid. Aqueous HCl (5%, 100 mL) was added to the yellow liquid, and under vigorous stirring at room temperature, a solution of PPh_3 (11.4 g, 0.041 mol) in 75 mL of ether was added dropwise. After stirring for 24 h, the ether was removed by rotary evaporation and the aqueous layer was extracted with CH_2Cl_2 until triphenylphosphine oxide was not detected in the aqueous layer. The aqueous layer was adjusted to pH=12, and amine was extracted from the aqueous layer with CH_2Cl_2 (6 × 50 mL). Drying under vacuum gave the product as a light yellow liquid (9.0 g 68%). ^{1}H NMR (500 MHz, $CDCl_3$) δ 3.72-3.58 (m, 10H), 3.48 (t, 2H, J = 5 Hz), 3.35 (t, 2H, J = 5 Hz), 2.84 (t, 2H, J = 5Hz), 2.24 (s, 2H); ^{13}C NMR (125 MHz, $CDCl_3$) 72.79, 70.50, 70.47, 70.43, 70.07, 69.85, 50.50, 41.44.

Synthesis of 2-[2-[2-[2-azidoethoxy]ethoxy]ethoxy]acetic acid (N34PEGCOOH) (Fig. 31D). A solution of [2-[2-[2-chloroethoxy]ethoxy]ethanol (16.8 g, 0.1 mol) and NaN_3 (13 g, 0.2 mol) in 75 mL of water was heated at 75 °C with stirring for 24 h. Water was removed by

rotary evaporation and the crude product was extracted from the salts with 200 mL of CH_2Cl_2. Concentration and drying under vacuum gave the product as a light yellow liquid (17 g, 97%), which was used without further purification. ^{1}H NMR (500 MHz, $CDCl_3$) δ 3.72-3.62 (m, 8H), 3.58 (m, 2H), 3.37 (t, 2H, *J* = 5 Hz). The light yellow liquid product (14 g, 0.08 mol), prepared above, was added to NaH (0.1 mol) in 350 mL of dry THF cooled in an ice bath. After stirring for 1 h at room temperature, ethyl bromoacetate (17.7 mL, 0.16 mol) was added dropwise to the solution and then stirred for 48 h at room temperature. The THF was removed by rotary evaporation, and then 150 mL of water was added. The aqueous layer was extracted with CH_2Cl_2 (3 × 50 mL), dried over anhydrous Na_2SO_4, and concentrated under reduced pressure at 55 °C to give an amber liquid (26 g), which was used without further purification. ^{1}H NMR (500 MHz, $CDCl_3$) δ 4.24 (q, 2H, *J* = 10 Hz), 4.17 (s, 2H), 3.77-3.65 (m, 10H), 3.41 (t, 2H, *J* = 5 Hz). The ester was hydrolyzed with 53 mL of 3M NaOH at room temperature for 18 h. After extracting the aqueous layer with CH_2Cl_2 (10 × 30 mL) to remove mineral oil and other impurities, the aqueous layer was acidified to pH=1 and extracted with EtOAc (1 × 80 mL, 7 × 30 mL). After drying over anhydrous Na_2SO_4, the residue was concentrated to a pale red liquid (14 g, 75%). ^{1}H NMR (500 MHz, $CDCl_3$) δ 4.18 (s, 2H), 3.78-3.67 (m, 10H), 3.41 (t, 2H, *J* = 5 Hz); ^{13}C NMR (125 MHz, $CDCl_3$) 177.88, 76.71, 75.95, 75.69, 75.48, 75.31, 74.02, 55.9.

Surface modification of SNPs

Synthesis of XXXXPTr: One-step alkyne modification of SNPs (Fig. 31E). XXXX represented different commercial SNPs, including LTM40, SNTXS, SNT20L, and SNTZL (9 g, 40% suspension in water), which were diluted with 75 mL of 1:1 EtOH-H_2O and sonicated.

Particle size was measured by DLS prior to modification. pH of the silica suspension was adjusted to ~9 by adding drops of aqueous ammonia. At room temperature, a solution of PPTrEOS (3 g, 10 mmol) in 10 mL of EtOH was added dropwise to the stirred silica suspension. After stirring for 3 days, the suspension was diluted with EtOH until it was homogeneous. The modified particles were purified by dialysis in EtOH and water (9:1) using dialysis tubing (MWCO: 300K). The surface coverage of the alkyne functional group was evaluated by TGA. The particle concentration (mg/g) was determined by evaporating 2 - 4 mL of purified particle solutions.

Synthesis of XXXXPTrgR' with different functional groups: "Click" chemistry of SNPs (Fig. 31E). Click chemistry between alkyne-modified SNPs and clicking reagents (R', including N34PEG, N34PEGOH, N34PEGNH2, and N34PEGCOOH) is described using the synthesis of LTM40PTrg4PEG as an example. LTM40PTr (100 mg, 0.036 mmol of alkyne functional groups) and N34PEG **(**41.9 mg, 0.18 mmol, 5 equiv.) were added to 13.8 g of EtOH and water (9:1). Then this mixture was diluted in 3:1 DMF/water until the solution was clear. After adding sodium ascorbate (14.3 mg, 2 equiv.) to the solution, trace O_2 was removed by three freeze-pump-thaw cycles. Aqueous $CuSO_4$ (72 µL, 0.1 M, 0.2 equiv.) was added to the solution followed by a final degassing process, and the solution changed to light brown-yellow. After stirring at room temperature for 36 h, 1 mL of aqueous EDTA (0.1M) was added and the solution was stirred for another 6 h. The resulting particles were dialyzed against (MWCO:12-14K) EtOH/water (9:1, 5 × 2 L) and against distilled water to afford purified surface-modified SNPs with different surface chemistry. For the synthesis of LTM40PTrg4PEGNH2, EDTA was not added after click chemistry, but was dialyzed directly

as stated above, and then the solution of LTM40PTrg4PEGNH2 was sonicated to be homogeneous. Ion exchange resin (2 g, Amberlite® IRC-748) was added to remove the Cu^{2+}, and it was removed via filtration after 8 h. The modified SNPs, including LTM40PTrg4PEG, LTM40PTrg4PEGOH, LTM40PTrg4PEGNH2, LTM40PTrg4PEGCOOH, SNTXSPTrg4PEGCOOH, SNT20LPTrg4PEGCOOH, and SNTZLPTrg4PEGCOOH, were kept in distilled water until further characterization. The surface coverage of surface functional groups after each step modification was evaluated by TGA. g indicates that the clicking reagents were grafted to the particles via "click" chemistry. DLS samples were prepared by diluting or concentrating solutions to 0.1 or 1 mg/mL. The particle concentration (mg/g) was determined by evaporating 2-4 mL of purified particle solutions.

Mice

Female OT-I and OT-II mice were purchased from Jackson Laboratory (Bar Harbor, ME, USA) and used at 8 -12 weeks of age. Mice were randomized at no more than 5 animals per cage and provided rodent chow (Harlan Teklad, Madison, WI) and water *ad libitum*. Rooms were kept on a 12-hr light/dark cycle at 21-24°C and 40-60% humidity. All experiments were performed following the guidelines set forth by Michigan State University Institutional Animal Care and Use Committee.

Cell culture conditions

DC2.4 cells (a kind gift from Dr. Kenneth Rock at University of Massachusetts) were maintained in complete RPMI media (10% BCS, 100 units/ml penicillin and 100 μg/ml streptomycin [pen/strep]).

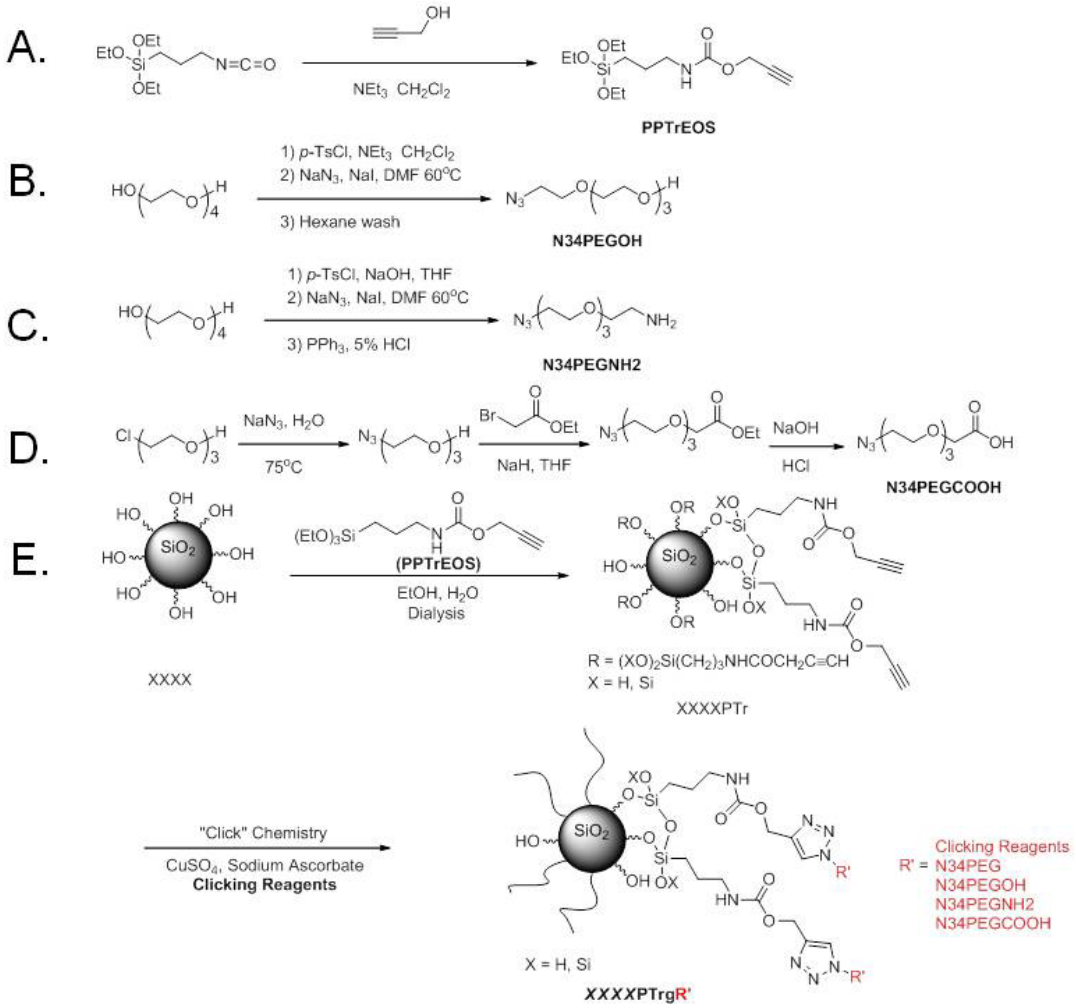

Figure 31. Synthesis of different SNPs. (A-D) Synthesis steps are illustrated for PPTrEOS (A), N34PEGOH (B), N34PEGNH2(C), and N34PEGCOOH (D). (E) Particle synthesis procedure is illustrated for modified SNPs. *XXXX* represents different commercial SNPs, including LTM40, SNTXS, SNT20L, and SNTZL. PTr represents particles modified with alkyne functional groups. R' represents different clicking reagents, including N34PEG, N34PEGOH, N34PEGNH2, and N34PEGCOOH, which are PEG chains of 4 repeating units terminated with -OMe, -OH, -NH_2, and -COOH functional groups, respectively. g represents that the clicking reagents were grafted to the particles via "click" chemistry.

Activation of OT-I or OT-II T cells with OVA peptides *in vitro*

Splenocytes were isolated aseptically from OT-I or OT-II mouse spleens and made into single-cell suspensions. Splenocytes (8 x 10^5 cells/well) were treated with various concentrations (10^{-8} – 10^{-2} μg/ml) of $OVA_{257-264}$ peptide SIINFEKL or $OVA_{323-339}$ peptide ISQAVHAAHAEINEAGR (Anaspec, San Jose, CA) in 48-well plates for 2 days in 2% BCS RPMI media (2% BCS, pen/strep, and 50 μM 2-mercaptoethanol). When DC2.4 cells were used as APCs, they were plated at 2 x 10^6 cell/well in 6-well pates and pretreated with 1 μg/ml LPS (*Salmonella typhosa*, Sigma-Aldrich) in 2% BCS RPMI media overnight. DC2.4 cells were then incubated with various concentrations of SIINFEKL (10^{-2} – 10 μg/ml) for 3 – 4 h, X-ray irradiated at 35 gray to prevent their proliferation, washed 3 times to remove the extra SIINFEKL, and plated 2 x 10^5 cell/well in 96 U-Bottom plates with 1 x 10^6 cells/well OT-I splenocytes for 4 days in 5% BCS RPMI media (5% BCS, pen/strep, and 50 μM 2-mercaptoethanol). Peptide concentration for suboptimal stimulation of T cell response was determined and used to further study the influence of modified SNPs on T cell function.

Modified SNPs treatment in cell culture

Once the suboptimal stimulation condition was determined, splenocytes were treated with modified SNPs with or without different surface functional groups or in different sizes, including LTM40PTrg4PEG, LTM40PTrg4PEGOH, LTM40PTrg4PEGNH2, LTM40PTrg4PEGCOOH, SNTXSPTrg4PEGCOOH, SNT20LPTrg4PEGCOOH and SNTZLPTrg4PEGCOOH. These modified SNPs were sonicated at 60°C for 35 min and then added to the splenocyte suspension at various concentrations (10^{-2} – 10 μg/ml) prior to the OVA peptide stimulation as describe above. As reviewed by Ganwal et al. [275], 10 μg/ml

concentration does not fall into the high-end concentrations (~30 – 400 μg/ml) of nanoparticles for *in vitro* assay testing based on estimates of lung deposition after occupational exposure.

Flow cytometry analysis

On day 2 post the initiation of peptide stimulation, brefeldin A (Biolegend, San Diego, CA) was added to the culture during the last 6 h of incubation to prevent cytokine release and allow for the identification of cytokine producing T cells. Cells were washed with 1 x HBSS buffer (Invitrogen, Carlsbad, CA) and incubated with LIVE/DEAD Fixable Near-IR Dead Cell Stain Kit (Invitrogen) to assess cell viability according to manufacturer's instructions. For surface molecule staining, cells were blocked for Fc receptors with purified rat anti-mouse CD16/CD32 ("Fc block", BD Pharmingen, San Diego, CA), then incubated with PE/Cy7-conjugated rat anti-mouse antibodies against CD8α (clone 53-6.7, Biolegend,) or CD4 (clone RM4-5, Biolegend), and fixed with Cytofix (BD Pharmingen). On the day of flow cytometric analysis, cells were permeabilized with 1 x Perm/Wash (BD Pharmingen) and stained with PE-conjugated anti-mouse IFNγ antibody (clone XMG1.2, Biolegend) and APC-conjugated anti-mouse IL-2 antibody (clone JES6-5H4, Biolegend). Single stain controls were included in all experiments to compensate for fluorescence interference between detectors. Cells were washed with 1 x Perm/Wash, resuspended in FACS buffer (1 x HBSS containing 1% BSA and 0.1% sodium azide), assessed on a FACS Canto II flow cytometer (BD Biosciences, San Jose, CA), and analyzed with FlowJo v8.8.6 (Tree Star, Ashland, OR) or Kaluza 1.1 (Beckman Coulter, Miami, FL) software. In the experiments where DC2.4 cells were used for elicitation, on day 4 post the initiation of the co-culture, cells were restimulated

with SIINFEKL (10 μg/ml) in the presence of brefeldin A for 6 h in 2% BCS RPMI media. Cells were then stained for viability, surface CD8 expression, and intracellular cytokine production as described above.

Statistical analysis

Graphing and statistical analyses were performed using GraphPad Prism v4.0 (Graphpad Software, San Diego, CA). The mean ± S.E. is presented in all bar graphs. To determine the statistically significant changes between peptide stimulated and unstimulated cells, two-way ANOVA for parametric data was performed. Bonferroni post-test was used to compare samples to their control group. Differences between means from each treatment group were determined using one-way ANOVA. When significant differences were detected, treatment groups were compared to the appropriate control using Dunnett's test.

RESULTS

Surface chemistry of modified LTM40PTrg4PEG SNPs

PPTrEOS was synthesized as a pure material with a high yield. Characterization by ^{1}H NMR and ^{13}C NMR indicated that further purification was not required [276, 277]. Commercial SNPs were condensed with PPTrEOS in basic EtOH-H_2O mixture for 3 days, as outlined in Fig. 31E. After condensation, alkyne-modified SNPs were purified via dialysis, using tubing with molecular weight cut off (MWCO) values appropriate for the sizes of the particles. Purification continued until no organic chemicals were detected in the dialysate residue by ^{1}H NMR analysis, usually lasting between 1.5 to 8 days. After dialysis was completed, particles were recovered by evaporating the dialysis solvent for further characterization. 'Click' chemistry on SNP surfaces was conducted to afford SNPs with different functional group moieties. These modified SNPs were purified by dialysis and used for further surface characterization, as well as in *in vitro* culture studies.

The changes in nanoparticle surface chemistry were tracked by FTIR. Fig. 32A showed normalized FTIR spectra of LTM40 and its modified SNPs as described in Materials and Methods. The band at 806 cm^{-1}, characteristic of bulk silica, allowed normalization of the IR data and semi-quantitative comparison of the nanoparticles. For example, LTM40PTr showed new absorption at 2900-3300 cm^{-1}, 2123 cm^{-1}, 1700 cm^{-1} and 1430 cm^{-1}, which corresponded to the alkyl group, triple bond, carbonyl group, and another alkyl group, respectively, and confirmed the functionalization of particle surface with alkynes. After "click" modification of the particles, bands at 2930 and 1640 cm^{-1} increased and were consistent with adding methylene groups from PEG units and the triazole ring (top 4 traces, Fig. 32A). FTIR was limited for characterizing pegylation, since the characteristic C-O bands of PEG were buried

under intense IR bands from the SNPs. However, C-H bending and stretching absorption bands were consistent with the PEG chain in LTM40PTrg4PEG (-OMe terminated) particles, as was seen in all other pegylated SNPs (-OH, -NH_2, and -COOH terminated particles).

TGA data in Fig. 32B and Table 3 confirmed the step-by-step modification of SNPs with different functional groups on the surface. The grafting density on particle surfaces was calculated from TGA mass loss in air, which corresponded to oxidation of the organic layer on the nanoparticle surfaces. Table 3 showed a 5.1% weight loss for alkyne-modified nanoparticles (LTM40PTr), which was calculated to a grafting density of 1.54 alkyne groups/nm^2. After clicking pegylated functional groups to LTM40PTr, TGA analyses showed 7.5-8.7% weight loss for all SNPs. The mass losses corresponded to a grafting density of ~1.5 chain/nm^2 and >90% high click conversion, indicating successful synthesis of water-dispersed nanoparticles.

DLS measurements were conducted with LTM40, LTM40PTr, and the four click products, LTM40PTrg4PEG (-OMe), LTM40PTrg4PEGOH (-OH), LTM40PTrg4PEGNH2 (-NH_2), and LTM40PTrg4PEGCOOH (-COOH) (Table 3 and Fig. 32C). All surface-modified nanoparticles had monomodal distributions. After modifying the surface of LTM40 with alkynyl groups to make LTM40PTr, its size increased from 30 nm to 37 nm with a zeta potential of -35mV measured in zwitterionic buffer (100mM KCl/10 mM HEPES). The sizes of the four products obtained from LTM40PTr using click chemistry increased to 56, 50, 66 and 51 nm for LTM40PTrg4PEG, LTM40PTrg4PEGOH, LTM40PTrg4PEGNH2, and LTM40PTrg4PEGCOOH, respectively, and zeta potentials were changed to -10mV, -13mV, -7mV, and -17mV, respectively. The DLS size of the click products slightly depended on the surface chemistry and their steric stabilization.

Surface chemistry of modified -COOH SNPs at different sizes

Grafting data from different sized -COOH SNPs are summarized in Table 4. The initial particle diameters ranged from 20 to 120 nm. Fig. 32D showed normalized FTIR spectra for SNPs terminated with -COOH groups, including LTM40PTrg4PEGCOOH, SNTXSPTrg4PEGCOOH, SNT20LPTrg4PEGCOOH, and SNTZLPTrg4PEGCOOH. Again, the IR band at 806 cm^{-1} (silica) was used to normalize the spectra and allowed semi-quantitative comparisons of the nanoparticles. All spectra showed IR absorption bands at 2900-3300 cm^{-1} and 1700 cm^{-1}, which corresponded to C-H stretching and a carbonyl group, respectively, confirming successful modification of the particle surface. Since the specific surface areas of small SNPs are higher than large particles, small particles appear to have higher grafted layers than larger particles. Therefore, the IR bands in Fig. 32D decreased in intensity from top to bottom (smallest particle to largest).

Table 4 and Fig. 32E showed TGA results for -COOH terminated SNPs. With increasing particle sizes (33 nm to 137 nm), TGA weight losses decreased from 15.9% to 2.2%, as expected due to the decreasing surface to mass ratios. The click conversion calculated from TGA data showed high conversion for all particles (>80%).

The DLS traces (Fig. 32F) and the data from SNPs modified with -COOH groups are presented in Table 4. All modified nanoparticles had monomodal distributions (intensity distribution), a result of the steric stabilization of surface modified particles.

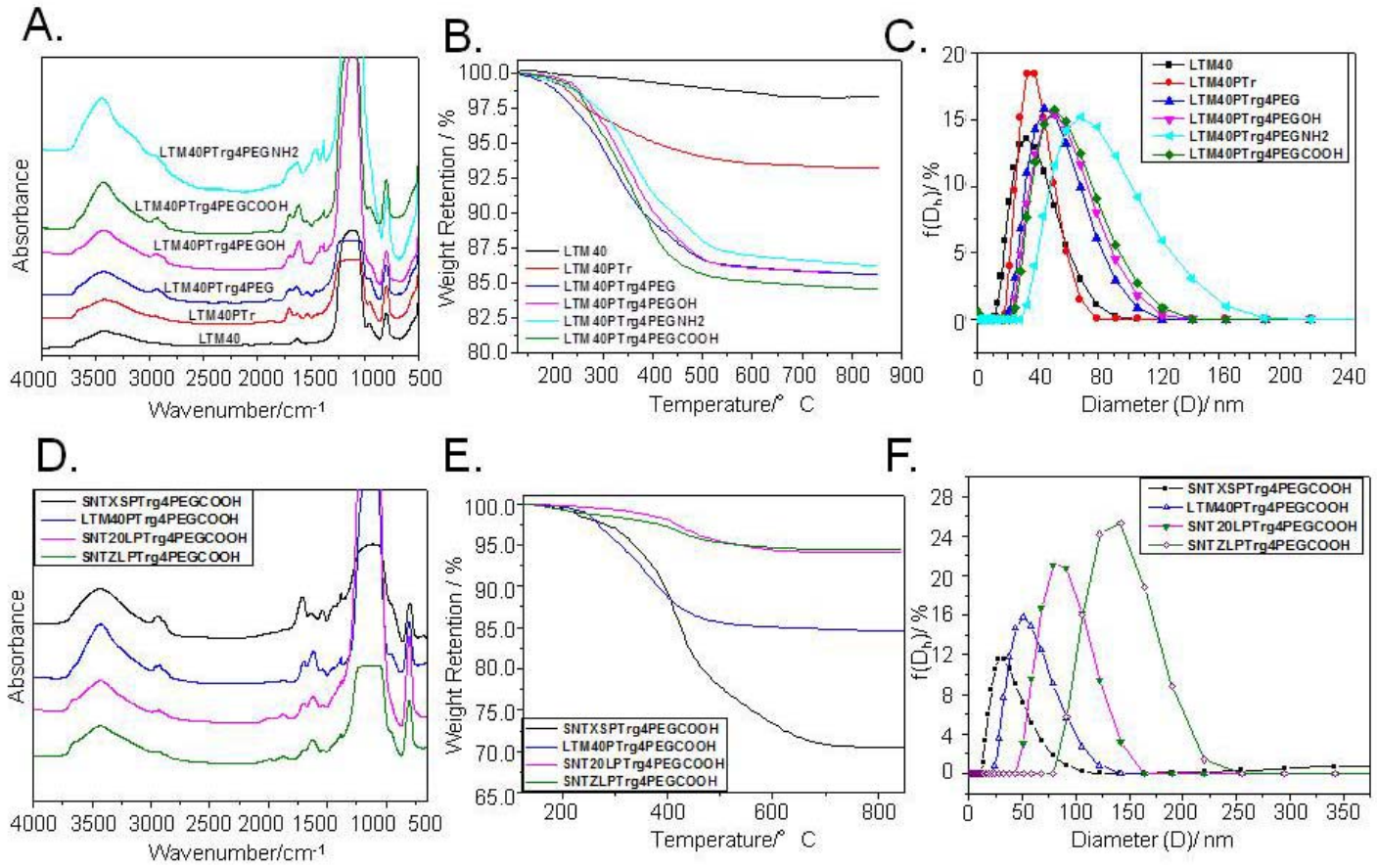

Figure 32. Surface chemistry of modified SNPs with different functional groups and at different sizes. (A and D) FTIR spectra were obtained by scanning the pellets of different SNPs and KBr from 500 to 4000 cm^{-1}, and the absorbance was recorded. FTIR spectra were normalized using the band intensity at 806 cm^{-1} for semi-quantitative comparison of the SNPs. (B and E) TGA traces of different SNPs were measured by burning the SNPs in air at a rate of 10 °C/min, and the weight retention of SNPs at different temperatures (120 to 850 °C) was recorded. (C and F) Different SNPs (100 µg/ml) were sonicated, and DLS data (size distribution by intensity) were measured at 25°C.

Table 3. Grafting amount and size of SNPs.

Sample	Weight Loss (%)[a]	Grafting Amount (mmol/g)[a]	Grafting Density (group/nm^2)[a]	Click Conversion[a] (%)	Size (nm)[b]
LTM40	--	--	--	--	30
LTM40PTr	5.1	0.36	1.5	--	37[c]
LTM40PTrg4PEG	7.6	0.33	1.4	92	56
LTM40PTrg4PEGOH	7.5	0.34	1.4	94	50
LTM40PTrg4PEGNH2	7.2	0.33	1.4	90	66
LTM40PTrg4PEGCOOH	8.7	0.37	1.5	97	51

[a] Weight loss, grafting amount, density and click conversion were determined after each modification step. [b] Size measured by DLS after sonication for 30 min in H_2O.

Table 4. Grafting data from different sized SNPs terminated with carboxylic acids.

Sample	Weight Loss (%)[a]	Grafting Amount (mmol/g)[a]	Grafting Density (group/nm^2)[a]	Click Conversion[a] (%)	Size (nm)[b]
SNTXS	--	--	--	--	20[b]
SNTXSPTr	10.4	0.74	0.8	--	19[c]
SNTXSPTrg4PEGCOOH	15.9	0.68	0.7	91.9	33[c]
LTM40	--	--	--	--	30[b]
LTM40PTr	5.1	0.36	1.5	--	37[c]
LTM40PTrg4PEGCOOH	8.7	0.37	1.5	100	51[b]
SNT20L	--	--	--	--	80[b]
SNT20LPTr	1.9	0.14	1.4	--	90[c]
SNT20LPTrg4PEGCOOH	2.8	0.12	1.2	84.3	82[b]
SNTZL	--	--	--	--	150[b]
SNTZLPTr	1.6	0.12	2.1	--	117[b]
SNTZLPTrg4PEGCOOH	2.2	0.10	1.7	79.2	137[b]

[a] Weight loss, grafting amount, density and click conversion were determined after each modification step. [b] Size measured in H_2O by DLS after sonication. [c] Size measured in EtOH.

Aqueous media dispersion stability of modified SNPs

DLS was used to determine whether the modified SNPs remained dispersed in cell culture media (RPMI containing 2% BCS) as well as their stability over time. Four SNPs with different surface chemistry (-OMe, -OH, -NH_2, and -COOH) were measured by DLS, and all were stabile for 2-3 days in the *in vitro* culture media without aggregation. For example, Fig. 33 showed data for LTM40PTrg4PEG (-OMe) in *in vitro* media. At 0 h in water, the distribution of the nanoparticles was monomodal with a hydrodynamic size of ~60 nm (black curve). The results from *in vitro* culture media showed two peaks, a small narrow peak at ~10 nm, and a broad particle population from >50 nm to <500 nm (red curve). After combining the particles and culture media (blue curve), the small peak at ~10 nm, seen in the culture media, shifted slightly to lower diameters (<10 nm), and the combined scattering from the nanoparticle and the media formed a single peak, which broadened toward higher particle sizes. On the high size of the distribution, the scattering was comprised of the sum of the particles and the media. Importantly, the onset for scattering from the particles, the near-constant slope of the low side of the distribution, and the peak of the distribution did not change as a function of time. We concluded that the pegylated SNPs in *in vitro* culture media showed no significant aggregation, and the main effect of the media was to broaden the distribution. The other three SNPs showed similar DLS behavior when added to *in vitro* culture media as presented in Fig. 34-36.

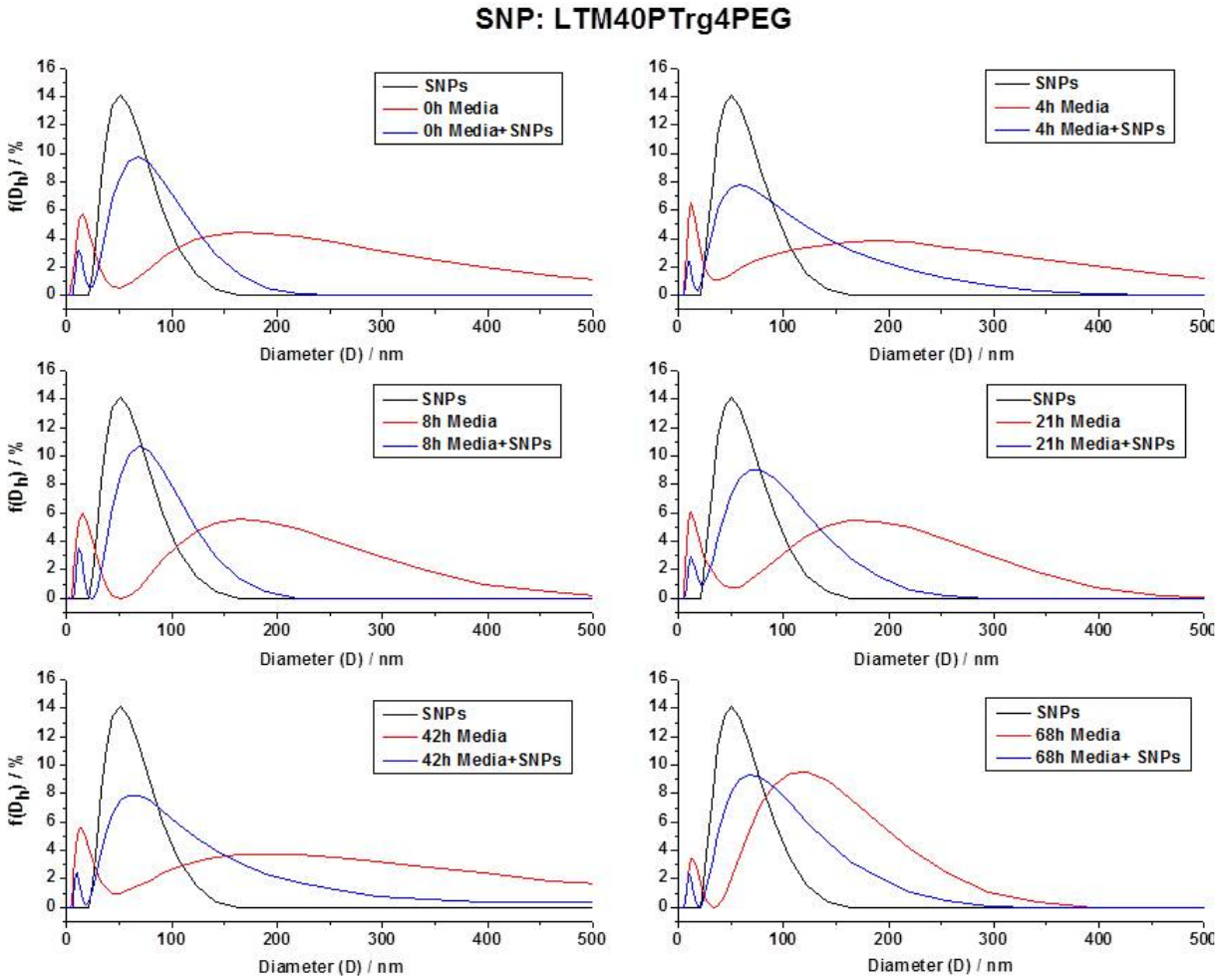

Figure 33. Aqueous dispersion stability of LTM40PTrg4PEG SNPs in *in vitro* culture media. LTM40PTrg4PEG SNPs were sonicated, and dispersed in culture media by vortexing. DLS data (size distribution by intensity) from LTM40PTrg4PEG SNPs alone (100 μg/ml, black curve), culture media alone (red curve), and LTM40PTrg4PEG SNPs in culture media (blue curve) at different time points (indicated on the graphs) were recorded.

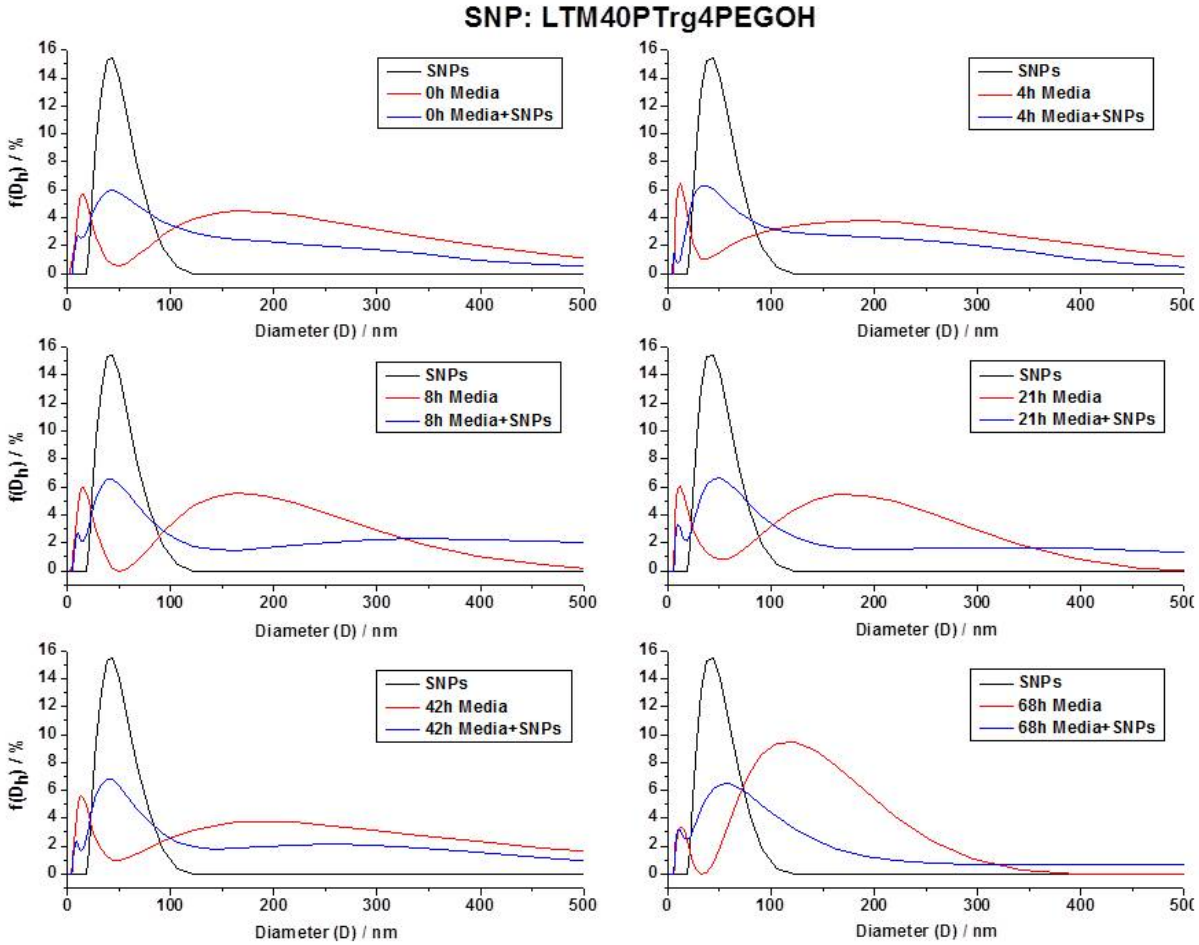

Figure 34. Aqueous dispersion stability of SNPs with -OH functional group in *in vitro* culture media. LTM40PTrg4PEGOH SNPs were sonicated, and dispersed in culture media by vortexing. DLS data (size distribution by intensity) from SNPs alone (100 μg/ml, black curve), culture media alone (red curve), and SNPs in culture media (blue curve) at different time points (indicated on the graphs) were recorded.

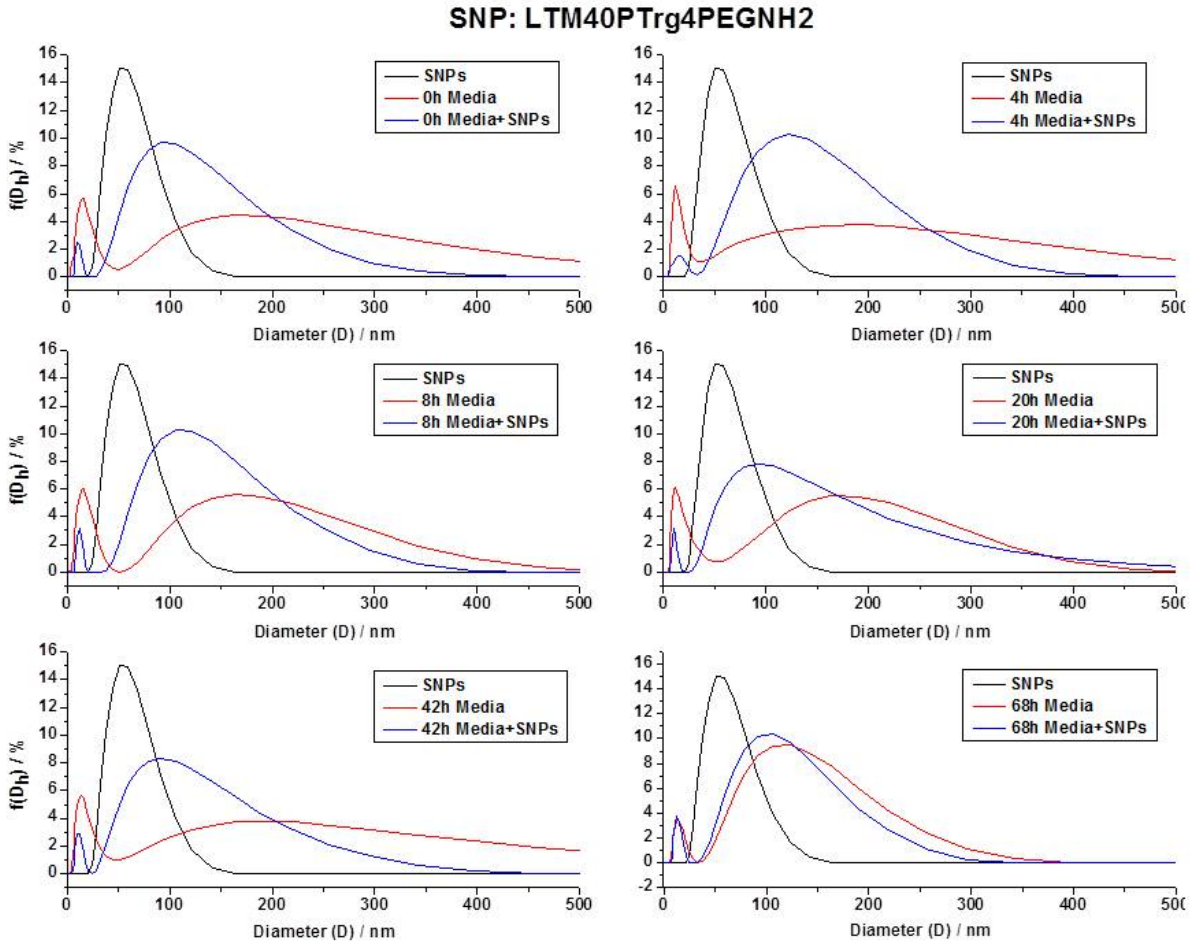

Figure 35. Aqueous dispersion stability of SNPs with –NH2 functional group in *in vitro* culture media. LTM40PTrg4PEGNH2 SNPs were sonicated, and dispersed in culture media by vortexing. DLS data (size distribution by intensity) from SNPs alone (100 μg/ml, black curve), culture media alone (red curve), and SNPs in culture media (blue curve) at different time points (indicated on the graphs) were recorded.

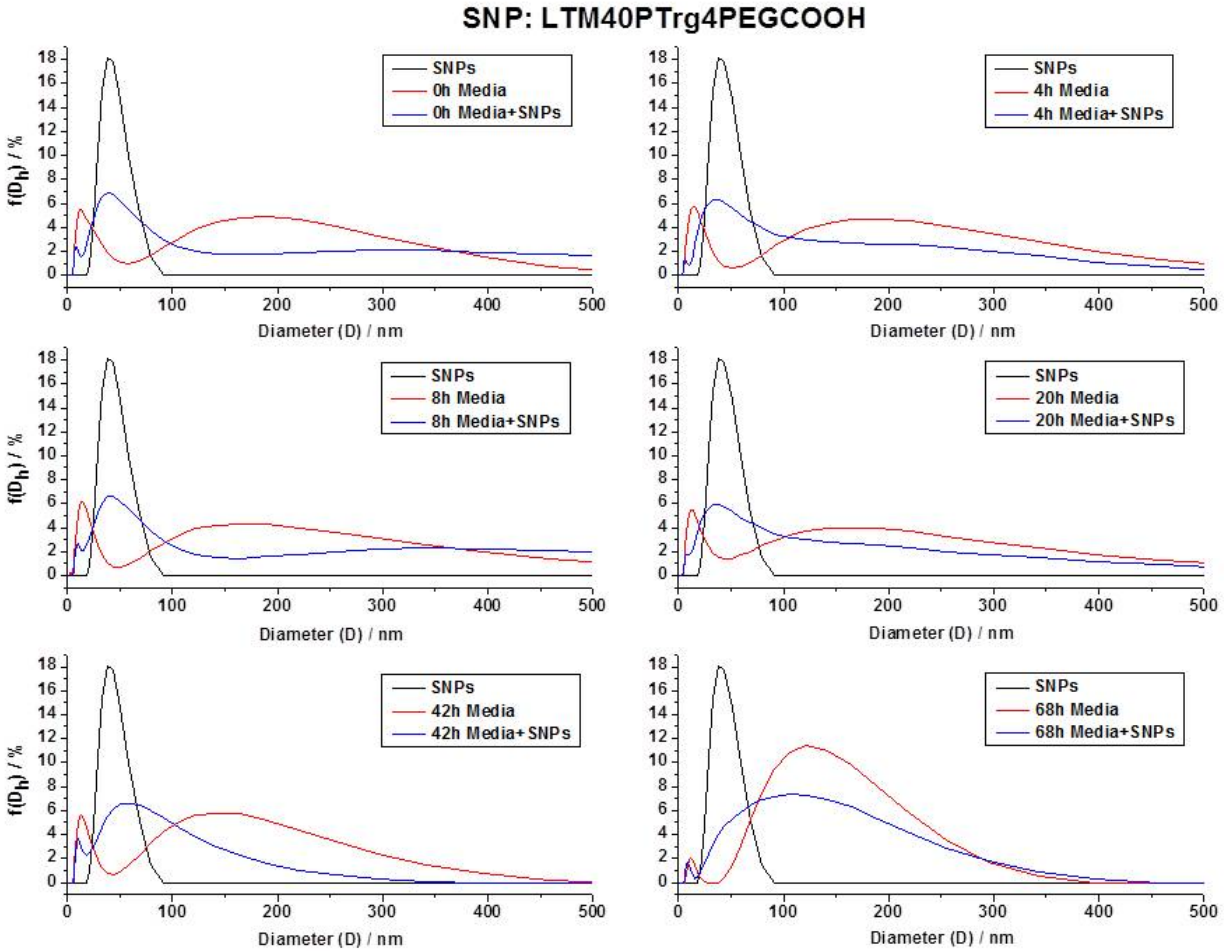

Figure 36. Aqueous dispersion stability of SNPs with -COOH functional group in *in vitro* culture media. LTM40PTrg4PEGCOOH SNPs were sonicated, and dispersed in culture media by vortexing. DLS data (size distribution by intensity) from SNPs alone (100 μg/ml, black curve), culture media alone (red curve), and SNPs in culture media (blue curve) at different time points (indicated on the graphs) were recorded.

$OVA_{257-264}$ (SIINFEKL)-stimulated cytokine production by $CD8^+$ T cells

Using the OT-I model in which SIINFEKL was presented by endogenous APCs to $CD8^+$ T cells, the percent of viable $CD8^+$ T cells that produced IFNγ (Fig. 37A, upper panel) or IL-2 (Fig. 37A, bottom panel) increased with increasing concentrations of SIINFEKL (S; 10^{-8} to 10^{-2} μg/ml). There was little background cytokine production in the absence of SIINFEKL stimulation (No S). In addition, the fluorescence intensity of IFNγ was higher than IL-2 (Fig. 37A). SIINFEKL (10^{-4} μg/ml) produced suboptimal, but measurable, stimulation of the $CD8^+$ T cell response and was used in subsequent experiments.

Cytokine production was also measured using the model in which DC2.4 cells were used as APCs to present SIINFEKL to OT-I $CD8^+$ T cells. DC maturation can be induced by various stimuli, including lipopolysaccharide (LPS) [278]. However, in this model under current conditions, LPS pretreatment of DC2.4 cells did not further increase IFNγ (Fig. 37B, left panel) or IL-2 (Fig. 37B, right panel) production by SIINFEKL-activated viable $CD8^+$ T cells. Thus, LPS pretreatment was not utilized in subsequent experiments. Production of IFNγ (Fig. 37C, upper panel) or IL-2 (Fig. 37C, bottom panel) by viable $CD8^+$ T cells was increased with increasing concentrations of SIINFEKL (0.01 – 1 μg/ml) loaded onto MHC I of DC2.4 cells. Also, there was more IFNγ production than IL-2, which was consistent with the trend observed in Fig. 37A. These studies showed that the concentration of SIINFEKL for MHC I loading on DC2.4, in order to achieve suboptimal activation of $CD8^+$ T cells, was 0.1 μg/ml.

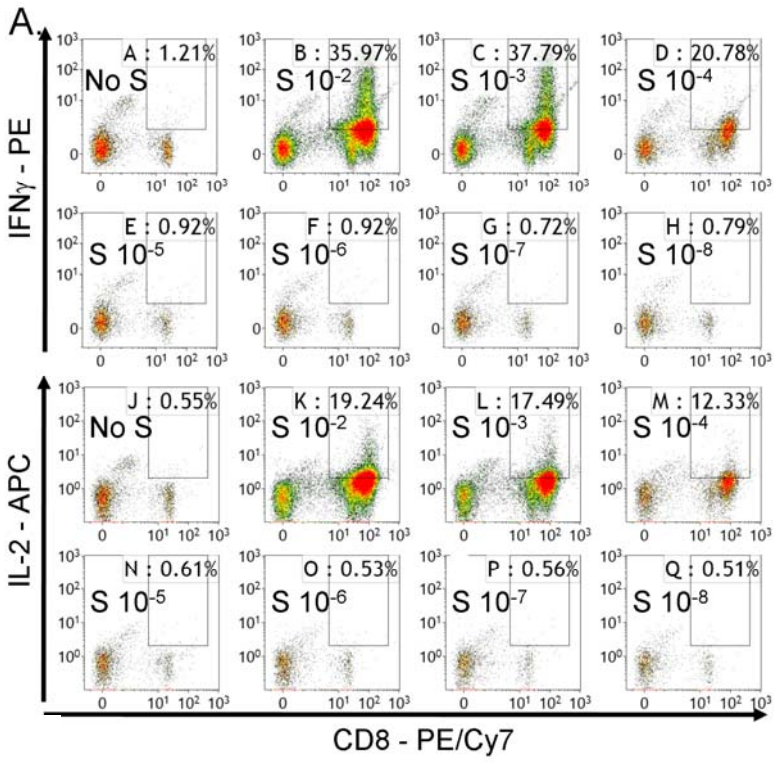

Figure 37. SIINFEKL concentration-dependent activation of CD8$^+$ T cell responses. (A) OT-I splenocytes (CD8$^+$ T cells, 8 x 10^5 cells/ well) were incubated with various concentrations of SIINFEKL (S) peptide (10^{-8} – 10^{-2} μg/ml) for 2 days. Brefeldin A was added during the last 6 h of incubation. Splenocytes were stained for viability, surface CD8 and intracellular IFNγ or IL-2 expression. The percent of IFNγ$^+$ or IL-2$^+$ cells within CD8$^+$ T cells is presented in the quadrants of dot plots, with X axis and Y axis representing the fluorescence intensity for CD8 and IFNγ or IL-2, respectively. (B) DC2.4 cells were pretreated with LPS (1 μg/ml) overnight, loaded with SIINFEKL peptide (1 μg/ml) for 3 – 4 h, irradiated, and plated at 2 x 10^5 cells/well with 1 x 10^6 cells/well OT-I splenocytes for 4 days. Splenocytes were restimulated with SIINFEKL (10 μg/ml) in the presence of brefeldin A for 6 h. Splenocytes were stained for viability, surface CD8 and intracellular IFNγ or IL-2 expression. The percent of IFNγ$^+$ or IL-2$^+$ cells within CD8$^+$ T cells is presented in histograms, with X axis representing fluorescence intensity for IFNγ or IL-2 and Y axis representing percent of CD8$^+$ T cells. (C) DC2.4 cells were not pretreated with LPS and incubated with various concentrations of SIINFEKL (10^{-2} – 1 μg/ml), co-cultured with OT-I splenocytes as described in (B). The dot plots are presented as described in (A). (A-C) Three replicates were concatenated for each treatment in the flow cytometric analysis. Data are representative of at least two separate experiments.

Figure 37 (cont'd)

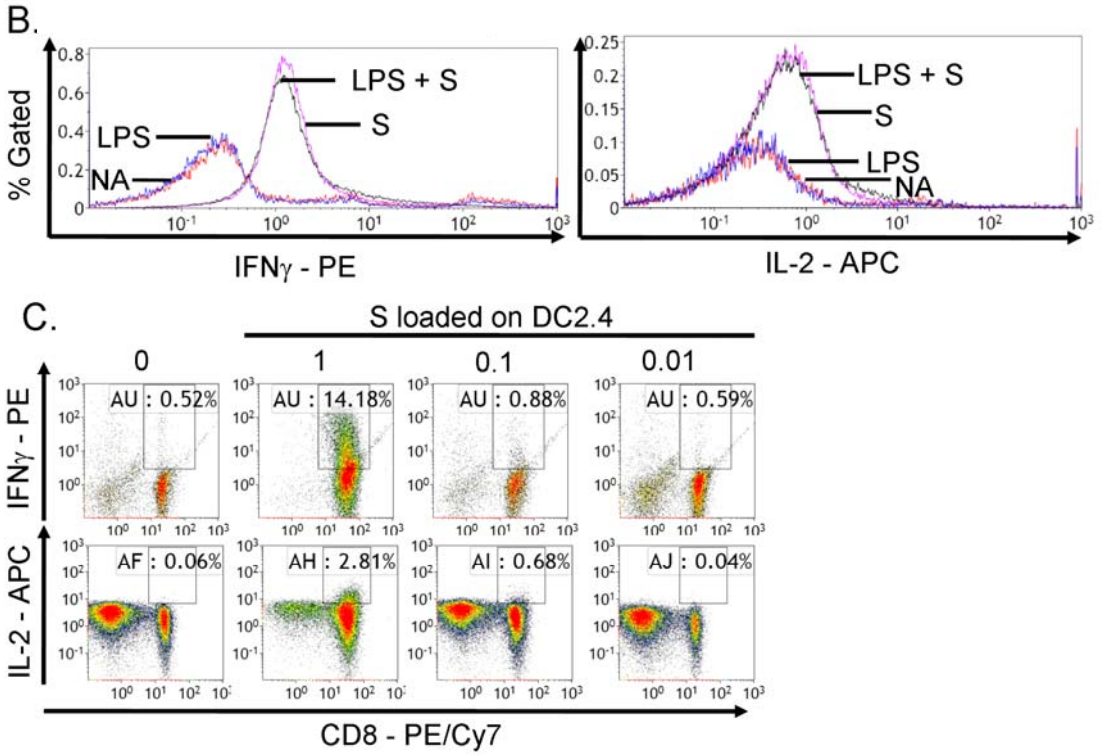

Modified SNPs enhanced SIINFEKL-activated $CD8^+$ T cell responses

LTM40PTrg4PEG SNPs alone showed minimal effects on IFNγ and IL-2 production by viable $CD8^+$ T cells; whereas LTM40PTrg4PEG enhanced the production of both cytokines by $CD8^+$ T cells that were suboptimally activated using SIINFEKL peptide directly (Fig. 38A and 38B). The effect was deemed statistically significant at multiple LTM40PTrg4PEG concentrations, including 0.01, 1, and 10 μg/ml for IFNγ, and all concentrations for IL-2. In the co-culture OT-I model in which irradiated DC2.4 cells were used as APCs, LTM40PTrg4PEG SNPs showed a similar trend of effect on $CD8^+$ T cell responses. LTM40PTrg4PEG had no effect in the absence of SIINFEKL activation; whereas in the presence of a suboptimal concentration of SIINFEKL loaded onto DC2.4 cells, LTM40PTrg4PEG at 10 μg/ml further enhanced IFNγ (Fig. 38C) and IL-2 (Fig. 38D) production by viable $CD8^+$ T cells, with the latter being significantly different from the no particle treatment control. This suggests that SNP-mediated enhancement is likely to act directly on $CD8^+$ T cell responses.

Different functional groups on SNPs influenced the immune enhancing effect to different levels

The effect of engineered SNPs on T cell responses was compared between particles with different surface functional groups, including LTM40PTrg4PEG (-OMe), LTM40PTrg4PEGOH (-OH), LTM40PTrg4PEGCOOH (-COOH), and LTM40PTrg4PEGNH2 ($-NH_2$). Similar to the above observations, in the absence of SIINFEKL stimulation, SNPs produced minimal effects on the cytokine response, especially for IL-2 (Fig. 38E and 38F). When OT-I $CD8^+$ T cells were suboptimally activated with 10^{-4}

μg/ml of SIINFEKL, all tested SNPs showed significant enhancement of IFNγ (Fig. 38E) and IL-2 (Fig. 38F) production by $CD8^+$ T cells. In particular, -COOH and $-NH_2$ particles exhibited concentration-dependent enhancement on cytokine production.

Absence of immune enhancement by SNPs on $OVA_{323-339}$-induced $CD4^+$ T cell responses

In the OT-II model in which $OVA_{323-339}$ is presented by MHC II molecules on endogenous APCs to OT-II $CD4^+$ T cells, production of IFNγ and IL-2 was minimal in the absence of $OVA_{323-339}$ peptide activation and increased with increasing concentrations of $OVA_{323-339}$ (0.01 – 0.1 μg/ml) (Fig. 39A). In contrast to the OT-I model, there was more IL-2 production than IFNγ in the OT-II model. The $OVA_{323-339}$ concentration for suboptimal $CD4^+$ T cell activation was determined to be 0.05 μg/ml. Next, effects of SNPs with different functional groups on $CD4^+$ T cell responses were characterized. In contrast to their enhancing effects on $CD8^+$ T cell responses, none of the particles showed enhancing activity on IFNγ and IL-2 production by $CD4^+$ T cells at any of the tested concentrations (Fig. 39B and 39C).

Enhancing effect of SNPs on $CD8^+$ T cell responses is size-dependent

Next, we investigated the role of particle size on the enhancement of $CD8^+$ T cell responses. Particles with the -COOH functional group at different sizes, including SNTXSPTrg4PEGCOOH (33 nm), LTM40PTrg4PEGCOOH (51 nm), SNT20LPTrg4PEGCOOH (82 nm), and SNTZLPTrg4PEGCOOH (137 nm), were compared. Interestingly, only the 51 nm -COOH particles at 10 μg/ml produced a significantly greater enhancement of IFNγ and IL-2 production by $CD8^+$ T cells activated with a suboptimal

concentration of SIINFEKL. SNPs either smaller or larger in size than 51 nm particles lacked immune enhancing activity as assessed by IL-2 and IFNγ production (Fig. 40A and 40B).

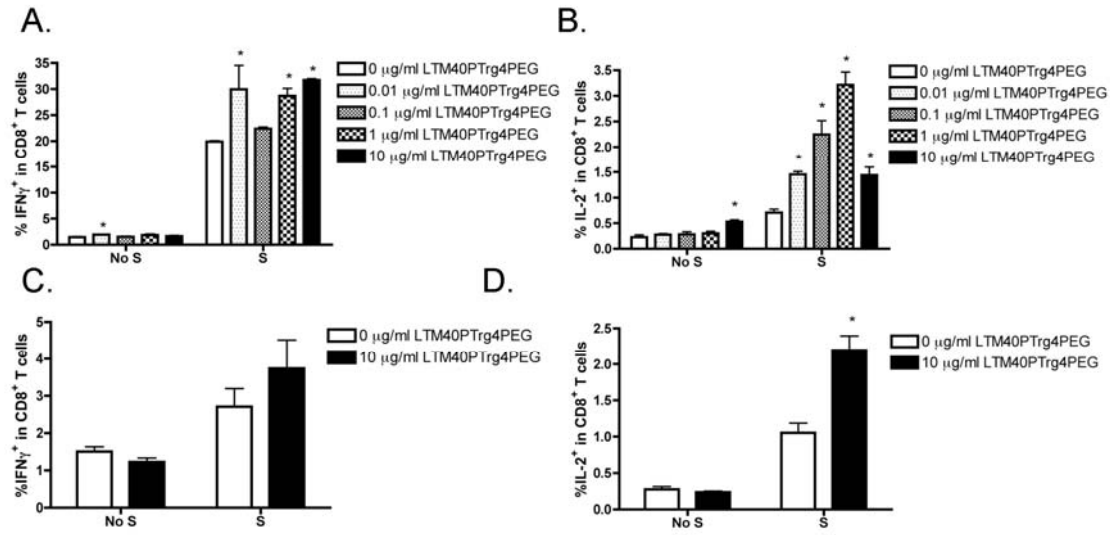

Figure 38. Enhancement by modified LTM40PTrg4PEG on CD8$^+$ T cell responses induced by a suboptimal concentration of SIINFEKL. (A-B) LTM40PTrg4PEG SNPs were sonicated and added to OT-I splenocytes (CD8$^+$ T cells, 8 x 10^5 cells/ well) at various concentrations (10^{-2} – 10 μg/ml) prior to SIINFEKL (S) stimulation (10^{-4} μg/ml) for 2 days. (C-D) SIINFEKL (S, 0.1 μg/ml)-loaded DC2.4 cells (2 x 10^6 cells/well) were irradiated and plated at 2 x 10^5 cells/well. OT-I splenocytes (1 x 10^6 cells/well) were treated with LTM40PTrg4PEG SNPs (10 μg/ml) and then co-cultured with SIINFEKL-loaded DC2.4 cells for 4 days. Splenocytes were restimulated with SIINFEKL (10 μg/ml) in the presence of brefeldin A. (E-F) SNPs with different functional groups, including LTM40PTrg4PEG (-OMe), LTM40PTrg4PEGOH (-OH), LTM40PTrg4PEGCOOH (-COOH), and LTM40PTrg4PEGNH2 (-NH_2), were sonicated and then added to OT-I splenocytes (8 x 10^5 cells/ well) at various concentrations (10^{-1} – 10 μg/ml) prior to SIINFEKL (S) stimulation (10^{-4} μg/ml) for 2 days. (A-F) Brefeldin A was added during the last 6 h of incubation. Splenocytes were stained for viability, surface CD8 and intracellular IFNγ or IL-2 expression. The percent of IFNγ$^+$ or IL-2$^+$ cells within CD8$^+$ T cells is presented as the mean % ± S. E. of triplicate cultures. * $p < 0.05$ as compared to respective no SNP treatment control. Data are representative of at least two separate experiments.

Figure 38 (cont'd)

E.

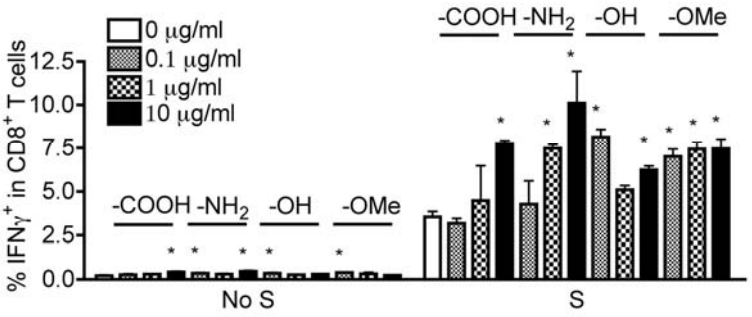

F.

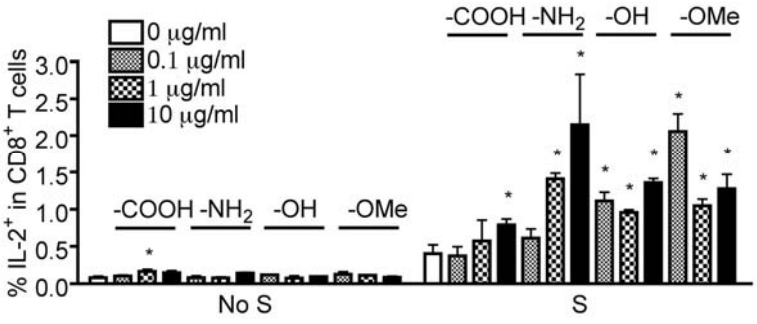

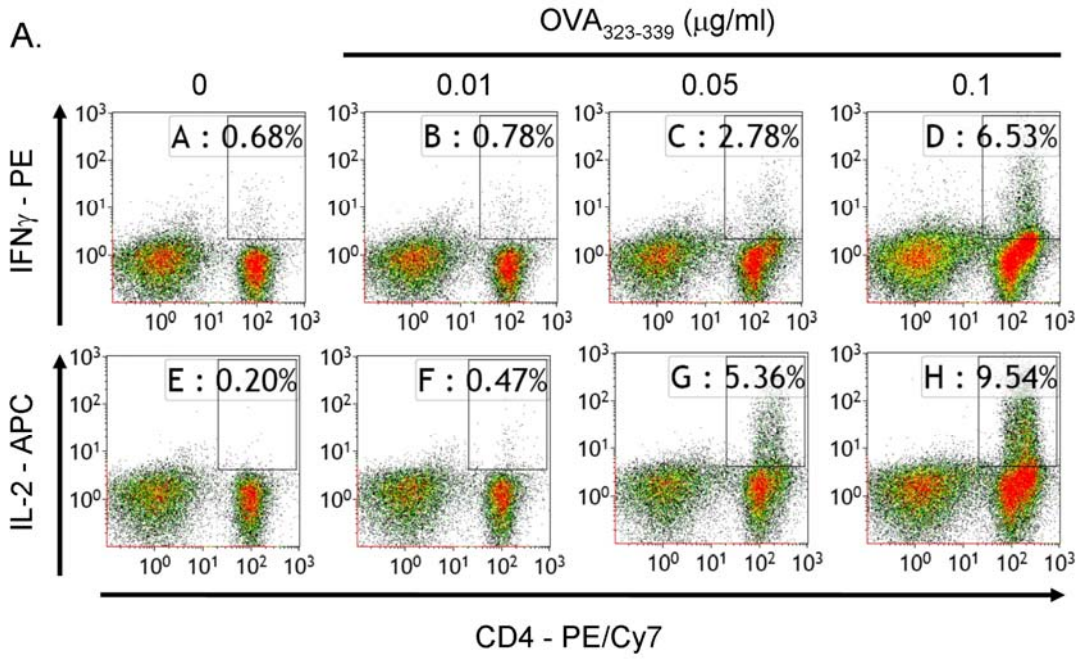

Figure 39. Absence of enhancement by SNPs with different functional groups on $CD4^+$ T cell responses under suboptimal $OVA_{323-339}$ stimulation. (A) OT-II splenocytes ($CD4^+$ T cells, 8 x 10^5 cells/well) were incubated with various concentrations of $OVA_{323-339}$ peptide (10^{-2} – 0.1 μg/ml) for 2 days. (B-C) SNPs with different functional groups, including LTM40PTrg4PEG (-OMe), LTM40PTrg4PEGOH (-OH), LTM40PTrg4PEGCOOH (-COOH), and LTM40PTrg4PEGNH2 ($-NH_2$), were sonicated and added to OT-II splenocytes at various concentrations (10^{-1} – 10 μg/ml) prior to $OVA_{323-339}$ peptide stimulation (0.05 μg/ml) for 2 days. (A-C) Brefeldin A was added during the last 6 h of incubation. Splenocytes were stained for viability, surface CD4 and intracellular IFNγ or IL-2 expression. The percent of $IFN\gamma^+$ or $IL\text{-}2^+$ cells within $CD4^+$ T cells is presented in the quadrants in dot plots (A), with X axis and Y axis representing fluorescence intensity for CD4 and IFNγ or IL-2, respectively. Three replicates were concatenated for each treatment in the flow cytometry analysis (A). The percent of $IFN\gamma^+$ (B) or $IL\text{-}2^+$ (C) cells within $CD4^+$ T cells is presented as the mean % ± S. E. of triplicate cultures. * $p < 0.05$ as compared to respective no SNP treatment control. Data are representative of at least two separate experiments.

Figure 39 (cont'd)

B.

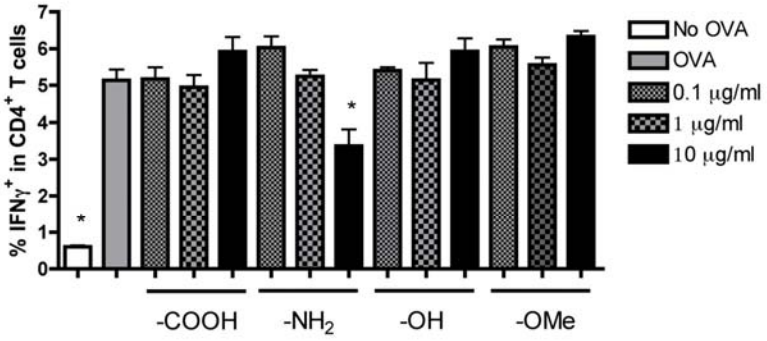

C.

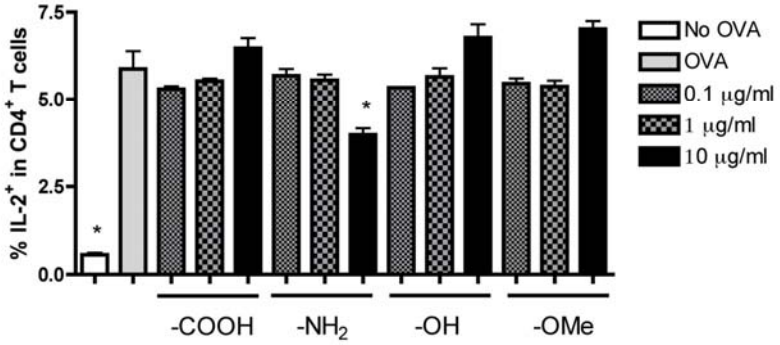

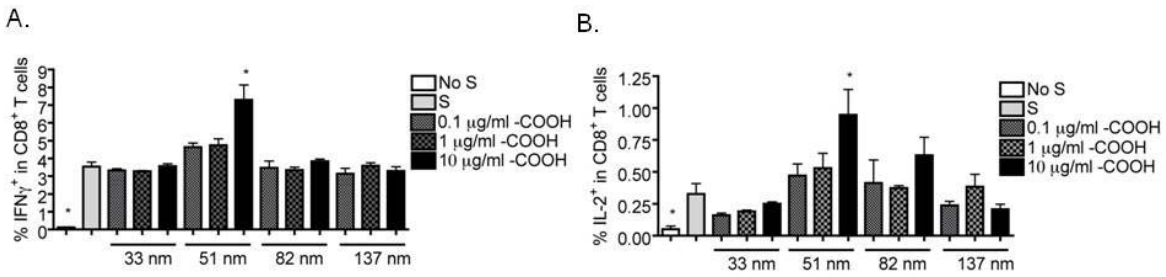

Figure 40. Effect of -COOH SNPs at different sizes on $CD8^+$ T cell responses under suboptimal induction. (A-B) SNPs with -COOH functional group at different sizes, including SNTXSPTrg4PEGCOOH (33 nm), LTM40PTrg4PEGCOOH (51 nm), SNT20LPTrg4PEGCOOH (82 nm), and SNTZLPTrg4PEGCOOH (137 nm) were sonicated and then added to OT-I splenocytes (8×10^5 cells/ well) at various concentrations (10^{-1} – 10 μg/ml) prior to SIINFEKL (S) stimulation (10^{-4} μg/ml) for 2 days. Brefeldin A was added during the last 6 h of incubation. Splenocytes were stained for viability, surface CD8 and intracellular IFNγ or IL-2 expression. The percent of $IFN\gamma^+$ (A) or $IL\text{-}2^+$ (B) cells within $CD8^+$ T cells is presented as the mean % ± S. E. of triplicate cultures. * $p < 0.05$ as compared to respective no SNP treatment control. Data are representative of at least two separate experiments.

DISCUSSION

As the commercial use of engineered nanoparticles has grown, their potential for causing adverse health issues has also received increasing attention. To date, most investigations focusing on the potential toxicity of engineered nanoparticles have been conducted in laboratory animals. Some of these studies have demonstrated that certain engineered nanoparticles possess adjuvant-like properties, especially on pulmonary inflammation and lung disease. Although inhalation is one of the principal routes of particle exposure [262-265, 279], little is still known concerning the effect of engineered nanoparticles on immune responses in airways or on the immune system in general. Here, we utilized unique *in vitro* mouse models to stimulate antigen-specific $CD8^+$ and $CD4^+$ T cell responses in order to investigate the effects of engineered nanoparticles on the functions of certain leukocyte populations. It is worth mentioning that two related but distinct OT-I models possessing either endogenous splenic APCs containing multiple cellular populations or the cell line, DC2.4, for antigen presentation of SIINFEKL showed similar trends, as evidenced by enhancement of antigen-specific $CD8^+$ T cell responses by engineered nanoparticles. As reviewed by Banchereau and co-workers, DCs are highly efficient antigen presenting cells [278]. DC2.4 cells were irradiated before co-culturing with splenocytes to arrest their proliferation, so they would not deplete the media of nutrients and/or outgrow naïve T cells; however, their ability to activate naïve T cells in the context of antigen-MHC complexes is not affected by irradiation [280, 281]. By using DC2.4 as the only APC population in the second OT-I model, OVA peptides were directly loaded onto DC2.4, therefore the effects of nanoparticles on antigen processing via APCs as a potential confounder were eliminated, allowing the direct assessment of their potential effects on T cell responses. With two OT-I

models, we demonstrated that SNPs produced their immune enhancing effects most likely by affecting T cell function directly.

The aqueous-dispersed engineered nanoparticles used in the present study underwent chemical modification by varying the surface functional group moieties and overall particle sizes. An important as well as rare physico-chemical property of the engineered nanoparticles employed in this study was that these intermediate-sized particles are resistant to undergoing aggregation even in the culture media, which allowed them to be used in *in vitro* assay systems to investigate their influence on leukocyte function in their true nanoscale context. Although the size distribution peak for the -NH_2 SNPs in culture media appeared to shift to the right, around 100 nm, distinct from the peaks for other particles, which appeared close to 50 nm, we believe they are unlikely to agglomerate in the culture media. Because if modest changes in the size of -NH_2 SNPs led to significant shifts between no agglomeration and agglomeration, one would expect to observe significant peaks at markedly larger sizes than 100 nm (i.e., which would be representative of association between 2 particles). Alternatively, the change in size could reflect an interaction between SNPs and serum proteins as previously suggested [282, 283]. However, if the nanoparticles interacted with protein components in the serum, the particle size would increase dramatically due to formation of agglomerates and keep increasing over time as reported in the literature [284], which were not detected by DLS here. In addition, a relatively low serum concentration in the RPMI media was used in our studies, which would not introduce a big amount of serum proteins, therefore keeping the zeta potentials relatively stable as compared to no serum condition. It is also worth mentioning that the average hydrodynamic diameters of the bare SNPs, measured by DLS in water, were larger than the sizes claimed by manufacturers, which

is likely due to the differences in methodologies for particle size measurement, such as using transmission electron microscopy (TEM) or scanning electron microscopy (SEM) images.

The zeta potential of all coated SNPs displayed higher values than the bare SNP, indicating that the silanol groups were covered by PEG layers. NH_2-modified SNPs showed the highest zeta potential, which indicates the zeta potential of bare SNP was compensated by both the PEG layer and the NH_2 (+) surface charge. COOH-modified SNPs with the lowest zeta potential, which was higher than bare SNP, is due to the PEG layer and carboxylate group in the buffer. PEG and OH-modified SNPs showed medium zeta potential, which is due to the neutral surface function and PEG layers. It has been reported recently that surface modified SNPs have a negative zeta potential for neutral surface layers and +0.6mV only for amine modified SNPs in PBS buffer [285, 286]. Our negative zeta potential is most likely due, at least in part, to the remaining negatively charged silanol groups.

Since surface chemistry of nanoparticles directly influences cellular uptake and thereby their activity as well as interaction with cellular compartments in the cells [273], three surface functional groups, including -COOH, -NH_2, and -OH, were engineered to modify the pegylated SNPs individually. Among these three functional groups, -COOH SNPs were chosen for further characterization, although both -COOH and -NH_2 SNPs showed concentration-dependent enhancement of the $CD8^+$ T cell response when compared with -OH SNPs in our assays (Fig. 38E and 38F). It has been suggested that -COOH particles help to facilitate cellular uptake and transport into intracellular compartments with less aggregation inside the cells [287]. Also, since -COOH, -NH_2, and -OH particles have different surface charges at physiological pH, cationic charge of the cell membrane due to interaction with -NH_2 particles may cause excessive proton transport and accumulate inside the cells, therefore

generating reactive oxygen species (ROS), which may injury mitochondria and eventually disrupt the cellular function [288, 289]. In addition, no agglomeration in culture media was observed with -COOH particles. Therefore, -COOH particles were selected for the subsequent size-dependent studies.

In this assay system, cytokine production by $CD8^+$, but not $CD4^+$, T cells was significantly increased by modified SNPs, suggesting that the particles selectively target $CD8^+$ T cell responses. It has been suggested that certain physico-chemical properties of modified SNPs may induce upregulation of MHC I expression on DCs by increasing phosphorylation of mitogen-activated protein kinases (MAPK), such as p38 kinase, c-Jun N-terminal kinases (JNK), and extracellular signal-regulated kinases (ERK), which are involved in DC activation signaling pathways, and thereby indirectly enhance $CD8^+$ T cell responses [290]. However, because DC2.4 cells were irradiated for experiments employing the co-culture model, MHC I expression on these cells should not be further regulated by SNPs, hence suggesting that SNPs did not enhance $CD8^+$ T cell responses via regulating APCs. Therefore, mechanisms underlining the observed enhancement on $CD8^+$ T cell responses remain to be elucidated. It is possible that engineered nanoparticles in our models specifically modulate $CD8^+$ T cell receptor signaling or directly interact with surface receptors on $CD8^+$ T cells, e.g. low-density lipoprotein receptor [291], and thereby increase particle cellular uptake to enhance $CD8^+$ T cell responses, but further investigations will be needed. In addition, there was no direct cytotoxicity from SNPs on the T cells, because all the flow cytometry analyses were performed using viable cells.

We have demonstrated that only particles at a size of 51 nm significantly enhanced $CD8^+$ T cell responses, suggesting that the nanoparticle-mediated enhancement of $CD8^+$ T cell

responses is size-dependent. Similar nanoparticle size-dependent effect has been demonstrated previously, indicating that within the size range of 2 - 100 nm, 50 nm gold nanoparticles showed the greatest effect on membrane receptor internalization, which in turn affected the downstream cellular proliferation and survival responses [292]. As suggested by others using gold naoparticles in cells or theoretical models, 50 nm particles might fall into the critical size range for receptor-mediated internalization. Smaller particles might dissociate from the receptors on the membrane before being endocytosed due to their small avidity; whereas large particles might cause decreased membrane wrapping efficiency, which would directly impair the nanoparticle internalization process [292-294].

Collectively, we demonstrated immune enhancing properties by engineered SNPs on DC-induced antigen-specific $CD8^+$ T cell responses using an OT-I model *in vitro*, suggesting the potential adjuvant-like effects of these engineered SNPs on immune function at the cellular level. We also show that by modifying the chemical and physical properties of the particles, such as the surface chemistry and size, the immunomodulatory properties of these particles can be differentially affected. Further studies at the organismal, cellular and subcellular level with special emphasis on engineered nanoparticle-membrane interactions are needed to provide more in-depth understanding of the mechanisms responsible for immune modulation by SNPs.

CONCLUSIONS

In summary, our results demonstrated that the engineered SNPs were successfully modified with different functional group moieties on the surface and in different sizes, which allowed them to be used to characterize the effect of diverse physical and chemical properties of SNPs on T cell function. In addition, modified SNPs, except for -NH_2 SNP, which might interact with proteins in the media, did not agglomerate in *in vitro* culture condition, which was critical for them to maintain their aqueous distribution at the nanoscale and was an essential prerequisite for studying their immunological effects (Fig. 33-36). Conditions for suboptimal stimulation of T cell responses were determined using OT-I and OT-II models (Fig. 37 and 39A) in order to measure the immune enhancing effects of the SNPs. Modified SNPs (up to 10 μg/ml) enhanced OVA-specific IFNγ and IL-2 production by $CD8^+$, but not $CD4^+$, T cells, suggesting a cell-type selective effect by engineered SNPs on immune function, in particular on antigen-specific $CD8^+$ T cell responses. Enhancement of $CD8^+$ T responses by SNPs was differentially affected by the surface functional groups placed on the SNPs, which is consistent with findings of others [273, 287]. SNPs with -COOH moieties were chosen for subsequent studies, since they exhibited concentration-dependent enhancement of $CD8^+$ T responses in the current assay system as well as advantages over SNPs with other functional groups as suggested in the literature [287-289], such as enhanced cellular uptake, less agglomeration, and limited cellular toxicity. Lastly, 51 nm sized SNPs showed greater enhancement of $CD8^+$ T cell responses than the other sized SNPs, which might be dictated by the nanoparticle size-dependent internalization processes as suggested by others [292-294]. Our findings provide strong evidence that nanoparticles have potential adjuvant-like properties by enhancing immune function, which will cause adverse effects on allergic airway

disease in humans. In addition, our studies have significant implications in understanding the role of particle size and other surface chemistry on regulating the biological responses and providing guidelines for the design of nanoproducts, with great potential for the development of novel biomedical applications in diagnostics and therapeutics.

BIBLIOGRAPHY

BIBLIOGRAPHY

1. Gilbert, P.B., McKeague, I.W., Eisen, G., Mullins, C., Gueye, N.A., Mboup, S., Kanki, P.J. (2003) Comparison of HIV-1 and HIV-2 infectivity from a prospective cohort study in Senegal. *Stat Med* 22, 573-93.

2. Buonaguro, L., Tornesello, M.L., Buonaguro, F.M. (2007) Human immunodeficiency virus type 1 subtype distribution in the worldwide epidemic: pathogenetic and therapeutic implications. *J Virol* 81, 10209-19.

3. Hemelaar, J., Gouws, E., Ghys, P.D., Osmanov, S. (2006) Global and regional distribution of HIV-1 genetic subtypes and recombinants in 2004. *Aids* 20, W13-23.

4. Gallo, R., Wong-Staal, F., Montagnier, L., Haseltine, W.A., Yoshida, M. (1988) HIV/HTLV gene nomenclature. *Nature* 333, 504.

5. Gallay, P., Swingler, S., Song, J., Bushman, F., Trono, D. (1995) HIV nuclear import is governed by the phosphotyrosine-mediated binding of matrix to the core domain of integrase. *Cell* 83, 569-76.

6. Lewis, P., Hensel, M., Emerman, M. (1992) Human immunodeficiency virus infection of cells arrested in the cell cycle. *Embo J* 11, 3053-8.

7. Harrison, G.P., Lever, A.M. (1992) The human immunodeficiency virus type 1 packaging signal and major splice donor region have a conserved stable secondary structure. *J Virol* 66, 4144-53.

8. Paxton, W., Connor, R.I., Landau, N.R. (1993) Incorporation of Vpr into human immunodeficiency virus type 1 virions: requirement for the p6 region of gag and mutational analysis. *J Virol* 67, 7229-37.

9. Loetscher, P., Moser, B., Baggiolini, M. (2000) Chemokines and their receptors in lymphocyte traffic and HIV infection. *Adv Immunol* 74, 127-80.

10. Ruben, S., Perkins, A., Purcell, R., Joung, K., Sia, R., Burghoff, R., Haseltine, W.A., Rosen, C.A. (1989) Structural and functional characterization of human immunodeficiency virus tat protein. *J Virol* 63, 1-8.

11. Kim, S.Y., Byrn, R., Groopman, J., Baltimore, D. (1989) Temporal aspects of DNA and RNA synthesis during human immunodeficiency virus infection: evidence for differential gene expression. *J Virol* 63, 3708-13.

12. Garcia, J.V., Miller, A.D. (1992) Downregulation of cell surface CD4 by nef. *Res Virol* 143, 52-5.

13. Luria, S., Chambers, I., Berg, P. (1991) Expression of the type 1 human immunodeficiency virus Nef protein in T cells prevents antigen receptor-mediated induction of interleukin 2 mRNA. *Proc Natl Acad Sci U S A* 88, 5326-30.

14. Miller, M.D., Warmerdam, M.T., Gaston, I., Greene, W.C., Feinberg, M.B. (1994) The human immunodeficiency virus-1 nef gene product: a positive factor for viral infection and replication in primary lymphocytes and macrophages. *J Exp Med* 179, 101-13.

15. von Schwedler, U., Song, J., Aiken, C., Trono, D. (1993) Vif is crucial for human immunodeficiency virus type 1 proviral DNA synthesis in infected cells. *J Virol* 67, 4945-55.

16. Re, F., Braaten, D., Franke, E.K., Luban, J. (1995) Human immunodeficiency virus type 1 Vpr arrests the cell cycle in G2 by inhibiting the activation of p34cdc2-cyclin B. *J Virol* 69, 6859-64.

17. Klimkait, T., Strebel, K., Hoggan, M.D., Martin, M.A., Orenstein, J.M. (1990) The human immunodeficiency virus type 1-specific protein vpu is required for efficient virus maturation and release. *J Virol* 64, 621-9.

18. Prevention, C.f.D.C.a. (2012) Monitoring selected national HIV prevention and care objectives by using HIV surveillance data - United States and 6 U.S. dependent areas - 2010. *HIV Surveillance Supplemental Report* 17.

19. Prevention, C.f.D.C.a. (2012) Estimated HIV incidence in the United States, 2007–2010. *HIV Surveillance Supplemental Report* 17.

20. Doms, R.W. (2001) Chemokine receptors and HIV entry. *Aids* 15 Suppl 1, S34-5.

21. Pierson, T., Hoffman, T.L., Blankson, J., Finzi, D., Chadwick, K., Margolick, J.B., Buck, C., Siliciano, J.D., Doms, R.W., Siliciano, R.F. (2000) Characterization of

chemokine receptor utilization of viruses in the latent reservoir for human immunodeficiency virus type 1. *J Virol* 74, 7824-33.

22. Kewenig, S., Schneider, T., Hohloch, K., Lampe-Dreyer, K., Ullrich, R., Stolte, N., Stahl-Hennig, C., Kaup, F.J., Stallmach, A., Zeitz, M. (1999) Rapid mucosal CD4(+) T-cell depletion and enteropathy in simian immunodeficiency virus-infected rhesus macaques. *Gastroenterology* 116, 1115-23.

23. Douek, D.C., Picker, L.J., Koup, R.A. (2003) T cell dynamics in HIV-1 infection. *Annu Rev Immunol* 21, 265-304.

24. McMichael, A.J., Borrow, P., Tomaras, G.D., Goonetilleke, N., Haynes, B.F. (2010) The immune response during acute HIV-1 infection: clues for vaccine development. *Nat Rev Immunol* 10, 11-23.

25. Ho, D.D., Neumann, A.U., Perelson, A.S., Chen, W., Leonard, J.M., Markowitz, M. (1995) Rapid turnover of plasma virions and CD4 lymphocytes in HIV-1 infection. *Nature* 373, 123-6.

26. Haase, A.T. (1999) Population biology of HIV-1 infection: viral and CD4+ T cell demographics and dynamics in lymphatic tissues. *Annu Rev Immunol* 17, 625-56.

27. Pantaleo, G., Graziosi, C., Fauci, A.S. (1993) The Immunopathogenesis of Human Immunodeficiency Virus Infection. *New England Journal of Medicine* 328, 327-335.

28. Zheng, Y.H., Lovsin, N., Peterlin, B.M. (2005) Newly identified host factors modulate HIV replication. *Immunol Lett* 97, 225-34.

29. Hiscott, J., Kwon, H., xE, nin, P. (2001) Hostile takeovers: viral appropriation of the NF-kB pathway. *The Journal of Clinical Investigation* 107, 143-151.

30. Pollard, V.W., Malim, M.H. (1998) The HIV-1 Rev protein. *Annu Rev Microbiol* 52, 491-532.

31. Rambaut, A., Posada, D., Crandall, K.A., Holmes, E.C. (2004) The causes and consequences of HIV evolution. *Nat Rev Genet* 5, 52-61.

32. Diebold, S.S., Kaisho, T., Hemmi, H., Akira, S., Reis e Sousa, C. (2004) Innate antiviral responses by means of TLR7-mediated recognition of single-stranded RNA. *Science* 303, 1529-31.

33. Stacey, A.R., Norris, P.J., Qin, L., Haygreen, E.A., Taylor, E., Heitman, J., Lebedeva, M., DeCamp, A., Li, D., Grove, D., Self, S.G., Borrow, P. (2009) Induction of a striking systemic cytokine cascade prior to peak viremia in acute human immunodeficiency virus type 1 infection, in contrast to more modest and delayed responses in acute hepatitis B and C virus infections. *J Virol* 83, 3719-33.

34. Lapenta, C., Santini, S.M., Proietti, E., Rizza, P., Logozzi, M., Spada, M., Parlato, S., Fais, S., Pitha, P.M., Belardelli, F. (1999) Type I Interferon Is a Powerful Inhibitor of in Vivo HIV-1 Infection and Preserves Human CD4+ T Cells from Virus-Induced Depletion in SCID Mice Transplanted with Human Cells. *Virology* 263, 78-88.

35. Brenchley, J.M., Price, D.A., Schacker, T.W., Asher, T.E., Silvestri, G., Rao, S., Kazzaz, Z., Bornstein, E., Lambotte, O., Altmann, D., Blazar, B.R., Rodriguez, B., Teixeira-Johnson, L., Landay, A., Martin, J.N., Hecht, F.M., Picker, L.J., Lederman, M.M., Deeks, S.G., Douek, D.C. (2006) Microbial translocation is a cause of systemic immune activation in chronic HIV infection. *Nat Med* 12, 1365-71.

36. Pope, M., Haase, A.T. (2003) Transmission, acute HIV-1 infection and the quest for strategies to prevent infection. *Nat Med* 9, 847-52.

37. Beignon, A.-S., McKenna, K., Skoberne, M., Manches, O., DaSilva, I., Kavanagh, D.G., Larsson, M., Gorelick, R.J., Lifson, J.D., Bhardwaj, N. (2005) Endocytosis of HIV-1 activates plasmacytoid dendritic cells via Toll-like receptor‚Äì viral RNA interactions. *The Journal of Clinical Investigation* 115, 3265-3275.

38. Kadowaki, N., Antonenko, S., Lau, J.Y., Liu, Y.J. (2000) Natural interferon alpha/beta-producing cells link innate and adaptive immunity. *J Exp Med* 192, 219-26.

39. Barblu, L., Machmach, K., Gras, C., Delfraissy, J.F., Boufassa, F., Leal, M., Ruiz-Mateos, E., Lambotte, O., Herbeuval, J.P. (2012) Plasmacytoid dendritic cells (pDCs) from HIV controllers produce interferon-alpha and differentiate into functional killer pDCs under HIV activation. *J Infect Dis* 206, 790-801.

40. Lubong Sabado, R., Kavanagh, D.G., Kaufmann, D.E., Fru, K., Babcock, E., Rosenberg, E., Walker, B., Lifson, J., Bhardwaj, N., Larsson, M. (2009) In vitro priming recapitulates in vivo HIV-1 specific T cell responses, revealing rapid loss of virus reactive CD4 T cells in acute HIV-1 infection. *PLoS One* 4, e4256.

41. Chang, J.J., Altfeld, M. (2010) Innate immune activation in primary HIV-1 infection. *J Infect Dis* 202 Suppl 2, S297-301.

42. Alter, G., Martin, M.P., Teigen, N., Carr, W.H., Suscovich, T.J., Schneidewind, A., Streeck, H., Waring, M., Meier, A., Brander, C., Lifson, J.D., Allen, T.M., Carrington, M., Altfeld, M. (2007) Differential natural killer cell-mediated inhibition of HIV-1 replication based on distinct KIR/HLA subtypes. *J Exp Med* 204, 3027-36.

43. Martin, M.P., Gao, X., Lee, J.H., Nelson, G.W., Detels, R., Goedert, J.J., Buchbinder, S., Hoots, K., Vlahov, D., Trowsdale, J., Wilson, M., O'Brien, S.J., Carrington, M. (2002) Epistatic interaction between KIR3DS1 and HLA-B delays the progression to AIDS. *Nat Genet* 31, 429-34.

44. Martin, M.P., Qi, Y., Gao, X., Yamada, E., Martin, J.N., Pereyra, F., Colombo, S., Brown, E.E., Shupert, W.L., Phair, J., Goedert, J.J., Buchbinder, S., Kirk, G.D., Telenti, A., Connors, M., O'Brien, S.J., Walker, B.D., Parham, P., Deeks, S.G., McVicar, D.W., Carrington, M. (2007) Innate partnership of HLA-B and KIR3DL1 subtypes against HIV-1. *Nat Genet* 39, 733-40.

45. Mavilio, D., Lombardo, G., Kinter, A., Fogli, M., La Sala, A., Ortolano, S., Farschi, A., Follmann, D., Gregg, R., Kovacs, C., Marcenaro, E., Pende, D., Moretta, A., Fauci, A.S. (2006) Characterization of the defective interaction between a subset of natural killer cells and dendritic cells in HIV-1 infection. *J Exp Med* 203, 2339-50.

46. Cresswell, P., Ackerman, A.L., Giodini, A., Peaper, D.R., Wearsch, P.A. (2005) Mechanisms of MHC class I-restricted antigen processing and cross-presentation. *Immunol Rev* 207, 145-57.

47. Neefjes, J., Jongsma, M.L., Paul, P., Bakke, O. (2011) Towards a systems understanding of MHC class I and MHC class II antigen presentation. *Nat Rev Immunol* 11, 823-36.

48. Strawbridge, A.B., Blum, J.S. (2007) Autophagy in MHC class II antigen processing. *Curr Opin Immunol* 19, 87-92.

49. Banchereau, J., Briere, F., Caux, C., Davoust, J., Lebecque, S., Liu, Y.J., Pulendran, B., Palucka, K. (2000) Immunobiology of dendritic cells. *Annu Rev Immunol* 18, 767-811.

50. Koup, R.A., Safrit, J.T., Cao, Y., Andrews, C.A., McLeod, G., Borkowsky, W., Farthing, C., Ho, D.D. (1994) Temporal association of cellular immune responses with the initial control of viremia in primary human immunodeficiency virus type 1 syndrome. *J Virol* 68, 4650-5.

51. Brown, D.M., Roman, E., Swain, S.L. (2004) CD4 T cell responses to influenza infection. *Semin Immunol* 16, 171-7.

52. Wong, P., Pamer, E.G. (2003) CD8 T cell responses to infectious pathogens. *Annu Rev Immunol* 21, 29-70.

53. Hadida, F., Vieillard, V., Mollet, L., Clark-Lewis, I., Baggiolini, M., Debre, P. (1999) Cutting edge: RANTES regulates Fas ligand expression and killing by HIV-specific CD8 cytotoxic T cells. *J Immunol* 163, 1105-9.

54. Wagner, L., Yang, O.O., Garcia-Zepeda, E.A., Ge, Y., Kalams, S.A., Walker, B.D., Pasternack, M.S., Luster, A.D. (1998) Beta-chemokines are released from HIV-1-specific cytolytic T-cell granules complexed to proteoglycans. *Nature* 391, 908-11.

55. Betts, M.R., Nason, M.C., West, S.M., De Rosa, S.C., Migueles, S.A., Abraham, J., Lederman, M.M., Benito, J.M., Goepfert, P.A., Connors, M., Roederer, M., Koup, R.A. (2006) HIV nonprogressors preferentially maintain highly functional HIV-specific CD8+ T cells. *Blood* 107, 4781-9.

56. Goonetilleke, N., Liu, M.K.P., Salazar-Gonzalez, J.F., Ferrari, G., Giorgi, E., Ganusov, V.V., Keele, B.F., Learn, G.H., Turnbull, E.L., Salazar, M.G., Weinhold, K.J., Moore, S., B, C.C.C., Letvin, N., Haynes, B.F., Cohen, M.S., Hraber, P., Bhattacharya, T., Borrow, P., Perelson, A.S., Hahn, B.H., Shaw, G.M., Korber, B.T., McMichael, A.J. (2009) The first T cell response to transmitted/founder virus contributes to the control of acute viremia in HIV-1 infection. *The Journal of Experimental Medicine* 206, 1253-1272 %R 10.1084/jem.20090365.

57. Salazar-Gonzalez, J.F., Salazar, M.G., Keele, B.F., Learn, G.H., Giorgi, E.E., Li, H., Decker, J.M., Wang, S., Baalwa, J., Kraus, M.H., Parrish, N.F., Shaw, K.S., Guffey, M.B., Bar, K.J., Davis, K.L., Ochsenbauer-Jambor, C., Kappes, J.C., Saag, M.S., Cohen, M.S., Mulenga, J., Derdeyn, C.A., Allen, S., Hunter, E., Markowitz, M., Hraber, P., Perelson, A.S., Bhattacharya, T., Haynes, B.F., Korber, B.T., Hahn, B.H., Shaw, G.M. (2009) Genetic identity, biological phenotype, and evolutionary pathways of transmitted/founder viruses in acute and early HIV-1 infection. *J Exp Med* 206, 1273-89.

58. Draenert, R., Le Gall, S., Pfafferott, K.J., Leslie, A.J., Chetty, P., Brander, C., Holmes, E.C., Chang, S.C., Feeney, M.E., Addo, M.M., Ruiz, L., Ramduth, D., Jeena, P., Altfeld, M., Thomas, S., Tang, Y., Verrill, C.L., Dixon, C., Prado, J.G., Kiepiela, P., Martinez-Picado, J., Walker, B.D., Goulder, P.J. (2004) Immune selection for altered antigen processing leads to cytotoxic T lymphocyte escape in chronic HIV-1 infection. *J Exp Med* 199, 905-15.

59. Tenzer, S., Wee, E., Burgevin, A., Stewart-Jones, G., Friis, L., Lamberth, K., Chang, C.H., Harndahl, M., Weimershaus, M., Gerstoft, J., Akkad, N., Klenerman, P., Fugger, L., Jones, E.Y., McMichael, A.J., Buus, S., Schild, H., van Endert, P., Iversen, A.K. (2009) Antigen processing influences HIV-specific cytotoxic T lymphocyte immunodominance. *Nat Immunol* 10, 636-46.

60. Turnbull, E.L., Wong, M., Wang, S., Wei, X., Jones, N.A., Conrod, K.E., Aldam, D., Turner, J., Pellegrino, P., Keele, B.F., Williams, I., Shaw, G.M., Borrow, P. (2009) Kinetics of expansion of epitope-specific T cell responses during primary HIV-1 infection. *J Immunol* 182, 7131-45.

61. Streeck, H., Jolin, J.S., Qi, Y., Yassine-Diab, B., Johnson, R.C., Kwon, D.S., Addo, M.M., Brumme, C., Routy, J.P., Little, S., Jessen, H.K., Kelleher, A.D., Hecht, F.M., Sekaly, R.P., Rosenberg, E.S., Walker, B.D., Carrington, M., Altfeld, M. (2009) Human immunodeficiency virus type 1-specific CD8+ T-cell responses during primary infection are major determinants of the viral set point and loss of CD4+ T cells. *J Virol* 83, 7641-8.

62. Wang, Y.E., Li, B., Carlson, J.M., Streeck, H., Gladden, A.D., Goodman, R., Schneidewind, A., Power, K.A., Toth, I., Frahm, N., Alter, G., Brander, C., Carrington, M., Walker, B.D., Altfeld, M., Heckerman, D., Allen, T.M. (2009) Protective HLA class I alleles that restrict acute-phase CD8+ T-cell responses are associated with viral escape mutations located in highly conserved regions of human immunodeficiency virus type 1. *J Virol* 83, 1845-55.

63. Rosenberg, E.S., Billingsley, J.M., Caliendo, A.M., Boswell, S.L., Sax, P.E., Kalams, S.A., Walker, B.D. (1997) Vigorous HIV-1-specific CD4+ T cell responses associated with control of viremia. *Science* 278, 1447-50.

64. Waldrop, S.L., Pitcher, C.J., Peterson, D.M., Maino, V.C., Picker, L.J. (1997) Determination of antigen-specific memory/effector CD4+ T cell frequencies by flow cytometry: evidence for a novel, antigen-specific homeostatic mechanism in HIV-associated immunodeficiency. *J Clin Invest* 99, 1739-50.

65. Pitcher, C.J., Quittner, C., Peterson, D.M., Connors, M., Koup, R.A., Maino, V.C., Picker, L.J. (1999) HIV-1-specific CD4+ T cells are detectable in most individuals with active HIV-1 infection, but decline with prolonged viral suppression. *Nat Med* 5, 518-25.

66. Kalams, S.A., Buchbinder, S.P., Rosenberg, E.S., Billingsley, J.M., Colbert, D.S., Jones, N.G., Shea, A.K., Trocha, A.K., Walker, B.D. (1999) Association between virus-specific cytotoxic T-lymphocyte and helper responses in human immunodeficiency virus type 1 infection. *J Virol* 73, 6715-20.

67. Grossman, Z., Feinberg, M.B., Paul, W.E. (1998) Multiple modes of cellular activation and virus transmission in HIV infection: a role for chronically and latently infected cells in sustaining viral replication. *Proc Natl Acad Sci U S A* 95, 6314-9.

68. Overbaugh, J., Morris, L. (2012) The Antibody Response against HIV-1. *Cold Spring Harbor Perspectives in Medicine %R 10.1101/cshperspect.a007039* 2.

69. Moir, S., Fauci, A.S. (2013) Insights into B cells and HIV-specific B-cell responses in HIV-infected individuals. *Immunol Rev* 254, 207-24.

70. Xu, W., Santini, P.A., Sullivan, J.S., He, B., Shan, M., Ball, S.C., Dyer, W.B., Ketas, T.J., Chadburn, A., Cohen-Gould, L., Knowles, D.M., Chiu, A., Sanders, R.W., Chen, K., Cerutti, A. (2009) HIV-1 evades virus-specific IgG2 and IgA responses by targeting systemic and intestinal B cells via long-range intercellular conduits. *Nat Immunol* 10, 1008-17.

71. Richman, D.D., Wrin, T., Little, S.J., Petropoulos, C.J. (2003) Rapid evolution of the neutralizing antibody response to HIV type 1 infection. *Proceedings of the National Academy of Sciences* 100, 4144-4149 %R 10.1073/pnas.0630530100.

72. Stamatatos, L., Morris, L., Burton, D.R., Mascola, J.R. (2009) Neutralizing antibodies generated during natural HIV-1 infection: good news for an HIV-1 vaccine? *Nat Med* 15, 866-70.

73. Wei, X., Decker, J.M., Wang, S., Hui, H., Kappes, J.C., Wu, X., Salazar-Gonzalez, J.F., Salazar, M.G., Kilby, J.M., Saag, M.S., Komarova, N.L., Nowak, M.A., Hahn, B.H., Kwong, P.D., Shaw, G.M. (2003) Antibody neutralization and escape by HIV-1. *Nature* 422, 307-12.

74. Moore, P.L., Gray, E.S., Choge, I.A., Ranchobe, N., Mlisana, K., Abdool Karim, S.S., Williamson, C., Morris, L. (2008) The c3-v4 region is a major target of autologous neutralizing antibodies in human immunodeficiency virus type 1 subtype C infection. *J Virol* 82, 1860-9.

75. Robinson, H.L., Amara, R.R. (2005) T cell vaccines for microbial infections. *Nat Med* 11, S25-32.

76. Korber, B.T., Letvin, N.L., Haynes, B.F. (2009) T-cell vaccine strategies for human immunodeficiency virus, the virus with a thousand faces. *J Virol* 83, 8300-14.

77. Walker, B.D., Burton, D.R. (2008) Toward an AIDS vaccine. *Science* 320, 760-4.

78. Dong, T., Stewart-Jones, G., Chen, N., Easterbrook, P., Xu, X., Papagno, L., Appay, V., Weekes, M., Conlon, C., Spina, C., Little, S., Screaton, G., van der Merwe, A., Richman, D.D., McMichael, A.J., Jones, E.Y., Rowland-Jones, S.L. (2004) HIV-specific Cytotoxic T Cells from Long-Term Survivors Select a Unique T Cell Receptor. *The Journal of Experimental Medicine* 200, 1547-1557 %R 10.1084/jem.20032044.

79. Turnbull, E.L., Lopes, A.R., Jones, N.A., Cornforth, D., Newton, P., Aldam, D., Pellegrino, P., Turner, J., Williams, I., Wilson, C.M., Goepfert, P.A., Maini, M.K., Borrow, P. (2006) HIV-1 epitope-specific CD8+ T cell responses strongly associated with delayed disease progression cross-recognize epitope variants efficiently. *J Immunol* 176, 6130-46.

80. Smith-Garvin, J.E., Koretzky, G.A., Jordan, M.S. (2009) T Cell Activation. *Annual Review of Immunology* 27, 591-619.

81. Bromley, S.K., Burack, W.R., Johnson, K.G., Somersalo, K., Sims, T.N., Sumen, C., Davis, M.M., Shaw, A.S., Allen, P.M., Dustin, M.L. (2001) The immunological synapse. *Annu Rev Immunol* 19, 375-96.

82. Quintana, A., Griesemer, D., Schwarz, E.C., Hoth, M. (2005) Calcium-dependent activation of T-lymphocytes. *Pflugers Arch* 450, 1-12.

83. Katso, R., Okkenhaug, K., Ahmadi, K., White, S., Timms, J., Waterfield, M.D. (2001) Cellular function of phosphoinositide 3-kinases: implications for development, homeostasis, and cancer. *Annu Rev Cell Dev Biol* 17, 615-75.

84. Rudd, C.E., Raab, M. (2003) Independent CD28 signaling via VAV and SLP-76: a model for in trans costimulation. *Immunol Rev* 192, 32-41.

85. Graef, I.A., Mermelstein, P.G., Stankunas, K., Neilson, J.R., Deisseroth, K., Tsien, R.W., Crabtree, G.R. (1999) L-type calcium channels and GSK-3 regulate the activity of NF-ATc4 in hippocampal neurons. *Nature* 401, 703-8.

86. Macian, F., Lopez-Rodriguez, C., Rao, A. (2001) Partners in transcription: NFAT and AP-1. *Oncogene* 20, 2476-89.

87. Pahl, H.L. (1999) Activators and target genes of Rel/NF-kappaB transcription factors. *Oncogene* 18, 6853-66.

88. Castagna, M., Takai, Y., Kaibuchi, K., Sano, K., Kikkawa, U., Nishizuka, Y. (1982) Direct activation of calcium-activated, phospholipid-dependent protein kinase by tumor-promoting phorbol esters. *J Biol Chem* 257, 7847-51.

89. Niedel, J.E., Kuhn, L.J., Vandenbark, G.R. (1983) Phorbol diester receptor copurifies with protein kinase C. *Proc Natl Acad Sci U S A* 80, 36-40.

90. Chatila, T., Silverman, L., Miller, R., Geha, R. (1989) Mechanisms of T cell activation by the calcium ionophore ionomycin. *J Immunol* 143, 1283-9.

91. Administration, S.A.a.M.H.S. (2013) Results from the 2012 National Survey on Drug Use and Health: Summary of National Findings. *NSDUH Series H-46, HHS Publication No. (SMA) 13-4795.*

92. Moore, T.H.M., Zammit, S., Lingford-Hughes, A., Barnes, T.R.E., Jones, P.B., Burke, M., Lewis, G. (2007) Cannabis use and risk of psychotic or affective mental health outcomes: a systematic review. *The Lancet* 370, 319-328.

93. Borgelt, L.M., Franson, K.L., Nussbaum, A.M., Wang, G.S. (2013) The pharmacologic and clinical effects of medical cannabis. *Pharmacotherapy* 33, 195-209.

94. Prentiss, D., Power, R., Balmas, G., Tzuang, G., Israelski, D.M. (2004) Patterns of marijuana use among patients with HIV/AIDS followed in a public health care setting. *J Acquir Immune Defic Syndr* 35, 38-45.

95. Cinti, S. (2009) Medical marijuana in HIV-positive patients: what do we know? *J Int Assoc Physicians AIDS Care (Chic)* 8, 342-6.

96. Gaoni, Y., Mechoulam, R. (1964) Isolation, Structure, and Partial Synthesis of an Active Constituent of Hashish. *Journal of the American Chemical Society* 86, 1646-1647.

97. Howlett, A.C., Barth, F., Bonner, T.I., Cabral, G., Casellas, P., Devane, W.A., Felder, C.C., Herkenham, M., Mackie, K., Martin, B.R., Mechoulam, R., Pertwee, R.G. (2002) International Union of Pharmacology. XXVII. Classification of cannabinoid receptors. *Pharmacol Rev* 54, 161-202.

98. Turner, J.C., Hemphill, J.K., Mahlberg, P.G. (1978) Cannabinoid composition and gland distribution in clones of Cannabis sativa L. (Cannabaceae). *Bull Narc* 30, 55-65.

99. Turner, C.E., Elsohly, M.A., Boeren, E.G. (1980) Constituents of Cannabis sativa L. XVII. A review of the natural constituents. *J Nat Prod* 43, 169-234.

100. Petitet, F., Jeantaud, B., Reibaud, M., Imperato, A., Dubroeucq, M.C. (1998) Complex pharmacology of natural cannabinoids: evidence for partial agonist activity of delta9-tetrahydrocannabinol and antagonist activity of cannabidiol on rat brain cannabinoid receptors. *Life Sci* 63, PL1-6.

101. Munro, S., Thomas, K.L., Abu-Shaar, M. (1993) Molecular characterization of a peripheral receptor for cannabinoids. *Nature* 365, 61-5.

102. Matsuda, L.A., Lolait, S.J., Brownstein, M.J., Young, A.C., Bonner, T.I. (1990) Structure of a cannabinoid receptor and functional expression of the cloned cDNA. *Nature* 346, 561-4.

103. Hanus, L.O. (2007) Discovery and isolation of anandamide and other endocannabinoids. *Chem Biodivers* 4, 1828-41.

104. De Petrocellis, L., Di Marzo, V. (2009) An introduction to the endocannabinoid system: from the early to the latest concepts. *Best Pract Res Clin Endocrinol Metab* 23, 1-15.

105. RodrÍGuez de Fonseca, F., Del Arco, I., Bermudez-Silva, F.J., Bilbao, A., Cippitelli, A., Navarro, M. (2005) THE ENDOCANNABINOID SYSTEM: PHYSIOLOGY

AND PHARMACOLOGY. *Alcohol and Alcoholism* 40, 2-14 %R 10.1093/alcalc/agh110.

106. Klein, T.W. (2005) Cannabinoid-based drugs as anti-inflammatory therapeutics. *Nat Rev Immunol* 5, 400-11.

107. Pertwee, R.G., Howlett, A.C., Abood, M.E., Alexander, S.P., Di Marzo, V., Elphick, M.R., Greasley, P.J., Hansen, H.S., Kunos, G., Mackie, K., Mechoulam, R., Ross, R.A. (2010) International Union of Basic and Clinical Pharmacology. LXXIX. Cannabinoid receptors and their ligands: beyond CB(1) and CB(2). *Pharmacol Rev* 62, 588-631.

108. Ferraro, L., Tomasini, M.C., Gessa, G.L., Bebe, B.W., Tanganelli, S., Antonelli, T. (2001) The Cannabinoid Receptor Agonist WIN 55,212-2 Regulates Glutamate Transmission in Rat Cerebral Cortex: an In Vivo and In Vitro Study. *Cerebral Cortex* 11, 728-733 %R 10.1093/cercor/11.8.728.

109. Huestis, M.A., Henningfield, J.E., Cone, E.J. (1992) Blood cannabinoids. I. Absorption of THC and formation of 11-OH-THC and THCCOOH during and after smoking marijuana. *J Anal Toxicol* 16, 276-82.

110. Lindgren, J.E., Ohlsson, A., Agurell, S., Hollister, L., Gillespie, H. (1981) Clinical effects and plasma levels of delta 9-tetrahydrocannabinol (delta 9-THC) in heavy and light users of cannabis. *Psychopharmacology (Berl)* 74, 208-12.

111. Ohlsson, A., Lindgren, J.E., Wahlen, A., Agurell, S., Hollister, L.E., Gillespie, H.K. (1980) Plasma delta-9 tetrahydrocannabinol concentrations and clinical effects after oral and intravenous administration and smoking. *Clin Pharmacol Ther* 28, 409-16.

112. Garrett, E.R., Hunt, C.A. (1974) Physiochemical properties, solubility, and protein binding of delta9-tetrahydrocannabinol. *J Pharm Sci* 63, 1056-64.

113. Ho, B.T., Fritchie, G.E., Kralik, P.M., Englert, L.F., McIsaac, W.M., Idanpaan-Heikkila, J. (1970) Distribution of tritiated-1 delta 9tetrahydrocannabinol in rat tissues after inhalation. *J Pharm Pharmacol* 22, 538-9.

114. Maykut, M.O. (1985) Health consequences of acute and chronic marihuana use. *Prog Neuropsychopharmacol Biol Psychiatry* 9, 209-38.

115. Matsunaga, T., Iwawaki, Y., Watanabe, K., Yamamoto, I., Kageyama, T., Yoshimura, H. (1995) Metabolism of delta 9-tetrahydrocannabinol by cytochrome P450 isozymes purified from hepatic microsomes of monkeys. *Life Sci* 56, 2089-95.

116. Narimatsu, S., Akutsu, Y., Matsunaga, T., Watanabe, K., Yamamoto, I., Yoshimura, H. (1992) Immunochemical characterization of a cytochrome P450 isozyme and a protein purified from liver microsomes of male guinea pigs and their roles in the oxidative metabolism of delta 9-tetrahydrocannabinol by guinea pig liver microsomes. *Biochem Pharmacol* 43, 1729-36.

117. Widman, M., Halldin, M., Martin, B. (1978) In vitro metabolism of tetrahydrocannabinol by rhesus monkey liver and human liver. *Adv Biosci* 22-23, 101-3.

118. Leighty, E.G. (1973) Metabolism and distribution of cannabinoids in rats after different methods of administration. *Biochem Pharmacol* 22, 1613-21.

119. Grotenhermen, F., Russo, E. (2002) *Cannabis and cannabinoids: Pharmacology, toxicology, and therapeutic potential.* . Binghamton (NY): Haworth Press.

120. Hollister, L.E. (1986) Health aspects of cannabis. *Pharmacol Rev* 38, 1-20.

121. Thompson, G.R., Rosenkrantz, H., Schaeppi, U.H., Braude, M.C. (1973) Comparison of acute oral toxicity of cannabinoids in rats, dogs and monkeys. *Toxicol Appl Pharmacol* 25, 363-72.

122. Mittleman, M.A., Lewis, R.A., Maclure, M., Sherwood, J.B., Muller, J.E. (2001) Triggering myocardial infarction by marijuana. *Circulation* 103, 2805-9.

123. Bachs, L., Morland, H. (2001) Acute cardiovascular fatalities following cannabis use. *Forensic Sci Int* 124, 200-3.

124. Pope, H.G., Jr. (2002) Cannabis, cognition, and residual confounding. *Jama* 287, 1172-4.

125. Solowij, N., Stephens, R.S., Roffman, R.A., Babor, T., Kadden, R., Miller, M., Christiansen, K., McRee, B., Vendetti, J. (2002) Cognitive functioning of long-term heavy cannabis users seeking treatment. *Jama* 287, 1123-31.

126. Gerard, C.M., Mollereau, C., Vassart, G., Parmentier, M. (1991) Molecular cloning of a human cannabinoid receptor which is also expressed in testis. *Biochem J* 279 (Pt 1), 129-34.

127. Abood, M.E. (2005) Molecular biology of cannabinoid receptors. *Handb Exp Pharmacol*, 81-115.

128. Griffin, G., Tao, Q., Abood, M.E. (2000) Cloning and pharmacological characterization of the rat CB(2) cannabinoid receptor. *J Pharmacol Exp Ther* 292, 886-94.

129. Lutz, B. (2002) Molecular biology of cannabinoid receptors. *Prostaglandins Leukot Essent Fatty Acids* 66, 123-42.

130. Szabo, B., Schlicker, E. (2005) Effects of cannabinoids on neurotransmission. *Handb Exp Pharmacol*, 327-65.

131. Onaivi, E.S., Ishiguro, H., Gong, J.P., Patel, S., Perchuk, A., Meozzi, P.A., Myers, L., Mora, Z., Tagliaferro, P., Gardner, E., Brusco, A., Akinshola, B.E., Liu, Q.R., Hope, B., Iwasaki, S., Arinami, T., Teasenfitz, L., Uhl, G.R. (2006) Discovery of the presence and functional expression of cannabinoid CB2 receptors in brain. *Ann N Y Acad Sci* 1074, 514-36.

132. Xi, Z.X., Peng, X.Q., Li, X., Song, R., Zhang, H.Y., Liu, Q.R., Yang, H.J., Bi, G.H., Li, J., Gardner, E.L. (2011) Brain cannabinoid CB(2) receptors modulate cocaine's actions in mice. *Nat Neurosci* 14, 1160-6.

133. Galiegue, S., Mary, S., Marchand, J., Dussossoy, D., Carriere, D., Carayon, P., Bouaboula, M., Shire, D., Le Fur, G., Casellas, P. (1995) Expression of central and peripheral cannabinoid receptors in human immune tissues and leukocyte subpopulations. *Eur J Biochem* 232, 54-61.

134. Schatz, A.R., Lee, M., Condie, R.B., Pulaski, J.T., Kaminski, N.E. (1997) Cannabinoid receptors CB1 and CB2: a characterization of expression and adenylate cyclase modulation within the immune system. *Toxicol Appl Pharmacol* 142, 278-87.

135. Borner, C., Hollt, V., Kraus, J. (2007) Activation of human T cells induces upregulation of cannabinoid receptor type 1 transcription. *Neuroimmunomodulation* 14, 281-6.

136. Carayon, P., Marchand, J., Dussossoy, D., Derocq, J.M., Jbilo, O., Bord, A., Bouaboula, M., Galiegue, S., Mondiere, P., Penarier, G., Fur, G.L., Defrance, T., Casellas, P. (1998) Modulation and functional involvement of CB2 peripheral cannabinoid receptors during B-cell differentiation. *Blood* 92, 3605-15.

137. Glass, M., Northup, J.K. (1999) Agonist selective regulation of G proteins by cannabinoid CB(1) and CB(2) receptors. *Mol Pharmacol* 56, 1362-9.

138. Felder, C.C., Joyce, K.E., Briley, E.M., Mansouri, J., Mackie, K., Blond, O., Lai, Y., Ma, A.L., Mitchell, R.L. (1995) Comparison of the pharmacology and signal transduction of the human cannabinoid CB1 and CB2 receptors. *Mol Pharmacol* 48, 443-50.

139. Gonzalez, G.A., Yamamoto, K.K., Fischer, W.H., Karr, D., Menzel, P., Biggs, W., 3rd, Vale, W.W., Montminy, M.R. (1989) A cluster of phosphorylation sites on the cyclic AMP-regulated nuclear factor CREB predicted by its sequence. *Nature* 337, 749-52.

140. Condie, R., Herring, A., Koh, W.S., Lee, M., Kaminski, N.E. (1996) Cannabinoid inhibition of adenylate cyclase-mediated signal transduction and interleukin 2 (IL-2) expression in the murine T-cell line, EL4.IL-2. *J Biol Chem* 271, 13175-83.

141. Hai, T., Curran, T. (1991) Cross-family dimerization of transcription factors Fos/Jun and ATF/CREB alters DNA binding specificity. *Proc Natl Acad Sci U S A* 88, 3720-4.

142. Kara, C.J., Liou, H.C., Ivashkiv, L.B., Glimcher, L.H. (1990) A cDNA for a human cyclic AMP response element-binding protein which is distinct from CREB and expressed preferentially in brain. *Mol Cell Biol* 10, 1347-57.

143. Rao, G.K., Zhang, W., Kaminski, N.E. (2004) Cannabinoid receptor-mediated regulation of intracellular calcium by delta(9)-tetrahydrocannabinol in resting T cells. *J Leukoc Biol* 75, 884-92.

144. Kaplan, B.L., Rockwell, C.E., Kaminski, N.E. (2003) Evidence for cannabinoid receptor-dependent and -independent mechanisms of action in leukocytes. *J Pharmacol Exp Ther* 306, 1077-85.

145. Faubert Kaplan, B.L., Kaminski, N.E. (2003) Cannabinoids inhibit the activation of ERK MAPK in PMA/Io-stimulated mouse splenocytes. *Int Immunopharmacol* 3, 1503-10.

146. Jeon, Y.J., Yang, K.H., Pulaski, J.T., Kaminski, N.E. (1996) Attenuation of inducible nitric oxide synthase gene expression by delta 9-tetrahydrocannabinol is mediated through the inhibition of nuclear factor- kappa B/Rel activation. *Mol Pharmacol* 50, 334-41.

147. Glass, M., Felder, C.C. (1997) Concurrent stimulation of cannabinoid CB1 and dopamine D2 receptors augments cAMP accumulation in striatal neurons: evidence for a Gs linkage to the CB1 receptor. *J Neurosci* 17, 5327-33.

148. Felder, C.C., Joyce, K.E., Briley, E.M., Glass, M., Mackie, K.P., Fahey, K.J., Cullinan, G.J., Hunden, D.C., Johnson, D.W., Chaney, M.O., Koppel, G.A., Brownstein, M. (1998) LY320135, a novel cannabinoid CB1 receptor antagonist, unmasks coupling of the CB1 receptor to stimulation of cAMP accumulation. *J Pharmacol Exp Ther* 284, 291-7.

149. Maneuf, Y.P., Brotchie, J.M. (1997) Paradoxical action of the cannabinoid WIN 55,212-2 in stimulated and basal cyclic AMP accumulation in rat globus pallidus slices. *Br J Pharmacol* 120, 1397-8.

150. Rhee, M.H., Bayewitch, M., Avidor-Reiss, T., Levy, R., Vogel, Z. (1998) Cannabinoid receptor activation differentially regulates the various adenylyl cyclase isozymes. *J Neurochem* 71, 1525-34.

151. Noguchi, K., Ishii, S., Shimizu, T. (2003) Identification of p2y9/GPR23 as a novel G protein-coupled receptor for lysophosphatidic acid, structurally distant from the Edg family. *J Biol Chem* 278, 25600-6.

152. Kotarsky, K., Boketoft, A., Bristulf, J., Nilsson, N.E., Norberg, A., Hansson, S., Owman, C., Sillard, R., Leeb-Lundberg, L.M., Olde, B. (2006) Lysophosphatidic acid binds to and activates GPR92, a G protein-coupled receptor highly expressed in gastrointestinal lymphocytes. *J Pharmacol Exp Ther* 318, 619-28.

153. McHugh, D., Page, J., Dunn, E., Bradshaw, H.B. (2011) Delta(9) - Tetrahydrocannabinol and N-arachidonyl glycine are full agonists at GPR18 receptors and induce migration in human endometrial HEC-1B cells. *Br J Pharmacol* 165, 2414-24.

154. Overton, H.A., Babbs, A.J., Doel, S.M., Fyfe, M.C., Gardner, L.S., Griffin, G., Jackson, H.C., Procter, M.J., Rasamison, C.M., Tang-Christensen, M., Widdowson, P.S., Williams, G.M., Reynet, C. (2006) Deorphanization of a G protein-coupled

receptor for oleoylethanolamide and its use in the discovery of small-molecule hypophagic agents. *Cell Metab* 3, 167-75.

155. Zygmunt, P.M., Petersson, J., Andersson, D.A., Chuang, H., Sorgard, M., Di Marzo, V., Julius, D., Hogestatt, E.D. (1999) Vanilloid receptors on sensory nerves mediate the vasodilator action of anandamide. *Nature* 400, 452-7.

156. Rosenbaum T, S.S. (2007) TRPV1 Receptors and Signal Transduction. In *TRP Ion Channel Function in Sensory Transduction and Cellular Signaling Cascades.* (H. S. Liedtke WB, ed) Boca Raton (FL): CRC Press;.

157. Raman, P., Kaplan, B.L., Kaminski, N.E. (2012) 15-Deoxy-Delta(1)(2),(1)(4)-prostaglandin J(2)-glycerol, a putative metabolite of 2-arachidonyl glycerol and a peroxisome proliferator-activated receptor gamma ligand, modulates nuclear factor of activated T cells. *J Pharmacol Exp Ther* 342, 816-26.

158. Raman, P., Kaplan, B.L., Thompson, J.T., Vanden Heuvel, J.P., Kaminski, N.E. (2011) 15-Deoxy-delta12,14-prostaglandin J2-glycerol ester, a putative metabolite of 2-arachidonyl glycerol, activates peroxisome proliferator activated receptor gamma. *Mol Pharmacol* 80, 201-9.

159. Kaplan, B.L., Springs, A.E., Kaminski, N.E. (2008) The profile of immune modulation by cannabidiol (CBD) involves deregulation of nuclear factor of activated T cells (NFAT). *Biochem Pharmacol* 76, 726-37.

160. Srivastava, M.D., Srivastava, B.I., Brouhard, B. (1998) Delta9 tetrahydrocannabinol and cannabidiol alter cytokine production by human immune cells. *Immunopharmacology* 40, 179-85.

161. Yea, S.S., Yang, K.H., Kaminski, N.E. (2000) Role of nuclear factor of activated T-cells and activator protein-1 in the inhibition of interleukin-2 gene transcription by cannabinol in EL4 T-cells. *J Pharmacol Exp Ther* 292, 597-605.

162. Springs, A.E., Karmaus, P.W., Crawford, R.B., Kaplan, B.L., Kaminski, N.E. (2008) Effects of targeted deletion of cannabinoid receptors CB1 and CB2 on immune competence and sensitivity to immune modulation by Delta9-tetrahydrocannabinol. *J Leukoc Biol* 84, 1574-84.

163. Rao, G.K., Kaminski, N.E. (2006) Cannabinoid-mediated elevation of intracellular calcium: a structure-activity relationship. *J Pharmacol Exp Ther* 317, 820-9.

164. Klein, T.W., Kawakami, Y., Newton, C., Friedman, H. (1991) Marijuana components suppress induction and cytolytic function of murine cytotoxic T cells in vitro and in vivo. *J Toxicol Environ Health* 32, 465-77.

165. Fischer-Stenger, K., Updegrove, A.W., Cabral, G.A. (1992) Delta 9-tetrahydrocannabinol decreases cytotoxic T lymphocyte activity to herpes simplex virus type 1-infected cells. *Proc Soc Exp Biol Med* 200, 422-30.

166. Schatz, A.R., Kessler, F.K., Kaminski, N.E. (1992) Inhibition of adenylate cyclase by delta 9-tetrahydrocannabinol in mouse spleen cells: a potential mechanism for cannabinoid-mediated immunosuppression. *Life Sci* 51, PL25-30.

167. Karmaus, P.W., Chen, W., Kaplan, B.L., Kaminski, N.E. (2011) Delta(9)-Tetrahydrocannabinol Suppresses Cytotoxic T Lymphocyte Function Independent of CB(1) and CB (2), Disrupting Early Activation Events. *J Neuroimmune Pharmacol* DOI: 10.1007/s11481-011-9293-4, 1-13.

168. Massi, P., Sacerdote, P., Ponti, W., Fuzio, D., Manfredi, B., Vigano, D., Rubino, T., Bardotti, M., Parolaro, D. (1998) Immune function alterations in mice tolerant to delta9-tetrahydrocannabinol: functional and biochemical parameters. *J Neuroimmunol* 92, 60-6.

169. Yuan, M., Kiertscher, S.M., Cheng, Q., Zoumalan, R., Tashkin, D.P., Roth, M.D. (2002) Delta 9-Tetrahydrocannabinol regulates Th1/Th2 cytokine balance in activated human T cells. *J Neuroimmunol* 133, 124-31.

170. Pross, S.H., Nakano, Y., McHugh, S., Widen, R., Klein, T.W., Friedman, H. (1992) Contrasting effects of THC on adult murine lymph node and spleen cell populations stimulated with mitogen or anti-CD3 antibody. *Immunopharmacol Immunotoxicol* 14, 675-87.

171. Nakano, Y., Pross, S., Friedman, H. (1993) Contrasting effect of delta-9-tetrahydrocannabinol on IL-2 activity in spleen and lymph node cells of mice of different ages. *Life Sci* 52, 41-51.

172. Jbilo, O., Derocq, J.M., Segui, M., Le Fur, G., Casellas, P. (1999) Stimulation of peripheral cannabinoid receptor CB2 induces MCP-1 and IL-8 gene expression in human promyelocytic cell line HL60. *FEBS Lett* 448, 273-7.

173. Derocq, J.M., Segui, M., Marchand, J., Le Fur, G., Casellas, P. (1995) Cannabinoids enhance human B-cell growth at low nanomolar concentrations. *FEBS Lett* 369, 177-82.

174. Jan, T.R., Kaminski, N.E. (2001) Role of mitogen-activated protein kinases in the differential regulation of interleukin-2 by cannabinol. *J Leukoc Biol* 69, 841-9.

175. Jan, T.R., Rao, G.K., Kaminski, N.E. (2002) Cannabinol enhancement of interleukin-2 (IL-2) expression by T cells is associated with an increase in IL-2 distal nuclear factor of activated T cell activity. *Mol Pharmacol* 61, 446-54.

176. Zimmerman, S., Zimmerman, A.M., Cameron, I.L., Laurence, H.L. (1977) delta1-tetrahydrocannabinol, cannabidiol and cannabinol effects on the immune response of mice. *Pharmacology* 15, 10-23.

177. Smith, S.H., Harris, L.S., Uwaydah, I.M., Munson, A.E. (1978) Structure-activity relationships of natural and synthetic cannabinoids in suppression of humoral and cell-mediated immunity. *J Pharmacol Exp Ther* 207, 165-70.

178. Kaminski, N.E., Abood, M.E., Kessler, F.K., Martin, B.R., Schatz, A.R. (1992) Identification of a functionally relevant cannabinoid receptor on mouse spleen cells that is involved in cannabinoid-mediated immune modulation. *Mol Pharmacol* 42, 736-42.

179. Schatz, A.R., Koh, W.S., Kaminski, N.E. (1993) Delta 9-tetrahydrocannabinol selectively inhibits T-cell dependent humoral immune responses through direct inhibition of accessory T-cell function. *Immunopharmacology* 26, 129-37.

180. Klein, T.W., Newton, C.A., Widen, R., Friedman, H. (1985) The effect of delta-9-tetrahydrocannabinol and 11-hydroxy-delta-9-tetrahydrocannabinol on T-lymphocyte and B-lymphocyte mitogen responses. *J Immunopharmacol* 7, 451-66.

181. Lee, M., Yang, K.H., Kaminski, N.E. (1995) Effects of putative cannabinoid receptor ligands, anandamide and 2-arachidonyl-glycerol, on immune function in B6C3F1 mouse splenocytes. *J Pharmacol Exp Ther* 275, 529-36.

182. Ngaotepprutaram, T., Kaplan, B.L., Carney, S., Crawford, R., Kaminski, N.E. (2013) Suppression by Delta(9)-tetrahydrocannabinol of the primary immunoglobulin M response by human peripheral blood B cells is associated with impaired STAT3 activation. *Toxicology* 310, 84-91.

183. Faris, M., Kokot, N., Stahl, N., Nel, A.E. (1997) Involvement of Stat3 in interleukin-6-induced IgM production in a human B-cell line. *Immunology* 90, 350-7.

184. Rachelefsky, G.S., Opelz, G., Mickey, M.R., Lessin, P., Kiuchi, M., Silverstein, M.J., Stiehm, E.R. (1976) Intact humoral and cell-mediated immunity in chronic marijuana smoking. *J Allergy Clin Immunol* 58, 483-90.

185. Nahas, G.G., Osserman, E.F. (1991) Altered serum immunoglobulin concentration in chronic marijuana smokers. *Adv Exp Med Biol* 288, 25-32.

186. El-Gohary, M., Eid, M.A. (2004) Effect of cannabinoid ingestion (in the form of bhang) on the immune system of high school and university students. *Hum Exp Toxicol* 23, 149-56.

187. Klein, T.W., Newton, C., Friedman, H. (1987) Inhibition of natural killer cell function by marijuana components. *J Toxicol Environ Health* 20, 321-32.

188. Kawakami, Y., Klein, T.W., Newton, C., Djeu, J.Y., Dennert, G., Specter, S., Friedman, H. (1988) Suppression by cannabinoids of a cloned cell line with natural killer cell activity. *Proc Soc Exp Biol Med* 187, 355-9.

189. Zhu, W., Igarashi, T., Friedman, H., Klein, T.W. (1995) delta 9-Tetrahydrocannabinol (THC) causes the variable expression of IL2 receptor subunits. *J Pharmacol Exp Ther* 274, 1001-7.

190. Kishimoto, S., Muramatsu, M., Gokoh, M., Oka, S., Waku, K., Sugiura, T. (2005) Endogenous cannabinoid receptor ligand induces the migration of human natural killer cells. *J Biochem* 137, 217-23.

191. Kusher, D.I., Dawson, L.O., Taylor, A.C., Djeu, J.Y. (1994) Effect of the psychoactive metabolite of marijuana, delta 9-tetrahydrocannabinol (THC), on the synthesis of tumor necrosis factor by human large granular lymphocytes. *Cell Immunol* 154, 99-108.

192. Massi, P., Fuzio, D., Vigano, D., Sacerdote, P., Parolaro, D. (2000) Relative involvement of cannabinoid CB(1) and CB(2) receptors in the Delta(9)-tetrahydrocannabinol-induced inhibition of natural killer activity. *Eur J Pharmacol* 387, 343-7.

193. Klein, T.W., Cabral, G.A. (2006) Cannabinoid-induced immune suppression and modulation of antigen-presenting cells. *J Neuroimmune Pharmacol* 1, 50-64.

194. Chandy, K.G., Wulff, H., Beeton, C., Pennington, M., Gutman, G.A., Cahalan, M.D. (2004) K+ channels as targets for specific immunomodulation. *Trends Pharmacol Sci* 25, 280-9.

195. Fischer, H.G., Eder, C. (1995) Voltage-gated K+ currents of mouse dendritic cells. *FEBS Lett* 373, 127-30.

196. Wacnik, P.W., Luhr, K.M., Hill, R.H., Ljunggren, H.G., Kristensson, K., Svensson, M. (2008) Cannabinoids affect dendritic cell (DC) potassium channel function and modulate DC T cell stimulatory capacity. *J Immunol* 181, 3057-66.

197. Karmaus, P.W., Chen, W., Crawford, R., Kaplan, B.L., Kaminski, N.E. (2013) Delta9-tetrahydrocannabinol impairs the inflammatory response to influenza infection: role of antigen-presenting cells and the cannabinoid receptors 1 and 2. *Toxicol Sci* 131, 419-33.

198. Puffenbarger, R.A., Boothe, A.C., Cabral, G.A. (2000) Cannabinoids inhibit LPS-inducible cytokine mRNA expression in rat microglial cells. *Glia* 29, 58-69.

199. Nakano, Y., Pross, S.H., Friedman, H. (1992) Modulation of interleukin 2 activity by delta 9-tetrahydrocannabinol after stimulation with concanavalin A, phytohemagglutinin, or anti-CD3 antibody. *Proc Soc Exp Biol Med* 201, 165-8.

200. Watzl, B., Scuderi, P., Watson, R.R. (1991) Influence of marijuana components (THC and CBD) on human mononuclear cell cytokine secretion in vitro. *Adv Exp Med Biol* 288, 63-70.

201. Coffey, R.G., Yamamoto, Y., Snella, E., Pross, S. (1996) Tetrahydrocannabinol inhibition of macrophage nitric oxide production. *Biochem Pharmacol* 52, 743-51.

202. McCoy, K.L., Gainey, D., Cabral, G.A. (1995) delta 9-Tetrahydrocannabinol modulates antigen processing by macrophages. *J Pharmacol Exp Ther* 273, 1216-23.

203. Sacerdote, P., Massi, P., Panerai, A.E., Parolaro, D. (2000) In vivo and in vitro treatment with the synthetic cannabinoid CP55, 940 decreases the in vitro migration of

macrophages in the rat: involvement of both CB1 and CB2 receptors. *J Neuroimmunol* 109, 155-63.

204. Klein, T.W., Newton, C.A., Nakachi, N., Friedman, H. (2000) Delta 9-tetrahydrocannabinol treatment suppresses immunity and early IFN-gamma, IL-12, and IL-12 receptor beta 2 responses to Legionella pneumophila infection. *J Immunol* 164, 6461-6.

205. Newton, C.A., Chou, P.J., Perkins, I., Klein, T.W. (2009) CB(1) and CB(2) cannabinoid receptors mediate different aspects of delta-9-tetrahydrocannabinol (THC)-induced T helper cell shift following immune activation by Legionella pneumophila infection. *J Neuroimmune Pharmacol* 4, 92-102.

206. Buchweitz, J.P., Karmaus, P.W., Harkema, J.R., Williams, K.J., Kaminski, N.E. (2007) Modulation of airway responses to influenza A/PR/8/34 by Delta9-tetrahydrocannabinol in C57BL/6 mice. *J Pharmacol Exp Ther* 323, 675-83.

207. Buchweitz, J.P., Karmaus, P.W., Williams, K.J., Harkema, J.R., Kaminski, N.E. (2008) Targeted deletion of cannabinoid receptors CB1 and CB2 produced enhanced inflammatory responses to influenza A/PR/8/34 in the absence and presence of Delta9-tetrahydrocannabinol. *J Leukoc Biol* 83, 785-96.

208. Karmaus, P.W., Chen, W., Crawford, R.B., Harkema, J.R., Kaplan, B.L., Kaminski, N.E. (2011) Deletion of cannabinoid receptors 1 and 2 exacerbates APC function to increase inflammation and cellular immunity during influenza infection. *J Leukoc Biol* 90, 983-95.

209. Rhee, M.H., Kim, S.K. (2002) SR144528 as inverse agonist of CB2 cannabinoid receptor. *J Vet Sci* 3, 179-84.

210. Landsman, R.S., Burkey, T.H., Consroe, P., Roeske, W.R., Yamamura, H.I. (1997) SR141716A is an inverse agonist at the human cannabinoid CB1 receptor. *Eur J Pharmacol* 334, R1-2.

211. Shire, D., Calandra, B., Bouaboula, M., Barth, F., Rinaldi-Carmona, M., Casellas, P., Ferrara, P. (1999) Cannabinoid receptor interactions with the antagonists SR 141716A and SR 144528. *Life Sci* 65, 627-35.

212. Krylatov, A.V., Maslov, L.N., Lasukova, O.V., Pertwee, R.G. (2005) Cannabinoid receptor antagonists SR141716 and SR144528 exhibit properties of partial agonists in experiments on isolated perfused rat heart. *Bull Exp Biol Med* 139, 558-61.

213. Karsak, M., Gaffal, E., Date, R., Wang-Eckhardt, L., Rehnelt, J., Petrosino, S., Starowicz, K., Steuder, R., Schlicker, E., Cravatt, B., Mechoulam, R., Buettner, R., Werner, S., Di Marzo, V., Tuting, T., Zimmer, A. (2007) Attenuation of allergic contact dermatitis through the endocannabinoid system. *Science* 316, 1494-7.

214. Winsauer, P.J., Molina, P.E., Amedee, A.M., Filipeanu, C.M., McGoey, R.R., Troxclair, D.A., Walker, E.M., Birke, L.L., Stouwe, C.V., Howard, J.M., Leonard, S.T., Moerschbaecher, J.M., Lewis, P.B. (2011) Tolerance to chronic delta-9-tetrahydrocannabinol (Delta-THC) in rhesus macaques infected with simian immunodeficiency virus. *Exp Clin Psychopharmacol* 19, 154-72.

215. Molina, P.E., Winsauer, P., Zhang, P., Walker, E., Birke, L., Amedee, A., Stouwe, C.V., Troxclair, D., McGoey, R., Varner, K., Byerley, L., Lamotte, L. (2010) Cannabinoid administration attenuates the progression of simian immunodeficiency virus. *AIDS Res Hum Retroviruses* 27, 585-92.

216. Abrams, D.I., Hilton, J.F., Leiser, R.J., Shade, S.B., Elbeik, T.A., Aweeka, F.T., Benowitz, N.L., Bredt, B.M., Kosel, B., Aberg, J.A., Deeks, S.G., Mitchell, T.F., Mulligan, K., Bacchetti, P., McCune, J.M., Schambelan, M. (2003) Short-term effects of cannabinoids in patients with HIV-1 infection: a randomized, placebo-controlled clinical trial. *Ann Intern Med* 139, 258-66.

217. Carbonetti, N.H., Tuskan, R.G., Lewis, G.K. (2001) Stimulation of HIV gp120-specific cytolytic T lymphocyte responses in vitro and in vivo using a detoxified pertussis toxin vector. *AIDS Res Hum Retroviruses* 17, 819-27.

218. Mirano-Bascos, D., Tary-Lehmann, M., Landry, S.J. (2008) Antigen structure influences helper T-cell epitope dominance in the human immune response to HIV envelope glycoprotein gp120. *Eur J Immunol* 38, 1231-7.

219. Palker, T.J., Matthews, T.J., Langlois, A., Tanner, M.E., Martin, M.E., Scearce, R.M., Kim, J.E., Berzofsky, J.A., Bolognesi, D.P., Haynes, B.F. (1989) Polyvalent human immunodeficiency virus synthetic immunogen comprised of envelope gp120 T helper cell sites and B cell neutralization epitopes. *J Immunol* 142, 3612-9.

220. Donnelly, J.J., Ulmer, J.B., Shiver, J.W., Liu, M.A. (1997) DNA vaccines. *Annu Rev Immunol* 15, 617-48.

221. Mo, Y., Quanquin, N.M., Vecino, W.H., Ranganathan, U.D., Tesfa, L., Bourn, W., Derbyshire, K.M., Letvin, N.L., Jacobs, W.R., Jr., Fennelly, G.J. (2007) Genetic alteration of Mycobacterium smegmatis to improve mycobacterium-mediated transfer of plasmid DNA into mammalian cells and DNA immunization. *Infect Immun* 75, 4804-16.

222. Hovav, A.H., Santosuosso, M., Bivas-Benita, M., Plair, A., Cheng, A., Elnekave, M., Righi, E., Chen, T., Kashiwagi, S., Panas, M.W., Xiang, S.H., Furmanov, K., Letvin, N.L., Poznansky, M.C. (2009) X4 human immunodeficiency virus type 1 gp120 down-modulates expression and immunogenicity of codelivered antigens. *J Virol* 83, 10941-50.

223. Barouch, D.H., Santra, S., Tenner-Racz, K., Racz, P., Kuroda, M.J., Schmitz, J.E., Jackson, S.S., Lifton, M.A., Freed, D.C., Perry, H.C., Davies, M.E., Shiver, J.W., Letvin, N.L. (2002) Potent CD4+ T cell responses elicited by a bicistronic HIV-1 DNA vaccine expressing gp120 and GM-CSF. *J Immunol* 168, 562-8.

224. Billaut-Mulot, O., Idziorek, T., Ban, E., Kremer, L., Dupre, L., Loyens, M., Riveau, G., Locht, C., Capron, A., Bahr, G.M. (2000) Interleukin-18 modulates immune responses induced by HIV-1 Nef DNA prime/protein boost vaccine. *Vaccine* 19, 95-102.

225. Billaut-Mulot, O., Idziorek, T., Loyens, M., Capron, A., Bahr, G.M. (2001) Modulation of cellular and humoral immune responses to a multiepitopic HIV-1 DNA vaccine by interleukin-18 DNA immunization/viral protein boost. *Vaccine* 19, 2803-11.

226. Livak, K.J., Schmittgen, T.D. (2001) Analysis of relative gene expression data using real-time quantitative PCR and the 2(-Delta Delta C(T)) Method. *Methods* 25, 402-8.

227. Faubert, B.L., Kaminski, N.E. (2000) AP-1 activity is negatively regulated by cannabinol through inhibition of its protein components, c-fos and c-jun. *J Leukoc Biol* 67, 259-66.

228. Lyakh, L., Ghosh, P., Rice, N.R. (1997) Expression of NFAT-family proteins in normal human T cells. *Mol Cell Biol* 17, 2475-84.

229. Azorlosa, J.L., Heishman, S.J., Stitzer, M.L., Mahaffey, J.M. (1992) Marijuana smoking: effect of varying delta 9-tetrahydrocannabinol content and number of puffs. *J Pharmacol Exp Ther* 261, 114-22.

230. Jan, T.R., Farraj, A.K., Harkema, J.R., Kaminski, N.E. (2003) Attenuation of the ovalbumin-induced allergic airway response by cannabinoid treatment in A/J mice. *Toxicol Appl Pharmacol* 188, 24-35.

231. Lu, H., Kaplan, B.L., Ngaotepprutaram, T., Kaminski, N.E. (2009) Suppression of T cell costimulator ICOS by Delta9-tetrahydrocannabinol. *J Leukoc Biol* 85, 322-9.

232. Kaplan, B.L.F., Lawver, J.E., Karmaus, P.W.F., Ngaotepprutaram, T., Birmingham, N.P., Harkema, J.R., Kaminski, N.E. (2010) The Effects of Targeted Deletion of Cannabinoid Receptors CB1 and CB2 on Intranasal Sensitization and Challenge with Adjuvant-free Ovalbumin. *Toxicologic Pathology* 38, 382-392 %R 10.1177/0192623310362706.

233. Pross, S.H., Nakano, Y., Widen, R., McHugh, S., Newton, C.A., Klein, T.W., Friedman, H. (1992) Differing effects of delta-9-tetrahydrocannabinol (THC) on murine spleen cell populations dependent upon stimulators. *Int J Immunopharmacol* 14, 1019-27.

234. Horsley, V., Pavlath, G.K. (2002) NFAT: ubiquitous regulator of cell differentiation and adaptation. *J Cell Biol* 156, 771-4.

235. Srinivasan, M., Frauwirth, K.A. (2007) Reciprocal NFAT1 and NFAT2 nuclear localization in CD8+ anergic T cells is regulated by suboptimal calcium signaling. *J Immunol* 179, 3734-41.

236. Jain, J., McCaffrey, P.G., Miner, Z., Kerppola, T.K., Lambert, J.N., Verdine, G.L., Curran, T., Rao, A. (1993) The T-cell transcription factor NFATp is a substrate for calcineurin and interacts with Fos and Jun. *Nature* 365, 352-5.

237. Shaw, J.P., Utz, P.J., Durand, D.B., Toole, J.J., Emmel, E.A., Crabtree, G.R. (1988) Identification of a putative regulator of early T cell activation genes. *Science* 241, 202-5.

238. Sweetser, M.T., Hoey, T., Sun, Y.L., Weaver, W.M., Price, G.A., Wilson, C.B. (1998) The roles of nuclear factor of activated T cells and ying-yang 1 in activation-induced expression of the interferon-gamma promoter in T cells. *J Biol Chem* 273, 34775-83.

239. Sica, A., Dorman, L., Viggiano, V., Cippitelli, M., Ghosh, P., Rice, N., Young, H.A. (1997) Interaction of NF-kappaB and NFAT with the interferon-gamma promoter. *J Biol Chem* 272, 30412-20.

240. Schwartz, R.H. (1996) Models of T cell anergy: is there a common molecular mechanism? *J Exp Med* 184, 1-8.

241. Schwartz, R.H. (2003) T cell anergy. *Annu Rev Immunol* 21, 305-34.

242. Puga, I., Rao, A., Macian, F. (2008) Targeted cleavage of signaling proteins by caspase 3 inhibits T cell receptor signaling in anergic T cells. *Immunity* 29, 193-204.

243. Refaeli, Y., Van Parijs, L., Alexander, S.I., Abbas, A.K. (2002) Interferon gamma is required for activation-induced death of T lymphocytes. *J Exp Med* 196, 999-1005.

244. Lee, C.Y., Wey, S.P., Liao, M.H., Hsu, W.L., Wu, H.Y., Jan, T.R. (2008) A comparative study on cannabidiol-induced apoptosis in murine thymocytes and EL-4 thymoma cells. *Int Immunopharmacol* 8, 732-40.

245. Ryan, D., Drysdale, A.J., Lafourcade, C., Pertwee, R.G., Platt, B. (2009) Cannabidiol targets mitochondria to regulate intracellular Ca2+ levels. *J Neurosci* 29, 2053-63.

246. Drysdale, A.J., Ryan, D., Pertwee, R.G., Platt, B. (2006) Cannabidiol-induced intracellular Ca2+ elevations in hippocampal cells. *Neuropharmacology* 50, 621-31.

247. Dolmetsch, R.E., Xu, K., Lewis, R.S. (1998) Calcium oscillations increase the efficiency and specificity of gene expression. *Nature* 392, 933-6.

248. Savignac, M., Mellstrom, B., Naranjo, J.R. (2007) Calcium-dependent transcription of cytokine genes in T lymphocytes. *Pflugers Arch* 454, 523-33.

249. Macian, F., Garcia-Rodriguez, C., Rao, A. (2000) Gene expression elicited by NFAT in the presence or absence of cooperative recruitment of Fos and Jun. *Embo J* 19, 4783-95.

250. Macian, F., Garcia-Cozar, F., Im, S.H., Horton, H.F., Byrne, M.C., Rao, A. (2002) Transcriptional mechanisms underlying lymphocyte tolerance. *Cell* 109, 719-31.

251. Surman, S., Lockey, T.D., Slobod, K.S., Jones, B., Riberdy, J.M., White, S.W., Doherty, P.C., Hurwitz, J.L. (2001) Localization of CD4+ T cell epitope hotspots to exposed strands of HIV envelope glycoprotein suggests structural influences on antigen processing. *Proc Natl Acad Sci U S A* 98, 4587-92.

252. Brown, S.A., Stambas, J., Zhan, X., Slobod, K.S., Coleclough, C., Zirkel, A., Surman, S., White, S.W., Doherty, P.C., Hurwitz, J.L. (2003) Clustering of Th cell epitopes on exposed regions of HIV envelope despite defects in antibody activity. *J Immunol* 171, 4140-8.

253. Wang, W.K., Dudek, T., Essex, M., Lee, T.H. (1999) Hypervariable region 3 residues of HIV type 1 gp120 involved in CCR5 coreceptor utilization: therapeutic and prophylactic implications. *Proc Natl Acad Sci U S A* 96, 4558-62.

254. Zhu, L.X., Sharma, S., Stolina, M., Gardner, B., Roth, M.D., Tashkin, D.P., Dubinett, S.M. (2000) Delta-9-tetrahydrocannabinol inhibits antitumor immunity by a CB2 receptor-mediated, cytokine-dependent pathway. *J Immunol* 165, 373-80.

255. Cabral, G.A., Mishkin, E.M., Marciano-Cabral, F., Coleman, P., Harris, L., Munson, A.E. (1986) Effect of delta 9-tetrahydrocannabinol on herpes simplex virus type 2 vaginal infection in the guinea pig. *Proc Soc Exp Biol Med* 182, 181-6.

256. Busch, L., Sterin-Borda, L., Borda, E. (2004) Expression and biological effects of CB1 cannabinoid receptor in rat parotid gland. *Biochem Pharmacol* 68, 1767-74.

257. Bonhaus, D.W., Chang, L.K., Kwan, J., Martin, G.R. (1998) Dual activation and inhibition of adenylyl cyclase by cannabinoid receptor agonists: evidence for agonist-specific trafficking of intracellular responses. *J Pharmacol Exp Ther* 287, 884-8.

258. Calandra, B., Portier, M., Kerneis, A., Delpech, M., Carillon, C., Le Fur, G., Ferrara, P., Shire, D. (1999) Dual intracellular signaling pathways mediated by the human cannabinoid CB1 receptor. *Eur J Pharmacol* 374, 445-55.

259. Cox, C.A., Shi, G., Yin, H., Vistica, B.P., Wawrousek, E.F., Chan, C.C., Gery, I. (2008) Both Th1 and Th17 are immunopathogenic but differ in other key biological activities. *J Immunol* 180, 7414-22.

260. Stern, S.T., McNeil, S.E. (2008) Nanotechnology safety concerns revisited. *Toxicol Sci* 101, 4-21.

261. Demento, S.L., Eisenbarth, S.C., Foellmer, H.G., Platt, C., Caplan, M.J., Mark Saltzman, W., Mellman, I., Ledizet, M., Fikrig, E., Flavell, R.A., Fahmy, T.M. (2009) Inflammasome-activating nanoparticles as modular systems for optimizing vaccine efficacy. *Vaccine* 27, 3013-21.

262. Colvin, V.L. (2003) The potential environmental impact of engineered nanomaterials. *Nat Biotech* 21, 1166-1170.

263. Nel, A., Xia, T., Mädler, L., Li, N. (2006) Toxic Potential of Materials at the Nanolevel. *Science* 311, 622-627 %R 10.1126/science.1114397.

264. Li, N., Wang, M., Bramble, L.A., Schmitz, D.A., Schauer, J.J., Sioutas, C., Harkema, J.R., Nel, A.E. (2009) The adjuvant effect of ambient particulate matter is closely reflected by the particulate oxidant potential. *Environ Health Perspect* 117, 1116-23.

265. Inoue, K.-i., Takano, H., Yanagisawa, R., Hirano, S., Sakurai, M., Shimada, A., Yoshikawa, T. (2006) Effects of Airway Exposure to Nanoparticles on Lung Inflammation Induced by Bacterial Endotoxin in Mice. *Environmental Health Perspectives* 114, 1325-1330.

266. Lin, Y.-S., Haynes, C.L. (2009) Synthesis and Characterization of Biocompatible and Size-Tunable Multifunctional Porous Silica Nanoparticles. *Chemistry of Materials* 21, 3979-3986.

267. Luhmann, T., Rimann, M., Bittermann, A.G., Hall, H. (2008) Cellular uptake and intracellular pathways of PLL-g-PEG-DNA nanoparticles. *Bioconjug Chem* 19, 1907-16.

268. Brandenberger, C., Rowley, N.L., Jackson-Humbles, D.N., Zhang, Q., Bramble, L.A., Lewandowski, R.P., Wagner, J.G., Chen, W., Kaplan, B.L., Kaminski, N.E., Baker, G.L., Worden, R.M., Harkema, J.R. (2013) Engineered silica nanoparticles act as adjuvants to enhance allergic airway disease in mice. *Part Fibre Toxicol* 10, 26.

269. Clarke, S.R., Barnden, M., Kurts, C., Carbone, F.R., Miller, J.F., Heath, W.R. (2000) Characterization of the ovalbumin-specific TCR transgenic line OT-I: MHC elements for positive and negative selection. *Immunol Cell Biol* 78, 110-7.

270. Sette, A., Buus, S., Colon, S., Smith, J.A., Miles, C., Grey, H.M. (1987) Structural characteristics of an antigen required for its interaction with Ia and recognition by T cells. *Nature* 328, 395-9.

271. Dobrovolskaia, M.A., Aggarwal, P., Hall, J.B., McNeil, S.E. (2008) Preclinical studies to understand nanoparticle interaction with the immune system and its potential effects on nanoparticle biodistribution. *Mol Pharm* 5, 487-95.

272. Dobrovolskaia, M.A., McNeil, S.E. (2007) Immunological properties of engineered nanomaterials. *Nat Nanotechnol* 2, 469-78.

273. Wilhelm, C., Billotey, C., Roger, J., Pons, J.N., Bacri, J.C., Gazeau, F. (2003) Intracellular uptake of anionic superparamagnetic nanoparticles as a function of their surface coating. *Biomaterials* 24, 1001-11.

274. Kitto, H.J., Schwartz, E., Nijemeisland, M., Koepf, M., Cornelissen, J.J.L.M., Rowan, A.E., Nolte, R.J.M. (2008) Post-modification of helical dipeptido polyisocyanides using the 'click' reaction. *Journal of Materials Chemistry* 18, 5615-5624.

275. Gangwal, S., Brown, J.S., Wang, A., Houck, K.A., Dix, D.J., Kavlock, R.J., Hubal, E.A. (2011) Informing selection of nanomaterial concentrations for ToxCast in vitro testing based on occupational exposure potential. *Environ Health Perspect* 119, 1539-46.

276. Lu, X., Sun, F., Wang, J., Zhong, J., Dong, Q. (2009) A Facile Route to Prepare Organic/Inorganic Hybrid Nanomaterials by ‘Click Chemistry’. *Macromolecular Rapid Communications* 30, 2116-2120.

277. Choualeb, A., Rosé, J., Braunstein, P., Welter, R. (2003) Routes to Ruthenium-Cobalt Clusters and Dicobalt Complexes with New Alkoxysilyl- or Sulfur-Functionalized Alkynes. X-ray Structures of [NEt4][RuCo3(CO)10{ μ 4- η 2-HC2(CH2)2OC(O)NH(CH2)3Si(OEt)3}] and [Co2(CO)6{ μ 2- η 2-HC2CH2NHC(O)NH(CH2)3Si(OEt)3}]. *Organometallics* 22, 2688-2693.

278. Banchereau, J., Steinman, R.M. (1998) Dendritic cells and the control of immunity. *Nature* 392, 245-252.

279. Li, N., Xia, T., Nel, A.E. (2008) The role of oxidative stress in ambient particulate matter-induced lung diseases and its implications in the toxicity of engineered nanoparticles. *Free Radical Biology and Medicine* 44, 1689-1699.

280. He, T., Tang, C., Xu, S., Moyana, T., Xiang, J. (2007) Interferon gamma stimulates cellular maturation of dendritic cell line DC2.4 leading to induction of efficient cytotoxic T cell responses and antitumor immunity. *Cell Mol Immunol* 4, 105-11.

281. Ni, H.T., Spellman, S.R., Jean, W.C., Hall, W.A., Low, W.C. (2001) Immunization with dendritic cells pulsed with tumor extract increases survival of mice bearing intracranial gliomas. *J Neurooncol* 51, 1-9.

282. Cohen, J., DeLoid, G., Pyrgiotakis, G., Demokritou, P. (2013) Interactions of engineered nanomaterials in physiological media and implications for in vitro dosimetry. *Nanotoxicology* 7, 417-431.

283. Jiang, J., Oberd √ ∂rster, G.n., Biswas, P. (2009) Characterization of size, surface charge, and agglomeration state of nanoparticle dispersions for toxicological studies. *Journal of Nanoparticle Research* 11, 77-89.

284. Katas, H., Hussain, Z., Awang, S.A.R. (2013) Bovine Serum Albumin-Loaded Chitosan/Dextran Nanoparticles: Preparation and Evaluation of Ex Vivo Colloidal Stability in Serum. *Journal of Nanomaterials* 2013, 9.

285. Yildirim, A., Ozgur, E., Bayindir, M. (2013) Impact of mesoporous silica nanoparticle surface functionality on hemolytic activity, thrombogenicity and non-specific protein adsorption. *Journal of Materials Chemistry B* 1, 1909-1920.

286. Kardys, A.Y., Bharali, D.J., Mousa, S.A.R. (2013) Amino-Functionalized Silica Nanoparticles: In Vitro Evaluation for Targeted Delivery and Therapy of Pancreatic Cancer. *Journal of Nanotechnology* 2013, 8.

287. Thevenot, P., Cho, J., Wavhal, D., Timmons, R.B., Tang, L. (2008) Surface chemistry influences cancer killing effect of TiO2 nanoparticles. *Nanomedicine* 4, 226-36.

288. Wang, C.C., Lu, J.N., Young, T.H. (2007) The alteration of cell membrane charge after cultured on polymer membranes. *Biomaterials* 28, 625-31.

289. Xia, T., Kovochich, M., Brant, J., Hotze, M., Sempf, J., Oberley, T., Sioutas, C., Yeh, J.I., Wiesner, M.R., Nel, A.E. (2006) Comparison of the Abilities of Ambient and Manufactured Nanoparticles To Induce Cellular Toxicity According to an Oxidative Stress Paradigm. *Nano Letters* 6, 1794-1807.

290. Uto, T., Akagi, T., Hamasaki, T., Akashi, M., Baba, M. (2009) Modulation of innate and adaptive immunity by biodegradable nanoparticles. *Immunology Letters* 125, 46-52.

291. Yeh, T.-C., Zhang, W., Ildstad, S.T., Ho, C. (1993) Intracellular labeling of T-cells with superparamagnetic contrast agents. *Magnetic Resonance in Medicine* 30, 617-625.

292. Jiang, W., KimBetty, Y.S., Rutka, J.T., ChanWarren, C.W. (2008) Nanoparticle-mediated cellular response is size-dependent. *Nat Nano* 3, 145-150.

293. Chithrani, B.D., Ghazani, A.A., Chan, W.C. (2006) Determining the size and shape dependence of gold nanoparticle uptake into mammalian cells. *Nano Lett* 6, 662-8.

294. Gao, H., Shi, W., Freund, L.B. (2005) Mechanics of receptor-mediated endocytosis. *Proc Natl Acad Sci U S A* 102, 9469-74.